Mode of Action of Fingolimod on Neurons:

The Role of the Sphingosine 1-Phosphate Receptor 1

Katharina Ursina Saeuberli

A thesis submitted to Cardiff University in accordance with the requirements for the

degree of Doctor of Philosophy in the discipline of Neuroscience

School of Biosciences, Cardiff University

January 2017

In memory of my brother Constantin

Declaration

This work has not been submitted in substance for any other degree or award at this or any other university or place of learning, nor is being submitted concurrently in candidature for any degree or other award.

Signed.. Date ....

STATEMENT 1

This thesis is being submitted in partial fulfilment of the requirements for the degree of PhD.

Signed.. Date ....

STATEMENT 2

This thesis is the result of my own independent work/investigation, except where otherwise stated, and the thesis has not been edited by a third party beyond what is permitted by Cardiff University's Policy on the Use of Third Party Editors by Research Degree Students. Other sources are acknowledged by explicit references. The views expressed are my own.

Signed.. Date ....

STATEMENT 4: PREVIOUSLY APPROVED BAR ON ACCESS

I hereby give consent for my thesis, if accepted, to be available online in the University's Open Access repository and for inter-library loans after expiry of a bar on access previously approved by the Academic Standards & Quality Committee.

Signed.. Date ....

Acknowledgements

I'd like to take this opportunity to thank my supervisor Prof Yves-Alain Barde for his support throughout my PhD. I learned a tremendous amount and I'm very grateful that you shared your knowledge with me. Thank you for giving me the opportunity to work on such an exciting and challenging PhD project.

Special thanks go to my co-supervisor Chris McGuigan who's knowledge and enthusiasm contributed to my wonderful PhD experience. He is greatly missed.

Special thanks go to Bridget Allen for supporting me with the ES cell harvest process. I'd like to thank Prof. Paul Kemp and his team for introducing me to the techniques of electrophysiology. I would also like to thank Dr. Isabel Martinez-Garay for providing me with the Cre-IRES-GFP plasmid, as well as Dr. Xinsheng Nan for providing me with the $Rosa26/Cre^{ERT2}$ ES cell line.

I would like to express my thanks to Dr. Pedro Chacón Fernández. Thank you for introducing me to all your secrets of cell culture, for all the interesting discussions and mostly for being such a good friend.

It was a wonderful experience to work in Yves' lab, not in the least because of the great team. Thank you all for creating such a pleasant working environment. For the many moments, full of laughter and for the support and fruitful discussions throughout my PhD.

Last, but not least I want to thank my family and friends for their love, support, and for always believing in me. Thank you mum and dad for all the sacrifices you've made on my behalf. Special thanks go to my sisters Barbara and Franziska and their partners for their continuous motivation and support. I would like to thank my friends in Switzerland, especially Stephanie for always being there for me, although I'm so far away. And finally, I would like to express my gratitude to Craig for being so patient, supporting me in every way and being my calm harbour. Thank you.

Abstract

Brain-derived neurotrophic factor (BDNF) is a secretory protein known to be essential for brain function, including key aspects of synaptic transmission. Its levels are decreased in a number of conditions including neurodegenerative diseases, thus generating a need for well-tolerated drugs increasing BDNF levels in the brain. The sphingosine analogue fingolimod, also designated FTY720, is one of a still very small number of drugs readily diffusing into the brain and extensively used in humans following its approval for the treatment of multiple sclerosis. It acts as a functional antagonist on the G protein-coupled receptor sphingosine 1-phosphate receptor 1 (S1P1R) thereby preventing the exit of lymphocytes from lymph nodes. Recently, FTY720 has been shown to increase BDNF levels in the brain and the main objective of the work was to investigate whether S1P1R plays a role in the action of the drug on neurons. This study reports on the successful generation of mutant neurons lacking S1P1R from mouse embryonic stem cells, using a modified differentiation protocol. While the interpretation of the data was complicated by a high variability encountered in the culture system, preliminary data suggests a role of S1P1R in the long-term effects of pFTY720 on BDNF levels *in vitro*. As the *BDNF* gene has been recently reported to be not only expressed by neurons, but also by megakaryocytes, FTY720-dependent effects were also investigated in primary rat megakaryocytes.

This work establishes that sphingosine receptors were found to be expressed at the mRNA level in ES cell-derived neurons and primary rat megakaryocytes and reveals an unexpected complexity of FTY720 signalling in these cells.

Abbreviations

Ø	control
#1 cells/neurons	ES cells derived from $S1p1r^{\text{loxP/loxP}}/Cre^{ERT2}$
#43 cells/neurons	$S1p1r^{-/-}$ cells/neurons
4-OHT	(Z)-4-hydroxytamoxifen
5-FdU	5-fluoro2'-deoxyuridin
Ab #1	monoclonal antibody anti-BDNF #1
AC	adenylyl cyclase
AD	Alzheimer's disease
ADP	adenosine diphosphate
AMPA	α-amino-3-hydroxy-5-methyl-4-isoxazolepropionic acid
ANOVA	analysis of variance
Arbp	attachment region binding protein
APP	amyloid precursor protein
AU	arbitrary units
AUC	area under the curve
B2 cells/neurons	subclone of #43 cells/neurons and $S1p1r^{-/-}$ cells/neurons
BBB	blood brain barrier
BCA	bicinchoninic acid
BDNF	brain-derived neurotrophic factor
$Bdnf^{-/-}$	$Bdnf$-null mice
Bis-Tris	bisamino-trismethan
BSA	bovine serum albumin
BW	bodyweight
CA	cellular aggregates
cAMP	cyclic adenosine monophosphate
CaRF	calcium responsive factor
cat.no.	catalogue number
cDNA	cyclic DNA
CerS	ceramide synthase 1
CHO	Chinese hamster ovary

CNS	central nervous system
CRE	calcium-responsive element
CREB	calcium-responsive element binding protein
CSF	cerebrospinal fluid
Ctip1	chicken ovalbumin upstream promoter transcription factor-interacting protein 1
Ctip2	chicken ovalbumin upstream promoter transcription factor-interacting protein 2
DAPI	4',6-diamidino-2-phenylindol dihydrochloride
DMEM	Dulbecco's Modified Eagle Medium
DMS	N,N-dimethylsphingosine
DMSO	dimethylsulfoxid
DNA	deoxyribonucleic acid
dNTP	deoxynucleotide
DTT	dithiothreitol
EAE	experimental autoimmune encephalomyelitis
EC_{50}	half-maximal effective concentration
EDG	endothelial differentiation gene
EDTA	ethylenediaminetetraacetic acid
ELISA	enzyme-linked immunosorbent assay
ERK pathway	Ras/Raf/MEK/ERK pathway
ERK1/2	extracellular signal-regulated kinase ½
EtOH	ethanol
EYFP	enhanced yellow fluorescent protein
FACS	fluorescence activated cell sorting
FBS	fetal bovine serum
FTY720	fingolimod
GAPDH	glyceraldehyde 3-phosphate dehydrogenase
GDP	guanosindiphosphate
GFAP	glial fibrillary acidic protein
GIRK	G-protein coupled inwardly rectifying potassium channel
GLAST	astrocyte-specific glutamate transporter
GSK3	glycogen synthase kinase-3

GTP	guanosintriphosphate
h	hour/s
HBSS	Hank's balanced salt solution
HCl	hydrochloric acid
HD	Huntington's disease
HDAC	histone deacetylase
HPRT	hypoxanthine-guanine phosphoribosyltransferase
i.p.	intraperitoneal
Igepal® CA-630	octylphenoxy poly(ethyleneoxy)ethanol
IP$_3$	inositol trisphosphate
J1 cells/neurons	cells derived from a 129S4/SvJae strain
kb	kilobase
KCl	potassium chloride
K_d	dissociation constant
LIF	leukemia inhibitory factor
LPA1	lysophosphatidic acid 1
LPP3	lipid phosphate phosphatase 3
LRP1	lipoprotein receptor-related protein 1
LTP	long-term potentiation
MEA	micro electrode array
MeCP2	methyl-CpG binding protein 2
MEF	mouse embryonic fibroblasts
MEK	mitogen-activated protein kinase kinase
MES	2-(N-morpholino)ethanesulfonic acid
mHtt	mutant huntingtin
min	minute/s
mM	millimolar
MOG	myelin oligodendrocyte glycoprotein
ms	millisecond/s
MSC	mesenchymal stem cells
NaCl	sodium chloride
NEAA	non-essential amino acids

NFAT	nuclear factor of activated T-cells
NF-κB	nuclear factor κ-light-chain-enhancer of activated B cells
nm	nanometer
nM	nanomolar
NMDA	*N*-methyl-*D*-aspartic acid
NMDARs	*N*-methyl-*D*-aspartic acid glutamate receptors
Oct4	octamer-binding transcription factor 4
p75^{NTR}	p75 neurotrophin receptor
PBS	phosphate buffered saline
PD	Parkinson's disease
pEC$_{50}$	-log(EC$_{50}$)
pERK1/2	phosphorylated extracellular signal-regulated kinase 1/2
pFTY720	(S)-phosphorylated fingolimod
PI3K	phosphoinositide 3-kinase
PKA	protein kinase A
PLCβ/γ	phospholipase C β/γ
PMSF	phenylmethylsulfonyl fluoride
Primer AS	Primer antisense
Primer S	Primer sense
PTEN	phosphatase and tensin homolog
PTX	pertussis toxin
RGS	regulator of G protein signalling
RNA	ribonucleic acid
ROCK	Rho-associated protein kinase
S1P	sphingosine 1-phosphate
S1P1R	sphingosine 1-phosphate receptor 1
S1p1r$^{-/-}$	*S1p1r*-null mice/cells
S1p1r$^{loxP/loxP}$	exon 2 of the *S1p1r* gene flanked by two loxP sites
S1P2R	sphingosine 1-phosphate receptor 2
S1P3R	sphingosine 1-phosphate receptor 3
S1P4R	sphingosine 1-phosphate receptor 4
S1P5R	sphingosine 1-phosphate receptor 5

S1PL	sphingosine 1-phosphate lyase
SCF	stem cell factor
SDO	sodium deoxycholate
SDS	sodiumdodecylsulphate
secs	seconds
SLICK	single-neuron labelling inducible Cre-mediated knockout
SMase	sphingomyelinase
SphK1/2	sphingosine kinase 1/2
Spns2	spinster 2
SPP	sphingosine 1-phosphate phosphatase
Tbr1	T-box brain gene 1
TFA	trifluoroacetic acid
Thy-1	thymocyte differentiation antigen 1
TPO	thrombopoietin
TrkA	tropomyosin receptor kinase A
TrkB	tropomyosin receptor kinase B
TrkC	tropomyosin receptor kinase C
USF1/2	upstream transcription factor ½
USFBE	USF binding element
VEGFD	vascular endothelial growth factor D
VGCC	voltage-gated calcium channels
vGlut1	vesicular glutamate transporter 1
vGlut2	vesicular glutamate transporter 2
vs.	*versus*
WAGR	Wilms tumour, Aniridia, Genitourinary anomalies, mental Retardation
WT	wild-type
μm	micrometer
μM	micromolar

Contents

List of Figures

List of Tables

Chapter 1

Introduction

1.1　Overview

Neurodegenerative diseases represent an ever growing problem for society due to the increased life expectancy in industrialised countries (Wyss-Coray 2016). While there is a wide spectrum of neurodegenerative disorders some of the most frequent diseases including Parkinson's (PD) as well as Alzheimer's disease (AD) have been shown to include cell death as well as the loss of synaptic contacts (Przedborski et al. 2003). These observations have increasingly focused attention on the potential use of neurotrophic factors to combat neurodegeneration. These factors are broadly defined as a class of substances preventing the death of neurons and positively regulating synaptic plasticity (Weissmiller and Wu 2012; Allen et al. 2013). By far the most thoroughly investigated molecule in this category is the growth factor designated brain-derived neurotrophic factor (BDNF; for review see Bibel and Barde 2000 and Park and Poo 2013). Like all other members of the family (see below), BDNF exerts its neuroprotective effects through the activation of a receptor tyrosine kinase. In the case of BDNF this is the tropomyosin receptor kinase B (TrkB) (Klein et al. 1990). The evidence for a significant "trophic" role of BDNF comes not only from the results of *in vitro* assays or of genetically manipulating animals lacking *BDNF* (Bibel and Barde 2000; Rauskolb et al. 2010; Park and Poo 2013), but also from human genetics including loss-of-allele mutation and a valine for methionine substitution in pro-BDNF (Egan et al. 2003; Gray et al. 2006; Notaras et al. 2015). Furthermore, BDNF turned out to be also present in human blood at relatively high concentrations (Yamamoto and Gurney 1990), and a number of studies have associated

BDNF levels in human blood with various conditions such as depression or Alzheimer's disease (Laske et al. 2011; Bus et al. 2015). Conversely physical exercise generally recognised to retard cognitive decline during ageing increases BDNF levels in human blood (Griffin et al. 2011; Tuon et al. 2014). Up until very recently, the origin of BDNF in human blood has remained unclear. BDNF was speculated to somehow diffuse from the brain into the blood circulation where it was thought to be accumulated by circulating platelets (Serra-Millas 2016). Indeed, it has been shown early on that human platelets, but not mouse platelets contain significant levels of BDNF (Yamamoto and Gurney 1990), As the levels of BDNF in mouse and human brains are comparable, it appears unlikely that BDNF in human platelets, would be brain-derived. Our laboratory recently reported that human and rat megakaryocytes express the *BDNF/Bdnf* gene and translate the corresponding mRNAs, thus clarifying the cellular origin of blood BDNF (Chacon-Fernandez et al. 2016). These non-neuronal cells express sphingosine 1-phosphate receptor mRNAs (see Chapter 7) and use the same promoters as neurons to transcribe the *BDNF/Bdnf* gene (Chacon-Fernandez et al. 2016).

Unlike growth factors acting on the hematopoietic lineage such as erythropoietin, BDNF cannot be administered as a recombinant protein to improve neuronal function. This is not just because of its unfavourable physicochemical characteristics including high isoelectric point (Barde et al. 1982), but also because of its short half-life in plasma it does not seem to be able to access the brain at therapeutically relevant quantities (Pardridge et al. 1994; Sakane and Pardridge 1997). Alternative strategies are being developed consisting in the development of drugs aiming at activating the BDNF receptor TrkB or at increasing BDNF transcription by using compounds accessing the brain and targeting neuronal receptors (Cazorla et al. 2011; English et al. 2013). In the brain, BDNF is primarily expressed by excitatory neurons and it has been known for some time that increased excitatory inputs on such neurons increase *Bdnf* mRNA and protein from

typically extremely low resting levels (Castren et al. 1993). In particular, glutamate receptor agonists, designated Ampakines, have been used extensively in an initial approach and with some success in animal models whereby it remained unclear whether excitotoxicity could be sufficiently separated from beneficial effects (Lauterborn et al. 2009). Additionally, it has been shown that the combined administration of Ampakines with BDNF is more effective in improving motor function in a post-stroke mouse model compared to Ampakine treatment alone (Clarkson et al. 2015). More recently, it was realised that a drug introduced for the treatment of multiple sclerosis increased BDNF levels, both *in vitro* and *in vivo* (Deogracias et al. 2012). In addition, it could be shown that this sphingosine analogue, designated fingolimod (FTY720) improves the locomotor behaviour of animals lacking the gene *Mecp2*, a model of a disease called Rett syndrome (Deogracias et al. 2012). Importantly, these findings formed the basis of a small clinical trial exploring the potential beneficial effects of FTY720 administered to children suffering from this neurodevelopmental disease (Naegelin et al. 2015). FTY720 is a sphingosine 1-phospate receptor modulator and there is overwhelming evidence to indicate that the downregulation of the sphingosine 1-phosphate receptor 1 (S1P1R) on T-lymphocytes explains its beneficial effects in the context of multiple sclerosis (Chun and Brinkmann 2011). In 2012, our group proposed that FTY720, well-known to diffuse into the brain (Foster et al. 2007), may activate S1P1R on neurons, potentially explaining the increase of BDNF levels in an activity-dependent manner (Deogracias et al. 2012). However, FTY720 is known to also activate other S1P receptors and both the cellular localisation of these receptors as well as their pre- or post-synaptic role in increasing neurotransmission remain unclear, including the important question as to whether the receptor itself or other molecules may be involved in regulating BDNF levels.

The core of this project was to clarify the role of the S1P1 receptor on neurons in mediating BDNF increase in the nervous system. To this end, neurons derived from

embryonic stem (ES) cells were used as a tool to dissect the role of this receptor in mediating the mode of action of FTY720. This system allows the generation of uniquely homogenous populations of neurons (Bibel et al. 2004; Bibel et al. 2007) and comparisons to be made between wild-type (WT) and mutant neurons lacking S1P1R. Additionally, given the expression of BDNF in a pattern similar to neurons in megakaryocytes, the expression of S1P1R was also investigated in these cells to explore possible effects of FTY720 on *Bdnf* mRNA levels outside the nervous system.

1.2 Sphingosine and its Receptors

1.2.1 Sphingosine metabolism

Sphingosine belongs to the family of sphingolipids. It is an 18-carbon amino alcohol with an unsaturated hydrocarbon chain and a primary constituent of sphingolipids, a class of cell membrane lipids (Figure 1.1 and 1.4; (Chun and Brinkmann 2011)). Sphingosine is generated from the membrane lipid sphingomyelin, which is first broken down to the intermediate ceramide by the enzyme sphingomyelinase, followed by its hydrolysis to sphingosine through the enzyme ceramidase. Sphingosine is phosphorylated by one of the two known sphingosine kinases 1 and 2 (SphK1 and 2) to sphingosine 1-phospate (S1P) (Pyne et al. 2016) and transported out of the cells by the transporter spinster 2 (Figure 1.1 and (Kawahara et al. 2009; Donoviel et al. 2015)). Cells such as red blood cells as well as blood platelets release considerable amounts of S1P so that its levels may reach about 1 μM in the blood and 0.1 μM in the lymph (Tani et al. 2005; Pappu et al. 2007; Yanagida and Hla 2016). These concentrations are thought to be considerably higher than in other interstitial fluids thus allowing lymphocytes *via* S1P receptor-mediated chemotaxis to exit the lymph nodes and enter the vascular system (Arnon et al. 2011; Zhang et al. 2012).
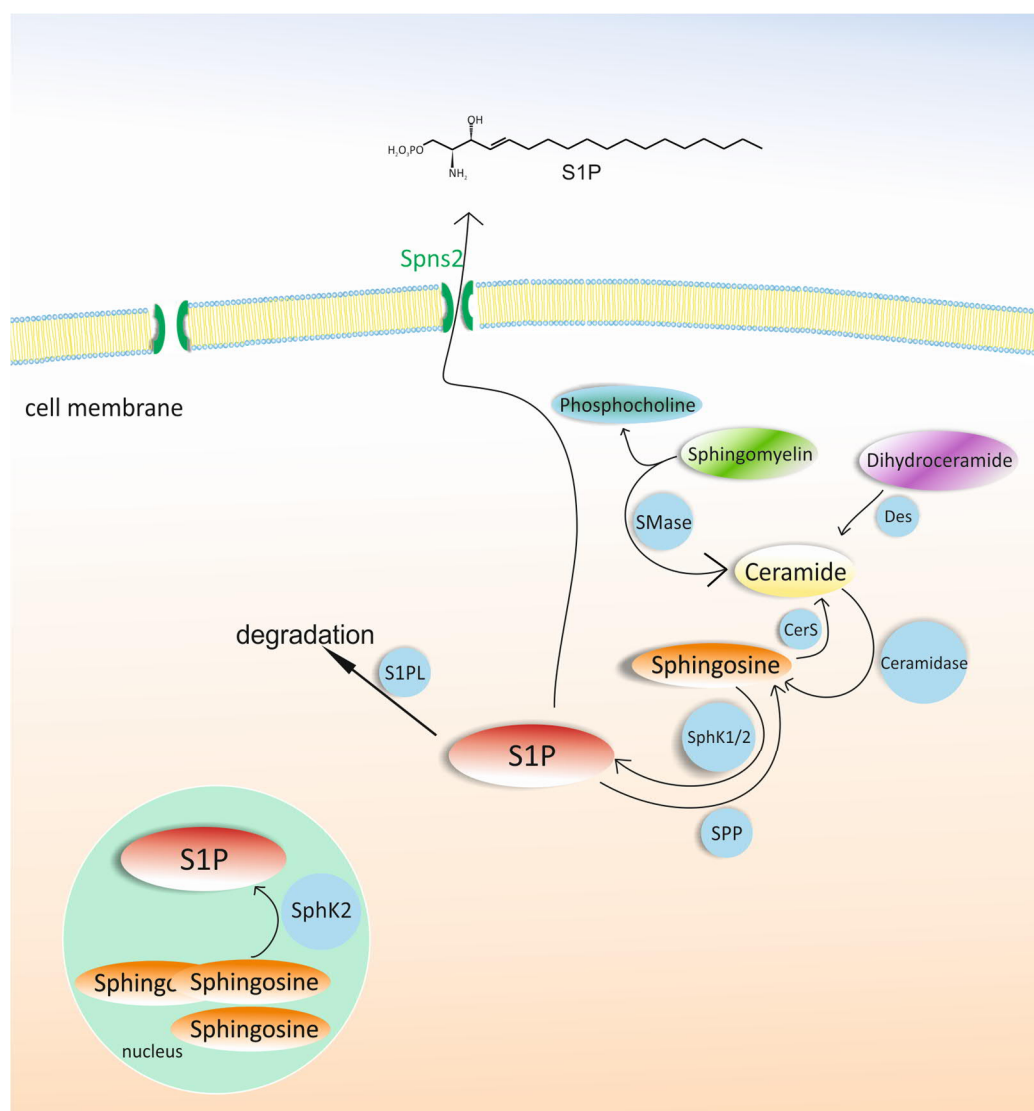
Figure 1.1 Sphingosine metabolism

Ceramide is either synthesised de novo from dihydroceramide via the dihydroceramide desaturase (Des) or by hydrolysis of sphingomyelin by the enzyme sphingomyelinase (SMase). Ceramidase cleaves ceramide and produces sphingosine, which can be converted back to ceramide via ceramide synthase 1 (CerS). One of the two sphingosine kinases (SphK1/2) phosphorylates sphingosine to its active form sphingosine 1-phosphate (S1P), which is also interconvertible due to the activity of the sphingosine 1-phosphate phosphatase (SPP). S1P is either transported out of the cell by the transporter spinster 2 (Spns2) or degraded by sphingosine 1-phosphate lyase (S1PL). Sphingosine also accumulates in the nucleus, where it is phosphorylated by SphK2. Figure adapted from (Pyne et al. 2016).

1.2.2   The five sphingosine receptors

Initially the sphingosine receptors were referred to as endothelial differentiation gene (EDG) receptors. The EDG family consists of eight members (Takuwa et al. 2002), with the first member EDG-1, having been discovered as a transcript expressed during the course of *in vitro* differentiation of endothelial cells (Hla and Maciag 1990). The later discoveries by homology cloning of EDG-3 and EDG-5 expanded the family (MacLennan et al. 1994; Yamaguchi et al. 1996), and it is only in 1998 that S1P was discovered as a high affinity ligand for EDG-1 (Lee et al. 1998; Zondag et al. 1998). Subsequent studies revealed that in fact S1P is a ligand for five members of the then orphan receptor family (Im et al. 2000; Spiegel 2000) and the receptors were renamed to S1P1R (EDG-1), S1P2R (EDG-5), S1P3R (EDG-3), S1P4R (EDG-6) and S1P5R (EDG-8) (Chun et al. 2002). S1P has a high affinity to four of the five receptors (K_d in the range of 2 – 27 nM) and binds S1P4R with a distinctly lower affinity (K_d = 63 nM) (Im et al. 2000; Spiegel 2000; Van Brocklyn et al. 2000). The S1P receptors exhibit about 20 % sequence identities with the cannabinoid receptors 1 and 2 and 30 % with the lysophosphatidic acid receptors 1-3 (Hla et al. 1999; Ishii et al. 2004).

1.2.3   Signal transduction through S1P receptors

All five S1P1Rs are heterotrimeric G protein-coupled receptors (GPCR) undergoing a conformational change after ligand binding, allowing the receptor to interact with a trimeric G protein (Figure 1.2 and (Blaho and Hla 2014).

Trimeric G proteins consist of three different subunits, namely G_α, G_β and G_γ and its inactive state, the G_α subunit is bound to guanosine diphosphate (GDP). Upon activation, GDP is replaced by guanosine triphosphate (GTP), leading to the interaction of the G_α subunit with membrane bound proteins signalling to downstream pathways (Oldham and Hamm 2008). Once the GTP bound-G_α subunit is hydrolysed by regulator of G protein

signalling (RGS) proteins it is inactivated and downstream signalling is terminated (Oldham and Hamm 2008).
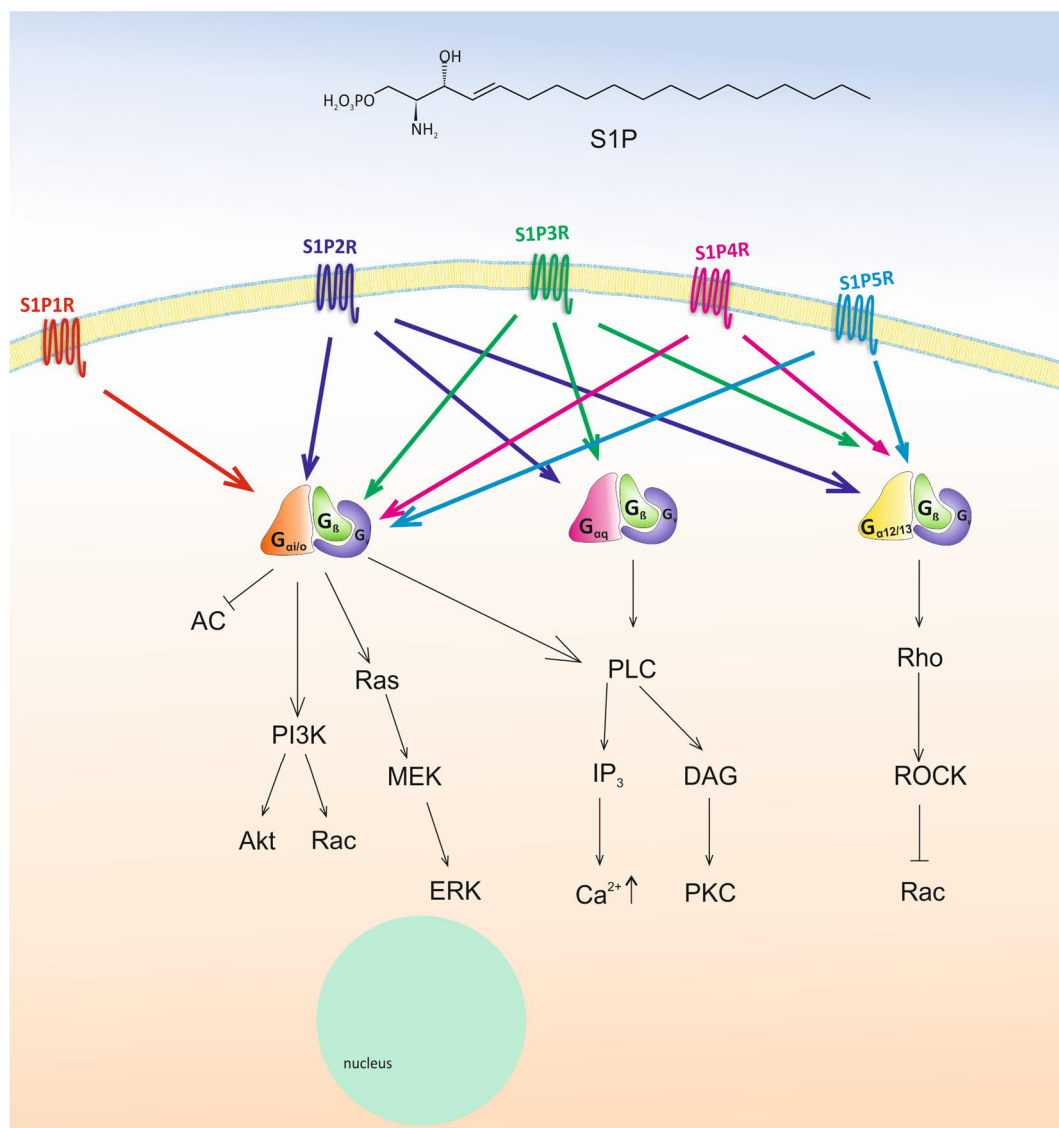
Figure 1.2 Downstream signalling pathways of S1P1-5R.

S1P1R signals through $G_{i/o}$ protein and thereby inhibits adenylyl cyclase (AC), activates PI3K-Akt/Rac, ERK and PLC pathway. S1P2R and S1P3R are both coupled to $G_{i/o}$, G_q and $G_{12/13}$ and activate the PI3K-Akt/Rac and ERK pathway, as well as PLC and Rho/ROCK. S1P4R and S1P5R both couple through $G_{i/o}$ and $G_{12/13}$. S1P4R was shown to inhibit AC and activate ERK pathway, whereas S1P activates AC and PI3K-Akt/Rac over S1P5R. Figure adapted from (Sanchez and Hla 2004; Brinkmann 2007).

The five sphingosine receptors are coupled to a variety of G proteins. Major contributors leading to different G protein associations are the cell types expressing the receptors, as well as the conformational change of the receptors induced by its ligands (Oldham and Hamm 2008; Nygaard et al. 2009). S1P1R is thought to be primarily coupled to $G_{i/o}$ protein, S1P2R and S1P3R to $G_{i/o}$, G_q and $G_{12/13}$, while S1P4R and S1P5R are coupled to $G_{i/o}$ and $G_{12/13}$ (Figure 1.2 and (Blaho and Hla 2014)). How the binding of S1P acts to each of these five receptors and which signalling pathways are activated has been the object of considerable work and the complexity of these interactions is not thoroughly clarified yet. Not least because of the difficulties in studying these interactions in relevant cells of sufficient purity.

S1P1R is thought to primarily signal through the $G_{i/o}$ protein thus leading to a decrease of cyclic adenosine monophosphate (cAMP) levels and an increase of intracellular Ca^{2+}. In addition, it activates the GTPase Ras/mitogen-activated protein kinase kinase (MEK)/extracellular signal-regulated kinase (ERK) pathway as well as Akt through the phosphoinositide 3-kinase (PI3K) pathway (Im et al. 1997; Lee et al. 1998; Okamoto et al. 1998; Zondag et al. 1998; Rakhit et al. 1999; Kim et al. 2000; Igarashi et al. 2001; Morales-Ruiz et al. 2001). In neurons, activation of ERK1/2 *via* the $G_{i/o}$ coupled S1P1R was confirmed by the demonstration of a S1P1R-dependent increase in neurogenesis in the hippocampus (Ye et al. 2016), as well as neuroprotective effects in cortical neurons (Di Menna et al. 2013). However, the S1P-elicited increase of intracellular Ca^{2+} levels is not completely inhibited by the addition of pertussis toxin (PTX), known to specifically ribosylate adenosine diphosphate (ADP) and inhibit $G_{i/o}$, thus suggesting the involvement of other G proteins. Indeed, the addition of specific phospholipase C (PLC) inhibitors completely abolishes the S1P-dependent Ca^{2+} increase (An et al. 1999), suggesting the activation of other receptor subtypes including S1P2R and S1P3R. The involvement of S1P4R can be excluded due to a complete inhibition of PLC activation after PTX addition

(Graler et al. 2003). S1P3R activation is thought to be the most effective pathway leading to increased intracellular Ca^{2+} levels by signalling through the G_q protein which binds and activates PLCβ (Ancellin and Hla 1999; Kon et al. 1999; McCudden et al. 2005). In addition, receptor deletion studies in mouse embryonic fibroblasts (MEFs) suggest that S1P2R is not involved in any PLC activation, as Ca^{2+} signalling is unaffected in $S1p2r^{-/-}$ cells while it is significantly reduced in the $S1p3r^{-/-}$ line (Ishii et al. 2002). This is in line with reduced inositol trisphosphate (IP_3) concentrations observed in $S1p3r^{-/-}$ MEFs by the same research group (Ishii et al. 2001). Activation of PLC not only increases the concentration of IP_3, leading to the release of Ca^{2+} from the endoplasmic reticulum (Putney and Tomita 2012), but also activates protein kinase C-dependent pathways involved in cell migration (Gonda et al. 1999; Gorshkova et al. 2008) and nuclear factor-κB (NF-κB) activation (Siehler et al. 2001). All of these pathways have been shown to involve G_q protein activation by the S1P3R. Importantly, cell migration is also regulated by S1P *via* the Rho family GTPase including Rac which is activated by the $G_{i/o}$ protein. Intriguingly, S1P activates cell migration upon binding of S1P1R and S1P3R, but inhibits it when signalling through S1P2R due to an altered Rac activity and the involvement of phosphatase and tensin homolog (PTEN) (Takuwa et al. 2002; Sanchez et al. 2005). This S1P2R mediated inhibition of Rac is preceded by activation of the Rho/Rho-associated protein kinase (ROCK) pathway through $G_{12/13}$ protein (Sugimoto et al. 2003) and interestingly it has been shown that the $G_{i/o}$ mediated activation of PI3K is still inducing the Akt pathway after S1P2R stimulation (Figure 1.2 and (Okamoto et al. 2000)).

In summary, signal transduction through S1P receptors is highly complex and far from being fully understood. The recent elucidation of the S1P1R crystal structure significantly advanced the field (Hanson et al. 2012), as it now allows the development of specific receptor agonists. The crystal structure also greatly helped to understand how different conformational changes of the receptor influences its signalling behaviour (Hanson et al.

2012) and it is to be expected that the elucidation of the structure of other sphingosine receptors will similarly facilitate the understanding of S1P signalling.

1.2.4   Functions of sphingosine receptors outside the nervous system

S1P receptors are involved in a variety of processes including cell survival, migration and proliferation (Pyne et al. 2016). Additionally, S1P is known to enhance endothelial barrier function by a variety of mechanisms including adherence and tight junction assembly (Wang and Dudek 2009), the deregulation of which may cause various pathologies such as inflammation, fibrosis and cancer (Pitman et al. 2015; Aoki et al. 2016; Gonzalez-Fernandez et al. 2016). S1P1-3R are also expressed ubiquitously outside the nervous system, including the immune and cardiovascular systems. The S1P4R is primarily found in the hematopoietic and lymphatic system while the S1P5R is expressed on endothelial cells (Brinkmann 2007; van Doorn et al. 2012). Studies of the S1P4R revealed that it is involved in immunosuppressive functions and regulates the release of specific cytokines by T cells (Wang et al. 2005). S1P5R on endothelial cells helps sustaining the integrity of the blood brain barrier (BBB) and reducing the ingress of immune cells into the brain (van Doorn et al. 2012). A deletion study of the S1P2R indicated that mice were born with no apparent defects outside the nervous system (MacLennan et al. 2001; Ishii et al. 2002). *S1p3r*$^{-/-}$ mice are viable and failed to reveal any specific phenotype (Ishii et al. 2001). Investigations of the effects of S1P in those mice revealed a role for S1P3R in the regulation of heart rate as S1P induced bradycardia in WT mice but not in mice lacking S1P3R (Forrest et al. 2004; Sanna et al. 2004). This is not surprising given that S1P3R is expressed on mouse ventricular myocytes (Forrest et al. 2004). The combined deletion of S1P2R and S1P3R revealed increased embryonic lethality compared with single receptor deletions (Ishii et al. 2002). By contrast, *S1p1r*$^{-/-}$ mice die at around E12 to E14.5 with early defects in vascular maturation explained by incomplete wrapping of blood vessels with vascular smooth muscle cells, frequently causing lethal intrauterine bleeding (Liu et

al. 2000; Kono et al. 2004). Defects were also observed in the developing brain, including increased cell death in the telencephalon and diencephalon (Liu et al. 2000; Mizugishi et al. 2005). *In situ* hybridisation results indicate that S1P1R is prominently expressed throughout the brain, including the ventricular zone at E14, a highly neurogenic region (McGiffert et al. 2002). Yet the cellular resolution of these experiments and the presence of S1P1R in blood vessels makes it difficult to dissect the molecular mechanisms leading to neuronal cell death during embryogenesis. In the context of human pathology, it is by far the expression of S1P1R by lymphocytes that received most attention (Garris et al. 2014). Indeed, the receptor plays a crucial role in allowing the cells to sense the S1P gradient between the interstitial compartment and the blood or lymph (Arnon et al. 2011). For example, the egress of immature T cells from the thymus is prevented by their low expression of S1P1R (Matloubian et al. 2004). As these cells mature, *S1p1r* mRNA levels increase, allowing them to sense the S1P gradient and to leave the thymus (Matloubian et al. 2004; Lo et al. 2005). Once in the blood, the high S1P concentration induces S1P1R internalisation on T and B cells which favours the interaction with specific chemokines and the subsequent uptake into the lymph node (Cyster and Schwab 2012). There the S1P1R is re-expressed but in case of an immune reaction where the sequestration of the lymphocytes in lymph nodes is needed for effector differentiation, the S1P1R is internalised and transcription of the *S1p1r* gene is only reactivated in effector T cells (Shiow et al. 2006). The crucial role of S1P1R for the egress of lymphocytes into the lymph by sensing the S1P gradient has been elegantly demonstrated in WT mice supplemented with T and B cells lacking S1P1R (Allende et al. 2004; Matloubian et al. 2004). This was supported by the finding that loss of the S1P concentration gradient by inhibition of S1P lyase (Schwab et al. 2005), or lack of both SphK1/2 in endothelial cells also blocked lymphocyte egress from the lymph node. This occurred despite the presence of S1P1R on lymphocytes (Pham et al. 2010). While the roles of the S1P gradient and of

the S1P1R in sensing it, are now well appreciated, the biochemistry of intracellular signalling is less clear. It is believed that S1P1R signalling either overcomes a retention signal induced by a chemokine receptor or that it promotes a trans-endothelial migration process (for review see (Cyster and Schwab 2012)). A similar chemotactic mechanism seems to be used by megakaryocytes as activation of S1P1R triggers the elongation of proplatelet extensions from the megakaryocytes into the sinusoids. The higher concentration of S1P in the blood compared to the bone marrow activates the Rac GTPase in megakaryocytes and thereby directs the formation of proplatelet extensions, eventually leading to the release of platelets into the circulation (Figure 1.3 and (Zhang et al. 2012)).
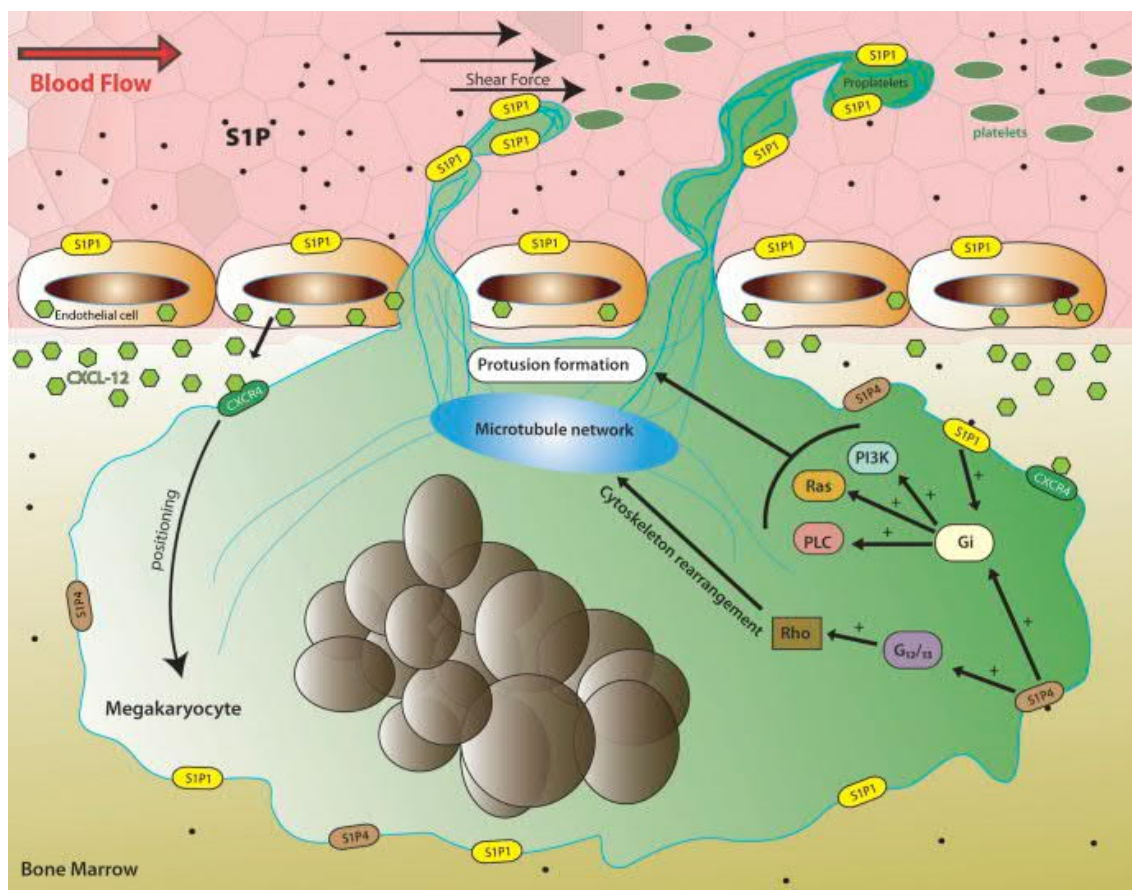
Figure 1.3 S1P1R in megakaryocytes is involved in platelet release into the blood circulation
The high concentration of S1P in the blood generates a gradient which is sensed by the S1P1R (yellow rectangular S1P1) expressed on megakaryocytes and thereby triggers the formation of platelet protrusions, called proplatelets across the endothelium. Megakaryocytes are multinucleated cells when mature as depicted by brown round objects in the figure. Figure taken from (Hla et al. 2012). Reprinted with permission.

1.2.5   Functions of sphingosine receptors in nerve cells

The generation of mice lacking *S1p1r*^{-/-} mice revealed an early essential role for the receptor with statistically significant losses of embryos starting at E13.5 (Liu et al. 2000). Given the high level of expression of the receptors by cells associated with blood vessels, the work largely focuses on the description of the developing vasculature and embryonic haemorrhage leading to the death of embryos (Liu et al. 2000). However, it later became clear that S1P1R, like the lysophosphatidic acid receptor LPA1 is expressed at significant levels next to the developing ventricles, including the lateral ventricles (McGiffert et al. 2002). The expression of both receptors also overlaps in the developing cortex (McGiffert et al. 2002). Massive cell death and a smaller number of mitotic cells were observed in the telencephalon of *S1p1r*^{-/-} mice (Mizugishi et al. 2005). However, it is not entirely clear if these dramatic effects on neurogenesis can be entirely dissociated from those on the developing vasculature eventually leading to the death of the embryos (see above). In the adult mouse brain S1P1R, S1P2R, S1P3R and S1P5R were found to be expressed on neurons, astrocytes, and microglia, while oligodendrocytes express S1P1R, S1P3R and S1P5R (O'Sullivan and Dev 2016). S1P5R is expressed on oligodendrocytes throughout their maturation and transduces distinct effects at different stages, including retraction of processes early on during development, inhibition of oligodendrocyte precursor cell migration and survival of mature oligodendrocytes (Jaillard et al. 2005; Novgorodov et al. 2007). Somewhat unexpectedly, the genetic deletion of the receptor suggested that it may not be essential for myelination (Jaillard et al. 2005). With regard to the possible roles of S1P1Rs in neurons, the germline deletion of S1P2R led to increased excitatory postsynaptic currents and to the development of lethal seizures in mice at about three weeks postnatally (MacLennan et al. 2001), indicative of a role for S1P in regulating neuronal excitability (Okada et al. 2009). Albeit these results were subsequently challenged (Ishii et al. 2002), additional studies supported the notion that S1P may be a

mediator of neuronal excitability (Zhang et al. 2006; Kajimoto et al. 2007). S1P2R was also proposed to be involved in counteracting cell migration as S1P2R antagonists increased migration of neuronal progenitor cells into ischemic brain regions with increased S1P concentrations following the release from microglial cells (Kimura et al. 2008). S1P is further involved in the regulation of cell apoptosis where the balance between the interconvertible lipids ceramide and S1P, also known as "ceramide/S1P rheostat", defines the fate of a cell (Cuvillier et al. 1996). Ceramide can be either synthesised *de novo* from dihydroceramide, recycled from sphingosine over ceramide synthase 1 or is else the result of sphingomyelin hydrolysis (Figure 1.1 and (Kitatani et al. 2008)). While low ceramide concentrations promote neurite outgrowth, neuronal survival and differentiation, high levels of the lipid lead to apoptosis (Czubowicz and Strosznajder 2014). In a human neuroblastoma cell line S1P was shown to counteract the ceramide-induced apoptosis by modulating pro- and anti-apoptotic factors through S1P1R and S1P3R signalling (Czubowicz and Strosznajder 2014). Both receptors were also found to be expressed on astrocytes with increased expression in multiple sclerosis lesions (Van Doorn et al. 2010; Dusaban et al. 2017). Astrocytes are known to induce neuroinflammation and several studies have reported on the role of S1P in this process (Pebay et al. 2001; Sorensen et al. 2003; Kimura et al. 2008; Van Doorn et al. 2010; Choi et al. 2011; Fischer et al. 2011). A recent publication now identified S1P3R as the main receptor activated by S1P. It couples to $G_{12/13}$ and activates RhoA thereby inducing the release of pro-inflammatory cytokines (Dusaban et al. 2017).

Over the last decade researchers showed that signalling of these receptors can be used to treat numerous neurological diseases. There are clinical studies ongoing (O'Sullivan and Dev 2016) for the treatment of amyotrophic lateral sclerosis (Potenza et al. 2016), acute stroke (Hasegawa et al. 2010), Rett syndrome (Deogracias et al. 2012), schizophrenia (Jang et al. 2011; Muhle et al. 2013) and glioblastoma (Zhang et al. 2015).

1.3 FTY720: Origin and Mode of Action

1.3.1 Discovery of FTY720

FTY720 is a sphingosine analogue and following its phosphorylation by endogenous SphK2 it initially acts as a S1P1R agonist. However, FTY720 is considered to act as a functional antagonist of S1P1R due to the realisation that chronic exposure to the drug triggers the internalisation of the receptor (Matloubian et al. 2004). FTY720 was the first oral drug approved for the treatment of relapsing-remitting multiple sclerosis (Figure 1.4 and (Chun and Brinkmann 2011)). Since 2010 it is traded under the name Gilenya® by Novartis and is a derivative of myriocin, a fungal metabolite isolated from Ascomycete *Isaria sinclairii*. *Isaria sinclairii* is the anamorph stage of the fungus *Cordyceps sinclairii* and is classified under the family *Clavicipitaceae* (Adachi et al. 1995; Paterson 2008). In traditional Chinese medicine *Isaria sinclairii* is used as a well-known remedy for the treatment of a range of diseases and claims to be the "elixir leading to eternal youth' (Chun and Brinkmann 2011). Another well-known fungus of the non-monophyletic family *Clavicipitaceae* is *Tolypocladium inflatum,* which is the anamorph stage of *Cordyceps subsessilis* (Sung et al. 2007). It is the source of cyclosporine, one of the most widely used immunosuppressant in transplantation medicine (Chun and Brinkmann 2011).

1.3.2 Mode of action of FTY720 in the immune system

In the context of multiple sclerosis, the primary target of FTY720 is thought to be S1P1R on lymphocytes following its phosphorylation to pFTY720 by the ubiquitously expressed kinase SphK2 (Figure 1.4 and (Zemann et al. 2006)). The drug induces the internalisation of S1P1R, thus preventing the lymphocytes to read S1P gradients and hindering their egress from lymph nodes (Graler and Goetzl 2004; Matloubian et al. 2004). Indeed,

decreased numbers of lymphocytes can readily be detected in the blood of FTY720-treated patients (Brinkmann et al. 2004). While FTY720 was initially developed as an immunosuppressant, clinical studies were discontinued as FTY720 did not show superior effects to other drugs used in the context of the prevention of organ graft rejection (Mansoor and Melendez 2008). Still, FTY720 does compromise the immune response and at present three cases of progressive multifocal leukoencephalopathy have been reported during the course of FTY720 treatment (FDA 2015; D'Amico et al. 2016). The other main side effect is bradycardia due to early agonistic actions of FTY720 (Camm et al. 2014). Studies in rodents explained these effects due to an agonistic action on the S1P3R expressed on heart tissue (Forrest et al. 2004; Sanna et al. 2004). In humans however, S1P3R in contrast to S1P1R, was not found to be expressed at significant levels on myocytes (Mazurais et al. 2002), and treatment in patients with specific S1P1R agonist still induced bradycardia (Gergely et al. 2012; Moberly et al. 2012). During early stages of treatment, FTY720 acts as an agonist at S1P1R on myocytes and leads to the activation of G-protein coupled inwardly rectifying potassium (GIRK) channels and subsequent heart rate reduction (Bünemann et al. 1995; Koyrakh et al. 2005). Prolonged treatment with FTY720 is thought to induce S1P1R internalisation as symptoms of bradycardia typically subside within the first 24 h of treatment (Vargas and Perumal 2013; Camm et al. 2014). This implies that close monitoring of patients treated with FTY720 is mandatory during the initial phase of drug administration (Sanna et al. 2004; Faber et al. 2013).

Sphingosine

S1P
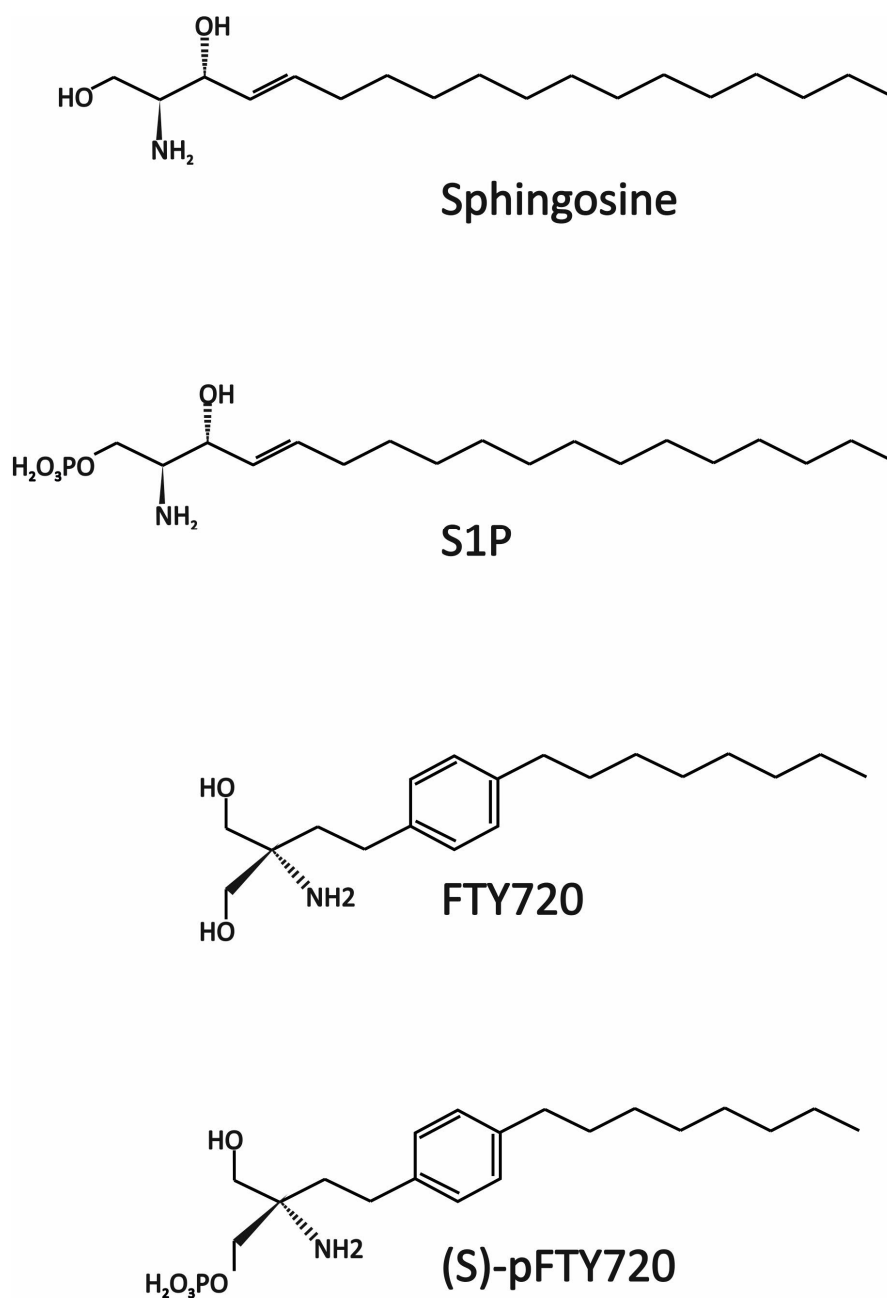
FTY720

(S)-pFTY720

Figure 1.4 FTY720 is a structural analogue of sphingosine

Both, sphingosine and FTY720 consist of an amino alcohol group and a hydrocarbon chain. These structural similarities led to the identification of S1P receptors as the primary target of the biologically active form of FTY720. Sphingosine and FTY720 are phosphorylated by SphK1/2 to S1P or (*S*)-pFTY720, respectively (Chun and Brinkmann, 2011). Chemical synthesis leads to the (*S*)- and (*R*)-enantiomer of pFTY720, but *in vivo* only (*S*)-pFTY720 is found and active (Albert et al. 2005).

1.3.3 Mode of action of FTY720 in the brain

Due to its lipophilicity FTY720 readily enters the brain and accumulates in the white matter (Foster et al. 2007). Given the expression of S1P receptors by most brain cells, including endothelial cells, it is then essential to better understand how FTY720 may act on brain cells, a question that is at the core of this PhD thesis. Previous studies by our laboratory revealed that FTY720 increases BDNF levels in the brain and ameliorates symptoms of a mouse model of Rett syndrome: FTY720 injections into mice lacking *Mecp2,* the gene mutated in most cases of Rett syndrome increases BDNF levels in the brain of mutant animals and markedly improves their locomotor activity (Deogracias et al. 2012). These findings also formed the basis of an exploratory clinical trial with a small number of Rett syndrome patients (Deogracias et al. 2012; Naegelin et al. 2015). Further experiments with primary cortical neurons showed that pFTY720 phosphorylated the calcium-responsive elements (CRE)-binding protein (CREB) through activation of the ERK pathway. In these studies, S1P1R was implicated as the primary target of pFTY720 as other S1P1R agonists elicited similar effects *in vitro* (Deogracias et al. 2012). The neuroprotective activity of FTY720 in the central nervous system (CNS) is further supported by a study demonstrating rapid reversal of neuronal damage in a rat model of multiple sclerosis, namely the experimental autoimmune encephalomyelitis (EAE) (Foster et al. 2009) and importantly, by studies indicating a reduced brain atrophy observed in patients treated with FTY720 in clinical phase III trials (Kappos et al. 2010). While there is little doubt that FTY720 also acts in the CNS in addition to its well-documented activity of T lymphocytes, there is still a great deal of uncertainty as to how the neuroprotective activity of FTY720 can be best explained. In an attempt to explore a possible role of FTY720 in the mouse CNS in the context of EAE, S1P1R flanked by loxP sites was deleted using a Cre driver under the control of a human glial fibrillary acidic protein (*GFAP*) promoter. The outcome of the study was that the excision of the

receptor rendered the animals unresponsive to FTY720 treatment and that S1P1R excision alone reduced astrogliosis and ameliorated symptoms of EAE (Choi et al. 2011). However, the interpretation of the results with regard to the identity of the cells targeted by the *S1p1r* deletion is complicated by the fact that the human *GFAP* promoter used in this study is expressed by most, if not all radial glial cells during development (Malatesta et al. 2003). These cells are now well appreciated to be the progenitors not only of astrocytes but also of major neuronal populations in the developing CNS (Hol et al. 2003; Malatesta et al. 2003). Given the expression of multiple receptors by most cells in the CNS including microglial cells, oligodendrocytes, and astrocytes it is not surprising that a number of different effects of FTY720 have been reported in the brain of rodents. Amongst the most intriguing physiological activities of S1P in the adult brain is the regulation of the proliferation of neural stem cells. S1P receptor expression was identified in stem cells isolated from the subventricular zone and S1P, possibly deriving from the cerebrospinal fluid (CSF), showed to contribute to the quiescence of these adult stem cells (Codega et al. 2014). FTY720 could therefore act as a functional antagonist explaining the increased neurogenesis observed after FTY720 administration, possibly contributing to improved learning and memory, an effect found in these animals (Efstathopoulos et al. 2015; Sun et al. 2016).

Elucidating the question of whether the effects of FTY720 on BDNF increase are receptor mediated is even more crucial as a recent study suggests a non-receptor mediated mode of action. Indeed, FTY720 has been shown to act through the inhibition of histone deacetylases (HDAC). Strikingly, pFTY720 can be generated in the nucleus due to the presence of SphK2 where it acts as a class I HDAC inhibitor on site (Hait et al. 2014). This finding is highly relevant as HDAC inhibition has long been known to increase BDNF levels and to facilitate fear extinction memory (Bredy et al. 2007).

1.3.4 FTY720 and neurodegenerative diseases

A hallmark of neurodegenerative disorders is the loss of neurons either in discrete brain regions such as the substantia nigra in the case of PD or the striatum in Huntington's disease (HD) or else more widespread in the case of AD, the most prevalent neurodegenerative disorder (Yuan and Yankner 2000). In AD, brain atrophy is evident with profound reductions in the volume of the hippocampus and the temporal lobe of the cerebral cortex where the accumulation of amyloid-β peptides is suggested to be the starting point of the neurodegenerative process (Hardy and Higgins 1992; Brunkhorst et al. 2014). Later in the disease, neurofibrillary tangles are also observed and consist of different protein aggregates, namely hyper-phosphorylated tau protein (Hyman et al. 2012). In terms of possible therapies, most attempts have targeted amyloid-β peptides using a variety of humanised monoclonal antibodies whereby thus far this strategy failed to halt the progression of the disease (Canter et al. 2016). Whether or not amyloid-β plaques may be the appropriate target is a question frequently asked in view of the failures of the clinical trials but at the same time human genetics indicate that a link between amyloid precursor protein (APP) and proteolytic enzymes such as presenilin is very strong indeed (Bagyinszky et al. 2014). This link is further strengthened by the observation that three copies of APP as observed in Trisomy 21 have been linked with early development of AD (Prasher et al. 1998). Interestingly, post-mortem analysis of AD brain tissue showed altered metabolism of sphingolipids (van Echten-Deckert and Walter 2012), including increased levels of the neurotoxic metabolite ceramide (Filippov et al. 2012) as well as decreased levels of S1P (see also section 1.2.5 and (Couttas et al. 2014)). The sphingosine analogue FTY720 is not only known to bind the S1P1R (section 1.3.3) but also to inhibit ceramide synthase. Thus, beyond its ability to increase BDNF levels (see below), this inhibitory activity on ceramide synthase is an additional reason to consider FTY720 as a potential treatment option for AD (Berdyshev et al. 2009;

Schiffmann et al. 2012). With regard to animal models of AD, a few studies have begun to explore the potential of FTY720 to act as a neuroprotective agent in AD (Asle-Rousta et al. 2013; Takasugi et al. 2013). In particular, Asle-Rousta and colleagues reported an attenuation of the amyloid-β induced learning and memory impairment in rats as well as protective effects of FTY720 on hippocampal neurons and inhibition of caspase-3 activation. Somewhat surprisingly, FTY720 was also shown to have a direct effect on amyloid-β 40 and amyloid-β 42 production by an unknown S1P1R-independent mechanism (Takasugi et al. 2013). Additionally, FTY720's potential to increase BDNF levels in the brain is increasingly appreciated (Doi et al. 2013; Fukumoto et al. 2014). This is of considerable interest given a recent meta-analysis revealed decreased BDNF levels in the blood of AD patients (Qin et al. 2016) and decreased levels of BDNF transcripts in the pre-frontal cortex of patients in parallel with their cognitive decline (Buchman et al. 2016). In cultures of cortical neurons FTY720 elicited its neuroprotective effect in a BDNF-dependent manner. *Bdnf* mRNA, as well as protein levels were increased after FTY720 exposure and attenuated amyloid-β toxicity (Doi et al. 2013). *In vivo*, FTY720 has been shown to restore decreased BDNF levels proposed to play a major role in the amelioration of amyloid-β induced memory impairment (Fukumoto et al. 2014).

Decreased BDNF levels have also been found in other neurodegenerative disorders including HD (Zuccato and Cattaneo 2007). The loss of striatal and cortical neurons in HD is caused by mutations in the *HUNTINGTIN* (*HTT*) gene, which then encodes for a mutant huntingtin protein. Huntingtin has been suggested to contribute to *BDNF* transcription in cortical neurons (Zuccato et al. 2001) and to facilitate the anterograde transport of BDNF from the cortex to the striatum (Gauthier et al. 2004). Both functions are compromised by mutations in the *HTT* gene leading to BDNF transport at reduced levels from the cortex to the striatum, thus compromising the functions of these neurons

(Ventimiglia et al. 1995). Due to its reported effects on BDNF levels (Deogracias et al. 2012), FTY720 was also tested in mouse models of HD and showed to increase life expectancy of FTY720-treated mice (Di Pardo et al. 2014). The treatment was accompanied by increased BDNF levels in the striatum as well as in the cortex, thus also supporting the notion that newly synthesized BDNF is anterogradely transported from the cortex to the striatum (Di Pardo et al. 2014). Interestingly, lipid metabolism is also disrupted in HD which may contribute to further increase the toxicity of mutated huntingtin (Di Pardo et al. 2012). In line with the beneficial effects of FTY720 injections in HD animal models, Di Pardo et al. also showed that the drug contributed to restore lipid imbalance thus reducing the toxicity of mutated huntingtin (Di Pardo et al. 2014).

PD is a disease characterized by the loss of neurons in the *substantia nigra* and the accumulation of Lewy Bodies consisting in large part of the presynaptic protein α-synuclein as well as ubiquitin (Abeliovich and Gitler 2016). Alpha-synuclein has an apolipoprotein-like structure (Clayton and George 1998) and while its physiological function is poorly understood it is believed to play a role in various cellular functions, ranging from neuroprotective actions to chaperone activities (Emamzadeh 2016). Interestingly, α-synuclein has been identified as an antigen recognized by T cell receptors in PD patients suggesting an autoimmune component in PD (Sulzer et al. 2017). Misfolded α-synuclein forms aggregates that may cause neurotoxicity *via* a number of different mechanisms including disrupted vesicular trafficking (Abeliovich and Gitler 2016). By contrast, the accumulation of ubiquitin may only represent an accompanying pathology resulting from defective protein trafficking (Ciechanover 2005). Lewy Bodies in the pathology of PD are found to be most abundant in neurons of the limbic as well as motor system (Braak and Braak 2000). Association studies have also reported a correlation between polymorphism of the *BDNF* gene and an increased risk of developing PD (Liu et al. 2012). Also, in PD as well as HD, physical exercise, well known to increase

BDNF levels in the CNS of rodents and in the blood of humans (see above) improves clinical symptoms in patients and is used increasingly in the context of HD. Importantly, exercise in mice prevents the decrease of BDNF in a mouse model of PD (Tuon et al. 2014). Interestingly, Lewy Bodies are not just found in the *substantia nigra*, but also in the enteric nervous system causing decreased intestinal motility. Very recently, a mouse model has been developed to replicate this pathology, and long-term treatment with FTY720 increased gut levels of BDNF in these mice, improved gut motility and reduced the aggregation of α-synuclein (Vidal-Martinez et al. 2016).

1.4 BDNF

1.4.1 Neurotrophin family

The neurotrophin family consists of four different members in mammals and include the founding member nerve growth factor (NGF), BDNF, neurotrophin-3 (NT-3) and neurotrophin-4 (NT-4). They interact with Trk receptors, leading to their dimerization and auto-phosphorylation of tyrosine residues (Kaplan et al. 1991; Barbacid 1995). BDNF, the most abundant neurotrophin in the CNS binds and activates the TrkB receptor (Barbacid 1994).

1.4.2 BDNF transcription and translation

In addition to the CNS, BDNF is known to be also expressed in several peripheral tissues, including liver, lung, kidney, stomach, and bladder (Maisonpierre et al. 1990). In rodents, the *Bdnf* gene encodes several transcripts from at least nine different tissue-specific promoters (Figure 1.5 and (Aid et al. 2007). All *Bdnf* mRNA species direct the translation of the same BDNF pre-pro-protein, with the exception of the transcripts including exon I that add eight amino acids to the signal sequence and is believed to enhance the translation efficiency of *Bdnf* (Koppel et al. 2015). Our group recently reported that in human and rat, but not in mouse megakaryocytes, the expression pattern of the *BDNF/Bdnf* transcripts is similar to the one found in neurons. Transcripts I and IV are found in megakaryocytes, both known to be regulated by intracellular calcium levels (Figure 1.6 and 1.7 and (Aid et al. 2007; Chacon-Fernandez et al. 2016). In neurons, calcium entry is activity-induced and regulated by L-voltage-gated calcium channels (L-VGCCs) and *N*-methyl-*D*-aspartic acid (NMDA)-type glutamate receptors (NMDARs). This calcium influx leads to the activation of calcium-responsive elements (CaRE) and thereby regulates the activity-dependent transcription of *Bdnf* promoters (West et al. 2001).
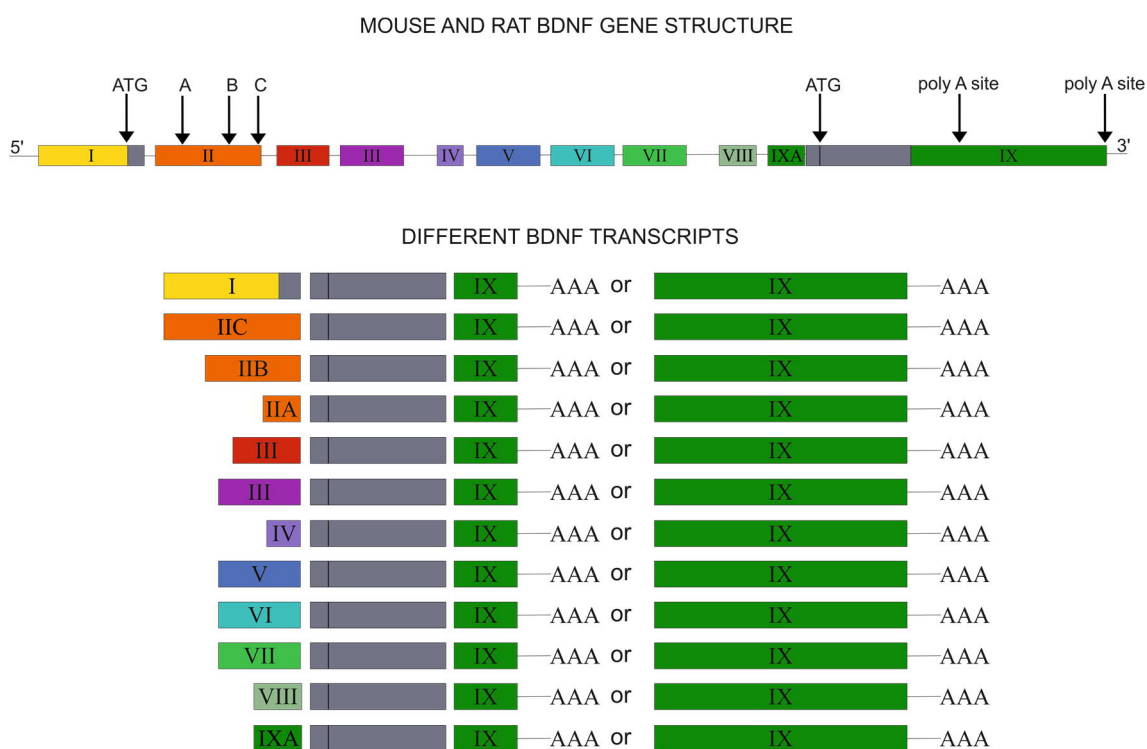
Figure 1.5 Mouse and rat *Bdnf* gene structure

The *Bdnf* gene in the mouse and rat consists of eight exons (I-VIII) on the 5' end and one exon (exon IX) on the 3' end. The protein coding region is depicted in grey, the introns as fine lines and the non-coding regions as coloured boxes. Every 5' end exon can be spliced to exon IX which has two different polyadenylation sites (poly A site). By initiating transcription in the intron before the coding region the IXA transcripts containing a 5' extended coding exon are generated. Additionally, exon II has three different splice-donor sites (arrow A, B and C) and therefore three different transcripts are known for this exon. Figure adapted from Aid et al. 2007 and Zheng et al. 2012.

One of the CaRE binding proteins is CREB which is of special interest as it is rapidly phosphorylated following neuronal activation (Figure 1.6 and 1.7 and (West et al. 2001; Chen et al. 2003; Zheng et al. 2011). CREB phosphorylation as well as activation of the calcium responsive factor (CaRF) is further induced after the activation of the ERK pathway, thereby regulating *Bdnf* transcription and its subsequent translation (Zheng et al. 2012). Interestingly, it has been suggested that dependent on the mediation of calcium influx by either L-VGCC or NMDAR, CaRF acts as an activator or repressor of *Bdnf* exon IV transcription (Figure 1.7 and (Zheng et al. 2011; Lyons et al. 2016)). The primary structure of pre-pro-neurotrophins including BDNF reveal the typical features of secretory proteins and they are thought to be secreted into the endoplasmic reticulum where pro-neurotrophins are N-glycosylated at a consensus sequence localized eight or nine amino acids upstream of the furin-type cleavage site (Leibrock et al. 1989). In the brain, BDNF is thought to be processed into its mature, biologically active form by a recently identified endoprotease designated pro-protein convertase PC7 (Wetsel et al. 2013). The processing of endogenous pro-BDNF is a rapid process presumably assisted by the chaperon function of its propeptide ensuring the correct formation of three disulphide bridges leading to a structure designated "cysteine knot" shared by other secretory proteins including transforming growth factor beta family members and platelet-derived growth factor (McDonald and Hendrickson 1993). Regarding the processing of pro-BDNF, pulse-chase experiments performed with cultured hippocampal neurons revealed that it is rapidly converted into its mature form within the neurons (Matsumoto et al. 2008). Like all neurotrophins, BDNF occurs in solution as a homodimer as demonstrated by biochemical experiments as well as its crystal structure (Radziejewski et al. 1992). Histochemical combined with biochemical studies suggest that the cleaved BDNF pro-peptide is stored pre-synaptically in large dense core vesicles together with mature BDNF (Dieni et al. 2012).
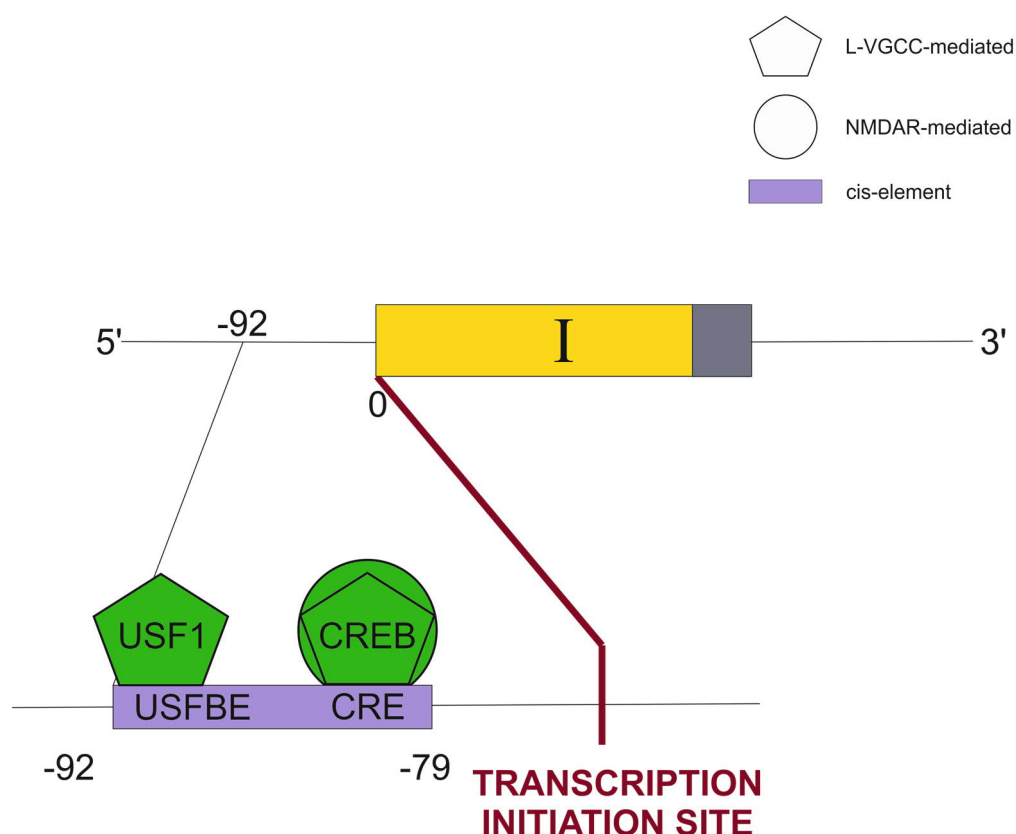
Figure 1.6 Transcription factor regulating *Bdnf* I mRNA transcription by neuronal activity
Exon I and its transcription regulatory sites. Positions of cis-regulatory elements (CRE) are depicted relative to the transcription initiation site (position 0). NMDARs and L-VGCCs mediates transcription of *Bdnf* I mRNA through CREB activation. The upstream stimulatory factor 1 (USF1) and the subsequent binding to its binding element (USFBE) is only mediated through L-VGCC. The continuous box of USFBE and CRE illustrates where their sequences overlap. Figure adapted from Zheng et al. 2012.
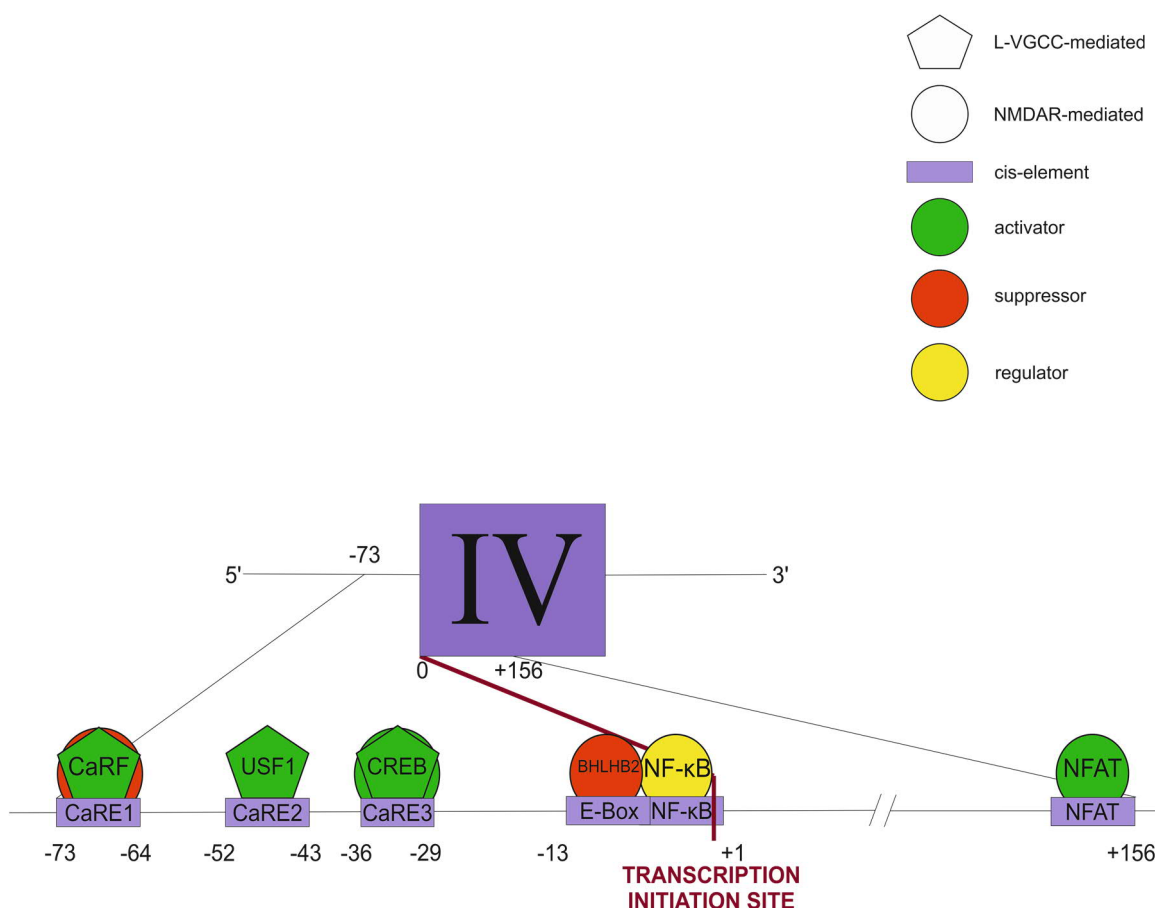
Figure 1.7 Activation of *Bdnf* IV mRNA transcription by neuronal activity in rodents

Exon IV and its transcription regulatory sites. Positions of cis-regulatory elements (CRE) are depicted relative to the transcription initiation site (position 0). Transcription factors are illustrated as pentagons if activated by Ca^{2+} influx through L-VGCC and circles if the activation is NMDAR-dependent. Suppressors are depicted in red, activators in green and positive or negative regulators in yellow. CaRE1-3 are found on the 5' end of the exon IV. CaRF has been shown to act as a repressor or activator of *Bdnf* transcription dependent on its mode of activation (Zheng et al. 2012; Lyons et al. 2016). The cis-elements E-box and NF-κB which regulate a further transcription start, overlap on one base pair. NF-κB is needed for an intact NMDAR response. It is suggested that it plays a role in *Bdnf* transcription, by regulating histone acetylation (Federman et al. 2013), and DNA methylation (Lyons et al. 2016). Also, upregulation of the nuclear factor of activated T cells (NFAT) increases NMDAR-dependent transcription of the exon IV mRNA. Figure adapted from Zheng et al. 2012.

1.4.3 BDNF signalling

Biochemical, physiological as well as histochemical data suggest that BDNF is released from presynaptic terminals (but see (Harward et al. 2016)) to activate TrkB receptors expressed both pre- as well as post-synaptically (Gartner et al. 2006; Dieni et al. 2012). The TrkB receptor is a single transmembrane domain protein and dimerises upon binding of mature BDNF (Chao 2003), phosphorylating tyrosine residues within the intracellular kinase domain and activating downstream pathways, including ERK, PI3K, as well as PLCγ pathway (Reichardt 2006). Presynaptic TrkB activation seems to enhance synaptic transmission by activating the ERK pathway and increasing intracellular Ca^{2+} levels (Xu et al. 2000), while post-synaptic activation of TrkB results in the phosphorylation of voltage-gated potassium and sodium channels (Tucker and Fadool 2002; Ahn et al. 2007), as well as NMDARs (Suen et al. 1997). BDNF thereby induces morphological changes, including increased dendritic arborisation as well as cell body area, changes that are most readily observed in inhibitory neurons (Ventimiglia et al. 1995; Marty et al. 1996; Rauskolb et al. 2010). In neurons of the peripheral nervous system, BDNF is thought to elicit its actions in cell bodies following the retrograde transport of the BDNF/TrkB complex in endosomes (Ito and Enomoto 2016). In the central nervous system, BDNF/TrkB signalling may occur primarily in dendrites following the presynaptic release of BDNF from excitatory nerve terminals (Dieni et al. 2012). Prolonged exposure of the receptor to its ligand BDNF decreased the expression of TrkB at the neuronal cell surface leading to rapid desensitisation reflected by loss of TrkB phosphorylation (Haapasalo et al. 2002). Interestingly, TrkB receptors can also be transactivated by GPCRs such as the adenosine receptor, known to activate downstream pathways by phosphorylating tyrosine residues on TrkB even in the absence of BDNF (Lee and Chao 2001; Lee et al. 2002; Swift et al. 2011). So far, no interaction have been reported between the sphingosine receptors and TrkB, but further investigations are warranted following

the observation that the NGF receptor TrkA is transactivated by the lysophosphatidic acid 1 (LPA1) receptor (Pyne et al. 2007), a receptor which as noted above shares around 30 % of its amino acid sequence with the S1P1R (Zhang et al. 1999). BDNF also binds to a TrkB splice variant designated the truncated TrkB receptor. Its transmembrane, as well as extracellular domain is identical to full-length TrkB, but it lacks the tyrosine kinase residue (Klein et al. 1990). Upon binding of BDNF, truncated TrkB may form a heterodimer with the full-length receptor thus exerting a dominant-negative inhibition by blocking the ERK, PI3K, as well as PLCγ pathways. Additionally, truncated TrkB may act to sequester BDNF to then trigger its internalization and degradation. In addition to its binding to TrkB, BDNF has also long been known to bind to the neurotrophin receptor p75[NTR] (Rodriguez-Tebar et al. 1990). This receptor is a member of the tumour necrosis factor receptor family and often exerts biological effects that counteract those resulting from TrkB activations, including the induction of programmed cell death (Roux et al. 1999; DeFreitas et al. 2001). Interestingly, pro-BDNF when released under pathological conditions seems to bind to p75[NTR] with an affinity that is even higher than that of mature BDNF (Taylor et al. 2012). However, pro-BDNF is not secreted under normal conditions (Dieni et al. 2012), the only reports postulating the contrary were conducted in cells overexpressing the protein, which presumably saturated the pro-BDNF processing capacity (Nagappan et al. 2009; Yang et al. 2009).

1.4.4   Roles of BDNF in the nervous system

BDNF is perhaps best known for promoting the survival of peripheral sensory neuron – indeed its ability to prevent the death of chick dorsal root ganglion neurons was used to monitor its purification from brain tissue (Barde et al. 1982). While later studies revealed that mouse dorsal root ganglion neurons are less responsive to BDNF than their chick counterparts, gene targeting experiments revealed that the absence of BDNF leads to the

loss of various cranial sensory neurons in the mouse (Ernfors et al. 1994). *Bdnf*[/-] mice die shortly after birth as a result of their inability to efficiently compete for milk with their littermates due to lack of balance following the loss of essentially all vestibular neurons (Ernfors et al. 1995). The loss of neurons in nodose and petrosal ganglia most likely also contribute to the early death of the animals following an impaired ability to adequately regulate blood pressure and oxygenation (Jones et al. 1994). While the pro-survival role of BDNF is evident in the peripheral nervous system, this is not the case in the CNS as the generation of a conditional mutation sparing the expression of BDNF in structures essential for the survival of peripheral sensory neurons failed to reveal significant cell losses in the CNS when the analyses were performed 2-month postnatal (Rauskolb et al. 2010). A slight decrease of total brain volume was detected, with the striatum being most affected in terms of size reduction amongst the main brain regions. Random cell filling indicated that striatal neurons are much smaller in BDNF-deprived animals, a reduction of dendritic complexity including branching as well as the number of spines in dendrites. *In vitro* experiments performed with the dissociated embryonic striatum revealed that these neurons show a strong growth response to the addition of BDNF, whereby this was not the case with neurons isolated from the embryonic hippocampus (Rauskolb et al. 2010). Further experiments suggest that in general, the growth promoting effects of BDNF are more marked on inhibitory, GABA-ergic neurons including interneurons in the developing cortex (unpublished results). Long-term more localised BDNF deprivation experiments in the mouse did reveal that the lack of BDNF does eventually lead to neuronal losses. Thus at 12 months the number of striatal neurons in mice carrying a specific BDNF deletion in the cortex is significantly reduced compared to WT mice, which is indicative of a long-term survival role of BDNF on striatal neurons (Baquet et al. 2004). Furthermore, these mice also revealed a phenotype reminiscent of the one seen in a mouse model of HD (Baquet et al. 2004). The importance of BDNF in the CNS

especially during aging is shown by the decreased life expectancy of only 8 months in mice with a deletion of BDNF in the entire CNS (Rauskolb et al. 2010). Additionally, contrasting with the modest morphological effects of BDNF on hippocampal neurons (but see (Harward et al. 2016)), BDNF has long been known to play a crucial role in functional plasticity, including in particular long-term potentiation. In particular, animals lacking even only one copy of *Bdnf* show reduced response in CA1 to high-frequency stimulation of Schaffer collaterals (Korte et al. 1995). While there is general agreement that this is best explained by a pre-synaptic release of BDNF, a recent study on structural plasticity of spines in CA1 suggest that there may be a post-synaptic component as well, resulting from the release of BDNF from spines (Harward et al. 2016). However, some of the key experiments performed by Harward et al. involve over-expression of *Bdnf* constructs targeting the protein to dendrites where it is not present under physiological conditions (Dieni et al. 2012). In addition, the biological activity of *Bdnf* constructs fused with reporters such as GFP remains to be convincingly demonstrated (Matsuda et al. 2009). Irrespective of remaining uncertainties about the sites of release of BDNF, resulting from the difficulties of working with proteins expressed at very low levels, it is known that decreased levels are associated with behavioural deficits in learning and memory (Hall et al. 2000; Heldt et al. 2007). Related to these findings in rodents, the discovery of a nucleotide polymorphism in the *BDNF* gene in humans leading to an amino acid replacement in pro-BDNF (valine for methionine) supports the notion that BDNF is required for episodic memory (Egan et al. 2003). How an amino acid substitution in pro-BDNF may affect its cell biology remains unclear though there have been suggestions that the mutant protein may be released at lower levels (Egan et al., 2003). The so-called Wilms tumour, Aniridia, Genitourinary anomalies, mental Retardation (WAGR) syndrome also illustrates the role of BDNF in humans. This syndrome results from deletions of various lengths on chromosome 11p13. All deletions including the *BDNF*

gene cause cognitive impairments in heterozygotes (Han et al. 2013). In addition, patients with *BDNF* haploinsufficiency have a higher incidence of childhood-onset obesity compared to subjects with an intact *BDNF* gene (Gray et al. 2006; Han et al. 2008). In line with this, animal experiments have revealed a crucial role for BDNF in the control of food intake. BDNF released from the ventro-lateral hypothalamic nucleus is known to have profound anti-orexic effects (Pelleymounter et al. 1995) and animals lacking one *Bdnf* copy show progressive obesity as they age (Kernie et al. 2000).

With regard to diseases of the nervous system and neurodegeneration, BDNF has been implicated in HD following suggestions that the mutant form of huntingtin may either decrease BDNF transcription in cortical neurons and/or interfere with the anterograde transport of the protein to the striatum (Zuccato et al. 2001; Gunawardena et al. 2003; Strand et al. 2007; Liot et al. 2013). In AD, the possible role of BDNF is less clear beyond observations that its serum levels may be decreased in patients and the levels of RNA transcripts decrease in the pre-frontal cortex of individuals affected by the disease (Nagahara et al. 2009; Laske et al. 2011; Qin et al. 2016). Beyond neurodegenerative diseases, depression is one of the most discussed condition where BDNF is thought to play an important role. Not only has been observed that animals lacking BDNF in the CNS show dramatically reduced activity (Rauskolb et al. 2010), but also serum levels of BDNF are decreased in depressed patients (Molendijk et al. 2014). The link between depression and BDNF levels in humans takes its origin with work in rodents that has indicated that BDNF injections into the brain exerts antidepressant effects followed by a series of experiments indicating that blocking the activity of BDNF or reducing its activity increases depressive symptoms in animal models (Lindholm and Castrén 2014). Interestingly, antagonising BDNF's effects has been suggested to block the actions of drugs typically used to treat depression, themselves shown to increase *Bdnf* transcription (Saarelainen et al. 2003). Importantly, BDNF has clear effects in supporting neurogenesis

in the adult brain and this is significant given reported anti-depressive effects of physical exercise and numerous reports indicating that exercise increases neurogenesis and BDNF levels in the brain (van Praag et al. 1999; Scharfman et al. 2005; Ernst et al. 2006; Erickson et al. 2012; Szuhany et al. 2015). Indeed, the generation of new neurons has been proposed to be a major component of the mode of action of antidepressants (Santarelli et al. 2003). Regarding animal models of diseases affecting the function of the developing nervous system, one of the best documented genetic link is with Rett syndrome, a progressive neurodevelopmental disorder caused by a mutation in the *MeCP2* gene (Amir et al. 1999). Not only do *Mecp2* mutant animals have reduced BDNF levels in several brain areas (Chang et al. 2006; Deogracias et al. 2012), but also the severity of the disease has been shown to be a function of BDNF levels. Thus, increasing BDNF levels by overexpressing it in the forebrain retards the development of symptoms in animals lacking MeCP2 (Chang et al., 2006). These results encouraged our laboratory to inject FTY720 into animals lacking *Mecp2* following the realisation that this drug increases BDNF levels (Deogracias et al. 2012). It turned out that FTY720 injections not only increase BDNF levels in animals lacking *Mecp2* but also that the drug markedly improves the locomotor symptoms of mutant animals and counteracts the effects of the *Mecp2* deletion on structures such as the striatum (Deogracias et al. 2012). These results are the foundation of the present work as major questions regarding the mode of action of FTY720 in the brain remain unresolved.

1.5   Aims and Hypothesis

The main goal of this PhD project was to understand the mechanisms of action of FTY720 on neurons. The key hypothesis was that FTY720 acts through the S1P1R. Accordingly, a major aim was to establish a system allowing to test the hypothesis using a previously

published protocol which allows the generation of excitatory, BDNF-expressing neurons from either wild-type or *S1p1r*$^{-/-}$ ES cells. The following aims were formulated:

1. Generation and characterisation of *S1p1r*$^{-/-}$ ES cell-derived neurons

2. Investigation of the effects of FTY720 on BDNF levels in WT and *S1p1r*$^{-/-}$ ES cell-derived neurons *in vitro*

3. Delineating the pathways activated by FTY720 in WT and *S1p1r*$^{-/-}$ ES cell-derived neurons *in vitro*

4. Validate the *in vitro* findings *in vivo* with WT and conditional *S1p1r*$^{-/-}$ mice

Chapter 2

Materials and Methods

2.1 Animal Husbandry

Mice were kept and handled according to the Animal Scientific Procedures Act (ASPA, Home Office 1986). They were held under a 10/14 h light cycle and received food and water *ad libitum*. Mice were weaned at four weeks and up to five mice were kept per cage.

2.2 Generation of the Mouse Line S*1p1r*$^{loxP/loxP}$/*Cre^{ERT2}*

A mouse line carrying the *S1p1r* gene, where exon 2 of the *S1p1r* gene is flanked by two loxP sites (B6.129S6(FVB)-S1pr1tm2.1Rlp/J), was obtained from Jackson Laboratory (Bar Harbor, ME, USA). This allows the removal of S1P1R conditionally (Figure 2.1A and 3.1). These mice were maintained on a C57BL/6J background (Jackson Laboratory).

In order to generate a line, where the *S1p1r* gene can be conditionally removed in neurons only, the mouse line mentioned above was crossed with the STOCK Tg(*Thy-1- Cre^{ERT2}, -EYFP*)HGfng/PyngJ mouse line (Jackson Laboratories) and maintained on a mixed CD1;C57BL/6J background (Jackson Laboratory). This line expresses a construct containing two copies of an altered mouse *Thy-1* promoter preceding either the transgene for the expression of the Cre^{ERT2} recombinase or the enhanced yellow fluorescent protein (EYFP) (Figure 2.1B). Both copies of the *Thy-1* promoter are needed to allow the expression of Cre^{ERT2} recombinase and EYFP in the same neuron, as one copy drives the expression of *Cre^{ERT2}* fusion gene, while the other drives the expression of the *EYFP* sequence (Young et al. 2008). In the CNS, *Thy-1* is only expressed by neurons. No

expression can be detected in oligodendrocytes, astrocytes, or non-neuronal cells (Gordon et al. 1987; Kollias et al. 1987). The Cre^{ERT2} stands for a Cre recombinase fused to a triple mutation of the human estrogen receptor ligand binding domain. This inhibits the binding of the endogenous estrogen to the receptor, but allows binding of 4-hydroxytamoxifen (4-OHT), the metabolite of tamoxifen. After binding of 4-OHT the Cre recombinase will be transported from the cytoplasm into the nucleus, where it will excise the genes flanked by two loxP sites (Figure 3.1). This mouse line is also widely known under the name of "single-neuron labelling inducible Cre-mediated knockout", short SLICK. There are a variety of different mouse lines, referred to as SLICK-3, -A, -H, -I, -P, -V and –X. Characteristic for these lines is the expression of the transgene in limited number of neurons within certain neuronal populations. For example, the SLICK-V line mainly expresses the transgene in hippocampal dentate granule cells. However, this is not the case for the SLICK-H line, where a widespread neuronal expression of transgenes can be found (Young et al. 2008). This is desirable for this project, as a general deletion of S1P1R is required. Therefore, the generation of the new mouse lines was undertaken using the SLICK-H mouse model.

The newly created lines (designated as *S1p1r*$^{loxP/loxP}$/*Cre*^{ERT2}) were bred until a line carrying the *Cre*^{ERT2} gene and being homozygous for the floxed *S1p1r* gene was established. Due to the random insertion of the *Thy-1/Cre*^{ERT2} construct, it was not possible to determine whether the mouse carried two copies or just one copy of the construct.

A

B
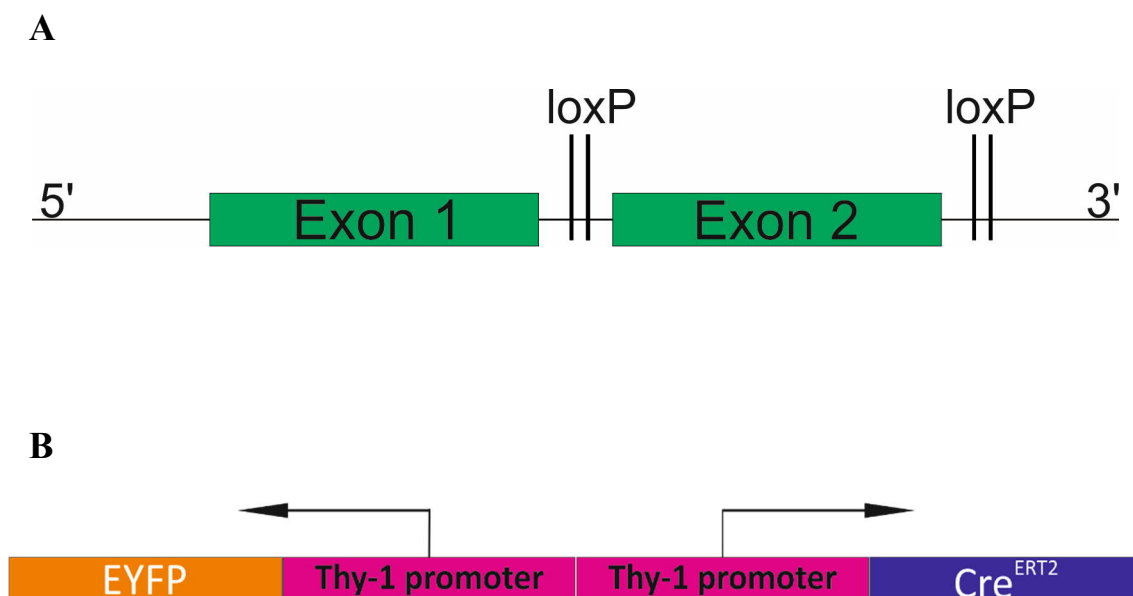
Figure 2.1 Floxed *S1p1r* gene and construct for neuron-specific Cre[ERT2] expression

A Exon 2 of the *S1p1r* gene is flanked by two loxP sites allowing the conditional deletion of S1P1R as exon 2 contains the entire coding region of *S1p1r*. **B** This construct was used by Young and colleagues to generate the SLICK-H mouse line. The two copies of the *Thy-1* promoter allow a comparable expression of EYFP and Cre[ERT2] in the same cell and therefore enables the detection of Cre[ERT2] positive neurons using fluorescence. Figure adapted from (Young et al. 2008).

2.3 Genotyping of Animals and ES Cells

2.3.1 DNA extraction

To genotype the animals, ear notches were obtained and processed on the same day. To genotype ES cells, the cells were trypsinised and centrifuged, and the pellet either processed immediately or stored at -20°C. For both animals and ES cells, the tissue/pellet was resuspended in 500 µl deoxyribonucleic acid (DNA) extraction buffer (10 mM Tris-HCL pH 8.0, 1 mM $CaCl_2$, 100 mM NaCl, 0.5 % sodiumdodecylsulphate (SDS)) containing 0.5 µg/µl proteinase K. Proteinase K stock was prepared as a 20 mg/ml stock solution in 50 mM Tris-HCL pH 8.0, 10 mM $CaCl_2$ and 40 % glycerol. After incubation overnight on a shaker at 50°C at 300 rpm, 500 µl phenol-chloroform-isoamyl alcohol was added and the mixture vortexed thoroughly for 30 sec and incubated on ice for 15 min. Samples were centrifuged at 4°C at full speed for 30 min to separate the two phases. The upper phase was collected and mixed with the same volume of isopropanol and 0.1 % sodium acetate 3 M. Samples were incubated at -20°C for 1 h and centrifuged thereafter at full speed and 4°C for 15 min. The supernatant was removed and the pellet washed with 70 % ethanol by further centrifugation. The dry pellet was resuspended in 30 µl ultrapure water and the DNA concentration was quantified using a BioSpectrometer® (Eppendorf).

2.3.2 Polymerase Chain Reaction

For the polymerase chain reaction (PCR) of amplicons below 1000 bp the following mix was prepared (2.5 µl Standard Taq Buffer (New England Biolab) + 0.5 µl 10 mM of deoxynucleotide (dNTP) mix (Promega) + 0.5 µl primer sense 10 µM (Table 2.1) + 0.5 µl primer antisense 10 µM (Table 2.1) + 0.12 µl Taq polymerase 5000 U/ml (cat.no. M0273S, New England Biolab) + 100 ng cDNA + H_2O *ad* 25 µl). For the long-range PCR which was used to amplify PCR products above 1000 bp the following SequalPrep™

Long Range PCR kit (Thermo Fisher Scientific) was used (2 μl Buffer + 2 μl Enhancer A + 0.4 μl DMSO + 1 μl primer sense 10 μM + 1 μl primer antisense 10 μM (Table 2.1) + 0.36 μl Long polymerase + 100 ng cDNA + H_2O *ad* 20 μl). If an internal control was required additional primers were added to the same mixture as the probe analysed. Internal control genes were used when no PCR product was expected, so that the amplification of the internal control gene would confirm that the lack of product was due to no template being present and not simply due to an inhibition or failure of the PCR reaction. PCR inhibition can occur because of several reasons including for example contamination by organic substances (Schrader et al. 2012). The PCR was performed using the BIORAD T100 Thermal Cycler with the corresponding programme (Table 2.1). The first step of the programme is used for the initial denaturation of the genomic DNA, followed by the indicated cycles of step two to step four. Step two allows yet again the separation of the two DNA strands after every synthesis. In step three the primers anneal to the DNA and the temperature which is chosen in this step is primer-dependent. Finally, during step four, which is typically at 72°C, the product between the two primers is synthesised (Table 2.1). After the amplification process the PCR mixture was loaded onto a 1.5 % (for detection of *Thy-1/Cre^{ERT2}*, *-EYFP,* exon 2 and sex determination) or 3 % (for detection of *S1p1r$^{loxP/loxP}$*) agarose gel for electrophoresis and visualised by ethidium bromide.

2.3.3 Genotyping of Thy-1/Cre^{ERT2}, -EYFP transgene

If the mice/cells were carrying the *Thy-1/Cre^{ERT2}*, *-EYFP* transgene a band at 300 bp was detected (The Jackson Laboratory). At the same time a reaction for the internal control was run. This reaction detected a band at 200 bp for the *T-cell receptor delta constant* (*Trdc-C*) gene (Figure 2.2 and Table 2.1). If the transgene was absent, only a band for the internal control was detected.

A

B
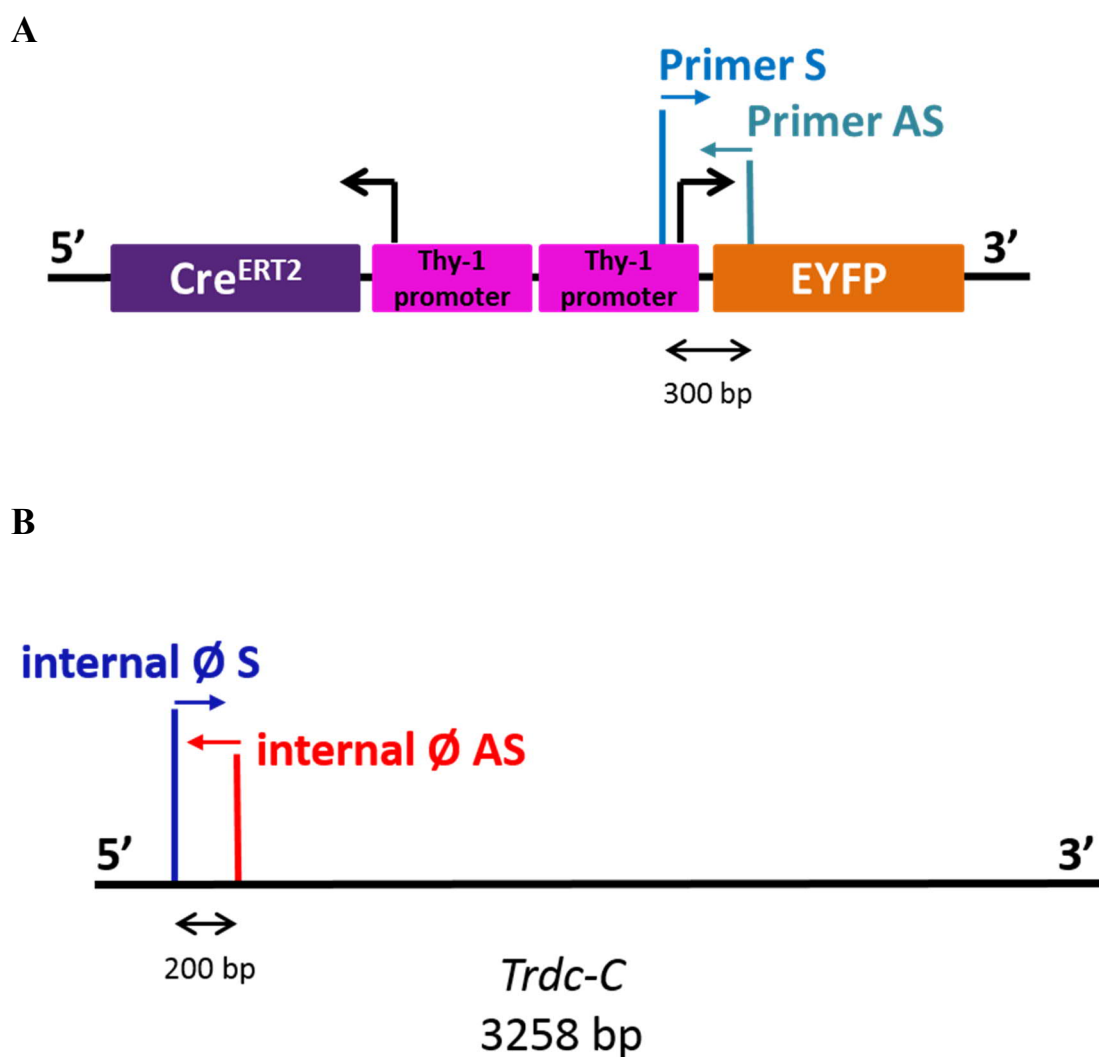
Figure 2.2 Primer binding sites to *Thy-1/Cre^ERT2* transgene and internal control *Trdc-C*

A The sense primer is located in the *Thy-1* promoter and is paired with the antisense primer having its binding site in the *EYFP* gene. The expected size of the PCR product is 300 bp. **B** The *Trdc-C* internal control gene was detected with the two primers depicted in the figure. The PCR using these primers generated a product of 200 bp.

2.3.4   Genotyping of S1p1r$^{loxP/loxP}$ transgene

To detect the loxP site on the 5' end of exon 2 of the *S1p1r$^{loxP/loxP}$* transgene the primer pair #1 and #2 was used (Figure 2.3). This primer pair amplified a PCR product of 216 bp if the loxP site was not present (WT cells/mice) and 250 bp in the mutant cells/mice carrying the loxP site. Therefore, in the case of a homozygous cell/mouse line only the product of the mutant allele was detected at 250 bp (Figure 2.3).

To confirm the excision of exon 2 in *S1p1r$^{loxP/loxP}$* cell lines the primer pair #1 and #3 was used (Figure 2.3). The PCR reaction using these primers led to a specific product of 200 bp when exon 2 was excised. For this reaction, an internal control primer pair was used, detecting a sequence of 275 bp in the *Rosa26* locus (Figure 2.5). To confirm the excision a further primer pair #1 and #5 was used. The binding site of primer #5 is located on the 5' end of exon 2. In the event of no excision, a product of 1462 bp was amplified in WT mice/cells which was 34 bp longer in the mutant *S1p1r$^{loxP/loxP}$* mice/cells due to the loxP site at the 5' end of exon 2 (Figure 2.3). After a successful excision of exon 2 no product was amplified by the primer pair #1 and #5 as primer #5 lost its binding site and the primer pair used for the internal control gene *Trdc-C* led to a product of 200 bp (Figure 2.3).

2.3.5   Genotyping for the X and Y chromosome gene Jarid1d

A primer pair detecting a sequence in the *Jarid1d* gene was used to determine the sex of the ES cells isolated (Clapcote and Roder 2005). The PCR product detected on the X chromosome was 331 bp long, which is longer than the 302 bp amplicon detected on the Y chromosome (Figure 2.4).
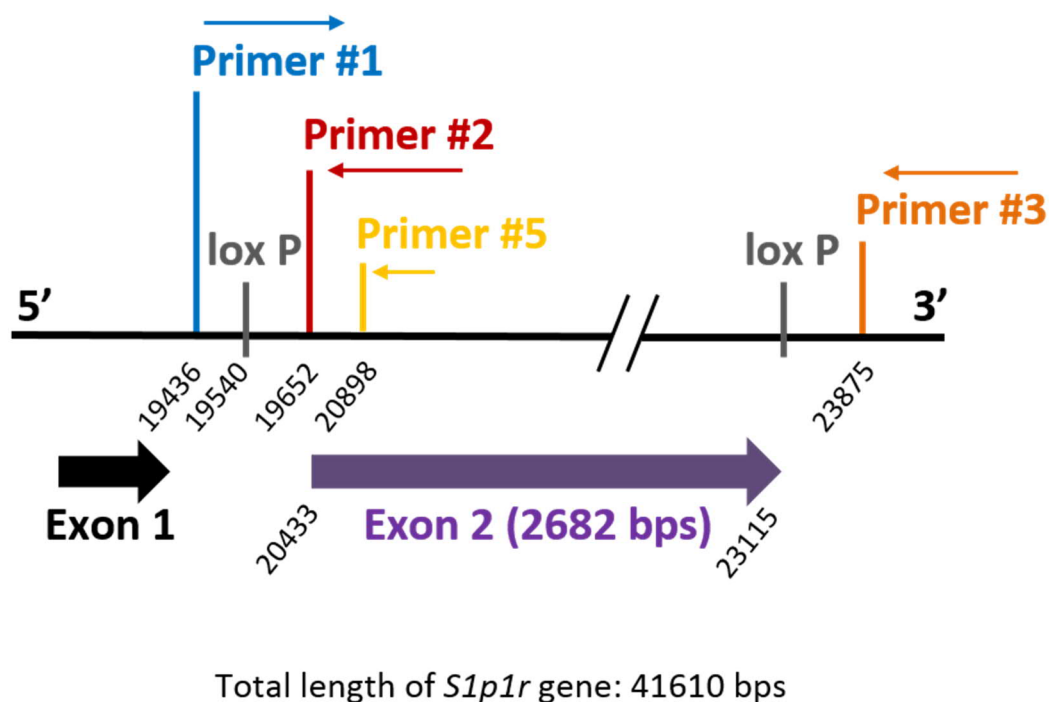
Figure 2.3 Illustration of the primer sites in the *S1p1r^(loxP/loxP)* gene

Primer #1 and #2 were used to detect the loxP site at the 5' end of exon 2. In WT mice, the generated PCR product was 216 bp and due to the loxP site the product was expected at 250 bp in mutant mice.

The primer pair #1 and #3 was used to detect the excision of exon 2. An amplicon of 200 bp was detected in the event of a successful excision.

Primer #5 was designed to detect exon 2. The primer was combined with primer #1 to amplify a PCR product of 1462 bp in WT mice and 1496 bp in mutant cell lines still carrying exon 2.
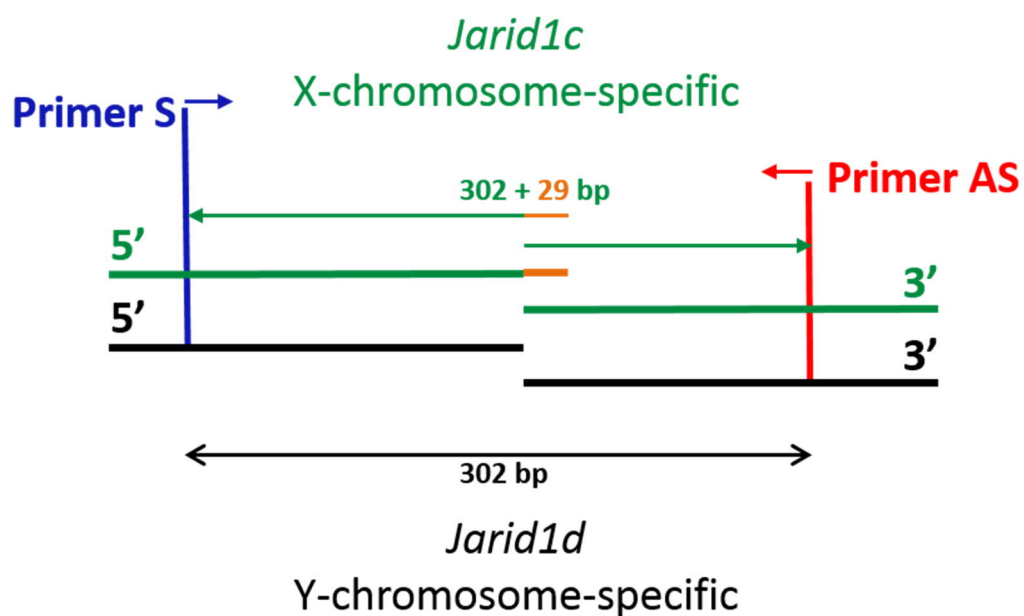
Figure 2.4 Sex determination by PCR

The *Jarid1d* gene was used to determine the sex of the ES cells isolated. The intron between exon 9 and exon 10 of the *Jarid1d* gene is 29 bp longer (depicted in orange) on the X chromosome compared to the Y chromosome. This allows for the generation of a 302 bp long product in male ES cells (depicted in black) and 331 bp product in female ES cells (depicted in green). Figure adapted from (Clapcote and Roder 2005).

Table 2.1 Primers to genotype *S1p1r*^{loxP/loxP}/*Cre*^{ERT2} mouse line and ES cells

S stands for sense; AS stands for antisense; Ø stands for control

Transgene	Sequence 5' to 3'	Programme
Thy-1-Cre^ERT2^, -EYFP		1. 94°C 3min
		2. 94°C 30sec
Primer S	TCTGAGTGGCAAAGGACCTTAGG	3. 60°C 1min
Primer AS	CGCTGAACTTGTGGCCGTTTACG	4. 72°C 1min
Internal Ø *Trdc-C* S	CAAATGTTGCTTGTCTGGTG	5. go to step 2 34x
Internal Ø *Trdc-C* AS	GTCAGTCGAGTGCACAGTTT	6. 72°C 2min
		7. 4°C ∞
loxP site at 5' end of *S1p1r*		1. 94°C 3min
		2. 94°C 30sec
		3. 55°C 30sec
Primer # 1 S	GAGCGGAGGAAGTTAAAAGTG	4. 72°C 30sec
		5. go to step 2 34x
Primer # 2 AS	CCTCCTAAGAGATTGCAGCAA	6. 72°C 2min
		7. 4°C ∞
Detection of exon 2 excision of *S1p1r*		1. 94°C 3min
		2. 94°C 30sec
		3. 60°C 30sec
Primer #3 AS	GATCCTAAGGCAATGTCCTAGAATGGGACA	4. 72°C 15sec
Internal Ø *Rosa26* S	AAGGGAGCTGCAGTGGAGTA	5. go to step 2 34x
Internal Ø *Rosa26* AS	GTCCCTCCAATTTTACACC	6. 72°C 2min
		7. 4°C ∞
Detection of exon 2 excision of *S1p1r*		1. 94°C 3min
		2. 94°C 30sec
		3. 61°C 30sec
Primer #5 AS	TAAGCCACGCCTGCTAATAGGTC	4. 72°C 90sec
Internal Ø *Trdc-C* S	CAAATGTTGCTTGTCTGGTG	5. go to step 2 34x
Internal Ø *Trdc-C* AS	GTCAGTCGAGTGCACAGTTT	6. 72°C 5min
		7. 4°C ∞
Sex determination		1. 94°C 5min
		2. 94°C 30sec
Primer S	CTGAAGCTTTTGGCTTTGAG	3. 54°C 1min
		4. 72°C 40sec
Primer AS	CCACTGCCAAATTCTTTGG	5. go to step 2 39x
		6. 72°C 5min
		7. 4°C ∞
Rosa26/Cre^ERT2^		1. 94°C 5min
Rosa26 S	AAGGGAGCTGCAGTGGAGTA	2. 94°C 30sec
Rosa26 AS	GTCCCTCCAATTTTACACC	3. 55°C 30sec
*Cre^ERT2^* S	GGTTATGCGGCGGATCCGAAAAGAAA	4. 72°C 30sec
*Cre^ERT2^* AS	ACCCGGCAAAACAGGTAGTTATTCGGATCA	5. go to step 2 34x
		6. 72°C 5min
		7. 4°C ∞

2.4 Isolation of Mouse ES Cells from $S1p1r^{\text{loxP/loxP}}/Cre^{ERT2}$ Mice

A day before the mating took place, $S1p1r^{\text{loxP/loxP}}/Cre^{ERT2}$ female mice were exposed to male's pheromones by putting them in contact with male bedding material. This procedure induces the natural oestrous cycle in females and no injections with the hormone gonadotropin are needed.

The next day male and female mice were crossed overnight. Females carrying a plug were sacrificed after two days and the oviducts were dissected and flushed using a mouth pipette. Obtained embryos were cultured in 35 mm dishes containing different drops of KSOM medium (cat.no. MR-020P-5D, Millipore) with 1 μM of the MEK inhibitor PD0325901 (cat.no. 1408-B5, Axon Medchem) and 3 μM of the GSK3 inhibitor Chir99021 (cat.no. 1386-B8, Axon Medchem). About four embryos were placed in each drop. Drops were covered with mineral oil to avoid evaporation and were incubated at 37°C and a concentration of 7 % CO_2.

After two days, the embryos were transferred into drops of N2B27 + 2i + LIF medium (1 part Neurobasal + 1 part DMEM/F12 + 0.5% N2 supplement + 1% B27 supplement without retinoic acid + 1% L-GlutaMAX™ + 50μM β-mercaptoethanol + 1μM PD0325901+ 3μM Chir99021, and 100 Units/ml leukemia inhibitory factor (LIF) (~100 ng/ml LIF, cat.no. ESG1106, Millipore)) by using the mouth pipette, and after covering with mineral oil incubated at 37°C and 7% CO_2.

As soon as the embryos hatched by themselves (usually one or two days) the inner cell mass was separated from the trophoblastic cells by following a previously described protocol with few modifications (Solter and Knowles 1975; Batlle-Morera et al. 2008). Embryos were placed into a drop of N2B27 containing 20% of rabbit anti-mouse serum antibody (cat.no. M5774, Sigma) for 1 h. In case they did not hatch, they were placed for

1-2 sec into a drop of acid tyrode solution, which removes the zona pellucida, followed by two washing steps in phosphate buffered saline (PBS) and further anti-mouse serum treatment.

Embryos were then subsequently transferred for 10 min to a drop of N2B27 containing 20 % of rat serum (produced in-house) as a source of the complement system, and after that they were incubated for 1 h in a drop of fresh N2B27 for recovery. The treatment with anti-mouse serum antibodies and subsequent rat serum is used to induce apoptosis of the outer trophoblastic cell mass and to keep the cells of the inner cell mass alive at the same time. This is enabled by the fact that the anti-mouse antibodies cannot reach the inner cell mass due to a lack of penetration. The rat serum provides the complement system to enhance the apoptotic process of anti-mouse antibody bearing cells. This procedure facilitates the isolation of the inner cell mass without the need for microsurgical procedures (Solter and Knowles 1975). During this time a 96-well plate was coated with 0.2 % gelatine. After 1 h incubation, it was possible to easily remove the trophectoderm mechanically and each isolated epiblast was placed into a separate well of the gelatine-coated 96-well plate with N2B27+2i+LIF medium.

The plate was incubated at 37°C and 7 % CO_2 until colonies could be detected. At that time the medium was changed every second day. As soon as the colonies were visible they were trypsinised with 200 µl of 0.05 % trypsin for 5 min at 37°C. Trypsin treatment was stopped by diluting it with N2B27+2i+LIF medium containing 10 % serum. Resuspended cells were transferred into a gelatine-coated 24-well plate, containing N2B27+2i+LIF and incubated for 2 h. As soon as the cells settled down, the medium was replaced by N2B27+2i+LIF without any serum. From a 24-well plate, the cells were subsequently passaged when they reached 80-90 % confluency. For these passages, the cells were centrifuged after trypsinisation to get rid of the serum used for stopping the

trypsin action. The ES cells were tested for mycoplasma using the 'LookOut®' Mycoplasma PCR Detection Kit' from Sigma (cat.no. MP0035) by following the manufacturer's instruction. Subsequently, the cells were frozen at -80°C in N2B27 containing 10 % fetal bovine serum (FBS) and 10 % DMSO.

During the expansion of the ES cells, DNA was extracted from the different clones as indicated before and genotyped to determine the sex (section 2.3.5). The PCR primers and protocol used are indicated in Table 2.1 and Figure 2.4.

2.5   ES Cell Lines used in the Study

2.5.1 J1 ES cell line

The WT J1 ES cell line (kindly provided from the Biozentrum, University of Basel, Switzerland), was first described by the Jaenisch group in 1992 (Li et al. 1992) and has been derived from a male agouti 129S4/SvJae (Stevens 1973; Simpson et al. 1997).

2.5.2 Rosa26/Cre^{ERT2} cell line

The *Rosa26-Cre^{ERT2}* mouse ES cell line (kindly provided by the research group of Meng Li) was generated by targeted homologous recombination. E14Tg2a ES cells were targeted with a vector containing 1 kb 5' arm, a 4.3 kb loxP-puro-loxP-Cre^{ERT2}-polyA cassette and a 4 kb 3' arm (Figure 2.5). Subsequently the Puro selection cassette (not shown in Figure 2.5) was removed by transient transfection with a Cre expression construct. The targeting event was screened by Southern Blot with external probes (not shown). Genotype is verified by PCR using primers which are depicted by green arrows for *Rosa26* and red arrows for *Cre^{ERT2}* transgene (Table 2.1). Sal 1 represents the location of the sequence recognised by the Sal 1 restriction enzyme (Dr. Xinsheng Nan, personal communication).
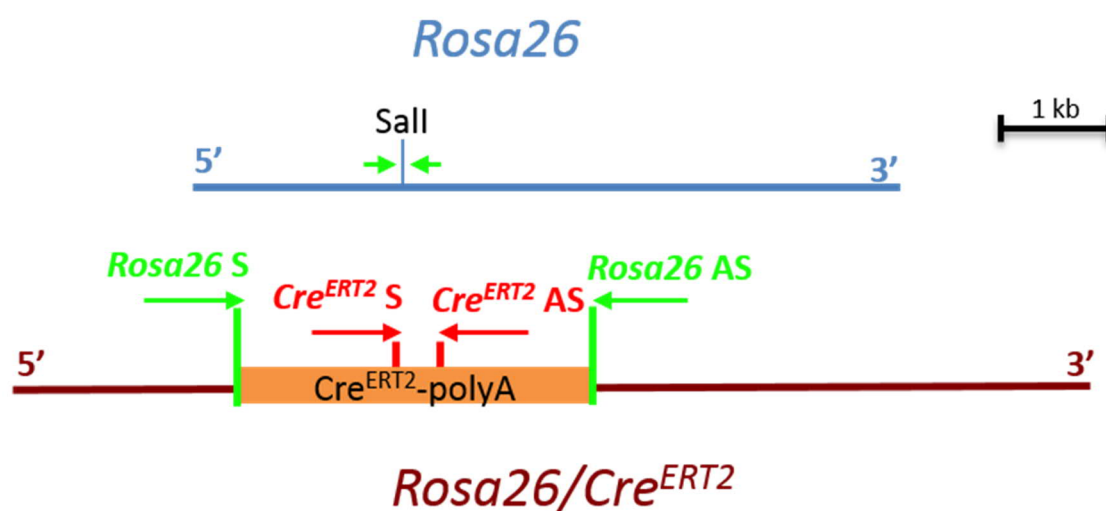
Figure 2.5 *Rosa26/Cre^{ERT2}* cell line

Figure shows map of the *Rosa26/Cre^{ERT2}* cell line which was provided by the research group of Meng Li. Green arrows depict the location of the primers used to detect a 275 bp long amplicon on the WT Rosa26 locus. The primers used for the detection of the *Cre^{ERT2}* transgene are shown in red and amplify a 381 bp long PCR product. Figure adapted from Dr. Xinsheng Nan, unpublished.

2.6 Isolation of Mouse Embryonic Fibroblasts

A pregnant WT female mouse was culled 14 days' *post coitum*. Embryos were harvested and kept on ice in 1 x Hank's Balanced Salt Solution (HBSS). Using dissection tools the internal organs of the embryos were removed. The embryos' cadavers were rinsed with HBSS and trypsinised with 400 µl of 10 mg/ml trypsin (Worthington Biochem) in 3.6 ml 1 x HBSS (to reach an end concentration of 1 mg/ml trypsin) in a water bath of 37°C for 20 min. The tube was vortexed every 5 min during this step. The trypsinisation was stopped by adding 1 mg/ml soybean trypsin inhibitor (Sigma) in 1 x HBSS. Suspension was pipetted up and down with 1000 µl pipette, while DNAse (Roche) at a final concentration of 0.05 mg/ml was added to the mixture. Tissue was left to settle down and supernatant was passed through a 40 µm strainer (BD Falcon) before centrifugation at 1200 rpm for 10 min. Pellet was resuspended in cellular aggregates (CA) medium (Dulbecco's Modified Eagle Medium (DMEM) + 10 % FBS + 1 % L-GlutaMAX™ + 1 % non-essential amino acids (NEAA) + 0.00001 % ß-mercaptoethanol). MEFs were counted using a NucleoCounter® NC-100™ (Chemometec) and $1x10^6$ cells were cultured on a 100 mm diameter Petri dish coated with 0.2 % gelatine (Sigma). As soon as the cells reached confluency they were passaged again. Before storage in liquid nitrogen in CA medium + 10 % DMSO, the cells were tested for mycoplasma using the 'LookOut® Mycoplasma PCR Detection Kit' from Sigma (cat.no. MP0035) by following the manufacturer's instruction.

2.7 MEF and ES Cell Culture

The MEFs were cultured on 60 mm Ø dish (Nunc) until they reached confluency. Subsequently, the proliferation of MEFs was inhibited by 10 µg/ml Mitomycin C (Sigma) in CA medium for 2 h. The medium was then removed and the MEFs were washed twice

with PBS. CA medium was added and the cells were left in the incubator for at least 1 h before the ES cells could be cultured on them. ES cells were cultured in ES cell medium (DMEM + 15 % FBS + 1 % GlutaMAX™ + 1 % NEAA + 100 Units/ml leukemia inhibitory factor (LIF) (~100 ng/ml LIF) + 0.00001 % ß-mercapto-ethanol) and were kept on MEF until homogenous colonies were formed and cells proliferated at a high rate. Typically, this required four to five passages on MEFs. Only then ES cells were cultured on 0.2 % gelatine.

2.8 Electroporation

The principle of the electroporation is summarised in Figure 2.6. The ES cells which were harvested from $S1p1r^{loxP/loxP}/Cre^{ERT2}$ mice were transfected with the Cre-IRES-GFP plasmid (kindly provided by I. Martinez-Garay, (Martinez-Garay et al. 2016)) using the Biosystems Microporator MP-100 with the Neon® Transfection System Kit (Thermo Fisher Scientific). Three pulses of 1400 volts were applied for 10 ms. After transfection, ES cells were plated onto 0.2 % gelatine dishes at various concentrations. Five days later colonies were picked. Every colony was resuspended in 100 µl of 0.01 % trypsin and 0.01 % ethylenediaminetetraacetic acid solution (EDTA, Thermo Fisher Scientific) in PBS in a well of a 96-well plate. After 3 min, trypsinisation was stopped by adding 100 µl of ES cell medium. The cell suspension was transferred to a well of a 12-well plate, where inactivated MEFs were precultured (see above, section 2.7). The different clones were expanded and subsequently genotyped (see above, section 2.3). For short-term storage cell lines were kept at -80°C and subsequently moved to liquid nitrogen for long-term storage. For the subcloning, cell line #43 was split 1:1000 and kept in culture for 10 days. Medium was exchanged every second day. On day 10 colonies were picked and same procedure was followed as elaborated above.
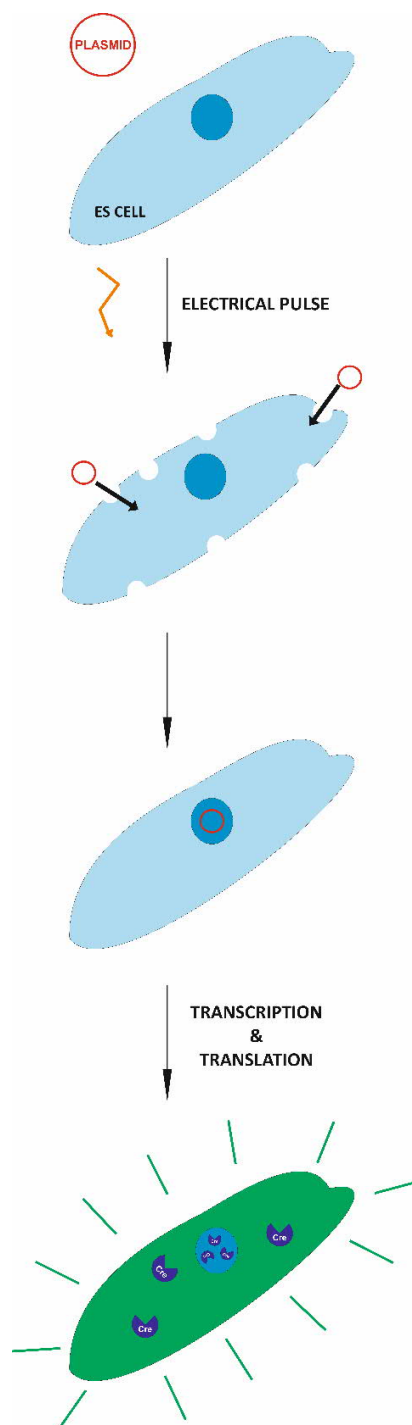
Figure 2.6 Principle of electroporation and transient expression of Cre-IRES-GFP plasmid
Cre-IRES-GFP plasmid is added to the cell suspension and an electrical pulse forms transient gaps into the cell membrane which allows the plasmid to enter the cell. Once in the cytoplasm the plasmid is translocated into the nucleus where it is transcribed followed by the subsequent translation of the mRNA. The Cre expressing cells can be identified by the GFP signal (green). The DNA of the plasmid is not integrated in the genome and its expression will therefore steadily decrease.

2.9   Differentiation of Mouse ES Cells into Neurons

The original protocol for the generation of glutamatergic-like neurons from mouse ES cells was taken from Bibel and colleagues (Bibel et al. 2007). The protocol was optimised by introducing minor changes which are elaborated in this paragraph. J1 ES cells were cultured on MEF in ES cell medium. Multiple passages of the cells were conducted to obtain high and synchronised proliferation. After reaching this point the cells were cultured on gelatine-coated dishes for 3-4 passages to get rid of the remaining MEFs. Subsequently, the ES cells were cultured on non-adherent plates in cellular CA medium, allowing them to aggregate together. Every second day the medium was replaced. On day four of culturing CAs, retinoic acid at a concentration of 5 μM was added to the cells. On day eight of CA culture, the CAs were dissociated using 0.05 % trypsin from bovine pancreas for 3 min at 37°C. Adding CA medium inactivated the trypsin and by pipetting up and down they were dissociated entirely. At this point it was possible to halt the protocol by freezing the CAs in 1 part ES cell medium and 1 part cryo medium (DMEM + 5% DMSO + 3.2% FBS). Otherwise the protocol continued by centrifuging and resuspending them in commercial N2 medium (DMEM/F12 + 1 % NEAA + 1 % N2 supplement + 1 % Penicillin/Streptomycin (Pen/Strep) + 25 μg/ml Insulin + 1 mM L-GlutaMAX™ + 50 μM ß-mercaptoethanol) or handmade N2 medium (50 % DMEM + 50 % F-12 + 2 mM GlutaMAX™ + 25 μg/ml Insulin + 50 μg/ml Transferrin + 20 nM Progesterone + 100 nM Putrescine + 30 nM Sodium Selenite + 1 % Pen/Strep). The neuronal progenitors were then plated on a 12-well plate at a density of 1 million cells per well (2.85×10^5 cells/cm^2) in 1.5 ml N2 medium per well. Plates were coated two days in advance. A poly-ornithine stock solution of 0.5 mg/ml in borate buffer (150 mM BH_3O_3, pH 8.3 adjusted with NaOH) was prepared and diluted 1:5 with ddH$_2$O. Each well was covered with 500 μl of the solution and left at 37 °C overnight. Plates were incubated at 37 °C overnight. Two hours after plating, the medium was replaced

completely, as well as after 24 h. On day 2 of the neuronal culture the medium was replaced by complete medium (Figure 2.7 and as previously described in (Bibel et al. 2007)) with or without 5 µg/ml 5-Fluorodeoxyuridine (5-FdU). Treatment with 5 µg/ml 5-FdU was stopped after two days. The 1.5 ml complete medium per well was then again completely changed on day 4, 8 and 12 and never again thereafter. On day 18, only 500 µl of fresh complete medium was added.

At the beginning, it was not possible to culture the $S1p1r^{loxP/loxP}/Cre^{ERT2}$ cell line on MEF, with FBS containing medium. Therefore, these cells had to be cultured on gelatine-coated dishes with the N2B27+2i+LIF medium. As soon as they were growing at a faster rate they were transferred onto MEF coated dishes. The rest of the protocol remained unchanged.

A

ingredients mix for complete medium	end concentration [µg/ml]	100 x stock [µg/ml]	for 200 ml of 100 x stock [mg]
L-alanine	2.00	200.00	40.00
biotin	0.10	10.00	2.00
L-carnitine	2.00	200.00	40.00
ethanolamine	1.00	100.00	20.00
D-galactose	15.00	1500.00	300.00
L-proline	7.76	776.00	155.20
putrescine	16.10	1610.00	322.00
sodium-pyruvate	25.00	2500.00	500.00
sodium-selenite	0.02	1.60	0.32
vitamin B12	0.34	34.00	6.80
zinc sulfate	0.19	19.40	3.88
catalase	2.56	256.00	51.20
glutathione	1.00	100.00	20.00
linoleic acid	1.00	100.00	20.00
linolenic acid	1.00	100.00	20.00
progesterone	0.01	0.63	0.13
all-trans retinol	0.10	10.00	2.00
retinylacetate	0.10	10.00	2.00
tocopherol	1.00	100.00	20.00
tocopherolacetate	1.00	100.00	20.00

dissolve in 26.6 ml of H$_2$O

dissolve in 1.4 ml of EtOH

→ **add everything to 172 ml DMEM**

B

Complete Medium

BSA/transferrin/insulin mix	dissolve in 30 ml DMEM [g]
BSA	1 g
transferrin	0.002 g
insulin	0.0016 g

complete medium	mix [ml]
DMEM	358.0
penicillin/streptomycin 100x	4.0
ingredients mix 100x	4.0
superoxidase dismutase 2.5 mg/ml	0.4
BSA/transferrin/insulin mix	30.0

Figure 2.7 Preparation of complete medium

A Once every 12 months a 100 x concentrated ingredients mix was prepared, which then was stored in 5 ml aliquots at -80°C. **B** Complete medium was prepared fresh and was kept for up to one month at 4°C. BSA, transferrin and insulin had to be weighed and dissolved in 30 ml before the other ingredients were added. Immediately before use 2 nM L-Glutamax™ was added to the medium.

2.10 Isolation of Primary Cortical Neurons

Mouse E16-16.5 embryos were harvested and brains isolated. During the entire procedure the tissue was kept on ice-cold 1 x HBSS (Thermo Fisher Scientific). Cortices were dissected and minced thoroughly with a scissor. To trypsinise the tissue, a stock solution of 10 mg/ml trypsin (Worthington Biochem) was prepared in 1x HBSS just before use. The tissue was distributed into 50 ml tube so that only tissue of six cortices was added to one 50 ml Falcon tube in 9 ml of 1x HBSS. One ml of the trypsin stock solution was added to get an end concentration of 1 mg/ml. Tissue was trypsinised for 20 min at 37 °C. Every 5 min the solution was gently stirred to allow optimum exposure of the tissue to the trypsin. Just before use a 10 mg/ml stock solution of trypsin inhibitor from soybean (Sigma) was prepared and 1.1 ml was added to each 50 ml tube containing 10 ml of cell suspension to reach an end concentration of approximately 1 mg/ml. The trypsin inhibitor binds with high affinity to trypsin thereby blocking its active site (Blow et al. 1974). This mixture was gently mixed and 100 µl of 1 mg/ml DNase (Roche) in H_2O was added. After mixing the cell suspension yet again it was passed through a strainer (BD Falcon) before a centrifugation step for 10 min at 900 rpm. The supernatant was carefully removed and the pellet was resuspended in primary culture medium (Figure 2.8 and (Chen et al. 2008)). Cell number was counted using a NucleoCounter® NC-100™ (Chemometec) and primary cortical neurons were plated at a density of 2.85 $x10^5$ cells/cm^2. 12-well plates were prepared the night before by coating each well with 500 µl of 0.5 mg/ml poly-L-lysine (Sigma). Just before use, the wells were washed two times with H_2O and dried. Cortical neurons were cultured in 1 ml primary culture medium (Figure 2.8). Every third day until 9 DIV, 200 µl fresh medium was added per well.

A

ingredients for NS21 supplement	end concentration [µg/ml]	stock solution [mg/ml]	for 400 ml of 100 x mix
bovine albumin	2500		50 g
catalase	2.5		50 mg
glutathione	1		20 mg
insulin	4	10.00	8 ml
superoxide dismutase	2.5		50 mg
holo-transferrin	5		100 mg
triiodol-l-thyronine	0.002	2.00	20 µl
L-carnitine	2		40 mg
ethanolamine	1	liquid sol. 1g/ml	20 ul
D(+)-galactose	15		300 mg
putrescine	16.1		322 mg
Na-selenite	0.01435	1.00	280 µl
corticosterone	0.02	2.00	0.2 ml
linoleic acid	1	100.00	0.2 ml
linolenic acid	1	100.00	0.2 ml
lipoic acid	0.047	4.70	0.2 ml
progesterone	0.0063	3.20	0.04 ml
retinol acetate	0.1	20.00	0.1 ml
all trans-retinol	0.1	10.00	0.2 ml
tocopherol	1	100.00	0.2 ml
tocopherolacetate	1	100.00	0.2 ml

B

primary culture medium	mix [ml]
Neurobasal	238.375
penicillin/streptomycin 100x	2.5
NS21 supplement 100x	2.5
L-Glutamax™ 200 mM	0.625

Figure 2.8 Preparation of primary culture medium

A The supplement NS21 was prepared as described by Chen et al. 2008 at a 100x concentration and stored at -20°C for up to 12 months. The compounds in yellow must be prediluted in EtOH to ensure their solubility at the concentration indicated in the column "stock solution". **B** Primary culture medium was prepared fresh by adding L-Glutamax at an end concentration of 0.5 mM, as well as Pen/Strep and NS21 supplement to Neurobasal medium. Medium was kept at 4°C for up to one month. Figure adapted from Chen et al. 2008.

2.11 Treatment of Cultured Neurons

Stock solutions of 10 mM (Z)-4-OHT (Sigma) were diluted in ethanol (EtOH, cat.no. 02860, Sigma) and stored at -20°C. Before use, 4-OHT was diluted to a concentration of 0.1 mM in EtOH and 1.5 µl were added directly to the neurons which were in 1.5 ml complete medium to get an end concentration of 0.1 µM. Control neurons were treated with EtOH only.

Stock solutions of 1 mM pFTY720 (kindly provided by Novartis AG, Basel Switzerland) were prepared by dissolving the powder in DMSO + 0.1 M HCl, aliquoted and stored at -80°C. Dilutions were prepared with DMSO and kept at -20°C for maximum a week.

ES-cell derived neurons or primary cortical neurons were treated by adding pFTY720 directly to the neurons in a 1:1000 dilution (e.g. in 1.5 ml medium 1.5 µl of pFTY720 were added). Wells were immediately agitated to mix the DMSO well. For the long-term treatment, fresh compound was added with fresh medium. In these cases, the pFTY720 dilution was prepared in a separate tube and directly added to the neurons during the medium exchange. Long-term treatments started on day two and lasted for three weeks. Fresh pFTY720 was added during each entire complete medium exchange (see above) and again on day 18. However, on that day no entire complete medium exchange was conducted, but 500 µl of medium containing pFTY720 in the relevant concentration was added to each well.

For experiments including pre-treatment of J1 ES cell-derived neurons with monoclonal anti-BDNF #9 (mAb#9, Developmental Studies Hybridoma Bank), neurons were exposed to 10 µg/ml from 14 DIV until the end of treatment at 21 DIV. Monoclonal Ab #9 (3 ng/ml) was directly added to the well in a dilution of 1:300. Treatment with pFTY720 at 21 DIV was as described above.

Stock solutions of potassium chloride (KCl) and sodium chloride (NaCl) were prepared at a concentration of 3 M in DMEM. To get an end concentration of 60 mM the stock solution was directly added to the neurons in a 1:500 dilution (e.g. to 1.5 ml medium 30 μl of 3 M KCl or NaCl solution were added). NaCl was used as a control to ensure equimolarity of the solution.

2.12 Electrophysiology

Neuronal progenitors were cultured on 24-well Multiwell Micro Electrode Array (MEA) plates (Multichannel System). Wells were coated as previously described (Bibel et al. 2007). At 14 DIV neuronal electrical activity was measured using the Multiwell-MEA system. Measurements were taken over a period of 2 min. At each time point three measurements were performed. During the recording cells were kept in a temperature controlled chamber at 37 °C.

2.13 *In vivo* Experiments

For the *in vivo* experiments, only adult male mice of the age of 12 – 16 weeks were used. Female mice were excluded of the study due to the treatment with an oestrogen receptor modulator and the unknown consequences resulting of it in females. To activate the Cre^{ERT2} recombinase, mice received an intraperitoneal (i.p). injection of 75 mg per kg bodyweight (BW) of tamoxifen for five consecutive days. Corn oil was used as a vehicle. Mice were left untreated for 7-12 days for the recombination to take place. Subsequently, the consecutive treatment was started.

For the long-term treatment, mice were i.p. injected every fourth day in the course of one month with either 0.1 mg FTY720 (Novartis) per kg BW or with vehicle saline. The

experiment was terminated 24 h after the last injection. Mice were culled by a "schedule 1" procedure and brains were immediately harvested. To increase the reproducibility of the dissection, the brains were cut into identical slices using a brain matrix (Acrylic Brain Matrix Adult Mouse, World Precision Instruments; Figure 2.9). The different regions of interest (cortex and hippocampus) were then isolated and snap frozen in liquid nitrogen. The tissue was kept at -80°C until it was further processed (section 2.14 and 2.15).

For the 30 min treatment, every mouse was injected with either FTY720 (0.1 mg/kg BW) or saline and placed into a new cage. Thirty minutes later, mice were culled using a "schedule 1" procedure, brains were harvested and immediately snap frozen in liquid nitrogen. They were stored at -80 °C. The different brain regions were dissected as described above just before the lysis.

In vivo experiments were performed under UK Home Office approval according to the Animal Scientific Procedures Act (ASPA, Home Office 1986).
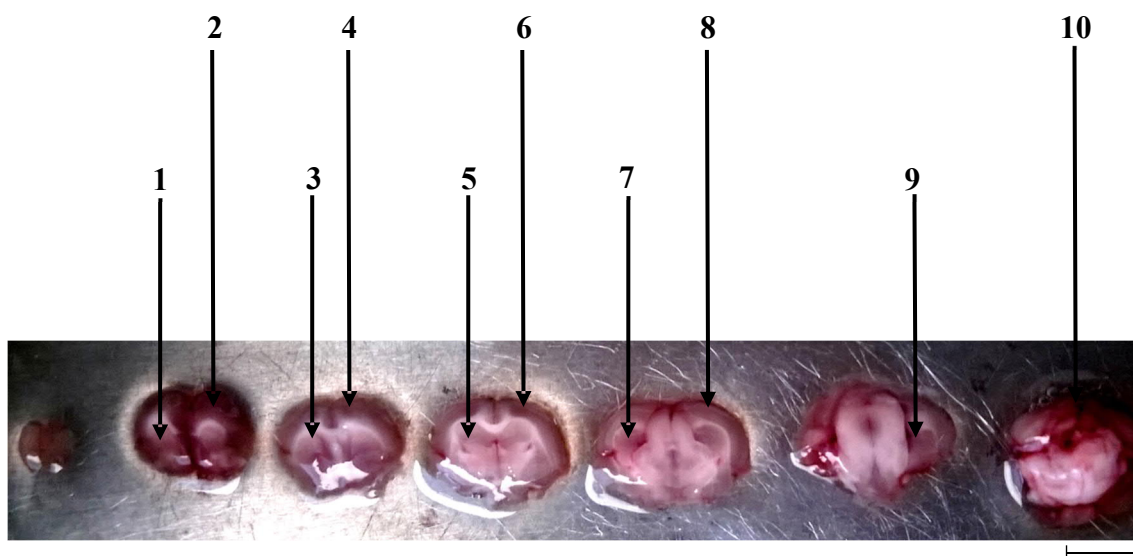
Figure 2.9 Coronal mouse brain sections obtained using a brain matrix

Brain sections were obtained using a brain mould. Section were 1.5 mm thick. Arrows indicate the different brain regions, which were dissected (Scale bar 5 mm.):

1: caudate putamen and nucleus accumbens (Striatum)

2: prefrontal cortex

3: caudate putamen and nucleus accumbens (Striatum)

4, 6, 8: cortex

5, 7, 9: hippocampus

10: cerebellum

2.14 RNA Isolation

2.14.1 ES cells and neurons

For RNA extraction from ES cells or neurons, cultures were washed with PBS and lysed with 350 µl of RLT RNA lysis buffer (RNeasy Mini Kit, QIAGEN) containing 1 % β-mercaptoethanol. Lysate was either immediately frozen at -80°C or processed with the 'RNeasy Mini Kit' (QIAGEN), following the manufacturer's instructions and including a DNase treatment for 15 min at room temperature.

2.14.2 Tissue

For RNA extraction from tissue TRIzol® reagent (Thermo Fisher Scientific) was used. Briefly, tissues were mixed with 1 ml of reagent and cut into small pieces using scissors. Samples were then sonicated and 200 µl of chloroform were added. After vortexing for 15 sec, an incubation step of 3 min at room temperature was performed. Samples were centrifuged at maximum speed for 15 min at 4°C. The upper aqueous phase was removed and 500 µl of isopropanol were added. The mixture was loaded into a RNeasy Mini Kit (QIAGEN) column and the manufacturer's instructions were followed.

2.15 Protein Isolation

2.15.1 Neurons

Sample lysis for the detection of BDNF, pERK1/2 and pCREB by Western blot was performed as follows. Neurons were washed twice with PBS. For a well of a 12-well plate 100μl of RIPA buffer (50 mM Tris base, 150 mM NaCl, 1 mM EDTA, 1 % Triton X-100, 0.2 % sodium deoxycholate, 0.1 % SDS, adjust pH to 7.4 with HCl and inhibitors (1 % phosphatase inhibitor cocktail 3 (Sigma), 1 % protease inhibitor cocktail (Sigma), 100 mM 6-aminohexanoic acid, 1.5 mM aprotinin, 1 mM dithiotreitol (DTT), 100 mM 1,10-phenanthroline, 1 mM phenylmethylsulfonyl fluoride (PMSF)) was used. Using a cell scraper, the cells were detached from the dish and transferred into an Eppendorf tube. Cell lysates were sonicated for 10 seconds at a pulse of 5 and 50 % amplitude if used for BDNF Western blot, otherwise this step was omitted. Lysates were vortexed every 5 min while they were kept on ice for 30 min. This was followed by a centrifugation step at 4°C and 15,000 rpm for 10 min. Lysates were then transferred into a fresh Eppendorf tube, protein concentrations were analysed (see below) and stored at -80°C.

Lysis of neurons for the analysis of Arc in Western blots was performed with the following lysis buffer (50 mM Tris base, 150 mM NaCl, 1 mM EDTA, 1 % Igepal® CA-630 (Sigma), adjust pH to 7.4 with HCl and phosphatase and protease inhibitors (see above). This lysis buffer was found to facilitate the extraction of Arc and used on the recommendations of Clive Bramham, an expert in the Arc field. The rest of the procedure was identical.

For BDNF enzyme-linked immunosorbent assay (ELISA) quantification in neurons, cells were lysed using RIPA buffer without SDS (50 mM Tris base, 150 mM NaCl, 1 mM EDTA, 1 % Triton X-100, 0.2 % sodium deoxycholate, adjust pH to 7.4 with HCl), followed by the lysis procedure stated above.

To quantify protein the Pierce^{TM} BCA Assay Protein Kit for cell samples (cat.no. 23235, Thermo Fisher Scientific) was used. The standard curve of the kit was adjusted to be able to analyse protein in cell lysates (Figure 2.10). Cell lysates were diluted 1:50 with ddH$_2$O and 100 µl of bicinchoninic acid (BCA) reagent was added to the samples as well as the standard curve. Plate was incubated at 37°C for 30 min and the absorbance was analysed at 562 nm using the plate reader (FLUOstar® Omega Microplate Reader).

2.15.2 Tissue

For Western blot analyses in tissue the exact amount of RIPA buffer with protease and phosphatase inhibitors was determined by weighing the tissue. For every mg of tissue 1µl of lysis buffer was added. Subsequently, the tissue was macerated by drawing it with a 1 ml syringe attached to a 25-gauge needle. After homogenization of the tissue, the samples were kept on ice for 30 min and vortexed every 5 min, centrifuged at 4°C and 15,000 rpm for 30 min. Lysates were then transferred into a fresh Eppendorf tube and centrifuged again at the same settings for 10 min to get rid of any tissue residues. After transferring the lysates into fresh tubes, they were kept at -80°C. After thawing and before using the samples in the ELISA, they were centrifuged at 4°C and 15,000rpm for 30 min. Protein was quantified using the Pierce^{TM} BCA Protein Assay Kit (Thermo Fisher Scientific) according to the manufacturer's instruction.

Standard	H$_2$O [µl]	BSA 2 mg/ml		Concentration [µg/ml]
A	1800	200 µl	1504 µl of A	200
B	496		1334 µl of B	150
C	666		1504 µl of C	100
D	496		1334 µl of D	75
E	666		400 µl of E	50
F	400		400 µl of F	25
G	400		400 µl of G	12.5
H	400			6.25
I	400			

Figure 2.10 Standard curve for protein quantification in cell lysates

Standard A was prepared by diluting the 2 mg/ml stock bovine serum albumin (BSA, Sigma) solution with water. Subsequently, a dilution series was performed. Standard I is the blank and therefore only contains water. Concentration indicates the BSA concentration of each standard.

2.16 Primary Rat Megakaryocytes

Two eight weeks old Wistar male rats were culled by a "schedule 1" procedure (Animals (Scientific Procedures) Act 1986) and *tibias* as well as *femurs* were removed from the hind limbs and placed in 1 x HBSS. Using a 25-gauge needle with a 5 ml syringe, bones were flushed with CATCH buffer (4.6 mM sodium acetate, 1 mM adenosine, 1 mM theophylline, 5 % FBS, 1 x HBSS) until they were transparent. Cell suspension was mixed and passed through a 40 μm strainer (BD Falcon) before it was centrifuged for 5 min at 1800 rpm at 4°C. The pellet was resuspended in hypotonic solution (H_2O) for 30 sec to lyse the red blood cells and 1.8 % NaCl solution was immediately added to keep cells in an isotonic condition. The suspension was centrifuged again at 1800 rpm for 5 min at 4°C and resuspended in CATCH buffer before it was centrifuged for the third and last time (as above). Pellet was resuspended in 'megakaryocyte complete medium' (IMDM (Thermo Fisher Scientific) + 5 % BSA + 2 mM GlutaMAX™ + 100 U/ml Pen/Strep + 25 ng/ml rat thrombopoietin (TPO) + 25 mg/ml rat stem cell factor (SCF) (both R&D Systems) and cells were distributed in nine non-adherent 100 mm Ø plates (Greiner). Per plate 8 ml complete medium was used and cells were incubated at 37°C and 4 % CO_2. After two days in culture plates were changed and 2 ml fresh complete medium was added per plate. After another four days in culture (six days in total) cells were harvested and centrifuged (as above). Pellet was resuspended in 10 ml of PBS. For the BSA gradient 2ml of 3 % BSA in PBS was added to a 15 ml Falcon conical tube. Subsequently, 2 ml of 1.5 % BSA in PBS was slowly added to the tube ensuring that the two phases did not mix. Finally, 2 ml of the cell suspension was slowly pipetted on top of the gradient and again being careful not to mix the different phases. Tubes were kept in a rack for up to 40 min to let the cells pass through the gradient. The upper 4 ml were harvested and centrifuged (as above) and the pellet was resuspended in complete medium and cultured for another two days. To the bottom phase 2 ml of PBS were added and the

cell suspension was centrifuged (as above). The pellet was resuspended in CellGro®

SCGM (CellGenix) medium containing 100 U/ml Pen/Strep. Cells were equally

distributed in three 25 mm Ø dishes, each containing 2 ml of medium. Treatment was

immediately started by either adding 2 µl of 10 µM pFTY720 to reach an end

concentration of 10 nM or by adding 2 µl of DMSO as a vehicle control. Megakaryocytes

were harvested by centrifugation (as above), washed with PBS and subsequently lysed by

addition of RNA RLT lysis buffer containing 0.1 % β-mercaptoethanol from the RNeasy

Mini Kit (Qiagen). RNA extraction was followed according to the manufacturer's

instruction. Primers used for the RT-qPCR are listed in Table 2.4 and 2.5.

2.17 ELISA

The principle of a two-site ELISA is elaborated in Figure 2.11. For the detection of BDNF

in ES cell-derived neurons a MaxiSorp white polystyrene 96-well plate (cat.no. 436110,

VWR) was coated with the monoclonal antibody anti-BDNF #1 (Ab #1, Developmental

Studies Hybridoma Bank). To each well 200 µl of 3 µg/ml Ab #1 diluted in coating buffer

(50 mM $NaHCO_3$, 50 mM Na_2CO_3, pH 9.7) was added. After overnight incubation, the

plate was washed once with PBS and blocked for 2 h at 30°C with blocking solution

(4 % BSA in PBS). The plate was washed again just once with PBS and 150 µl of

incubation buffer (0.1 M KH_2PO_4, 0.1 M Na_2HPO_4, pH 7.6) were added to each well. The

standard curve was prepared using recombinant BDNF protein starting at a concentration

of 25 ng/ml, followed by eight subsequent 1:2 dilutions. Triplicates of 50 µl of standard,

blank or sample were added to each well. The samples were then incubated at room

temperature on a rotating platform. After 3 h the samples were removed and the wells

were washed five times with PBS. The secondary antibody anti-BDNF #9 conjugated

with horseradish peroxidase (HRP) (Ab #9-HRP, Developmental Studies Hybridoma

Bank) using HRP-linkage kit (Thermo Fisher Scientific). was prepared at a concentration of 1:4000 in incubation buffer containing 4 % BSA. To each well 200 µl of the mixture was added and incubated for 3 h at room temperature. The wells were then washed five times with PBS before 100 µl of developing solution (BM chemiluminescence ELISA Substrate POD, cat.no. 11582950001, Roche) were added to each well. Luminescence was measured using the plate reader (FLUOstar$^®$ Omega Microplate Reader).
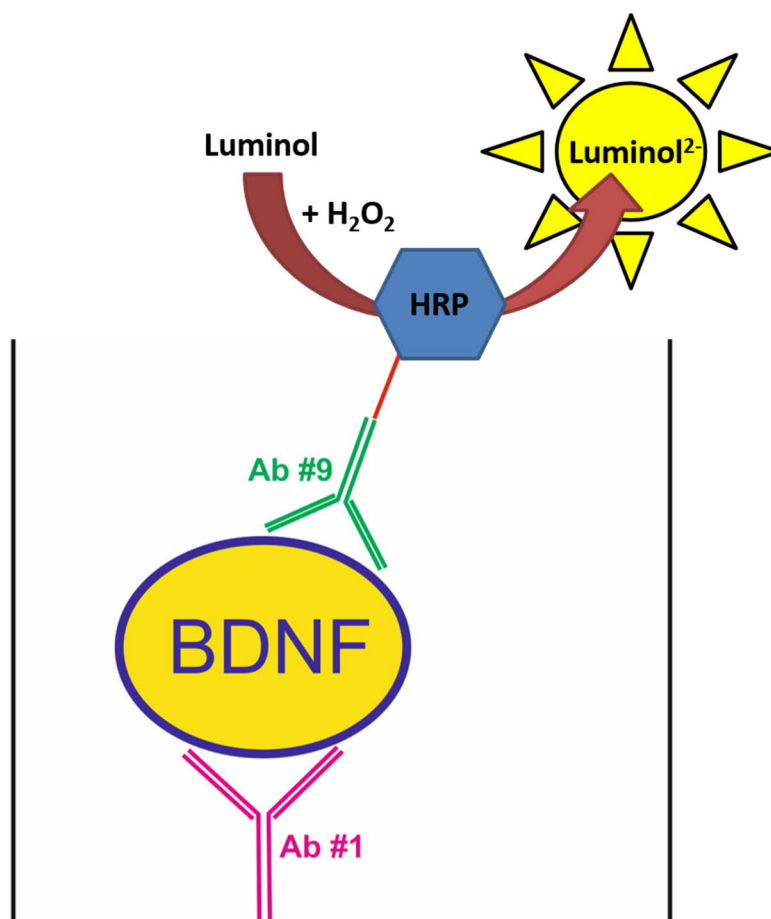
Figure 2.11 Principle of two-site ELISA

Two specific antibodies are used to detect and quantify BDNF. The first antibody (Ab #1) attached to the surface of the well via covalent bonds. Lysate containing BDNF is then incubated in the well and BDNF will therefore be immobilised. During subsequent washing steps unbound BDNF is removed and the secondary antibody which is linked to the enzyme HRP (Ab #9-HRP) detects the immobilised BDNF. After removal of any excessive Ab#9, the substrate, containing hydrogen peroxide and luminol is added and the chemiluminescent reaction is started, which results in oxidisation of luminol and subsequent light emission.

2.18 Western Blot

Lysates were mixed with 1x lithium dodecyl sulphate (LDS) buffer (1 M Glycerol, 140 mM Tris Base, 106 mM Tris HCl, 0.5 mM EDTA, 0.22 mM Brilliant Blue G-250, 0.175 mM Phenol Red, 74 mM LDS, pH 8.5) and 50 mM DTT and boiled at 70ºC for 10 min. Subsequently they were loaded on a NuPAGE™ Novex™ 4-12 % Bis-Tris gel (Thermo Fisher Scientific) and run at 120 V for 90 min in 2-(N-morpholino)ethanesulfonic acid (MES) running buffer (50 mM MES, 50 mM Tris base, 0.1% SDS, 1 mM EDTA, pH 7.3). Proteins were then transferred to a nitrocellulose membrane, by applying 80 V for 1 h at 4°C, using the wet transfer technique. The gel and the membrane were placed between two blotting papers and put in a cassette which was completely immerged in transfer buffer (25mM Bicine, 25mM Bis-Tris, 1mM EDTA, 20% MeOH). Following transfer, the membrane was blocked using blocking solution for at least 30 min. The blocking solution used for BDNF Western blots consisted of 3 % Amersham ECL Prime blocking reagent (GE Healthcare) + 3 % BSA in TBS-T (24.7 mM Tris base, 137 mM NaCl, 2.6 mM KCl, 0.1 % Tween-20, pH 7.5). For all the other Western blots 5 % blotting-grade blocker (Bio-Rad) in TBS-T was used (Table 2.2). The membrane was incubated at 4°C overnight with primary antibody diluted in blocking solution (Table 2.2). The next morning the membrane was washed three times 15 min with TBS-T, before it was incubated with an either HRP- or Alexa 647-conjugated secondary antibody for 1 h at room temperature (Table 2.3). The membrane was washed again three times 15 min in TBS-T. For development of the membrane LumiGLO® ReserveChemiluminescent Substrate kit (seracare) was used. Membrane was covered with 1 ml of substrate and incubated at room temperature for 1 min. The substrate was removed and the signal was detected using the ChemiDoc™ MP system together with the Image Lab™ software (Bio-Rad). This camera system allows the detection of chemiluminescent and fluorescence signal and to control for saturation. Exposure times

was adjusted to avoid saturation. For the analysis of the signal refer to section 2.19. After development, the membrane was washed three times for 10 min with TBS-T and blocked with blocking solution at 4°C for 30 min (Table 2.2), before primary antibody of the internal control was incubated overnight at 4°C. The next morning the membrane was washed three times for 15 min with TBS-T and secondary antibody of the internal control was incubated for 1 h at room temperature. In the case of βIII-tubulin, the secondary antibody was always conjugated to the Alexa-647 fluorophore. Membrane was washed again three times 15 min with TBS-T and developed as above. If the Alexa-647 fluorophore was used the signal was detected by using red epi-illumination as the excitation source and a 695/55 emission filter. Thereafter, the membrane was only stripped if an incubation with another primary antibody apart from βIII-tubulin was desirable. The membrane was stripped for 30 min with stripping buffer (Thermo Fisher Scientific) and then washed three times for 15 min with TBS-T. Subsequently, standard procedures like those specified above were followed. Finally, to control the loading with a second method, all the protein on the membrane were stained with the Pierce™ Reversible Protein Stain Kit (Thermo Fisher Scientific). This was to verify that the internal control was representative of the loading and not affected by subsequent treatments. Then in the case of a total protein stain, one did not just control for one specific protein but for all the detectable protein. The principle is similar to a Ponceau Red staining with the advantage that the staining does not fade and pictures can be taken without the loss of signal. The staining was not performed according to the manufacturer's instruction, as only 1 ml per membrane was used and the membrane was incubated for 5 min on the shaker. Subsequently, the membrane was washed three times for 5 min with water and pictures were taken (Figure 2.12).

Table 2.2 Primary antibodies used for Western blot applications

Antibody	Type	Dilution End Conc.	Species	Blocking Solution	Distributor
anti-Arc	mAb	1:250 1 µg/ml	mouse	5 % Blotting Grade Blocker	BD Bioscience cat.no. 612603
anti-β-actin	pAb	1:5000 0.2 µg/ml	chicken	5 % Blotting Grade Blocker	Abcam cat.no. ab13822
anti-βIII-tubulin	mAb	1:10000 0.1 µg/ml	mouse	5 % Blotting Grade Blocker	Biolegend cat.no. 801202
anti-BDNF	mAb	1:2000 0.5 µg/ml	mouse	3 % ECL 3 % BSA	Icosagen cat.no. 3C11
anti-BDNF N-20	pAb	1:750 0.13 µg/ml	rabbit	3 % ECL 3 % BSA	Santa Cruz cat.no. sc-546
anti-Cre	mAb	1:1000	rabbit	5 % Blotting Grade Blocker	Cell Signaling cat.no. 15036S
anti-GAPDH	pAb	1:5000 0.2 µg/ml	chicken	5 % Blotting Grade Blocker	Abcam cat.no. ab83956
anti-pCREB (Ser111)	mAb	1:1000 -	rabbit	5 % Blotting Grade Blocker	Cell Signaling cat.no. 9198S
anti-pERK1/2 (Thr202/Tyr204)	mAb	1:10000 -	rabbit	5 % Blotting Grade Blocker	Cell Signaling cat.no. 4370
anti-S1P1R	pAb	1:500 2 µg/ml	rabbit	5 % Blotting Grade Blocker	Cayman Chemicals cat.no. 10005228
anti-S1P1R	mAb	1:1000 -	mouse	5 % Blotting Grade Blocker	Millipore cat.no. MABC94
anti-synaptophysin	mAb	1:1000 10 µg/ml	mouse	5 % Blotting Grade Blocker	Sigma cat.no. S5768
anti-GFAP	mAb	1:1000 -	mouse	5 % Blotting Grade Blocker	Cell Signaling cat.no. 3670S
anti-vGlut2	mAb	1:1000 1µg/ml	mouse	5 % Blotting Grade Blocker	Synaptic System cat.no. 135421

Table 2.3 Secondary antibodies used for Western blot applications

Antibody	Dilution End Conc.	Species	Distributor
anti-mouse HRP	1:7500 0.13 µg/ml	goat	Promega cat.no. W4021
anti-rabbit HRP	1:7500 0.13 µg/ml	goat	Promega cat.no. W4011
anti-chicken HRP	1:7500 0.27 µg/ml	goat	Abcam cat.no. ab6877
anti-mouse Alexa 647	1:5000 0.4 µg/ml	donkey	Thermo Fisher Scientific cat.no. A31571
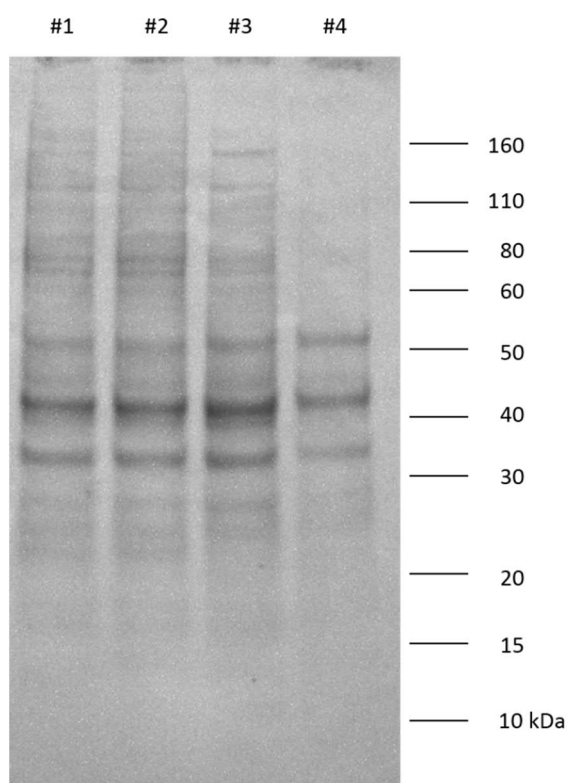
Figure 2.12 Pierce™ Reversible Protein staining

Illustration of a total protein staining using the Pierce Reversible Protein Stain kit. Four different neuronal lysates were loaded and it is apparent that from lysate #4 less protein was loaded. In such a case the lysates were reloaded and protein amounts were adjusted.

2.19 Densitometric Analysis

Western blot data were quantified using ChemiDoc™ MP system together with the Image Lab™ software (BioRad). Manually, a square was matched around each lane, making sure that each band was surrounded (Figure 2.13A). With the help of the software the lane was automatically detected. Next, each peak which was generated was analysed to make sure that the lane was detected completely and that the area under the curve correlated to the density of the band (Figure 2.13B). The software then subtracted the background and calculated the area under the curve (AUC). This value was now used to compare the intensity of the signal from the different groups. The AUC of the target of interest, was divided by the AUC of the internal control. To determine changes in percentage *versus* the control, each sample value was divided by the value obtained from the control treatment (e.g. DMSO).

A
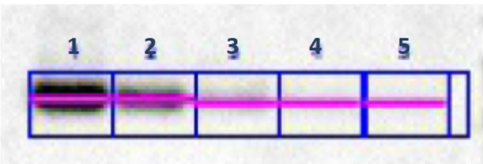
B

Lane 1
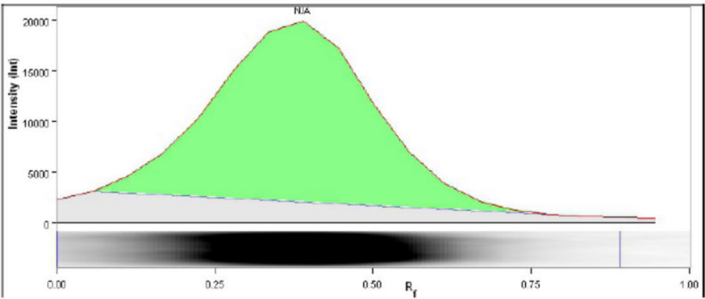
Band No.	Band Label	Mol. Wt. (KDa)	Relative Front	Volume (Int)	Abs. Quant.	Rel. Quant.	Band %	Lane %
1		N/A	0.444	2,378,090	N/A	N/A	100.0	100.0

Lane 2
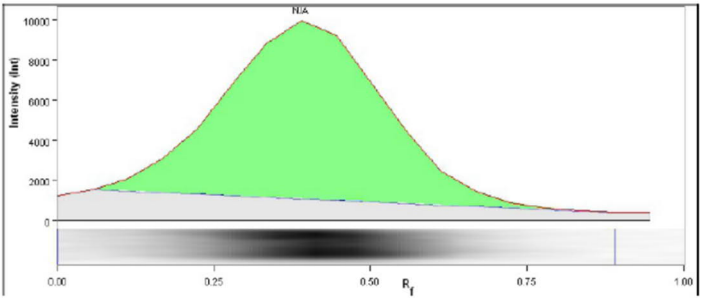
Band No.	Band Label	Mol. Wt. (KDa)	Relative Front	Volume (Int)	Abs. Quant.	Rel. Quant.	Band %	Lane %
1		N/A	0.444	1,092,366	N/A	N/A	100.0	100.0

Lane 3
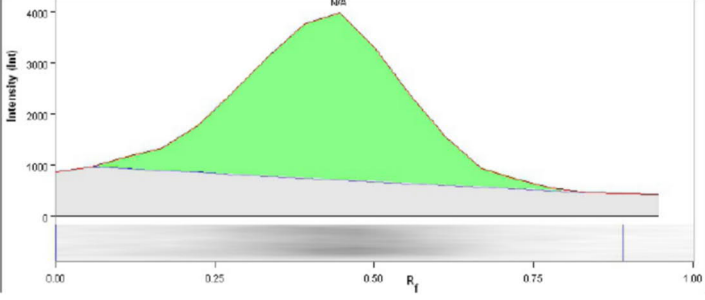
Band No.	Band Label	Mol. Wt. (KDa)	Relative Front	Volume (Int)	Abs. Quant.	Rel. Quant.	Band %	Lane %
1		N/A	0.500	392,898	N/A	N/A	100.0	100.0

Lane 4
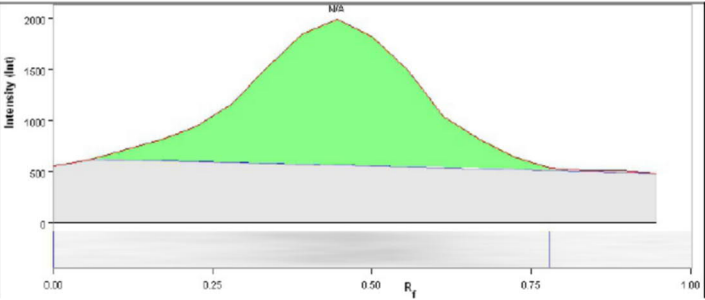
Band No.	Band Label	Mol. Wt. (KDa)	Relative Front	Volume (Int)	Abs. Quant.	Rel. Quant.	Band %	Lane %
1		N/A	0.500	190,124	N/A	N/A	100.0	99.7

Figure 2.13 Densitometric analysis of a BDNF Western blot

Figure 2.13 Densitometric analysis of a BDNF Western blot

A BDNF Western blot analysed with secondary anti-mouse HRP. ImageLab™ Software was used to detect bands on the Western blot. Blue squares were placed by hand and software then detected the band automatically. **B** From these bands the software calculated the intensity of the signal and blotted the intensity against the relative front (R_f). The software first substracted the background and then specified the AUC, which corresponds to the entire intensity of the band specified as volume. In this particular case the volume for lane 1 was 2,378,090, for lane 2 it was 1,092,366, for lane 3 it was 392,898 and for lane 4 it was 190,124, corresponding to the decrease of signal.

2.20 RT-qPCR

The real-time quantitative poly chain reaction (RT-qPCR) was performed to analyse the relative expression of different genes. RNA was extracted as mentioned in section 2.14. RNA was quantified using a BioSpectrometer® (Eppendorf), which apart from the concentration of RNA also quantifies the 260/280 nm absorbance ratio. This value was supposed to be in the range of 1.8 to 2.0 to be free of protein contamination. If this was not the case the samples were discarded. Between 500 ng – 1000 ng of total RNA were reverse transcribed using the SuperScript® III reverse transcriptase (Thermo Fisher Scientific). First, 1 mM of dNTP mix (Promega) and 0.025 µg/µl of Random Hexamer Primers (Promega) were mixed with the RNA and diluted with ddH$_2$O to a final volume of 13 µl. The mixture was heated to 65°C for 5 min, while the master mix (4 µl 5x First-Strand Buffer (Thermo Fisher Scientific) + 1 µl of 0.1 M DTT (Invitrogen) + 1 µl 20 – 40 U/µl RNasin® Ribonuclease Inhibitor (Promega) +1 µl 200 U/µl the SuperScript® III reverse transcriptase) was prepared. The 7 µl of master mix were then added to the RNA/dNTP/Random Primer mix and was incubated at 50°C for 2 h. Subsequently, the reaction was inactivated by heating the mixture to 70°C for 15 min. The complementary DNA (cDNA) was then either directly used for a qPCR or stored at -80°C. Primers were either manually designed, using the primer design software https://www.genscript.com/ssl-bin/app/primer with a subsequent analysis of the primers using clone manager software (version 7) and a specificity test using the BLAST homepage (https://blast.ncbi.nlm.nih.gov/Blast.cgi) or TaqMan® probes were acquired from Thermo Fisher Scientific. Primers for the detection of *S1pr* mRNA in the rat megakaryocytes were taken from a recent publication which looked at the expression of *S1pr* in the rat dorsal root ganglia and sensory neurons (Kays et al. 2012). The manual designed primers had to fulfil the following criteria: They had to be between 17-25 bp long, have a GC content of minimum 55 – 65 % and a melting temperature around 60 –

70°C. Although a genomic DNA digestion step with DNase enzyme was performed, primers were still designed to span an intron sequence where applicable to avoid genomic DNA amplification.

For each RT-qPCR between 25-50 ng of cDNA was used which corresponded 1.5-2.5 µl of final reverse transcription mix. For each reaction on the 96-well plate, the same amount of cDNA was used. For one sample of the FAST SYBR® Green RT-qPCR 12.5 µl FAST SYBR® Green master mix (Thermo Fisher Scientific) + 0.625 µl of 10 µM oligo sense + 0.625 µl of 10 µM oligo antisense + 1.5 – 2.5 µl cDNA + H_2O ad 25 µl were mixed. Each reaction was prepared in triplicates in one tube, mixed well and distributed in a MicroAmp® Fast Optical 96-well plate (Thermo Fisher Scientific). For each sample a reaction for the internal control was performed at the same time (Table 2.4). For the PCR reaction, the StepOnePlus™ Real-Time PCR system (Thermo Fisher Scientific) was used with the following programme. In the first 10 min, the temperature was raised to 95°C, the reaction then started by denaturation of the DNA at 95°C for 30 sec. The temperature dropped to 57°C for 30 sec to allow the annealing of the probe and then increased again to 70°C for 1 min to allow amplification. The last three steps were repeated for 39 times. Subsequently, a melting curve was generated to identify if unspecific fluorescence signal was detected as the SYBR® dye detects any double-stranded DNA. The melting curve was generated by increasing the temperature slowly at a rate of 1°C per minute up to 99°C to detect the fluorescence signal released by the now denatured products which incorporated the fluorescent dye during the PCR reaction. The obtained values by the RT-qPCR were analysed using Word Excel.

For a TaqMan® RT-qPCR the mix included 12.5µl FAST TaqMan® master mix (Thermo Fisher Scientific) + 1.25 µl of TaqMan® primer/probe set (Thermo Fisher Scientific) + 1.5-2.5 µl cDNA + H_2O ad 25 µl. For each sample, a reaction for the internal control was

performed at the same time (Table 2.5). In the first 20 secs, the temperature was risen to 95°C, the reaction then started by denaturation of the DNA at 95°C for 1 sec. The temperature dropped to 60°C for 20 secs to allow the annealing of the probe and to extend the product. The last two steps were repeated for 39 times.

Table 2.4 Primers used for SYBR® Green RT-qPCR.

Transgene	Oligonucleotide	Species	Primer 5' to 3'
Thy-1	sense antisense	mus musculus	CCAGAATCCAAGTCGGAACT GGACACCTGCAAGACTGAGA
Cre^{ERT2}	sense antisense	mus musculus	TCCATATTGGCAGAACGAAA CAGCTACACCAGAGACGGAA
vGlut1	sense antisense	mus musculus	GGAGGAGCGCAAATACATTGAGG CATAGACGGGCATGGACGTAAAG
vGlut2	sense antisense	mus musculus	TGCAAAGCATCCTACCATTACAG GCAGAAGTTGGCAACAATTATCG
Tbr1	sense antisense	mus musculus	ACAACAAGGGAGCATCAAACAAC TCTGTGCCATCCTCATTCACTTC
S1p1r	sense antisense	mus musculus	TCGCCGACAGCAGCAAGATG AACCTCCGGGATGCTAGTGG
S1p2r	sense antisense	mus musculus	ACCGAGCACAGCCAACAGTC GAGGTGGTCTCCTGCATGTC
S1p3r	sense antisense	mus musculus	GATGCGCCTTGCAGAACGAG CCATGGCTTCCTAGAGACAG
S1p4r	sense antisense	mus musculus	TGGTGGTCTTCGCCCTCATC TGAGTAGCCTGCGGGACTTG
S1p5r	sense antisense	mus musculus	TCTGGAGTGCCGGTTACAGG GGAGCTTGCCGGTGTAGTTG
β-actin	sense antisense	mus musculus	CAATAGTGATGACCTGCCGT AGAGGGAAATCGTGCGTGAC
S1p1r	sense antisense	rattus norvegicus	TTCAGCCTCCTTGCTATCGC AGGATGAGGGAGATGACCCAG
S1p2r	sense antisense	rattus norvegicus	GACGCTGGACATGCAGGAG TACATGGCTGAGTGGAACTTGC
S1p3r	sense antisense	rattus norvegicus	GCCACCCGCCAGTCTTG GCCAGCTTCCCCACGTAAT
S1p4r	sense antisense	rattus norvegicus	CGTTTCCAGCATCCGCAG CCAGTCCCTTCTCACCTCTCCT
S1p5r	sense antisense	rattus norvegicus	CCTATGTGCTCTTCTGCGTGCTG CGCACCTGACAGTAAATCCTTG
Hprt	sense antisense	rattus norvegicus	GCAGACTTTGCTTTCCTTGG TACTGGCCACATCAACAGGA

Table 2.5 Protocols and primer/probe sets used for TaqMan® RT-qPCR.

Transgene	Species	Product Size	Primer
Bdnf	mus musculus	92 bp	Mm04230607_s1
S1p1r	mus musculus	133 bp	Mm00514644_m1
Vegfd	mus musculus	57 bp	Mm01131929_m1
18s rRNA	mus musculus	61 bp	Mm03928990_g1
Bdnf	rattus norvegicus	142 bp	Rn02531967_s1
Gapdh	rattus norvegicus	174 bp	Rn01775763_g1

2.21 Analysis of C_t values

The RT-PCR was repeated three times for each sample and the values from each reaction were averaged. The RT-PCR data was analysed using the $2^{-\Delta\Delta Ct}$ method (Schmittgen and Livak 2008). The ΔC_t values were calculated by subtracting the C_t values of the reference gene from the gene of interest. When analysing the gene expression changes relative to a calibrator, the ΔC_t value of the calibrator was further subtracted from any other value to obtain the $\Delta\Delta C_t$ value for each condition. The calibrator was typically the untreated control. The fold-change difference was calculated by converting the $\Delta\Delta C_t$ to a linear form using $2^{-\Delta\Delta Ct}$. In the absence of a calibrator the ΔC_t values were compared to each other by plotting the $2^{-\Delta Ct}$ value, as this value represents the variation between samples more accurately than the C_t values (Schmittgen and Livak 2008).

2.22 Immunocytochemistry

Cells were cultured and differentiated as described earlier. They were cultured on glass coverslips, which were pre-treated with pure nitric acid overnight and washed with ultrapure water until neutral pH is attained. The water was removed and the coverslips were washed in 1 M HCL at 40-50°C for 4 h. Coverslips were then washed again with ultrapure water until neutral pH was attained, before washing them for 1 h with pure ethanol. This was followed by drying the coverslips on a filter paper and autoclaving them. The staining was performed according to a previously published protocol with slight modifications (Ippolito and Eroglu 2010). In brief, cultured cells were washed with PBS and fixed for 15 min with 4 % paraformaldehyde (PFA). The cells were then washed three times with 0.1 % Triton X-100 in PBS (PBS-T) and blocked for 30 min with blocking solution (50 % antibody buffer (150 mM NaCl, 50 mM Tris Base, 1 % BSA, 100 mM L-Lysine) + 50 % donkey serum containing 0.2 % Triton X-100). The primary antibody (Table 2.6) was diluted in antibody solution (90 % antibody buffer + 10% donkey serum). Cells were incubated with primary antibody overnight in a humidified chamber at 4°C. Cells which were used for the no primary control were incubated with antibody solution (see above) only. The next morning the cells were washed three time for 10 min each with PBS-T. The secondary antibody (Table 2.7) was also diluted in antibody solution (see above) and cells were incubated for 1 h in a dark chamber. Four washes with PBS-T for 15 min each were carried out and nuclei were stained with 4',6-diamidino-2-phenylindole dihydrochloride (DAPI) (cat.no. D9542, SIGMA) at a concentration of 1:10,000 in PBS for 5 min. Cells were washed with ultrapure water and coverslips were mounted with Dako mounting medium (Dako North America, USA). For detection of S1P1R no Triton X-100 was used at any point to avoid permeabilization of the membrane and all washing steps were performed with PBS only.

Table 2.6 Primary antibodies used for immunocytochemistry

Antibody	Type	Dilution End Conc.	Species	Distributor
anti-S1P1R	pAb	1:250 4 µg/ml	rabbit	Cayman Chemicals cat.no. 10005228
anti-Cre	mAb	1:1000 -	rabbit	Millipore cat.no. ab5392

Table 2.7 Secondary antibodies used for immunocytochemistry

Antibody	Dilution End Conc.	Species	Distributor
anti-rabbit Alexa 647	1:1000 2 µg/ml	donkey	Thermo Fisher Scientific cat.no. A31573

2.23 Imaging

Images were acquired at 63x magnification using a confocal microscope (LSM 780, Carl Zeiss) together with the ZEN Black software (version 2.0, Carl Zeiss).

2.24 Analysis

Image Lab™ software (BioRad) was used for densitometry analysis on Western blots.

MARS software (BMG labtech) was used to analyse the luminescence data from ELISA measurements as well as data acquired from protein quantification assays.

The StepOne™ Software was used to analyse the C_t values obtained in the RT-qPCR.

ImageJ was used to perform colocalization analysis.

For further analyses Word Excel software was used.

2.25 Statistical Analysis

For statistical analysis GraphPad Prism software (version 7.02) was used. Only in cases where a normality test had to be performed was SPSS software (version 23) consulted. If only three independent experiments were undertaken a non-parametrical t test, also known as Mann-Whitney test, was performed or when two or more groups were to be compared a Kruskal-Wallis test was considered. If the Kruskal-Wallis test showed a significant difference, the test was followed up by the Dunn's multiple comparison post-hoc test. Data from experiments which were repeated more than three times were analysed for Gaussian distribution, *via* performing a Q-Q-Plot. When the z values of the skewness and kurtosis (mean/standard deviation) was in the range of -1.96 and +1.96, the p value of the Shapiro-Wilk test was greater than 0.05 and the Q-Q-Plot indicated normality, the

data was considered normally distributed and an Unpaired t-test was performed or where two or more groups were to be compared a One-way analysis of variance (ANOVA) which was followed up by a Bonferroni post-hoc test if it showed a significant difference was considered. Unless otherwise stated, the number n stands for the number of independent experiments conducted.

Chapter 3

Generation and Characterisation of the *S1p1r*$^{-/-}$ ES Cell Line B2

3.1   Introduction

Currently there is a high degree of uncertainty as to the distribution of the S1P1R in the brain, not least because of the lack of reliable, specific antibodies and the limited cellular resolution of *in situ* hybridisation in the CNS. While there is agreement that several different cell types express the receptor, including vascular endothelial cells and astrocytes based on work with transgenic animals the suggestion has been made that neurons may not express S1P1R (Choi et al. 2011). This conclusion has been subsequently challenged following the discovery that FTY720 increases BDNF levels in the brain and the knowledge that neurons are the primary site of *Bdnf* expression in the CNS (Deogracias et al. 2012). As the germline deletion of *S1p1r* causes early embryonic death as blood vessels fail to develop normally an alternative is to generate genetically modified embryonic stem (ES) cells and to differentiate them into neurons. Indeed, protocols have been developed allowing the *in vitro* generation of highly enriched populations of excitatory neurons (Bibel et al. 2004), which unlike inhibitory neurons, express the *Bdnf* gene (Baquet et al. 2004). As detailed in "Materials and Methods" a new mouse line *S1p1r*$^{loxP/loxP}$/*Cre*^{ERT2} was generated by crossing mice carrying floxed *S1p1r* alleles with animals expressing a tamoxifen-inducible form of Cre placed under the control of a randomly inserted *Thy-1* promoter (Figure 3.1). This strategy allows the conditional excision of the *S1p1r* in neurons. Subsequently, ES cells were harvested from the inner cell mass of *S1p1r*$^{loxP/loxP}$/*Cre*^{ERT2} blastocysts to differentiate them into neurons.
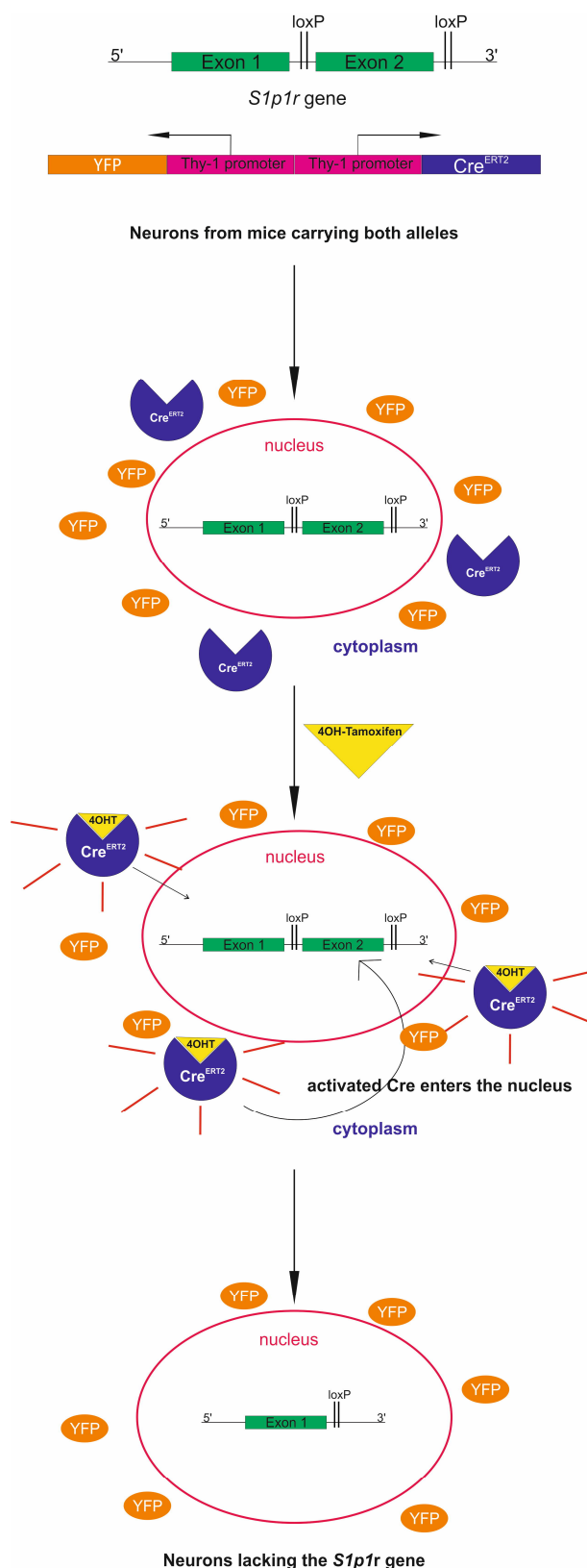
Figure 3.1 Scheme of *S1p1r* excision following 4-OHT addition

All cells of this mouse line carry two floxed *S1p1r* alleles as well as a randomly inserted *Thy-1/Cre^{ERT2}* construct. After activation of the Cre recombinase with 4-hydroxytamoxifen (4-OHT) exon 2 of the *S1p1r* can be excised from neurons.

3.2   ES Cell Harvest

S1p1r$^{\text{loxP/loxP/}}$*Cre*^{ERT2} mice were bred and female mice sacrificed after two days to harvest the blastocysts (Materials and Methods, section 2.4). A total of eight blastocysts were isolated and cells cultured either until the blastocysts spontaneously hatched or following the manual removal of the *zona pellucida*. The "embryo proper" or epiblast was separated from the trophectoderm and subsequently cultured in a 96-well plate (Figure 3.2). From these eight blastocysts, eight epiblasts were cultured and four cell lines were viable, which equals a success rate of 50 %. In female mouse, unlike human ES cells, both X chromosomes are active and are therefore not suitable for their use in the differentiation protocol. Typically mouse XX ES cells eventually die with time in culture as the process of X inactivation cannot be readily recapitulated *in vitro* (Barakat and Gribnau 2010). Male ES cells were selected by genotyping and the ES cell lines #1 - #4 used in subsequent experiments (Figure 3.3). These cell lines were expanded until a high enough number of cells could be obtained to allow their storage in liquid nitrogen. ES cells were initially cultured using the N2B27 + 2i + LIF protocol introduced by Ying and colleagues, a procedure that eased the isolation of ES cells from blastocysts (Ying et al. 2008). The ES cell line #1 was kept in culture and was subsequently cultured on MEF (Figure 3.4) and differentiated into neurons using the protocol from Bibel et al. 2007 (Materials and Methods, section 2.9).
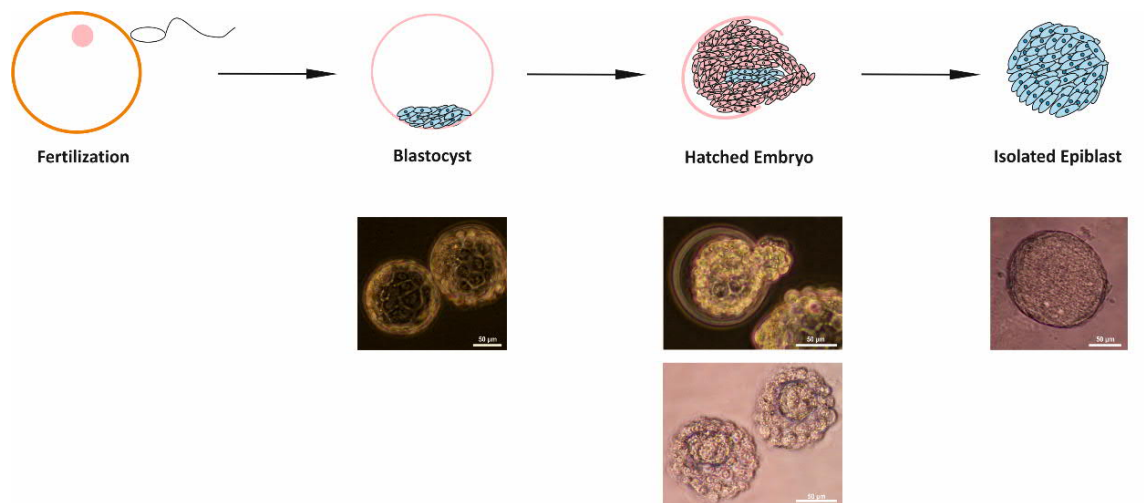
Figure 3.2 Scheme of ES cells harvest

The bright field pictures illustrate early mouse embryos and the scale bar is 50 µm.
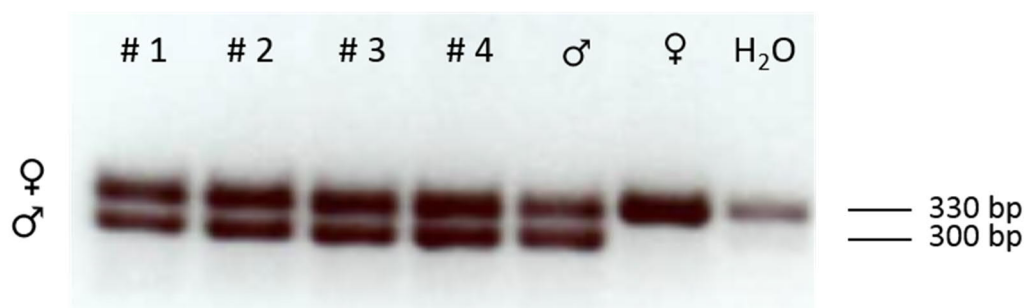
Figure 3.3 Sex determination by PCR

Amplicons were separated by electrophoresis on a 1.5 % agarose gel labelled with ethidium bromide. Genomic DNA isolated from *S1p1r*^{loxP/loxP/}*Cre*^{ERT2} ES cell lines #1 - #4 were analysed. Positive control samples (male (♂) and female (♀)) and negative control sample without DNA (H_2O) were used. 331 bp and 302 bp amplicons represent a sequence found on the X or Y chromosome, respectively.
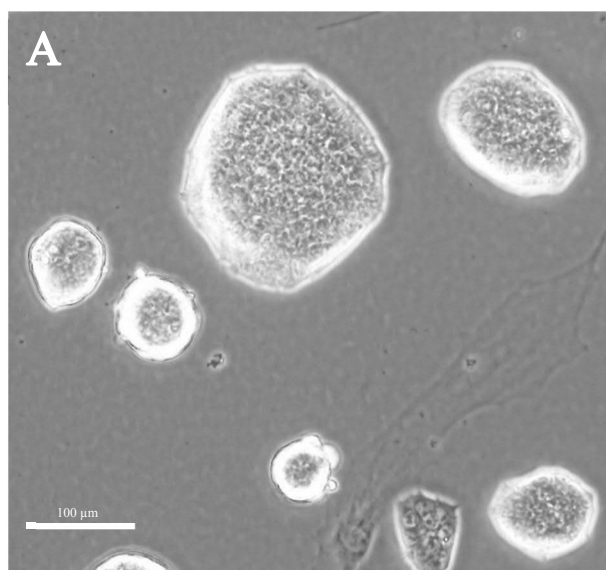
Figure 3.4 Culture of ES cells

A ES cells cultured with the N2B27 + 2i + LIF protocol (Materials and Methods, section 2.4).
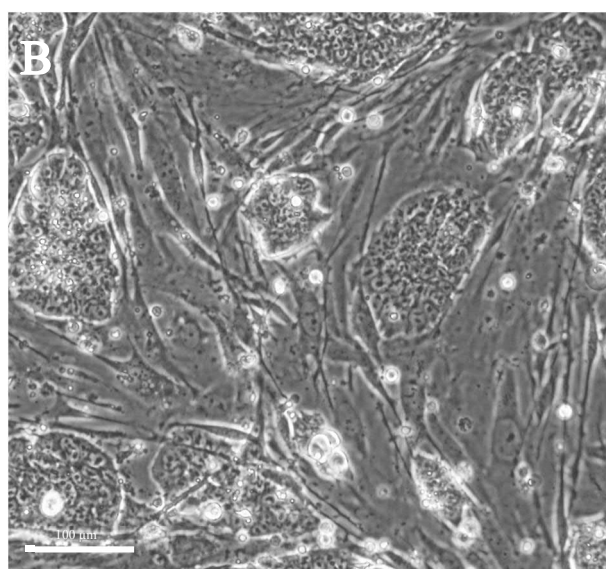
B ES cells of the mutant cell line #1 after transfer from the N2B27 + 2i + LIF system to the culture on MEF with DMEM/FBS and LIF.
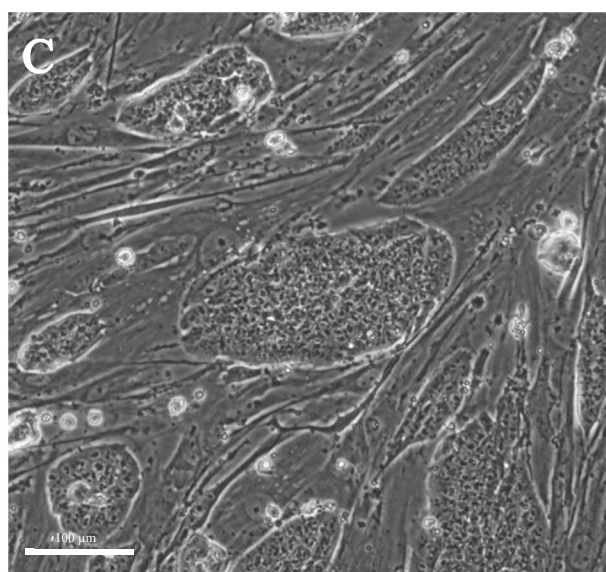
C ES cells from the WT ES cell line J1 cultured on MEF.

Scale bar 100 μm

3.3   ES Cell-Derived Neurons

ES cells were cultured for at least four and for up to seven passages on MEFs. Multiple passages markedly improved the quality of the differentiation procedure and greatly helped generating homogeneous populations of ES cells by selecting the most rapidly dividing cells (Bibel et al. 2007). This simple procedure turned out to select for pluripotent cells as asymmetric cell division slows down the cell cycle. The last two passages on MEFs were conducted with a lower number of MEFs, i.e. less than 1×10^6 cells were plated per 60-mm dish to decrease the number of MEFs as these interfere with the formation of cellular aggregates. Subsequently, two rounds of passages onto gelatine-coated dishes was found to be optimal for the complete elimination of MEFs from the culture. Following dissociation of the cellular aggregates, neuronal progenitors were then cultured in commercial N2 medium (Materials and Methods, section 2.9) which appeared to improve the general quality of the neurons when compared to handmade N2 medium as described by Bibel and colleagues (Figure 3.5, Materials and Methods section 2.9). After two days, the cells were cultured in complete medium (Materials and Methods, Figure 2.7). Other attempts with primary culture medium (Material and Methods, Figure 2.8) led to a high number of non-neuronal cells, as well as neuronal aggregation. Apart from the medium, the density at which the neurons were cultured was also found to make a significant difference regarding the quality of the cultures. While higher densities improved the survival rate, they also markedly increased the degree of neuronal aggregation that eventually compromised the long-term survival of the cultures. The optimal cultures density was determined to be 2.85×10^5 cells per cm^2.
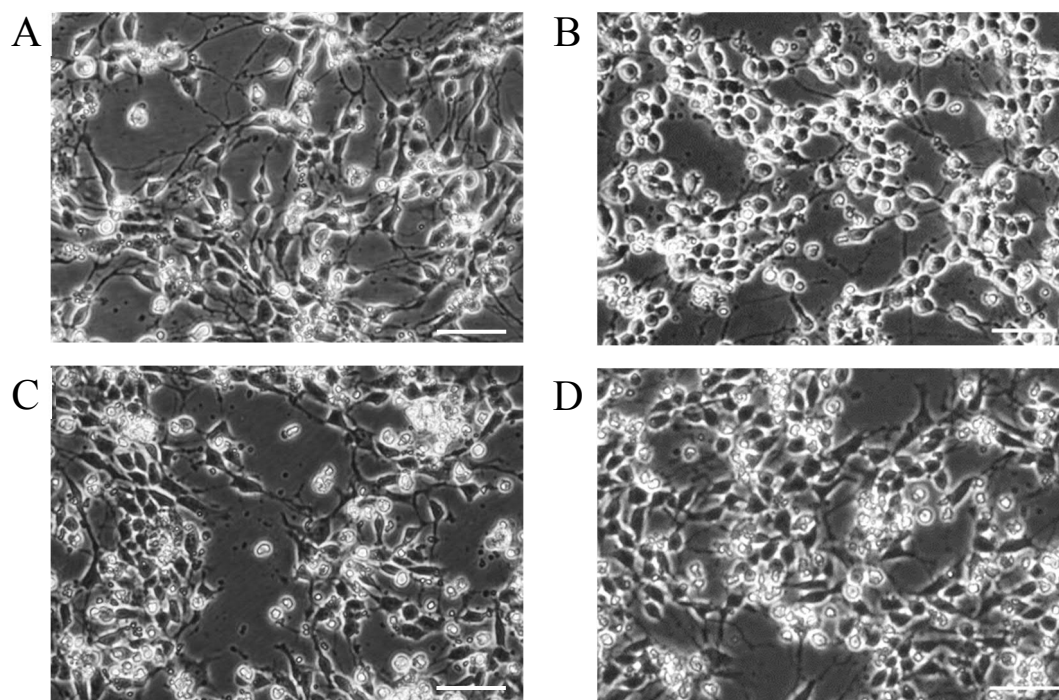
Figure 3.5 Neurons cultured with handmade and commercial N2 medium

Neuronal progenitors 1 DIV were cultured with handmade N2 (A and C) and commercial N2 medium (B and D). When cultured with N2 commercial medium more cells appeared to have a round neuronal like profile compared to cells cultured with handmade N2 medium. Observations are from four independent experiments. Scale bar 50 μm.

3.4   *S1p1r* Excision

3.4.1 Tamoxifen treatment

To excise S1P1R specifically on neurons, $S1p1r^{loxP/loxP}/Cre^{ERT2}$ ES cell-derived neurons, referred to thereafter as #1 neurons, were treated with 4-OHT at different time points. In parallel, *Thy-1* as well as Cre^{ERT2} expression was analysed to identify potential optimal time points of 4-OHT addition (Figure 3.6 and 3.7). ES cell-derived neurons were treated overnight with 0.1 µM 4-OHT due to the results obtained from pilot experiments indicating that concentrations above 0.1 µM 4-OHT were toxic for ES cell-derived neurons. In addition, the quality and efficiency of 4-OHT was analysed using a control cell line expressing Cre^{ERT2} under the control of the *Rosa26* promoter expressed in ES cells. Overnight exposure of these cells to 0.05 µM 4-OHT was shown to be effective to induce Cre-mediated excision of a transgene flanked by two loxP sites in ES cells (Appendix, Figure A.1).

As expected, *Thy-1* mRNA levels increased with the maturation of the neurons. At 6 DIV, following the start of differentiation, *Thy-1* mRNA levels already reached a seven-fold increase compared to 3 DIV and then increased further to reach significance at 13 DIV with a 50-fold increase (* p (day 3 *vs.* day 13) < 0.05, Figure 3.6). In line with this, Cre^{ERT2} mRNA was detectable at 6 DIV though it was noted that unexpectedly, mRNA levels failed to increase further with the maturation of the neurons (Figure 3.7A). Unsurprisingly, Cre^{ERT2} mRNA levels did not change after exposure to 0.1 µM 4-OHT (Figure 3.7B). The expression of the *S1p1r* gene was then determined in neurons treated either with 4-OHT or the vehicle EtOH at 6 DIV, as well as 13 DIV (Figure 3.8). At both time points excision of *S1p1r* could not be achieved. The possible reasons for the failure of excision was investigated by looking at the nuclear translocation of Cre^{ERT2} after 4-OHT treatment in #1 neurons *via* immunostaining.
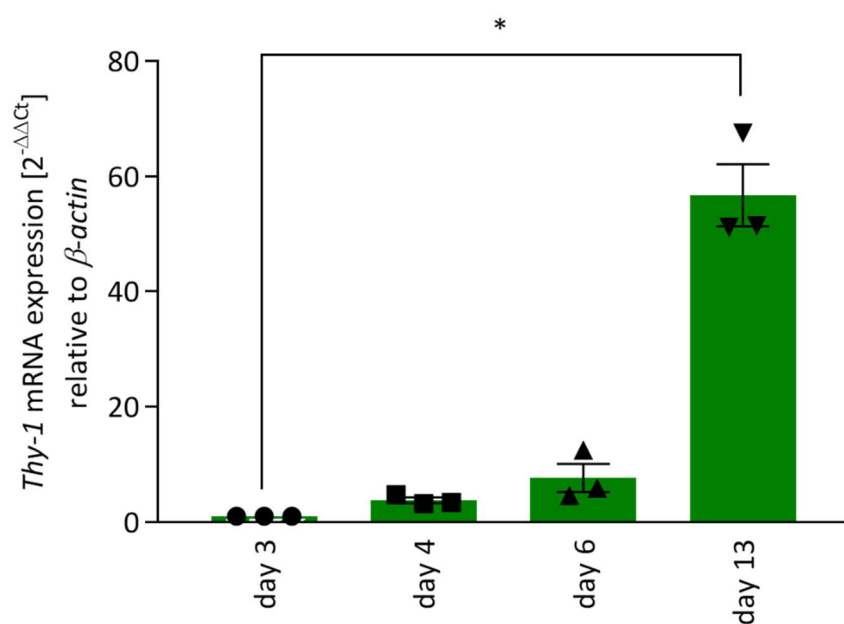
Figure 3.6 *Thy-1* mRNA levels increased during the maturation of #1 neurons

At 3 DIV *Thy-1* mRNA was detected in #1 neurons and its expression increased significantly over the next 10 days (Kruskal-Wallis test followed by a Dunn's multiple comparison test, * p (day 3 *vs.* day 13) < 0.05, n = 3). Data are represented as mean of $2^{-\Delta\Delta Ct} \pm$ SEM.
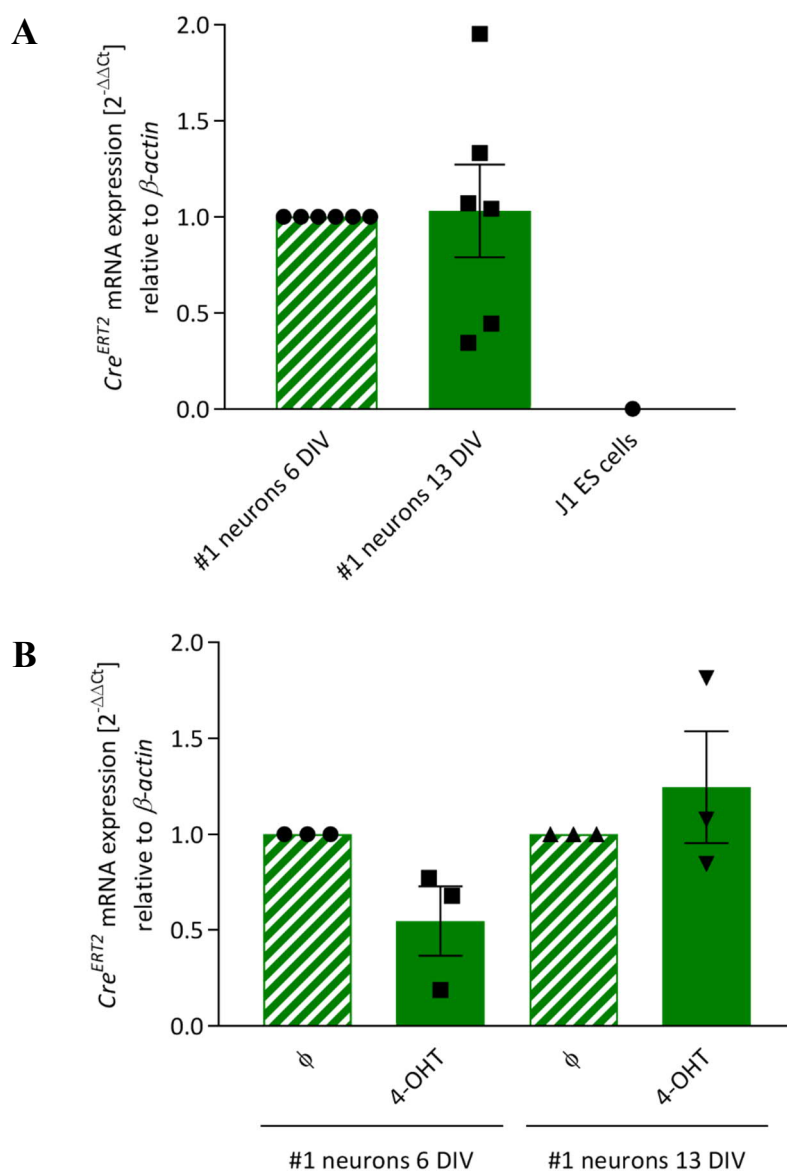
Figure 3.7 *Cre^{ERT2}* mRNA expression stayed constant after 6 DIV in #1 neurons

A *Cre^{ERT2}* mRNA was expressed in #1 neurons at 6 DIV. *Cre^{ERT2}* did not increase further during the maturation of #1 neurons (Mann-Whitney test, $p > 0.05$, $n = 6$ repeats from 3 independent experiments). J1 ES cells served as a negative control. **B** At both time points *Cre^{ERT2}* mRNA levels were unaffected by the 4-OHT treatment (Mann-Whitney test, $p > 0.05$, $n = 3$). Data are represented as mean of $2^{-\Delta\Delta Ct} \pm$ SEM. Ø: vehicle (EtOH) treated cells.
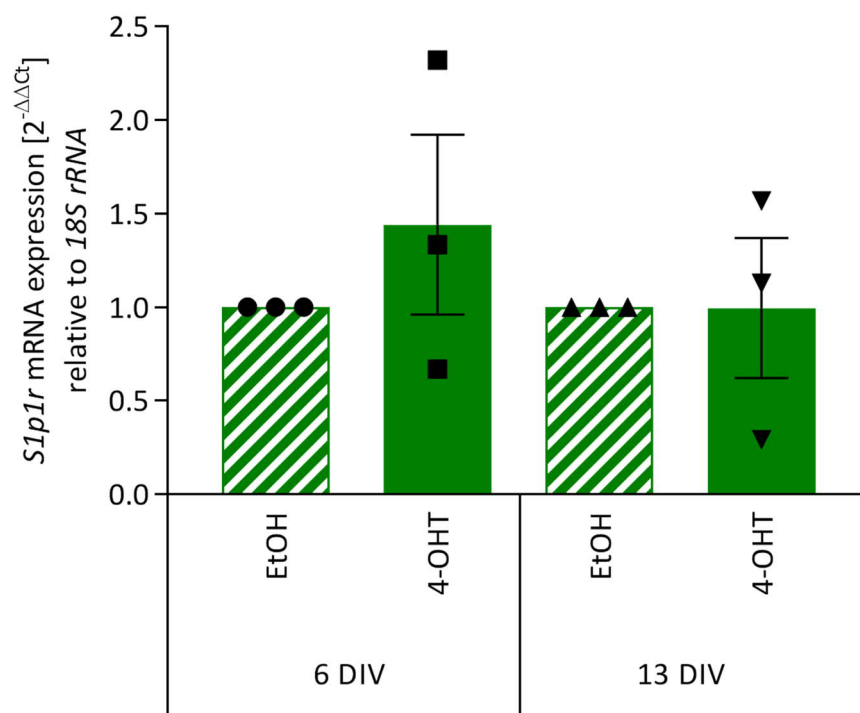
Figure 3.8 4-OHT treatment unexpectedly failed to decrease *S1p1r* mRNA expression in mutant #1 neurons.

#1 neurons were treated with 0.1 μM 4-OHT or vehicle overnight and lysed at the indicated days. *S1p1r* mRNA levels were analysed using a TaqMan® RT-PCR assay. *S1p1r* mRNA levels remained unchanged after tamoxifen treatment (Mann-Whitney test, $p > 0.05$, n = 3). Data are represented as mean of $2^{-\Delta\Delta Ct} \pm$ SEM.

3.4.2 Cre^{ERT2} immunostaining and Western blot

The possible reasons for the unsuccessful *S1p1r* excision in the #1 neurons was further investigated. To identify if the 4-OHT treatment used would induce the expected nuclear translocation of Cre^{ERT2}, #1 neurons were treated with 0.1 μM 4-OHT or vehicle (EtOH) overnight and an immunostaining was performed. In six days old #1 neurons a staining for Cre^{ERT2} could be detected with its highest intensity found in the cytoplasm (Figure 3.9 and 3.10). However, no difference was detected when comparing the Cre^{ERT2} staining intensity in the nucleus of 4-OHT and vehicle treated neurons (Figure 3.10). This is in contrast to the obvious translocation seen in the ES cell line *Rosa26/Cre^{ERT2}* (Materials and Methods, section 2.5.2), which was used as a positive control to validate the immunostaining (Figure 3.11) and activity of 4-OHT (Figure 3.12). This indicates that while 4-OHT was active, 4-OHT treatment did not activate nuclear translocation of Cre^{ERT2} in #1 neurons 6 DIV. To investigate if treatment with 4-OHT would lead to Cre^{ERT2} activation in more mature neurons the experiment was repeated in 14 days old #1 neurons (Figure 3.13). These neurons express higher levels of *Thy-1* mRNA compared to less mature neurons (Figure 3.6), and although the *Cre^{ERT2}* mRNA levels were similar in six days old neurons compared to 13 days old neurons (Figure 3.7A), it was unclear if Cre^{ERT2} protein levels would follow the same pattern. However, Cre^{ERT2} could not be detected in cultures of #1 neurons 14 DIV (Figure 3.13), and the staining was similar to that seen in the cell line used as a negative control, J1 (Figure 3.14).
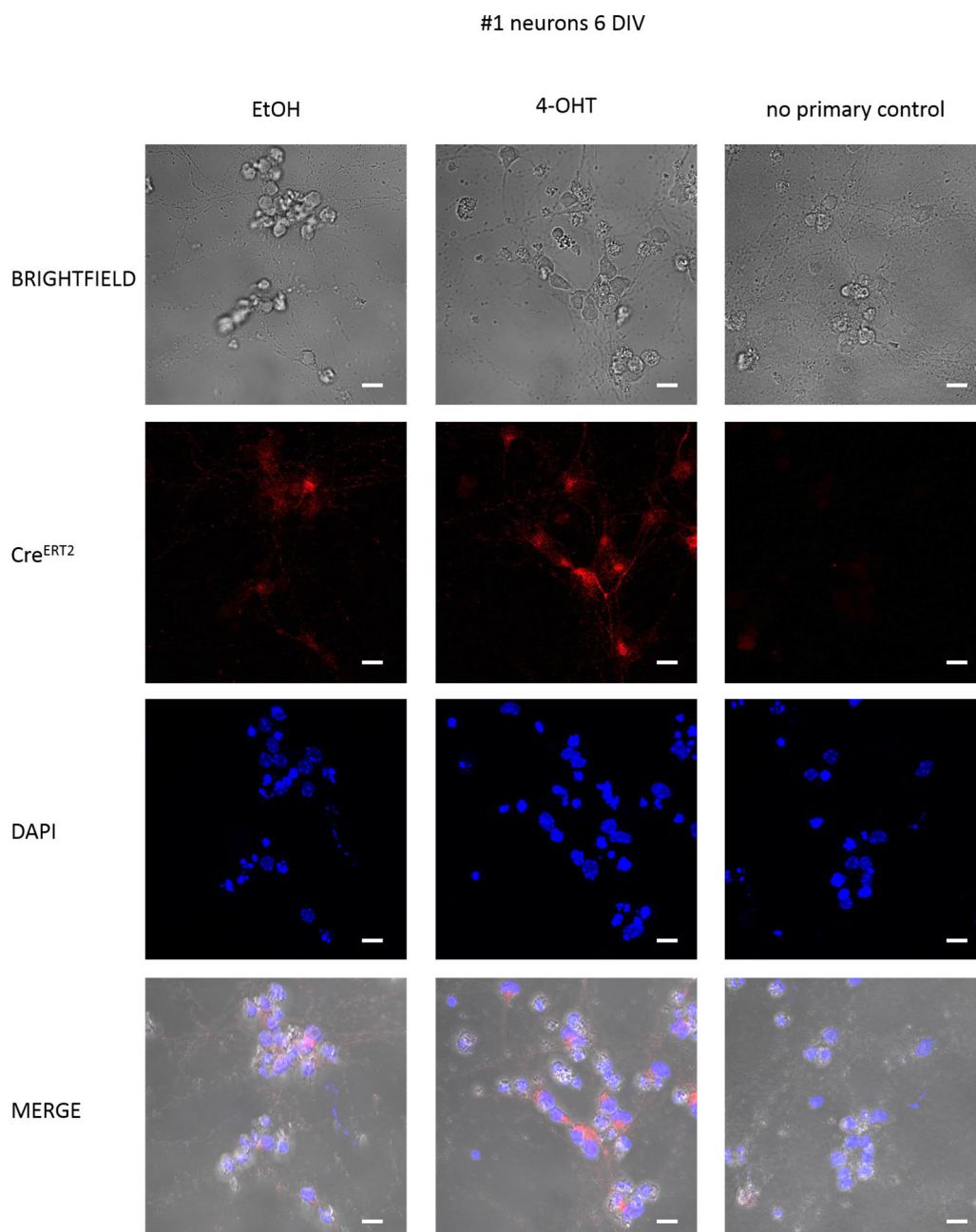
#1 neurons 6 DIV

Figure 3.9 Cre^ERT2 immunostaining in #1 neurons 6 DIV

#1 neurons 6 DIV were treated with 0.1 μM 4-OHT or vehicle overnight and fixed thereafter. Cells were stained for Cre^ERT2 (Alexa-647, red). Brightfield image illustrates a single plane scan to facilitate identification of neurons. Nuclei were stained with DAPI (blue). Cre^ERT2 staining was mainly detected in the cytoplasm. Right panel shows neurons stained with no primary antibody. Scale bar 20 μm.
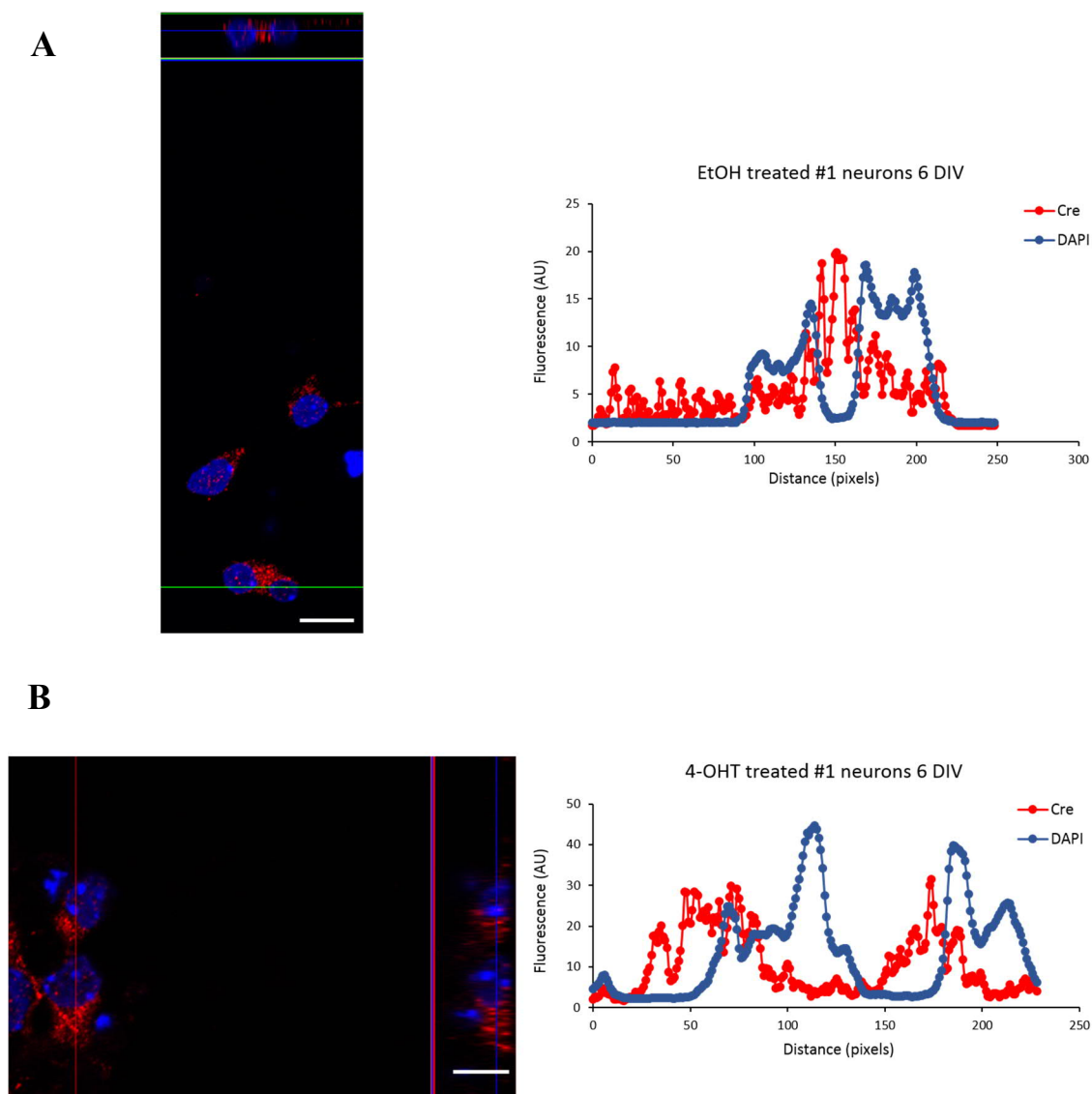
Figure 3.10 Colocalisation analysis of Cre^{ERT2} with DAPI in #1 neurons 6 DIV

#1 neurons 6 DIV were treated with **A** vehicle (EtOH) or **B** 0.1 μM 4-OHT overnight, followed by an immunocytochemistry staining for Cre^{ERT2}. Staining was analysed for nuclear translocation of Cre^{ERT2} (Alexa-647, red). 4-OHT did not induce nuclear translocation of Cre^{ERT2} as no colocalisation of the Cre^{ERT2} staining with DAPI could be observed. Scale bar 10 μm.

Rosa26/Cre^{ERT2} ES cells
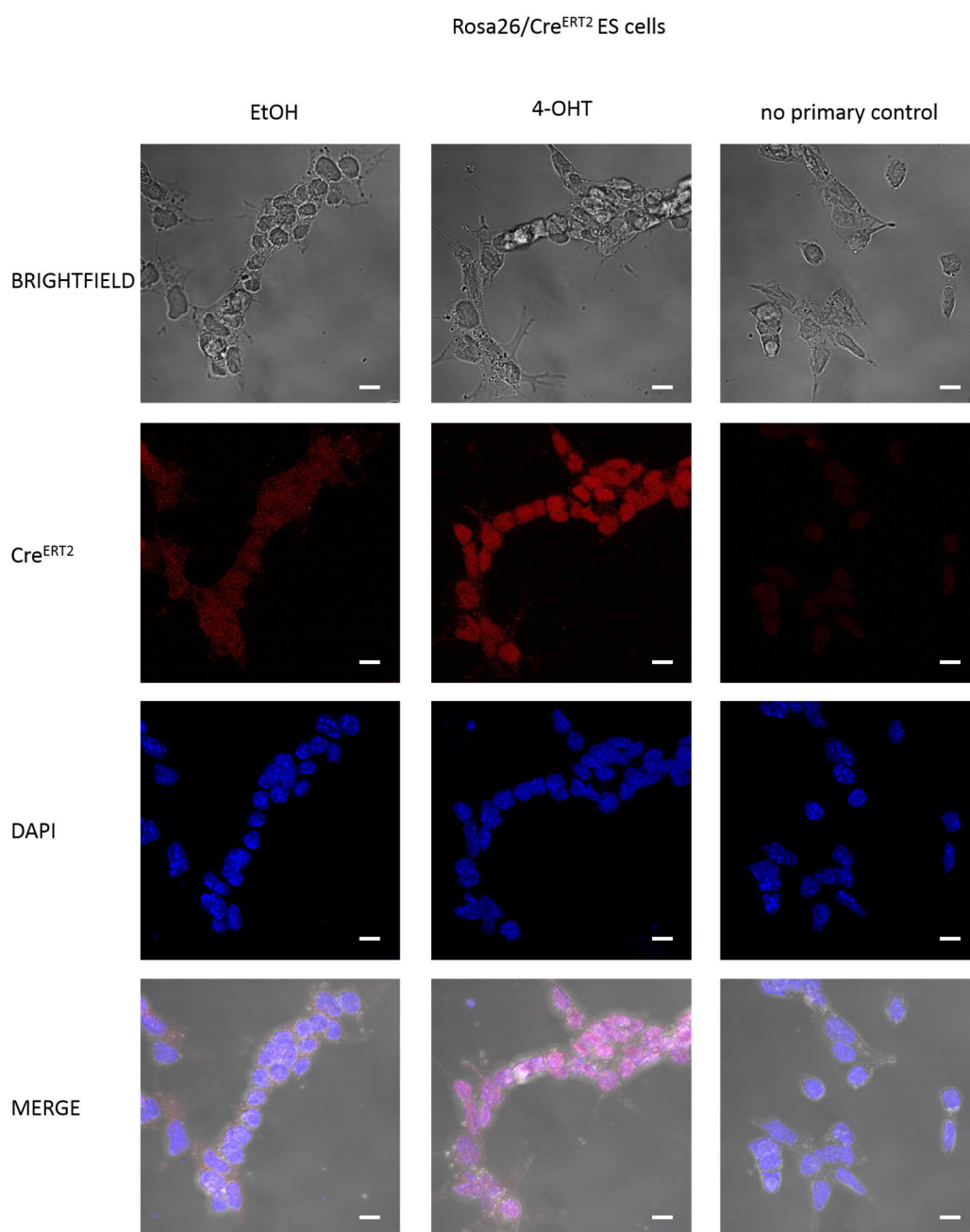
Figure 3.11 Positive control for Cre^{ERT2} immunostaining

Rosa26/Cre^{ERT2} ES cells were treated with 0.1 μM 4-OHT or vehicle overnight and fixed thereafter. Cells were stained for Cre^{ERT2} (Alexa-647, red). Brightfield image illustrates a single plane scan. Nuclei were stained with DAPI (blue). Cre^{ERT2} staining was detected in the nucleus after 4-OHT treatment. Right panel shows neurons stained with no primary antibody. Scale bar 20 μm.

A

B
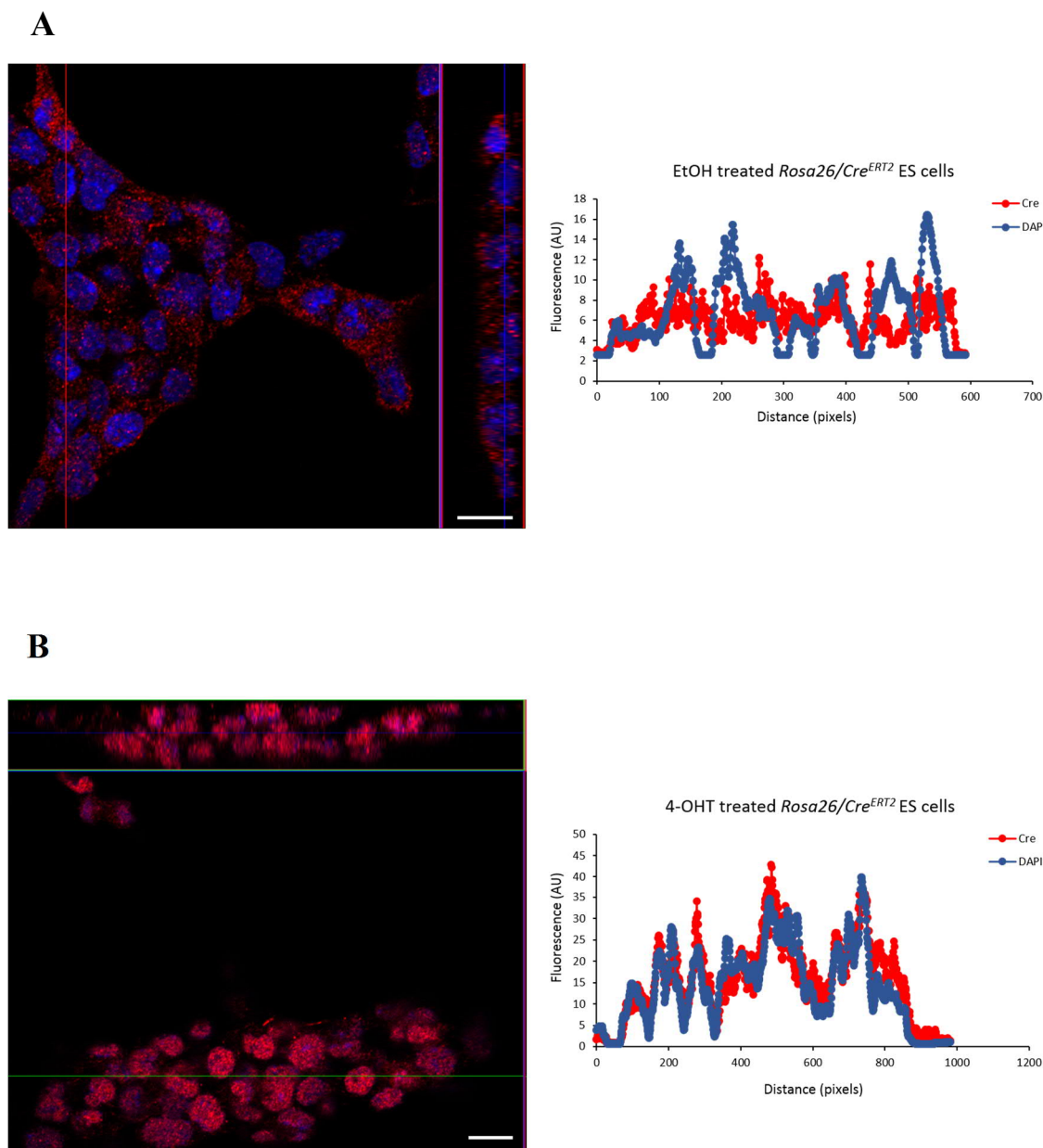
Figure 3.12 Nuclear translocation of Cre^{ERT2} in *Rosa26/Cre^{ERT2}* ES cells

Rosa26/Cre^{ERT2} cells were treated with **A** vehicle (EtOH) or **B** 0.1 μM 4-OHT overnight, followed by immunocytochemistry staining for Cre^{ERT2}. Staining was analysed for nuclear translocation of Cre^{ERT2} (Alexa-647, red). 4-OHT induced nuclear translocation of Cre^{ERT2} which is represented by the overlay of the DAPI and Cre^{ERT2} fluorescence signal in **B** compared to weak Cre^{ERT2} signal in the nucleus in **A**. Scale bar 10 μm.
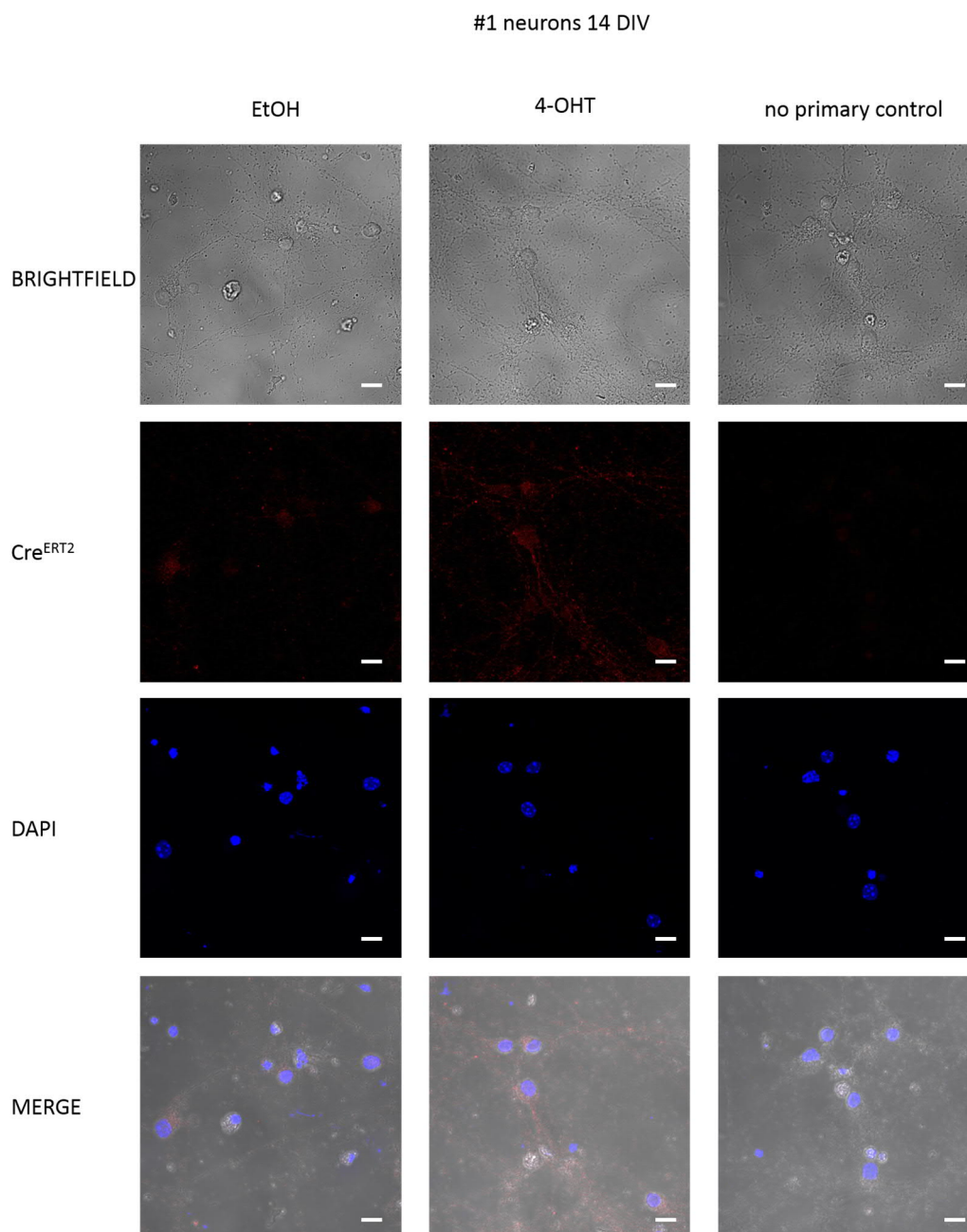
#1 neurons 14 DIV

Figure 3.13 Cre^{ERT2} was not detectable in #1 neurons 14 DIV

#1 neurons 14 DIV were treated with vehicle (EtOH) or 0.1 μM 4-OHT overnight, followed by immunocytochemistry staining for Cre^{ERT2}. Cells were stained for Cre^{ERT2} (Alexa-647, red). To identify neuronal cells bodies a single plane brightfield image is shown. Nuclei were stained with DAPI (blue). No staining for Cre^{ERT2} could be detected. The signal obtained is close to the no primary control and is similar to the staining found in the negative control cell line J1 (see below). Right panel shows neurons stained with no primary antibody. Scale bar 20 μm.

J1 neurons 14 DIV

no primary control
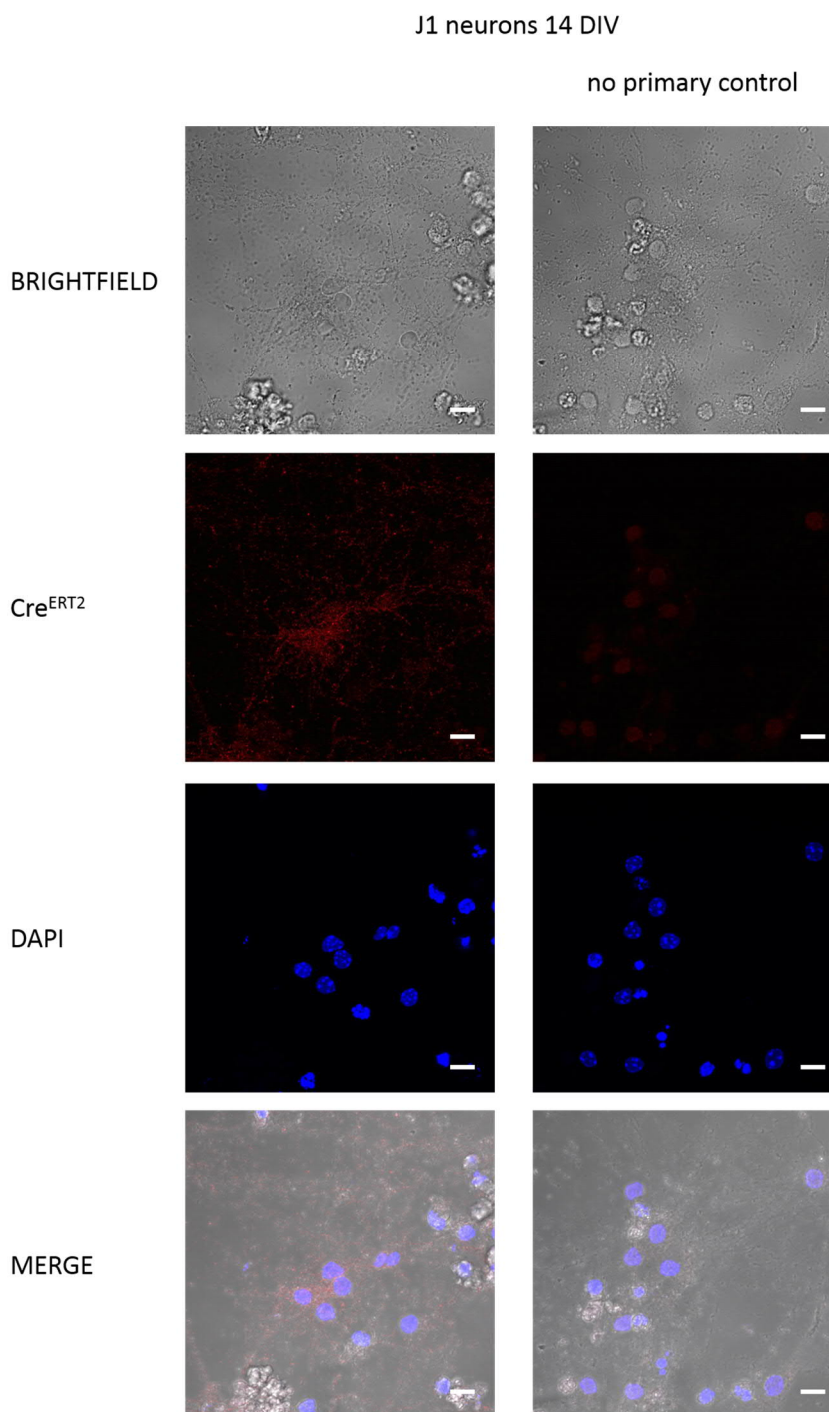
Figure 3.14 Negative control for Cre^ERT2 immunostaining

J1 neurons 14 DIV were stained for Cre^{ERT2} (Alexa-647, red). A single plane brightfield image is shown to identify neurons. Nuclei were stained with DAPI (blue). Only background signal can be detected which is similar to that detected in #1 neurons 14 DIV. Right panel shows neurons stained with no primary antibody. Scale bar 20 μm.

3.4.3 Cre^{ERT2} Western blot

A Western blot analysis was performed to verify Cre^{ERT2} expression. These experiments were complicated by the very low expression levels of Cre^{ERT2} whereby surprisingly, it seemed that 14 days old #1 neurons expressed even slightly lower levels of Cre^{ERT2} (Figure 3.15B). Additionally, #1 neurons clearly expressed less Cre^{ERT2} than the positive control cell line *Rosa26/Cre^{ERT2}* where 4-OHT treatment led to a clear translocation of Cre^{ERT2} (Figure 3.12) and induced successful target excision (Appendix, Figure A.1).
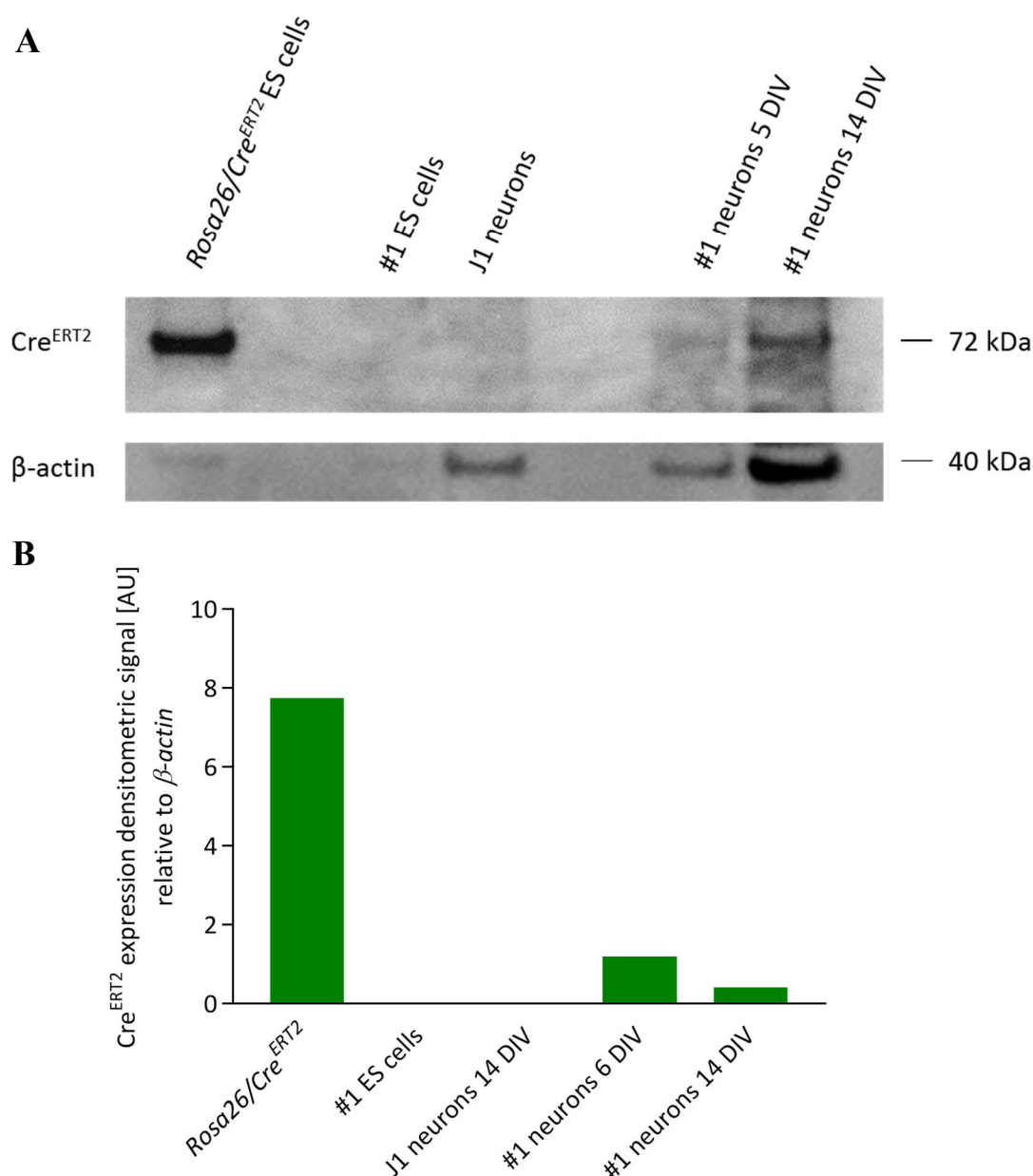
Figure 3.15 Cre^{ERT2} Western blot

Western blot for Cre^{ERT2} was performed. *Rosa26/Cre^{ERT2}* cell line served as a positive control alongside J1 neurons and #1 ES cells as negative control. **A** While high levels of Cre^{ERT2} could be readily detected in the *Rosa26/Cre^{ERT2}* lysates, barely detectable levels could be observed in #1 lysates at 5 DIV that hardly seem to increase at 14 DIV. Note that to ensure Cre^{ERT2} detection in these #1 lysates, comparatively higher levels of proteins were loaded at 14 DIV **B** Quantification of the corresponding Western blot by densitometry. It appears that the levels of Cre^{ERT2} expression seemed to even decrease between 6 DIV and 14 DIV.

3.4.4 Cre electroporation

Given the lack of detectable excision of the *S1p1r* gene following 4-OHT treatment, #1

ES cells were electroporated with a Cre-IRES-GFP plasmid to ease the detection of Cre

in transfected ES cells (Materials and Methods, section 2.8). Forty-eight clones were

picked between five and seven days after electroporation and cultured on a 24-well plate.

Eighteen turned out to be viable and were used for genotyping using primer #1 and #2

(Figure 3.16A). Primer #1 and #2 detect the loxP site at the 5' end of exon 2 (Figure 3.16).

If the excision of exon 2 was successful, primer #2 will have lost its binding site and no

product will be amplified. In WT ES cells, no loxP site is in place and the exon 2 is still

present. Therefore, primer #1 and #2 will amplify a product of 216 bp (Materials and

Methods, section 2.3 and Figure 3.16). It is smaller than the band found in mutant ES

cells carrying the loxP site where a PCR product of 250 bp will be amplified (Figure

3.16A and B). In clone #43 and #46 a band of approximately 200 bp was amplified. The

signal was considerably weaker in clone #43. This band corresponded to the same one

detected in WT J1 ES cells (Figure 3.16B). As the mother cell of clone #43 and #46 was

a mutant cell carrying the loxP site it is not possible to detect a WT band even after the

excision. Therefore, this band can only be explained by the presence of WT MEF in the

culture at the time of genomic DNA extraction. Clone #48 represents a cell line where the

excision was not complete and the loxP site is still present (Figure 3.16B).
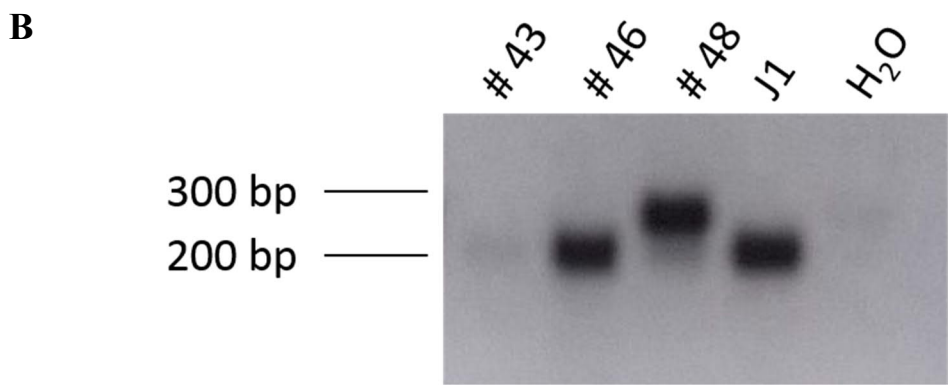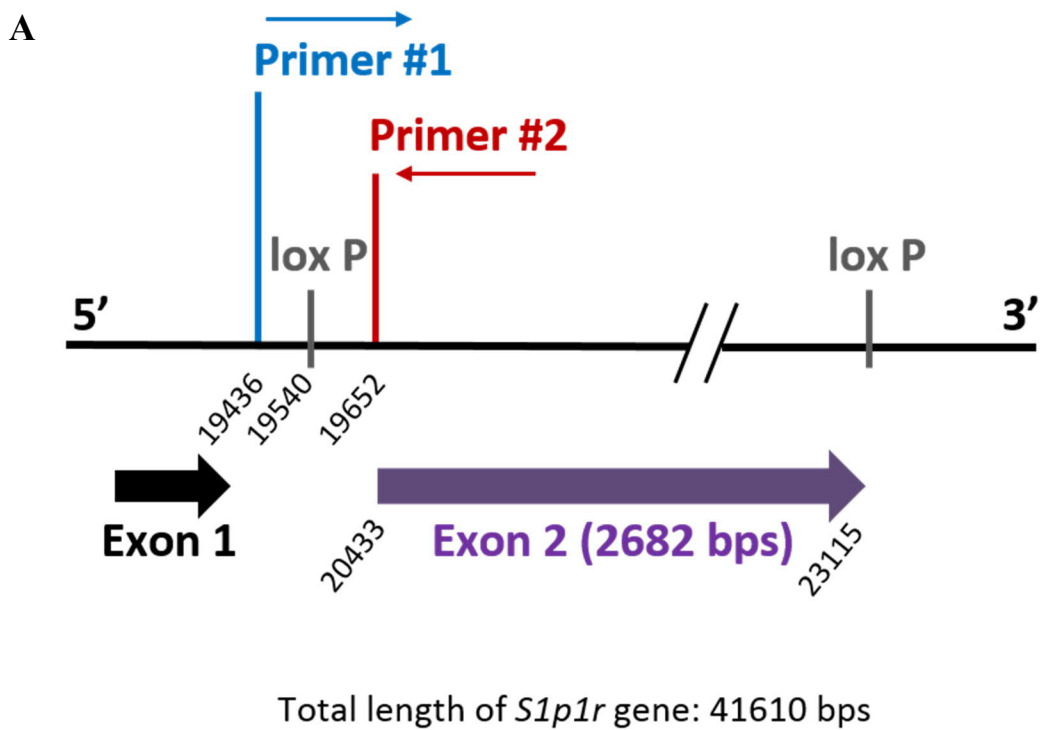
Figure 3.16 Successful excision of exon 2 of the *S1p1r* in cell line #43 and #46

Figure 3.16 Successful excision of exon 2 of the *S1p1r* in cell line #43 and #46

A Schematic of the binding sites of primer #1 and #2, as well as loxP sites on the *S1p1r* gene.

B Different clones were analysed using primer #1 and #2, which detect the loxP site at the 5'

end of the exon 2 and generates a product of 216 bp in WT cells and 250 bp in cells carrying

the loxP site. Note that in clone #43 and #46 a band of 200 bp was amplified, identical to the

band found in WT J1 ES cells. This suggests that the loxP site was successfully excised in

clone #43 and #46, but that genomic DNA contamination with MEF cell DNA was occurring.

In clone #48 a product of 250 bp is amplified, as the loxP site is still present.

Another primer was used to further confirm the excision (Figure 3.17A). Primer #1 and #3 flank the exon 2. Those primers were chosen to detect a product of 200 bp length which will only be amplified if exon 2 was removed (Figure 3.17A). As expected in clone #43 the amplicon of 200 bp is detected, which proved the excision of the exon 2 (Figure 3.17B). The genotyping results suggested that the excision of the *S1p1r* exon 2 was successful in clone #43. However, a contamination of the clone with cells still carrying the *S1p1r* is possible due to the nature of colony picking. If the number of ES cells still expressing the *S1p1r* is low, the PCR may fail to detect it. Therefore, a subcloning procedure was undertaken to ensure clone purity. This resulted in another 12 colonies which were genotyped using the same techniques and clone B2 was chosen due to a clear detection of the product generated with primer #1 and #3 at 200 bp (Figure 3.17B). This PCR was performed with an internal control (*Rosa26*) generating an amplicon of 275 bp to demonstrate that a lack of bands is not due to an inhibition of the PCR reaction (Figure 3.17B and Materials and Methods, section 2.3).

To further confirm the excision, another primer pair #1 and #5 was tested (Figure 3.18). In the event of a successful excision, primer #5 would lose its binding site and no product is expected in *S1p1r*$^{-/-}$ cell lines. Without an excision of exon 2 however, primer #1 and #5 will amplify a PCR product of 1462 bp in WT cell lines and 1496 bp in cell lines carrying the *S1p1r*$^{loxP/loxP}$ gene. Indeed, no product around 1400 bp was detected in cell line #43 and B2 and the expected PCR products were amplified in the J1 and #1 cell line (Figure 3.18B)

A

Total length of *S1p1r* gene: 41610 bps

B
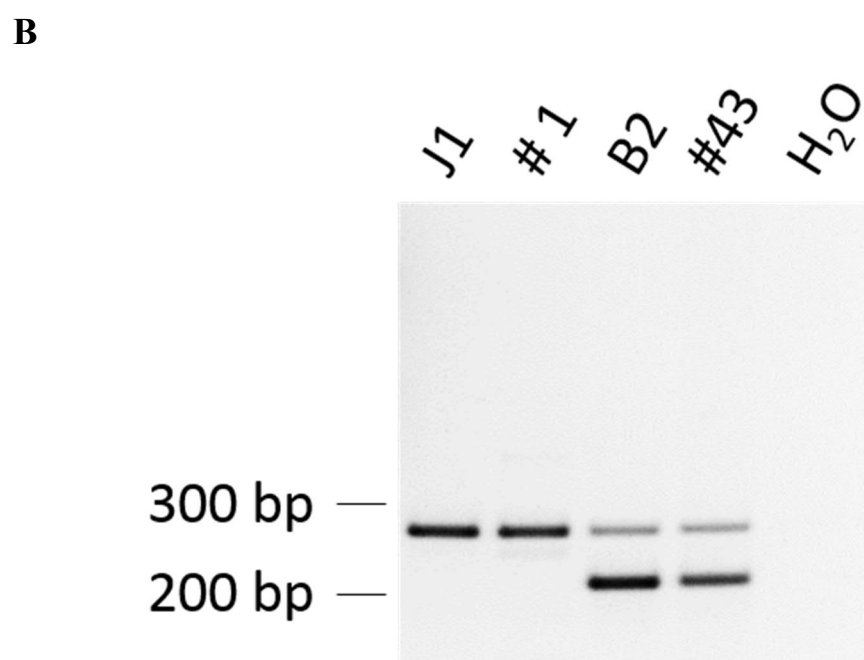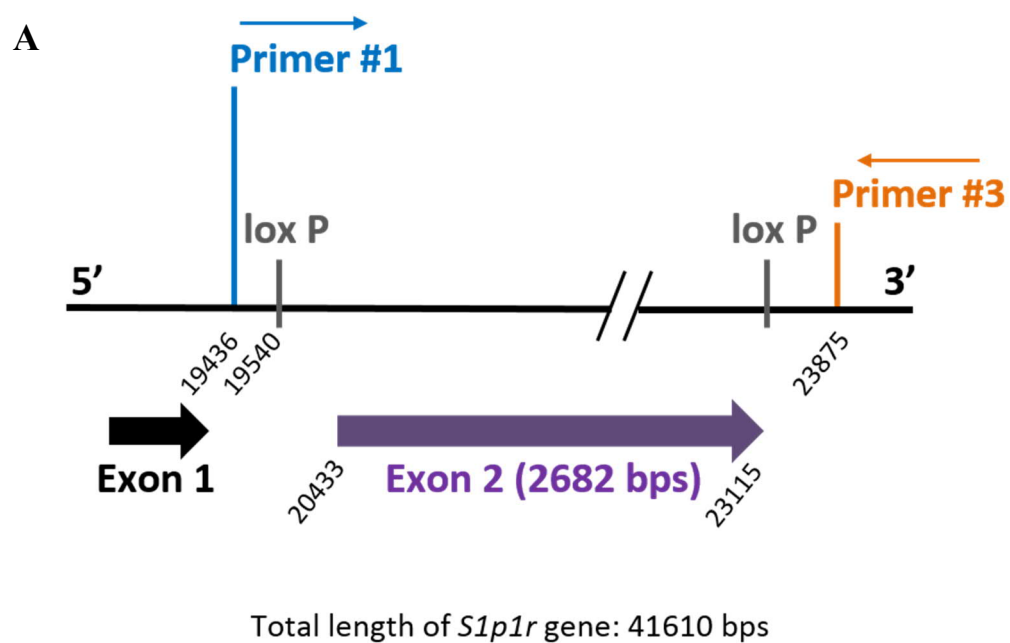
Figure 3.17 Exon 2 was successfully removed in cell lines #43 and B2

Figure 3.17 Exon 2 was successfully removed in cell lines #43 and B2

A Schematic of the binding sites of primer #1 and #3 as well as loxP sites on the *S1p1r* gene.

B The #43 clone was sub-cloned to generate clone B2. Genotyping with primer #1 and #3 detected a PCR product of 200 bp in cell line #43 and B2 which proves the excision of exon 2. The amplicon detected at 275 bp reflects the amplification of the internal control detecting the *Rosa26* locus and demonstrates that the PCR reaction was not inhibited. The 200 bp amplicons were extracted from the gel and sequenced (see below).
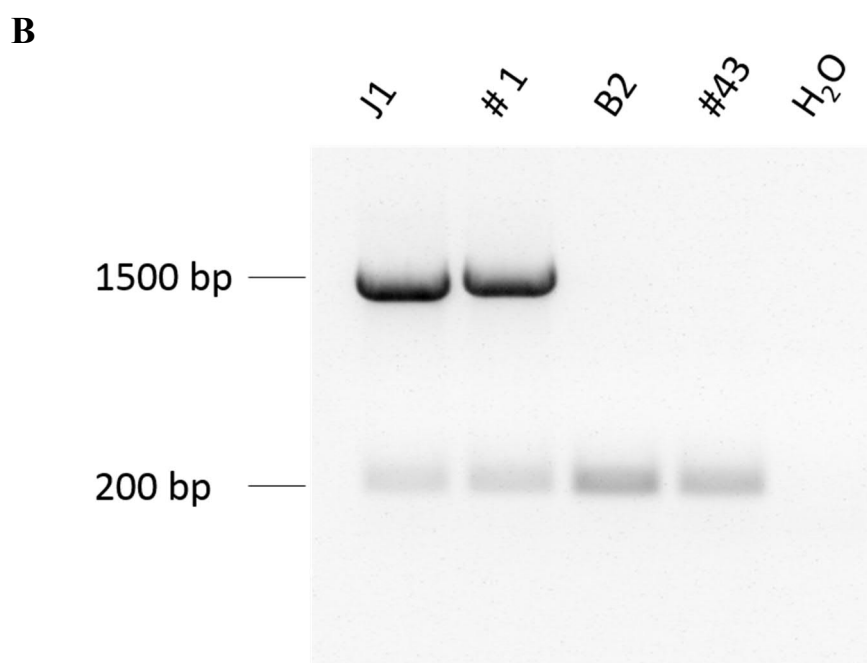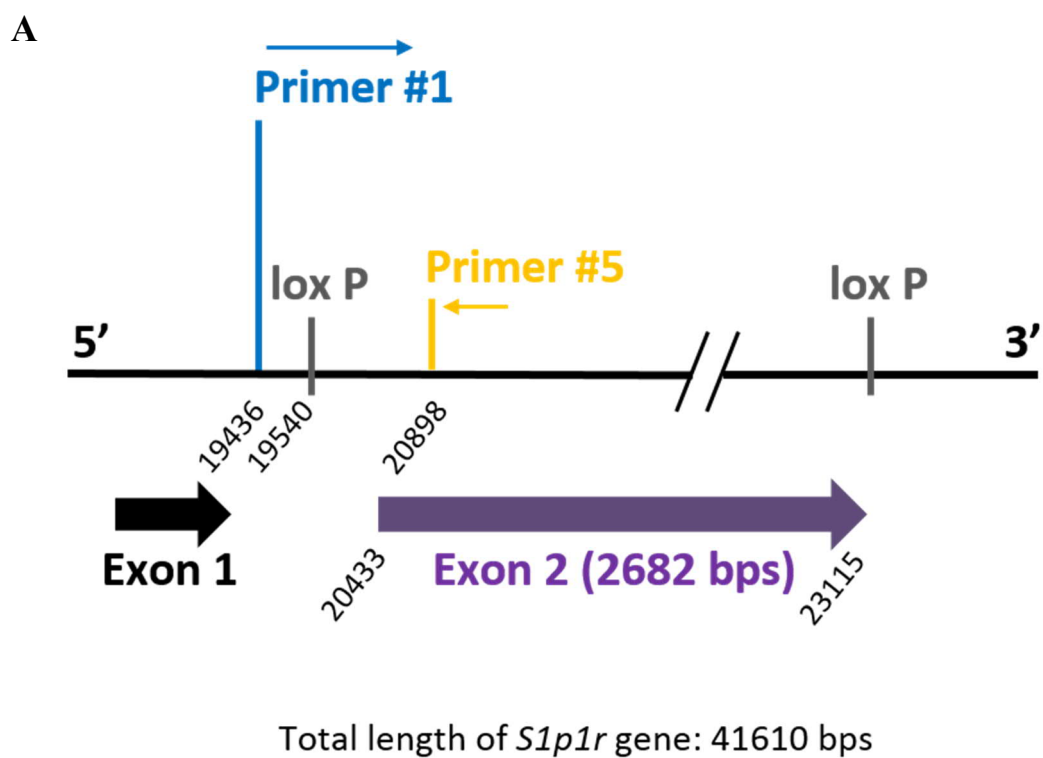
Figure 3.18 PCR with primer #1 and #5 confirmed exon 2 excision in cell line B2 and #43

Figure 3.18 PCR with primer #1 and #5 confirmed exon 2 excision in cell line B2 and #43

A Schematic representation of the binding sites of primer #1 and #5, as well as loxP sites on the *S1p1r* gene. **B** PCR was performed with primers for the internal control *Trdc-c*. In the J1 cell line exon 2 was detected which is represented by the amplicon at 1462 bp. In the #1 cell line the loxP site at position 19540 is detected with primer #1 and #5 and therefore a bigger PCR product of 1496 bp was amplified. In cell line #43 and B2 only the amplicon for the internal control at 200 bp was detected which confirms the excision of exon 2.

The amplicons detected by the primer #1 and #3 in clone #43 and B2 (Figure 3.17C), were sequenced to affirm the excision. The sequence of clone #43 (AGTATGTGTTTCTAGGATTAATGTACCTGAAGTTAAAACAAAGTGGCGTGC TTCGTTATCGCTAGCGCTGCAGGATAACTTCGTATAATGTATGCTATACAAA GTTATCTAGGCCGCCACCGCGGTGGAGCTCCATCTCCAGCCTCTAAGTTGTC CCATTCTAGGACATTGCCTTAGGATCAAA) and B2 (CGTATGTGTTTCTGGAT TAATGTACCTGAAGTTAAAACAAAGTGGCGTGCTTCGTTATCGCTAGCGCTG CAGGATAACTTCGTATAATGTATGCTATACAAAA) matched part of the sequence of the *S1p1r* gene and contained the loxP site at the 5' end of exon 2 (Figure 3.19). These results therefore confirmed the successful excision of exon 2 of the *S1p1r* gene in the #43 and B2 cell line.

Figure 3.19 Alignment of the *S1p1r* sequence with PCR amplicon of #43 and B2 cell lines

Amplicons of the #43 and B2 cell line which were generated with primer pair #1 and #3 were sequenced and aligned with the *S1p1r* sequence. Both sequences aligned from position 19473 shortly after primer #1 (highlighted in blue) until 19540 with the *S1p1r* sequence. At 19540 the full loxP sequence (highlighted in red) could be detected in cell line #43. Only part of it was detected in the B2 cell line as the sequencing was aborted, shown by the polyadenylation tail (highlighted in dark green). The sequence of #43 continued shortly before primer #3 (highlighted in purple) at position 23822 and ended with a polyadenylation tail (highlighted in dark green) after primer #3. Part of the sequence of the 200 bp amplicon in #43 and B2 ES cells therefore corresponded to the *S1p1r* gene and confirmed the excision of exon 2.

3.4.5 Analysing S1p1r excision using Western blot

To explore whether the removal of *S1p1r* could also be documented at protein level, Western blots were performed using two frequently used and commercially available antibodies targeting S1P1R. Specifically, the membrane was first incubated with the polyclonal antibody from Cayman Chemical (Figure 3.20), then stripped and incubated with the monoclonal antibody from Millipore (Figure 3.21). The polyclonal antibody revealed a main band of about 50 kDa expressed at similar levels in both WT and B2 neurons. The monoclonal antibody showed a single band of about 43 kDa with again similar intensity in B2 neurons (Figure 3.21). According to the literature murine S1P1R is detected at around 47 kDa (Crousillac et al. 2009; Brizuela et al. 2014; Efstathopoulos et al. 2015) or 37 kDa (Silva et al. 2017). Additionally, a range between 35 kDa to 75 kDA has been reported when the S1P1R was tagged with a human influenza hemagluttinin (HA) or Flag epitope and recognised by the corresponding antibodies (Kohno et al. 2002; Shiow et al. 2006). This range can be explained by the glycosylation of the receptor and other possible posttranslational modifications (Kohno et al. 2002).

3.4.6 Analysing S1p1r excision using immunocytochemistry

Further analysis was performed using an immunocytochemistry staining with the same polyclonal antibody from Cayman Chemical. In line with the data obtained in Western blot, a signal for the S1P1R was detected in J1 as well as B2 neurons. The staining intensity was similar in all neurons and lacked specificity, indicated by the ubiquitous signal detection which was close to background levels (Figure 3.22 and 3.23).

A
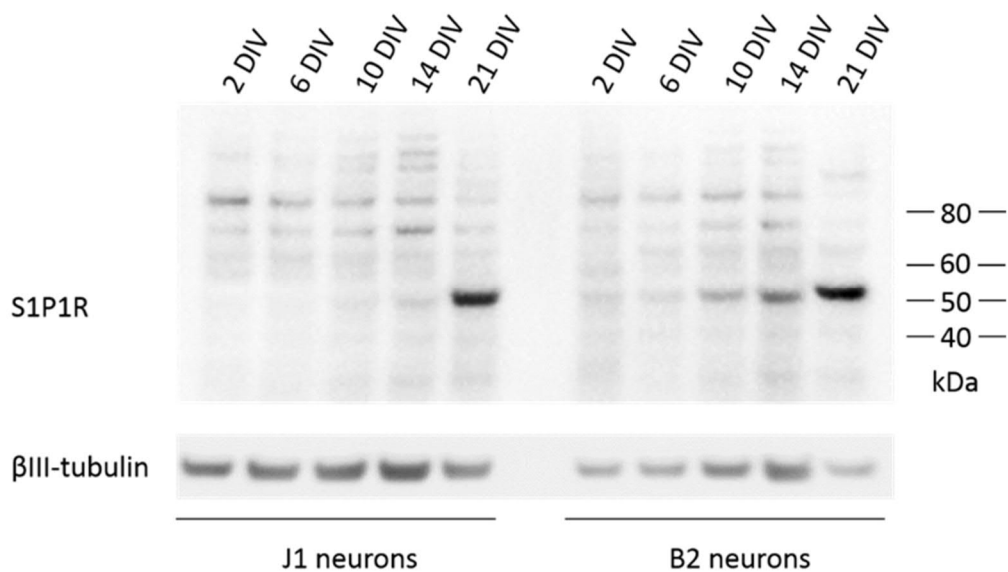
B
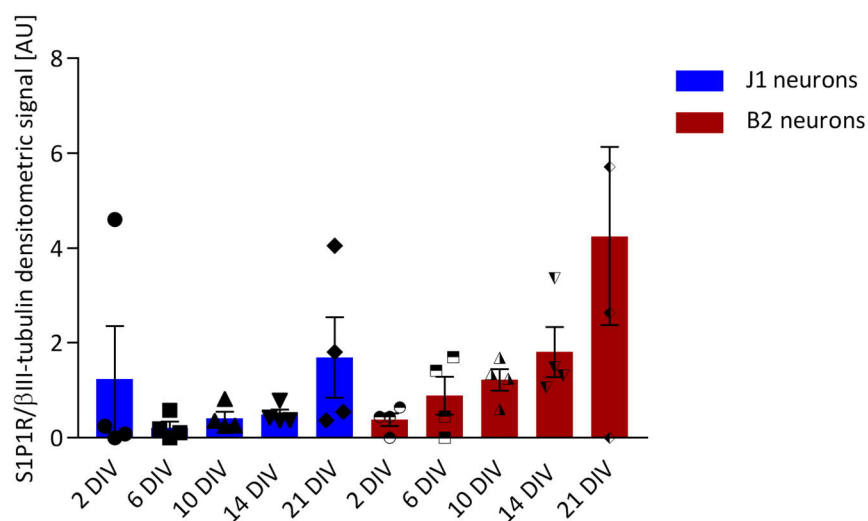
Figure 3.20 Polyclonal antibody detected S1P1R in both cell lines by Western blot

A Western blot representing S1P1R expression in J1 and B2 neurons between 2 and 21 DIV. The polyclonal antibody from Cayman Chemical detected a protein around 50 kDa. 20 µg of protein were loaded per lane. **B** Graph shows densitometric analysis. S1P1R expression was similar in both cell lines (Kruskal-Wallis test, $p > 0.05$, $n = 4$). βIII-tubulin was used as internal control. Graph represents values of the mean ± SEM.
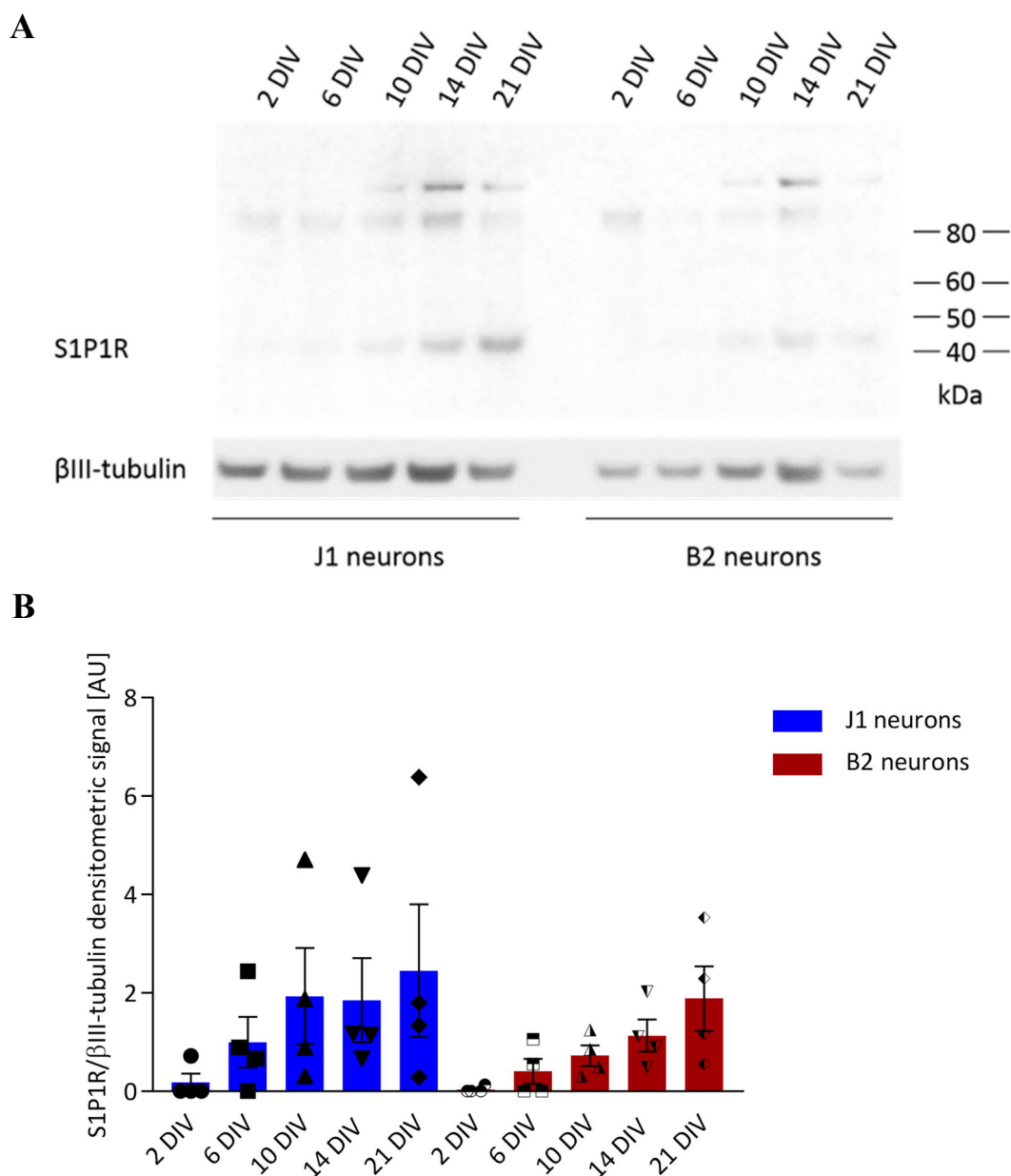
Figure 3.21 S1P1R detection by Western blot using a monoclonal antibody

A Western blot representing longitudinal S1P1R expression in J1 and B2 neurons between 2 and 21 DIV. The monoclonal antibody from Millipore detected a protein around 43 kDa. 20 μg of protein were loaded per lane. **B** Graph shows densitometric analysis. S1P1R expression was similar in both cell lines (Kruskal-Wallis followed by a Dunn's multiple comparison, $p > 0.05$, $n = 4$). βIII-tubulin was used as internal control. Graph represents values of the mean ± SEM.

J1 neurons 14 DIV

no primary
control

BRIGHTFIELD

S1P1R

DAPI

MERGE
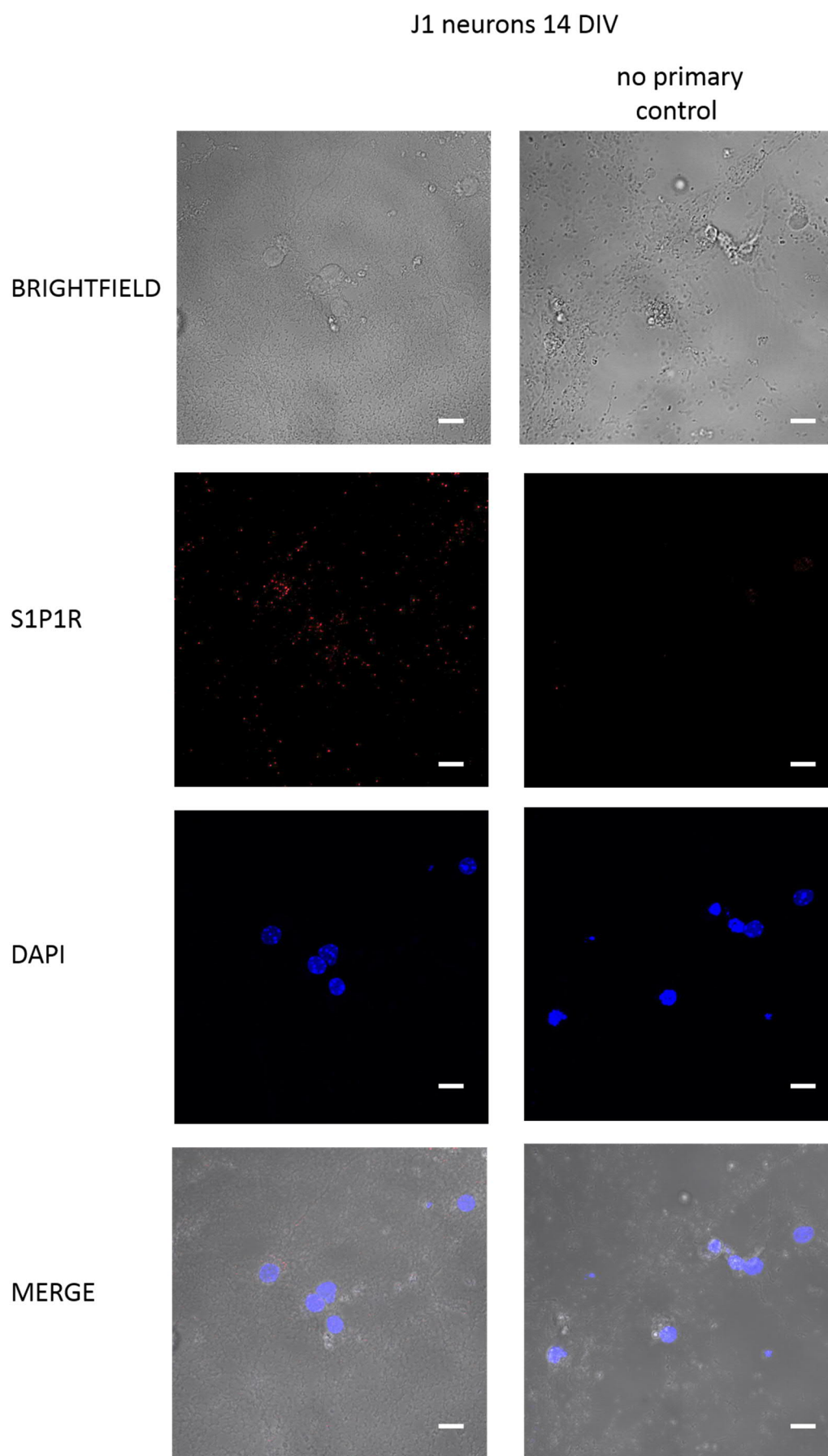
Figure 3.22 S1P1R antibody detected a weak signal in J1 neurons

Figure 3.22 S1P1R antibody detected a weak signal in J1 neurons

J1 neurons 14 DIV were stained with anti-S1P1R (Alexa Fluor 647 – red). Brightfield picture illustrates a single plane scan to allow identification of neurons. The rest of the images illustrate maximum intensity projections. Nuclei were stained with DAPI. In J1 neurons a faint staining for the S1P1R could be detected throughout the culture at the same intensity as high background staining, indicative of a lack of antibody specificity. Right panel corresponds to a control staining with no primary antibody. Scale bar 20 µm.

B2 neurons 14 DIV

no primary
control

BRIGHTFIELD

S1P1R

DAPI

MERGE
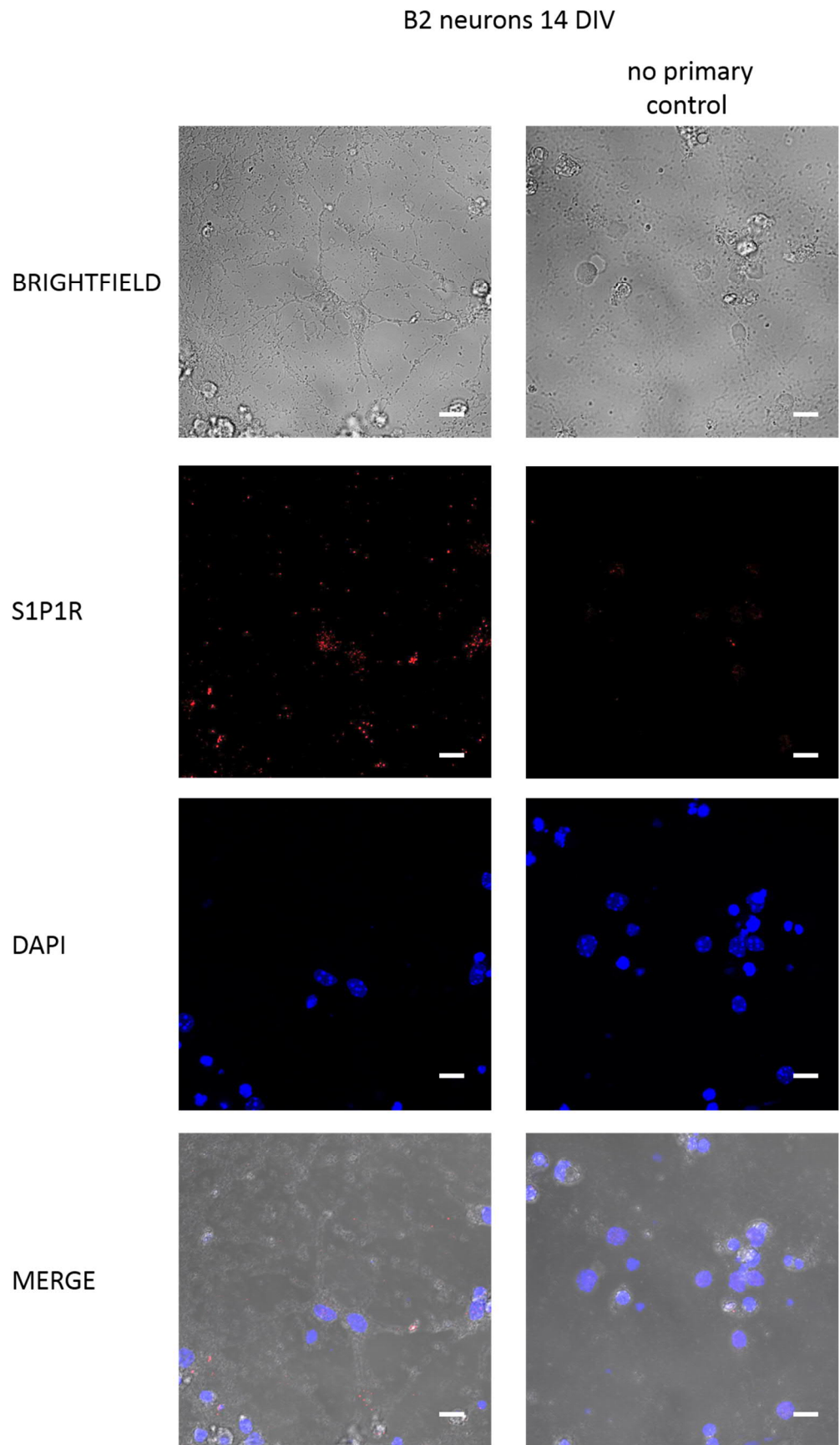
Figure 3.23 S1P1R antibody detected unspecific signal in B2 neurons

Figure 3.23 S1P1R antibody detected unspecific signal in B2 neurons

B2 neurons 14 DIV were stained with anti-S1P1R (Alexa Fluor 647 – red). Brightfield picture illustrates a single plane scan to allow identification of neurons. The rest of the images illustrate maximum intensity projections. Nuclei were stained with DAPI. In B2 neurons a staining for S1P1R of a similar intensity to that found in J1 neurons was detected throughout the culture. Right panel corresponds to a control staining with no primary antibody. Scale bar 20 μm.

3.4.7 Analysing S1p1r excision using RT-qPCR

Next, the mRNA was extracted of 14 days old J1 and B2 neurons and analysed using a TaqMan® RT-PCR Assay. These experiments revealed that no *S1p1r* mRNA could be detected in the B2 *S1p1r*$^{-/-}$ cell line, further confirming receptor excision (Figure 3.24).
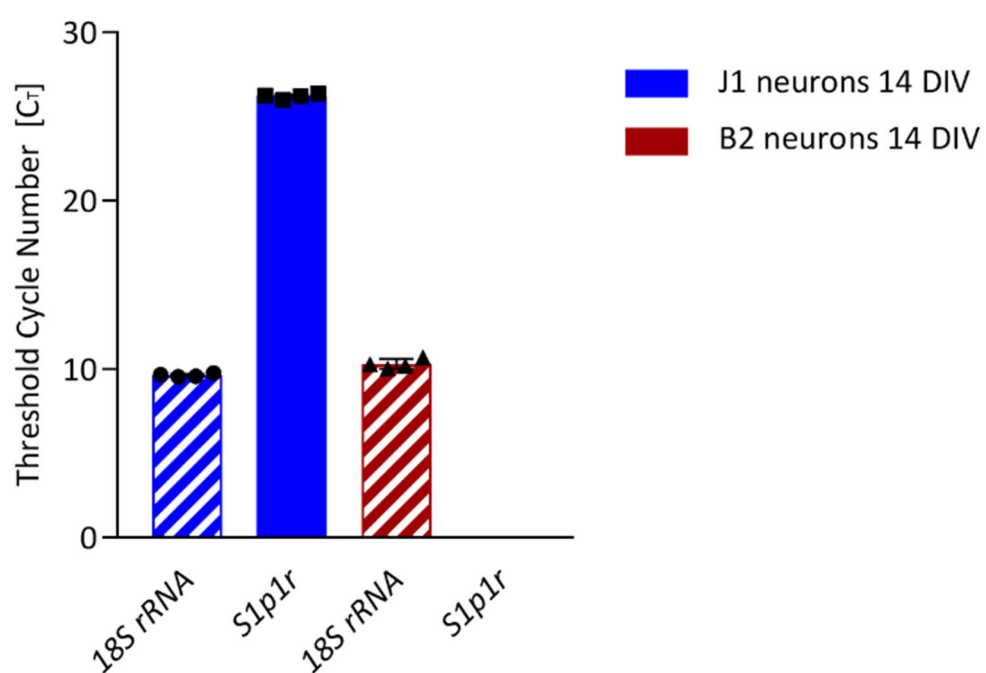
Figure 3.24 RT-PCR confirmed the successful *S1p1r* excision in B2 neurons

No *S1p1r* expression was detected in the *S1p1r*$^{-/-}$ cell line B2. As a positive control WT J1 neurons

were used. Threshold cycle numbers are presented.

3.5 Differentiation of B2 ES Cells into Neurons

In contrast to the differentiation of J1 ES cells, known to give rise to essentially pure cultures of glutamatergic-like neurons (Bibel et al. 2004), the differentiation of the mutant B2 ES cells while also generating neurons (see below), gave rise to large numbers of non-neuronal cells alongside neurons. In addition, mutant B2 neurons did not survive for longer than 12 DIV using the standard cell culture protocol, possibly as a result of being outcompeted by the rapidly growing non-neuronal cell population (Figure 3.25 and 3.26). To reduce the number of non-neuronal cells, the mitotic inhibitor 5-FdU was added to the culture. To determine the best time point for, as well as duration of drug treatment, different protocols were tested and it turned out that the addition of 5 µg/ml 5-FdU from 2 DIV to 4 DIV of the neuronal culture gave the best results.

Glial fibrillary acidic protein (GFAP), a widely used marker for astrocytes (Middeldorp and Hol 2011), was used to demonstrate the successful reduction of GFAP-expressing cells after 5-FdU treatment in the J1 and B2 cultures (Figure 3.27). Indeed, after 5-FdU treatment GFAP was not detectable anymore by Western blot in J1 and B2 cultures (Figure 3.27). GFAP levels were normalised to β-actin. The neuronal marker βIII-tubulin could not be used as a loading control as its levels varied significantly between the different conditions. Expression levels of βIII-tubulin were significantly reduced in untreated B2 cultures compared to treated J1 neurons (*p (Ø B2 *vs.* 5-FdU J1) < 0.05, Figure 3.27D). This also shows that 5-FdU selectively kills proliferating cells and as neurons are post-mitotic this treatment should not and did not detectably affect them under the conditions used here (Figure 3.27).
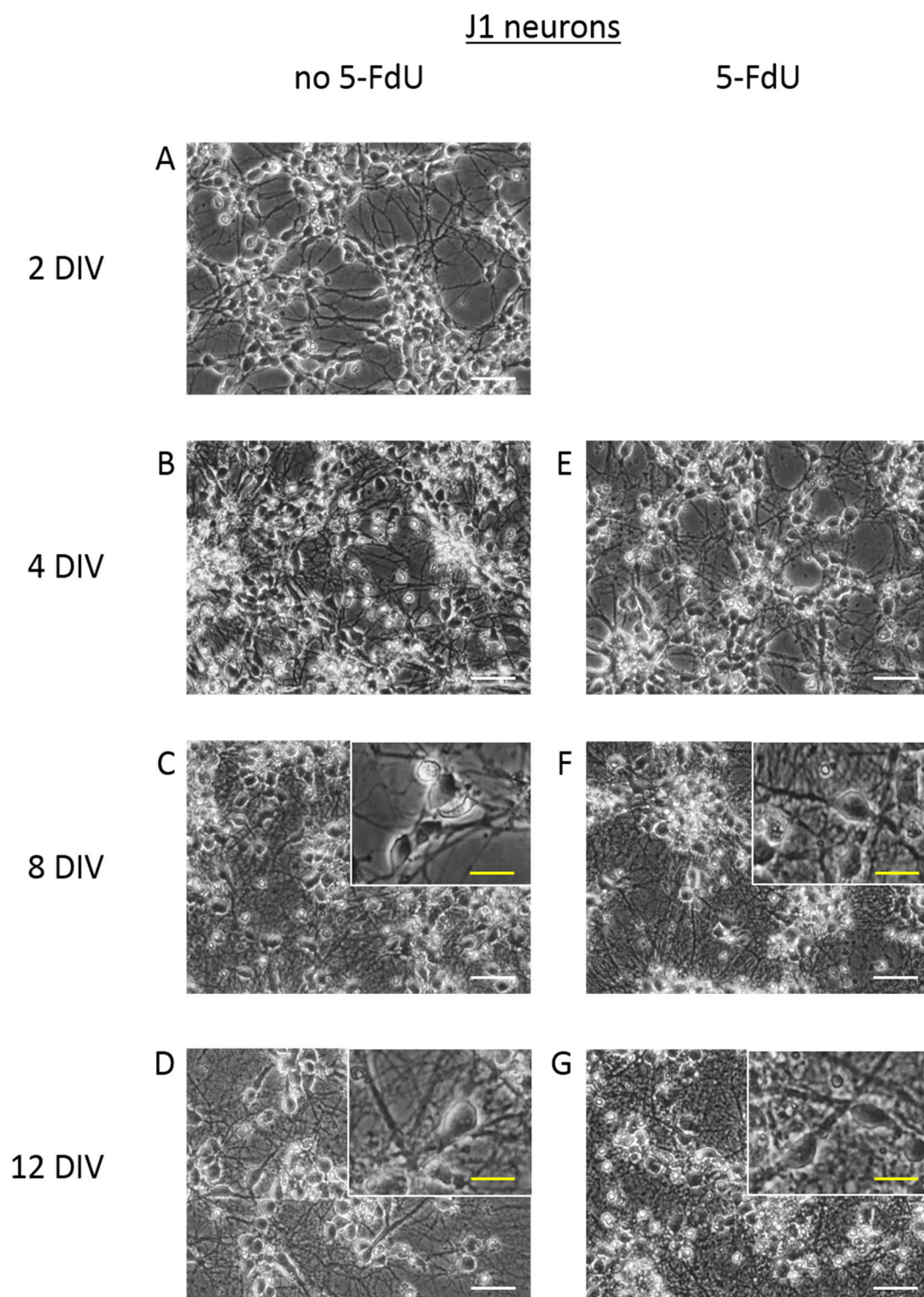
Figure 3.25 Survival and purity of J1 neurons with and without 5-FdU treatment

J1 neurons treated with 5 µg/ml 5-FDU at 2 DIV (E – G) were not different with regard to survival or apparent number of non-neuronal cells compared with untreated controls (A – D). White scale bar 50 µm. Yellow scale bar 20 µm.
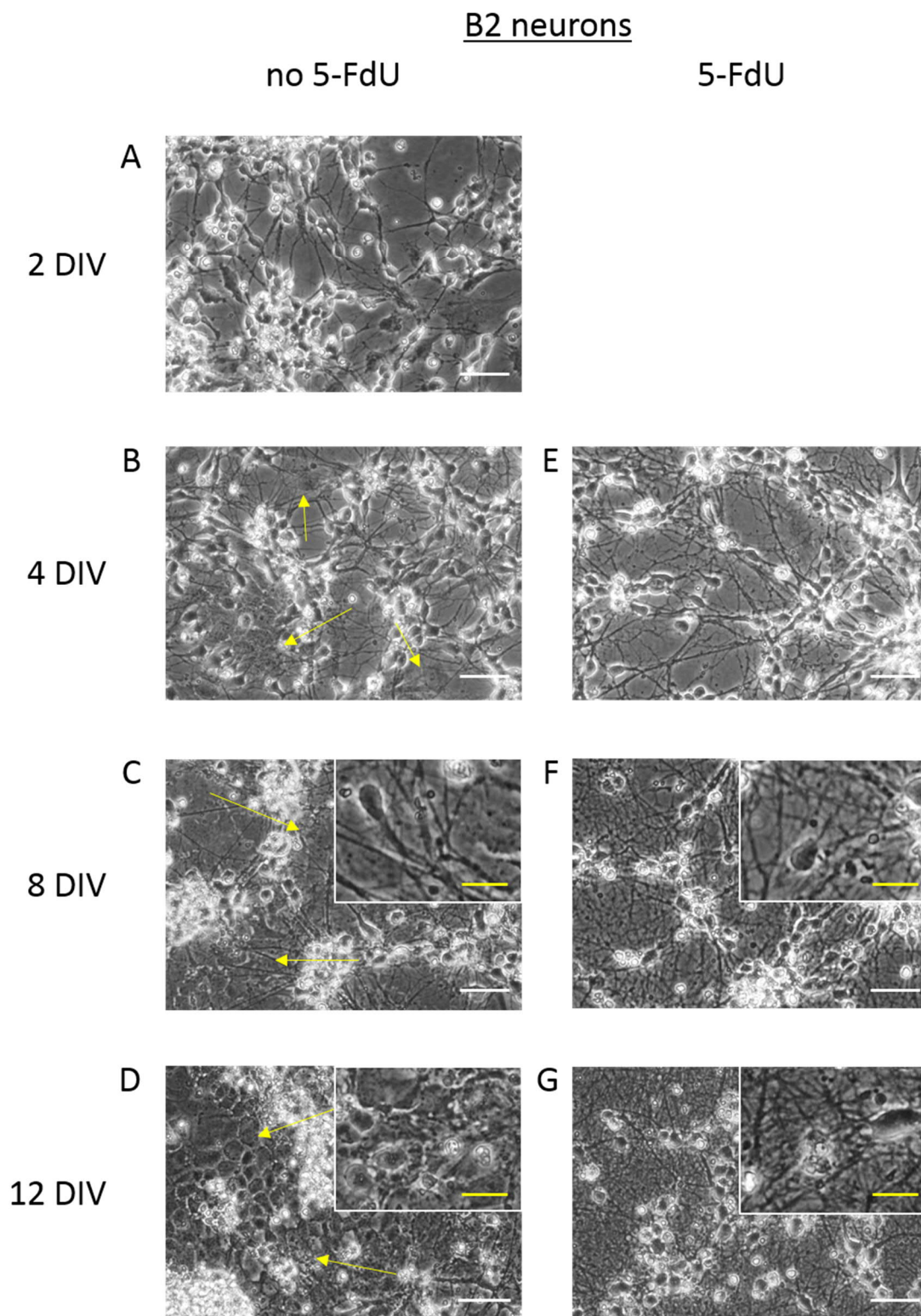
Figure 3.26 Survival and purity of B2 neurons with and without 5-FdU treatment

The survival of B2 neurons was dramatically improved following the addition of 5 µg/ml 5-FdU from 2 DIV – 4 DIV (compare D and G). At 12 DIV hardly any neurons are visible in the untreated B2 culture (note the lack of neuronal processes in D). Arrows point to non-neuronal cells (C and D). White scale bar 50 µm. Yellow scale bar 20 µm.

A

B

C

D
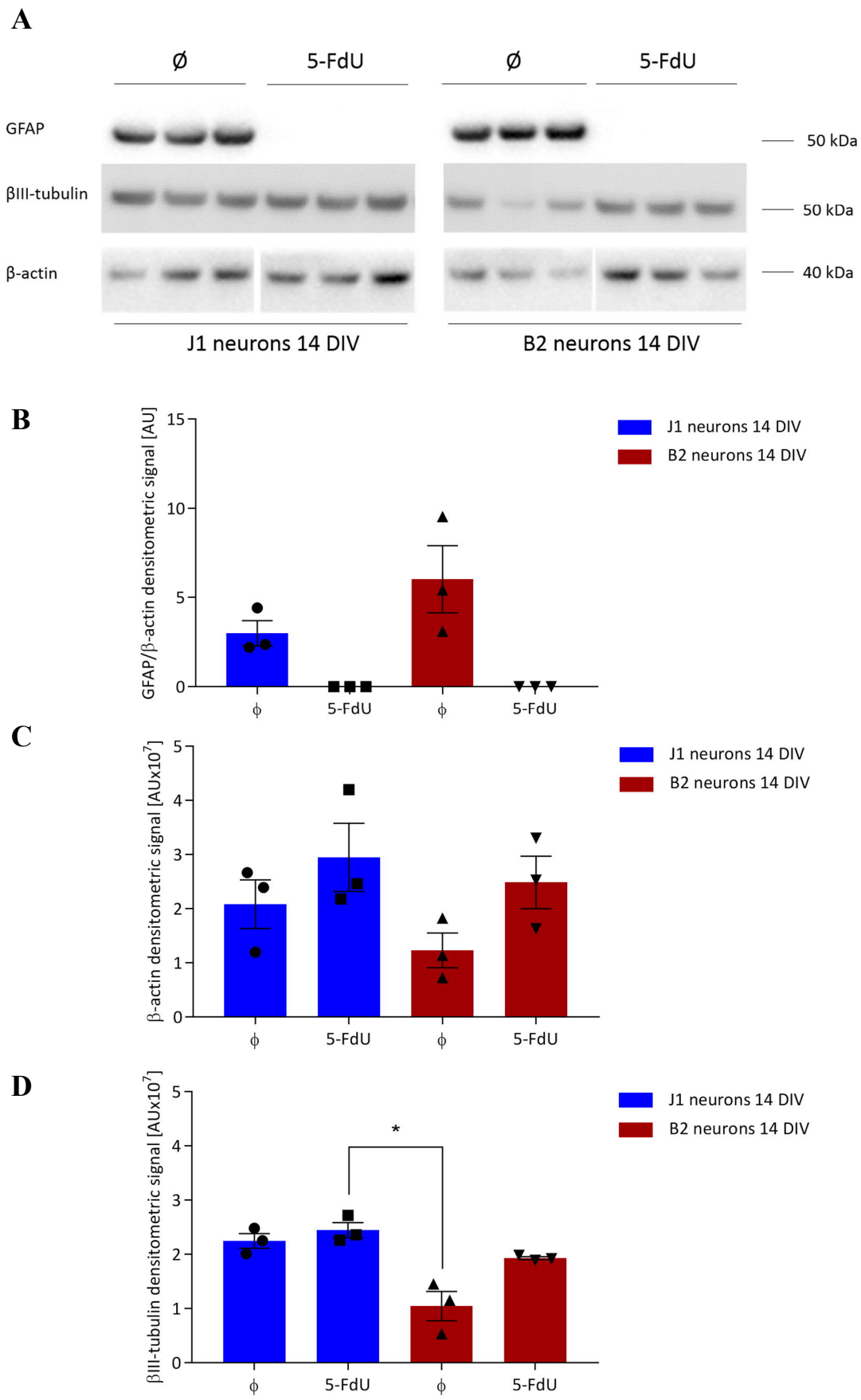
Figure 3.27 5-FdU treatment depleted cultures of GFAP-expressing cells

Figure 3.27 5-FdU treatment depleted cultures of GFAP-expressing cells

A Western blot reflects the expression of GFAP in 5-FdU treated and untreated J1 and B2 neurons. 20 µg of protein loaded per lane. **B** GFAP was no longer detectable in J1 and B2 neurons treated with 5-FdU. Levels were normalised to β-actin as **C** β-actin (Kruskal Wallis test, $p > 0.05$, n = 3) were similar between conditions opposed to **D** βIII-tubulin. In untreated B2 neurons βIII-tubulin levels were significantly reduced compared to 5-FdU treated J1 neurons (Kruskal Wallis test followed by Dunn's multiple comparison, *p (Ø B2 vs. 5-FdU J1) < 0.05, n = 3). Untreated samples are three different samples of one differentiation, whereas treated samples are of three independent differentiations. All graphs represent densitometric analysis. Data are represented as mean ± SEM. Ø: untreated cells.

3.6 Characterisation of J1 and B2 Neurons

The differentiation of mouse ES cells into neurons using the protocol of Bibel and colleagues is known to lead to the generation of excitatory neurons, as previously established using antibodies to the glutamate vesicular transporters (Bibel et al. 2004; Bibel et al. 2007) as well as other neuronal markers such as synaptophysin and the AMPA receptor subunit GluR1 (Bibel et al. 2004).

3.6.1 Synaptophysin expression in J1 and B2 neurons

To test whether the excision of the S1P1R from ES cells would influence the differentiation process, neuronal markers were used to monitor neuronal maturation in B2 neurons compared with J1 WT neurons. This is an important point as S1P1R has been previously shown to be somehow involved in neurogenesis. Indeed, the receptor is expressed in the mouse brain during embryogenesis and *S1p1r*$^{-/-}$ mice show severe cell loss in the forebrain (McGiffert et al. 2002; Mizugishi et al. 2005). To investigate whether maturation of WT and B2 mutant neurons would proceed similarly, the levels of the synaptic protein synaptophysin were quantified by Western blot (Figure 3.28). Synaptophysin expression levels followed a similar expression pattern in J1 and B2 neurons resulting in no statistically significant difference detected at any time point measured ($p > 0.05$, Figure 3.28). Synaptophysin was not detectable in J1 and B2 cultures before 10 DIV (Figure 3.28). These results suggest that S1P1R may not be required for synaptophysin expression by excitatory neurons.

A
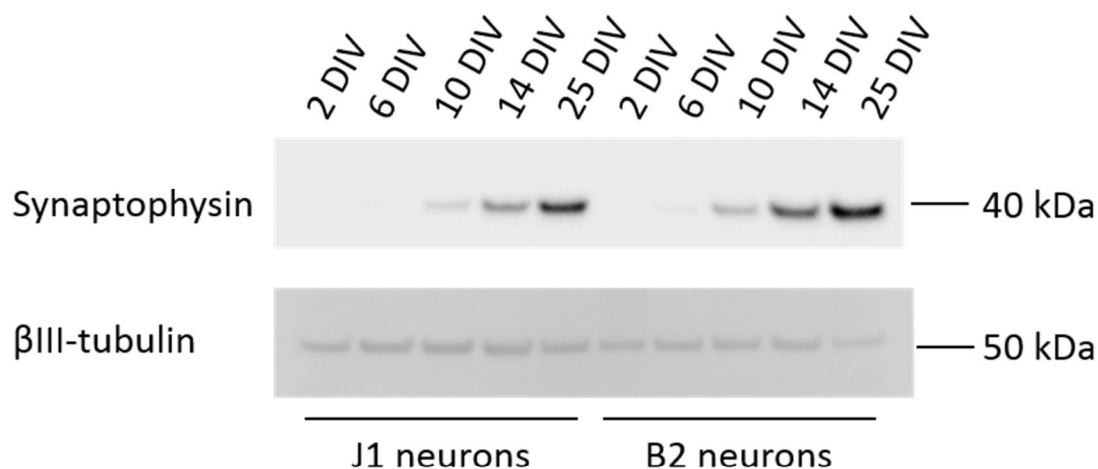
B
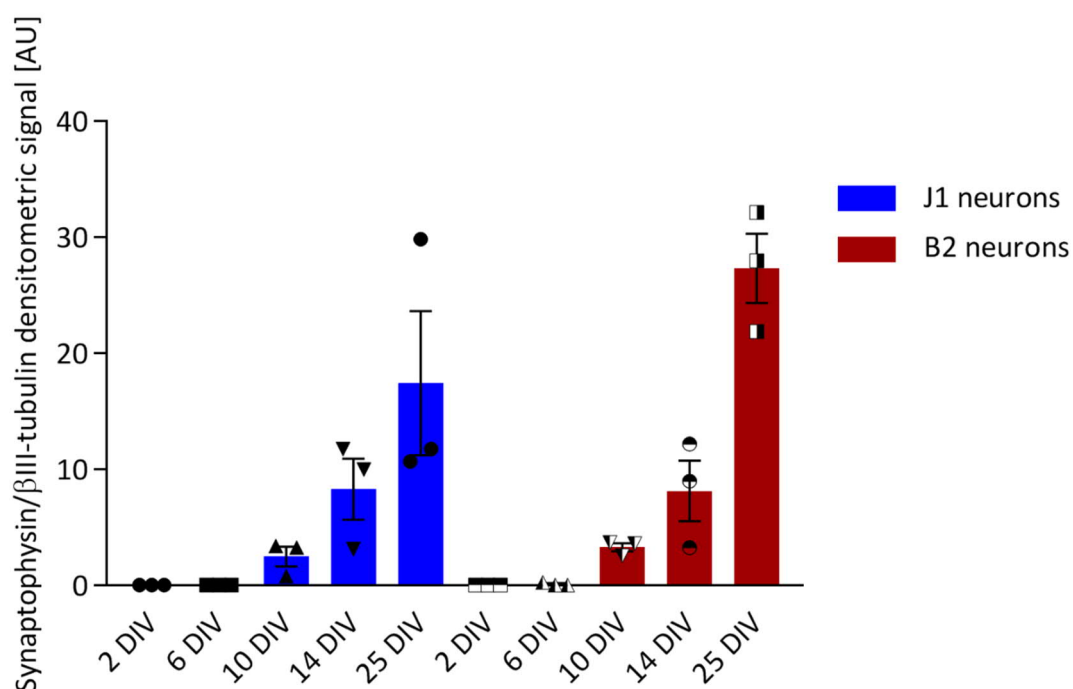
Figure 3.28 J1 and B2 neurons matured at similar rates as assessed by synaptophysin expression
Synaptophysin levels were analysed in J1 and B2 neuronal cultures at different time points. **A** Western blot for synaptophysin showed expression after 10 DIV and subsequent increase during maturation of the neurons. 20 µg of protein were loaded per lane. **B** Graph represents densitometric analysis. Both cultures expressed similar levels of synaptophysin (Kruskal-Wallis test followed by Dunn's multiple comparison test, $p > 0.05$, $n = 3$). Data was normalised to internal control βIII-tubulin. Graphs represent values of the mean ± SEM.

3.6.2 BDNF expression levels in J1 and B2 neurons

Given that a main goal of the project is to investigate the role of the S1P1R in the regulation of BDNF levels by FTY720, it was essential to establish that BDNF is detectable in B2 neurons. BDNF levels were barely detectable at early time points but higher levels were detectable over time, in both J1 and B2 neurons (Figure 3.29). These results suggest that the lack of S1P1R may not directly affect BDNF protein levels in ES cell-derived neurons.

A
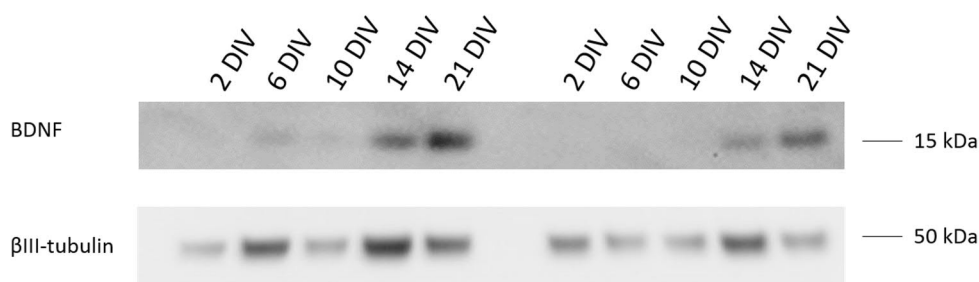
B
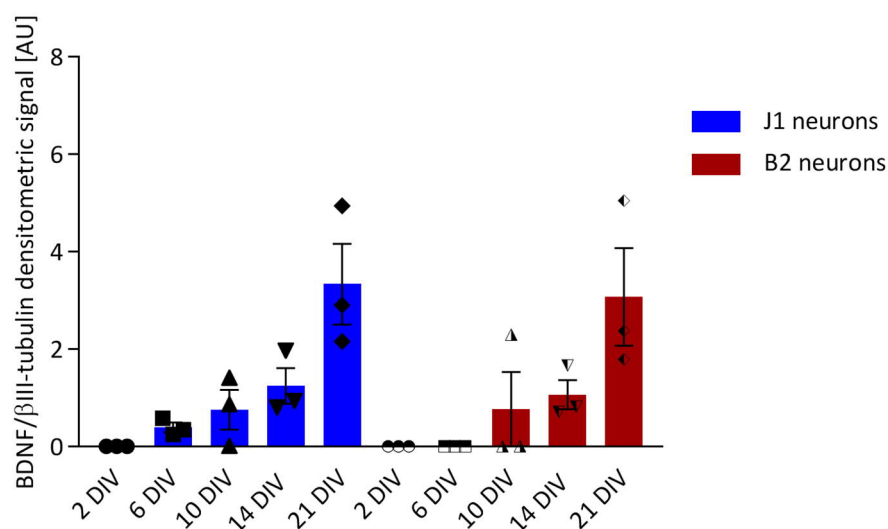
Figure 3.29 BDNF expression levels were similar in J1 and B2 neurons

Longitudinal BDNF protein expression levels were investigated in J1 and B2 neurons from 2 – 21 DIV. **A** Western blot represents BDNF expression in J1 and B2 neurons. 20 µg of protein were loaded per lane. BDNF levels were barely detectable before 10 DIV. **B** Graph represents densitometric analysis. No difference between the BDNF expression in J1 and B2 neurons was detected at any time point during the maturation of the neurons (Kruskal Wallis test followed by Dunn's multiple comparison, $p > 0.05$, n = 3). Data was normalised to internal control βIII-tubulin. Graph represents values of the mean ± SEM.

3.6.3 vGlut1 and vGlut2 mRNA expression in J1 and B2 neurons

To further compare the maturation of J1 and B2 neurons, the expression of the vesicular glutamate transporters 1 and 2 (*vGlut1* and *2*) were analysed using RT-qPCR. RNA was extracted from two and 14 days old neurons and the levels of *vGlut1* mRNA found to be identical in both cultures, with no significant changes during neuronal maturation (Figure 3.30A). Likewise, the expression levels of *vGlut2* mRNA were identical in J1 and B2 neurons. Levels of *vGlut2* mRNA increased significantly during the maturation of the J1 neurons (2 DIV *vs.* 14 DIV: 51-fold increase) as well as B2 neurons (2 DIV *vs.* 14 DIV: 33-fold increase, Figure 3.30B).

3.6.4 vGlut2 protein expression in J1 and B2 neurons

To investigate if the mRNA levels reflect the expression levels of vGlut2 on protein levels in J1 and B2 neurons a Western blot was performed. The analysis was focused on vGlut2 only as our group has previously shown that vGlut1 could not be reliably discriminated from vGlut2 in Western blot and immunocytochemistry (Schrenk-Siemens et al. 2008). Unexpectedly, vGlut2 protein levels were significantly higher expressed in B2 neurons compared to J1 neurons (*p < 0.01) after 14 days in culture (Figure 3.31).

A

B
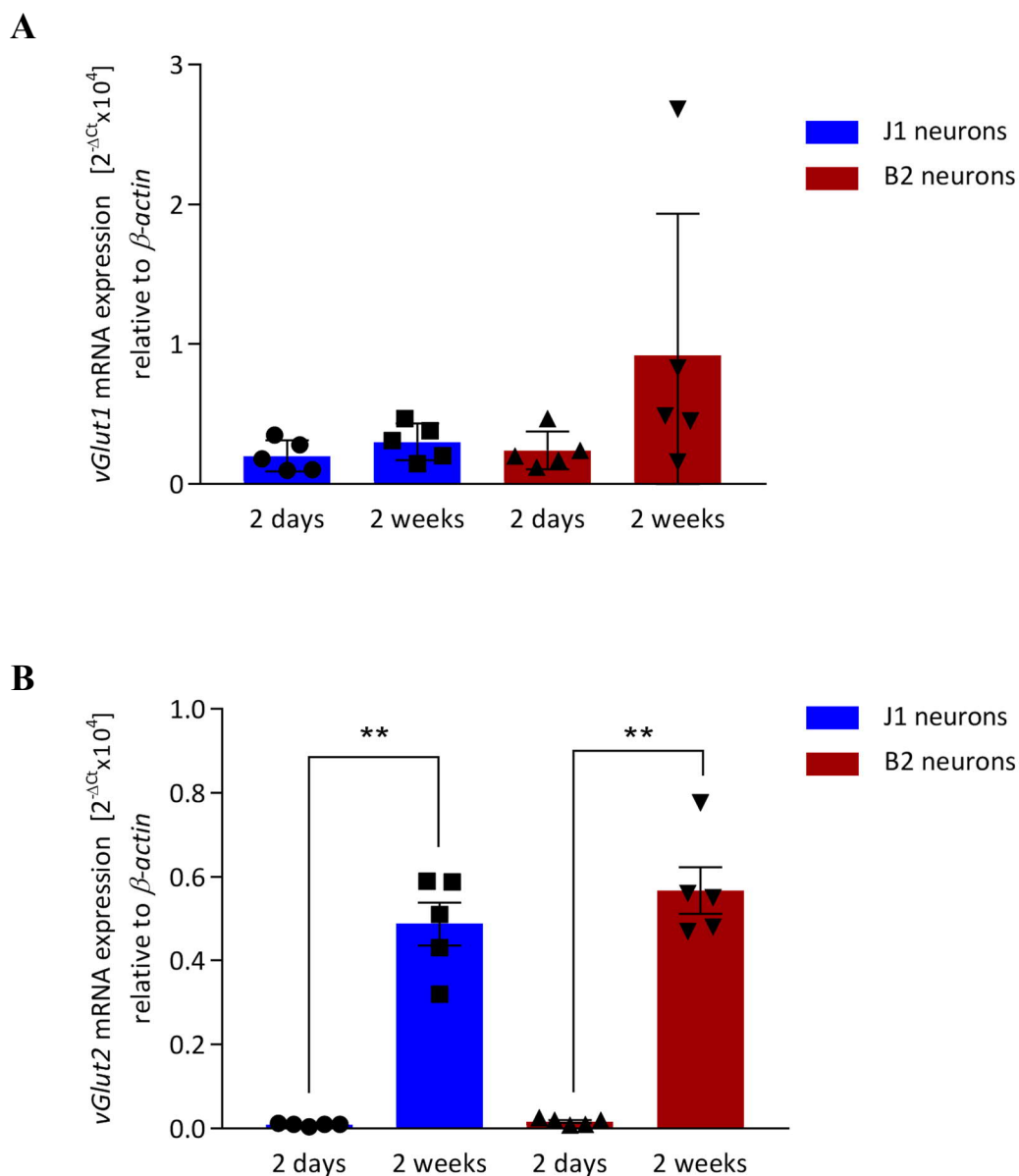
Figure 3.30 *vGlut1* and *vGlut2* expression levels were similar in J1 and B2 neurons

Expression pattern of vGlut1 (One-way ANOVA, p (J1 vs. B2) > 0.05, n = 5) and vGlut2 (Kruskal Wallis test, p (J1 vs. B2) > 0.05, n = 5) mRNA was identical in J1 and B2 neurons at both time points. **A** vGlut1 expression stayed constant over the course of 14 days, whereas **B** vGlut2 expression increased during maturation of the neurons (Mann-Whitney test, **p (2 days vs. 2 weeks) < 0.01, n = 5). Data is presented as 2-ΔCtx104. Data was normalised to internal control β-actin. Graphs represent values of the mean ± SEM.

A

B
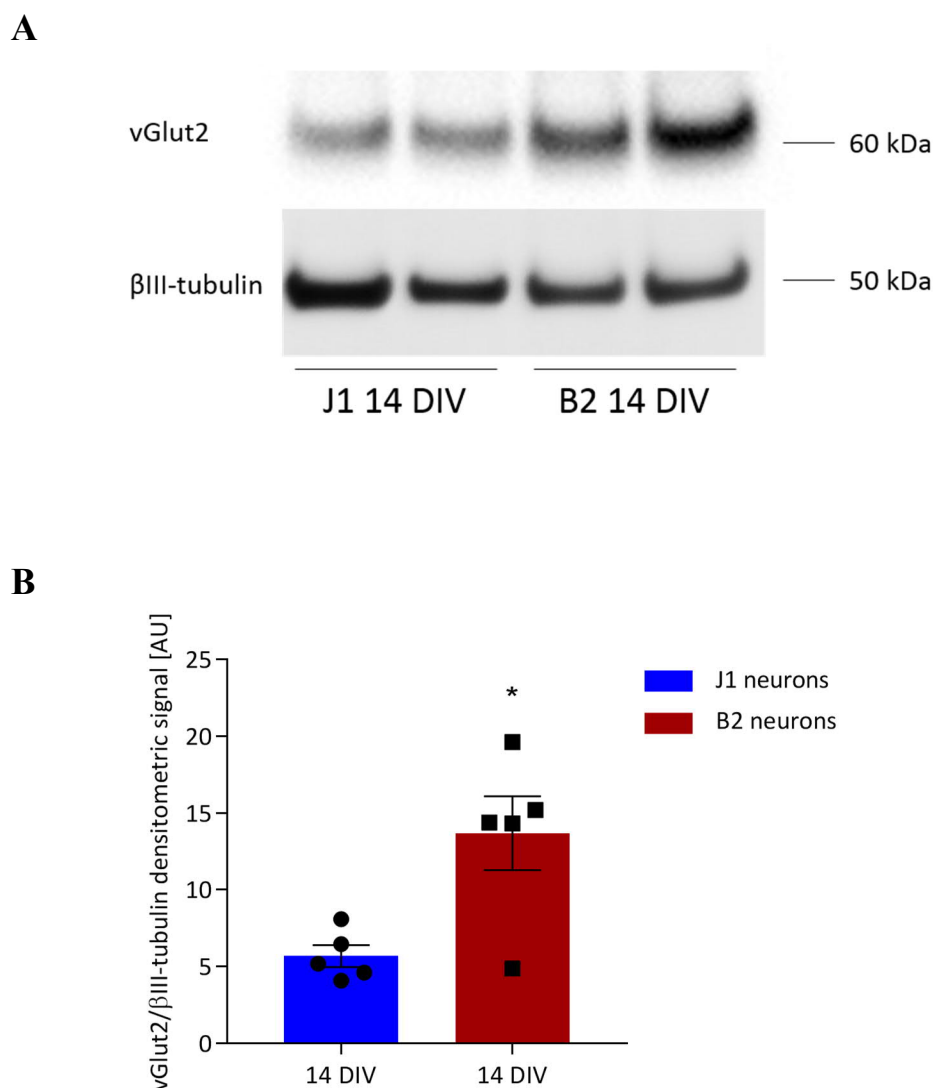
Figure 3.31 vGlut2 protein expression in J1 and B2 neurons after 14 days in culture

Protein levels of vGlut2 were analysed in 14 days old J1 and B2 neurons. **A** Western blot represents vGlut2 expression in J1 and B2 neurons 14 DIV. 20 μg total protein were loaded per lane. **B** Graph shows densitometric analysis. Levels of vGlut2 were expressed at significantly higher levels in B2 compared to J1 neurons after 14 days in culture (Unpaired t test, $*p < 0.05$, n = 5). Data was normalised to internal control βIII-tubulin. Graph represents values of the mean ± SEM.

3.6.5 Tbr1 mRNA expression in J1 and B2 neurons

To explore a possible cortical identity of J1 and B2 neurons, expression levels of the T-box brain gene 1 (*Tbr1*) mRNA were analysed by RT-qPCR. *Tbr1* is one of the markers expressed in the cortical pre-plate as well as in cortical layer VI (Hevner et al. 2001). Both cell lines showed an identical expression pattern. *Tbr1* levels varied considerably at 14 DIV in both cultures and no increase during the maturation of the neurons was observed (Figure 3.32).

3.6.6 Expression pattern of S1p1 – 5 receptors in J1 and B2 neurons

To explore the possibility of compensatory increases in expression of other S1P receptors, expression levels were analysed using RT-qPCR. As expected *S1p1r* mRNA levels were significantly different between the two cell lines after two days in culture ($*p < 0.05$ (2 days B2 *vs.* 2 days J1)), as well as two weeks ($***p < 0.001$ (2 weeks B2 *vs.* 2 weeks J1)). As a positive control sample cDNA from mouse hippocampus was used and resulted in a $2^{-\Delta Ct} \times 10^4$ value of 11. This is close to the levels found in J1 neurons after 14 days in culture ($2^{-\Delta C} \times 10^4 = 10.2$). It was also observed that *S1p1r* expression increased during the maturation of J1 neurons ($**p < 0.01$ (2 days J1 *vs.* 2 weeks J1)). No significant differences were found between the two cell lines when comparing the mRNA levels of the other four S1P receptors, apart from *S1p3r* (Figure 3.33). While high levels of *S1p3r* mRNA were found in J1 and B2 neurons, there was a clear trend towards decreased expression levels during the maturation of the B2 neurons. In the J1 and B2 neurons the *S1p3r* mRNA was expressed at significantly higher levels than the *S1p2r* mRNA ($*p < 0.05$). In both cultures, no expression of the *S1p4r* and *S1p5r* mRNA could be detected (Figure 3.33).
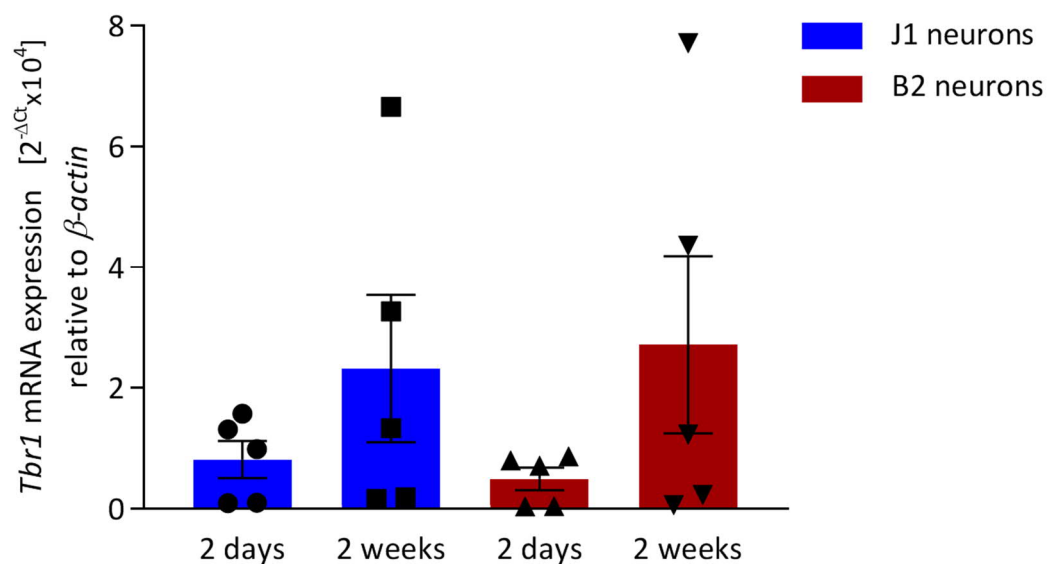
Figure 3.32 *Tbr1* mRNA levels were comparable between J1 and B2 neurons

Expression levels of *Tbr1* mRNA were similar between J1 and B2 neurons (One-way ANOVA, $p > 0.05$, n = 5). In both cultures no difference in Tbr1 levels was observed during neuronal maturation at 14 DIV. Data is presented as 2-ΔCtx104. Data was normalised to internal control β-actin. Values are mean ± SEM.

Figure 3.33 *S1p1 – 5 receptor* mRNA levels in J1 and B2 neurons

While in general, no significant differences were found between the expression levels of *S1p2-5r* mRNA levels in J1 and B2 neurons (Mann-Whitney test, $p > 0.05$, $n = 3$), B2 neurons showed a burst of high expression of *S1p3r* mRNA after 2 DIV that came back to WT levels after two weeks (Kruskal-Wallis test, *p (*S1p2r vs. S1p3r)* < 0.05). *S1p1r* mRNA expression was significantly reduced in the B2 neurons at two days (Unpaired t-test, *p (*S1p1r* 2 days *vs.* 2 days) < 0.05, $n = 4$) as well as 2 weeks (Unpaired t-test, ***p (*S1p1r* 2 weeks *vs.* 2 weeks) < 0.001, $n = 4$) compared to J1 neurons. In J1 neurons a significant increase of *S1p1r* levels was observed after 2 weeks compared to 2 days (Unpaired t-test, **p (*S1p1r* 2 days *vs.* 2 weeks) < 0.01, $n = 4$). Data is presented as $2^{-\Delta Ct} \times 10^4$. Data was normalised to internal control *β-actin*. Values are mean ± SEM.

3.7   Discussion

The focus of this Chapter was on the generation of ES cell-derived neurons lacking the

S1P1R. The initial attempt to directly excise the S1P1R from neurons *via* the addition of

tamoxifen failed (Figure 3.8), possibly because of the lack of significant nuclear

translocation of Cre^{ERT2} after tamoxifen addition (Figure 3.9 and 3.10). The activity of

tamoxifen was tested on control cells expressing Cre^{ERT2} under a different promoter and

led to the expected positive results (Figure 3.11 and 3.12, Appendix, Figure A.1).

Therefore, it appears likely that under the culture conditions used, the activity of the

Thy-1 promoter may be too low to drive the expression of significant levels of Cre^{ERT2} in

these neurons (Figure 3.9, 3.13 and 3.15). *Thy-1* mRNA data suggested that expression

levels would increase during maturation of the neurons (Figure 3.6). Hence, it is unclear

why *Cre^{ERT2}* mRNA levels stayed unchanged between 6 DIV and 13 DIV (Figure 3.7A)

and why Cre^{ERT2} expression levels in 14 days old #1 neurons were below detection limits

in the immunostaining (Figure 3.13). What this study does not address and what should

be investigated in the future, is the proportion of Cre^{ERT2} expressing cells in #1 cultures.

Then the presence of cells not expressing *Thy-1* and therefore Cre^{ERT2} could also

contribute to the *S1p1r* levels quantified. Then the genomic analysis of *S1p1r* expression

(Figure 3.8), does involve the entire population of cultured cells. In view of these results,

a different approach was followed, namely the excision of exon 2 following

electroporation of the *S1p1r*$^{loxP/loxP}$/*Cre^{ERT2}* ES cells with a Cre-IRES-GFP plasmid. This

strategy led to a successful excision, as confirmed by genotyping, sequencing and RT-

qPCR analysis, resulting in the generation of ES cells designated B2 (Figure 3.16 - 3.19

and 3.24). Confirmation of S1P1R deletion at the protein level was not possible as due to

the lack of specific antibodies, as neither of the two antibodies tested could specifically

detect S1P1R (Figure 3.22 and 3.23). Whether or not the signals detected both before and

after Cre-mediated excision correspond to other members of this family remains unclear (Discussion, section 8.2).

A close examination of the cultures by phase-contrast revealed that a high number of non-neuronal cells were present in the culture of B2 neurons (Figure 3.25), a conclusion supported by GFAP Western blot analysis (Figure 3.27B). This Western blot showed that after 5-FdU treatment GFAP was no longer detectable. Similar levels of GFAP were also detected in J1 neuronal cultures not treated with 5-FdU (Figure 3.27B). The differentiation protocol used in this study normally gives rise to a very high proportion of glutamatergic neurons and only few ramified astrocytes detected by GFAP antibodies (Bibel et al. 2004). It does seem however that certain unknown conditions and the absence of mitotic inhibitors led to an increase of this proportion of cells, explaining the results presented in Figure 3.27. Furthermore, it seems conceivable that the relatively high levels of *S1p3r* mRNA detected in B2 neurons at 2 DIV may derive from an increased number of dividing cells in B2 compared to J1 cultures (Figure 3.25 and 3.26). Indeed, a marked reduction of *S1p3r* mRNA levels was observed between 2 days and 2 weeks following 5-FdU treatment (Figure 3.33). The detection of GFAP in Western blot suggests that a proportion of these dividing cells are likely to be astrocytes (Figure 3.27). It has been shown that astrocytes express high levels of S1P3R (Dusaban et al. 2017); the lower levels of *S1p3r* mRNA in J1 neurons might be due to differences in GFAP-expressing cells between single differentiations or because additional non-neuronal cell types might contribute to the high levels of *S1p3r* mRNA in B2 neurons. This is a real possibility given the near ubiquitous expression of S1P3R (Blaho and Hla 2014). This result should be followed up by a detailed analysis of the cellular composition of the cultures via immunocytochemistry, including cell-type specific markers for microglia (Bennett et al. 2016) and oligodendrocytes (Bronstein et al. 1997). The RT-PCR experiment also

revealed that there was no long-term compensatory expression of any of the other sphingosine receptors following S1P1R excision.

With regard to the maturation of the neurons generated from J1 and B2 ES cells, it is of note that the levels of synaptophysin and BDNF showed a similar expression pattern (Figure 3.28 and 3.29). This was expected as firstly, BDNF is known to be regulated by neuronal activity (West et al. 2002) and secondly BDNF also enhances functional and morphological maturation of synapses (Park and Poo 2013). To follow the neuronal maturation of the J1 and B2 neurons more closely the analysis of a number of additional maturation markers could be investigated as well as synaptic activity *via* functional assays including calcium imaging and/or patch clamp recordings as previously practiced with these cultures (Barth et al. 2014). Directly supporting the notion that the neurons generated from both J1 and B2 cells are excitatory and therefore express the *Bdnf* gene (Baquet et al. 2004 and Introduction), the levels of the glutamate transporters *vGlut1* and *vGlut2* were measured and found to be similar (Figure 3.30). The higher expression of *vGlut2* at 14 DIV seen in both cell lines, is due to its localisation to synaptic vesicles which is in line with the increased number of synapses represented by the synaptophysin levels (Figure 3.28; (Fremeau Jr et al. 2001; Todd et al. 2003). Surprisingly, B2 neurons expressed significantly higher levels of vGlut2 protein levels at 14 DIV compared to J1 neurons (Figure 3.31), for reasons that are unknown. As this difference had no measurable impact on BDNF protein levels between J1 and B2 neurons (Figure 3.29), the functional significance of this observation remains unclear at this point.

To better define if the neuronal subtypes differ between B2 and J1 neurons, additional neuronal markers to *Tbr1* could be used, such as the chicken ovalbumin upstream promoter transcription factor-interacting protein 1 and 2 (*Ctip1*, *Ctip2*). *Ctip2* is found to

be primarily expressed in the intermediate zone of the developing mouse cerebral cortex at E18.5, whereas *Ctip1* is distributed throughout the cerebral cortex (Leid et al. 2004).

In summary, the excision of the S1P1 receptor in ES cells appeared to have been successful, allowing the generation of neurons with some similar characteristics to those generated from the wild-type J1 ES cells. In particular, the degree of BDNF expression seemed to follow a developmental time course which was similar in both neuronal cultures (Figure 3.29). However, further detailed analysis is needed to make a conclusion on the role of the S1P1R in the differentiation of ES cell-derived neurons into glutamatergic-like neurons and their maturation. Future experiments should also involve the characterisation of a cell line of the same background as the B2 ES cells which still express S1P1R, like #48 (Figure 3.16). This would help to understand if certain differences observed between J1 and B2 neurons, for example the expression of vGlut2 protein at 14 DIV is due to the lack of S1P1R or solely due to background differences. This could be followed up by RNA sequencing analysis in all three cell lines to clearly define if there is any compensatory gene expression due to the excision of the *S1p1r* gene.

Chapter 4

Quantifying BDNF Protein Levels in ES Cell-Derived Neurons

4.1   Introduction

The next objective was to establish a method allowing the reliable quantification of BDNF in ES cell-derived neurons. In principle, immunoassays of solubilized material represent the method of choice to quantify the levels of cytokines and growth factors. Indeed, so-called two-site ELISAs based on the use of antibodies have already been extensively used in the BDNF field, especially with human serum as documented in many publications linking BDNF levels with various conditions such as depression (Introduction, section 1.1 and (Lee and Kim 2010; Buckley et al. 2011; Bathina and Das 2015). However, a recent publication comparing six commercially available BDNF ELISAs indicated surprising variations in the results obtained with these ELISAs used to measure BDNF levels in the serum of over 30 volunteers, raising questions about the suitability of such assays (Polacchini et al. 2015). Our laboratory developed specific, well-characterized antibodies to BDNF (Kolbeck et al. 1999; Heyden et al. 2011; Deogracias et al. 2012) so that a major source of variability could be minimised, namely the quality of the antibody reagents and the coating of the ELISA plates. Nonetheless, initially it was unclear if this ELISA would be sensitive enough to detect the low levels of BDNF in neurons derived from ES cells. As detailed in the following, this turned out not to be the case whereby an alternative possibility arose during the project with the introduction of the first monoclonal antibody suitable for the detection of BDNF by Western blots.

4.2 BDNF ELISA

4.2.1 ELISA measurement of lysates from ES cell-derived neurons

To validate the reproducibility of the BDNF ELISA protocol, BDNF levels of the same sample were measured twice. Two different lysates of ES cell-derived neurons were loaded onto different ELISA plates and both experiments performed independently of each other. Surprisingly, BDNF content varied between the two measurements (Mann-Whitney test, actual difference between medians (sample 1 #1 *vs.* sample 1 #2) = -1.89 and (sample 2 #1 *vs.* sample 2 #2 = -4.31), n = 3 technical repeats) (Figure 4.1).

4.2.2 Background values varied between wells of the ELISA plate

To investigate the cause of this unexpected variability between identical samples, a BDNF ELISA was performed to determine background values potentially caused by the lysis buffer used to extract the material from cultured neurons, but this time in the absence of cell lysates. Surprisingly, high background levels were measured (yellow highlighted in Figure 4.2) as well as alarming variations between different wells of the ELISA plate (red numbers in Figure 4.2). These background values are highly relevant not just because they are variable but also because they are too close (theoretically calculated to correspond to about 18 pg BDNF per ELISA-well) to the real BDNF values expected from neurons derived from ES cells, i.e. in the range of 20-30 pg/well.
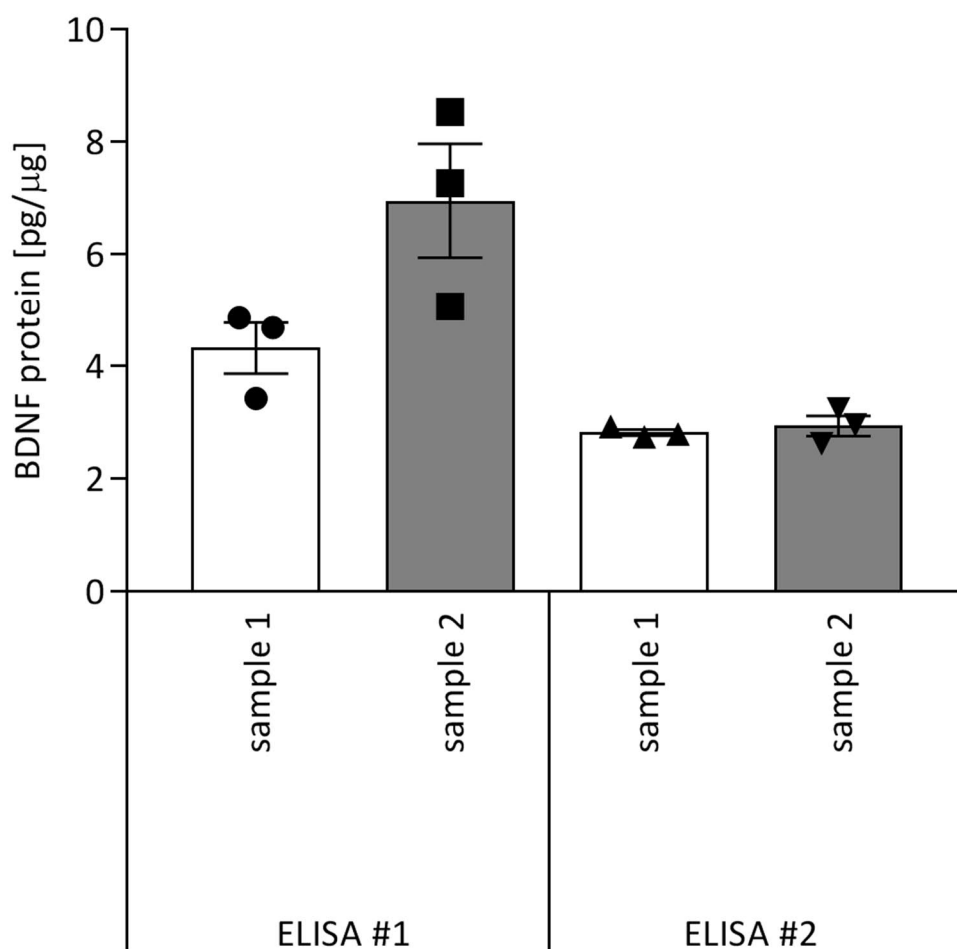
Figure 4.1 Variability of BDNF concentrations determined by ELISA

The exact same triplicates were analysed twice by BDNF ELISA. The only difference being the position of the samples on the 96-well plate. When re-tested, the different samples show different BDNF protein levels (Mann-Whitney test, actual difference between medians (sample 1 #1 *vs.* sample 1 #2) = -1.89 and (sample 2 #1 *vs.* sample 2 #2 = -4.31), n = 3 technical repeats). Values are presented as pg of BDNF per μg total protein. Data is represented as mean ± SEM.

A

	1	2	3	4	5	6	7	8	9	10	11	12
	Wells containing only lysis buffer no addition of BDNF								BDNF in pg/well (as pipetted) in triplicates			
A							2.44	2.44	2.44	625.00	625.00	625.00
B										312.50	312.50	312.50
C										156.25	156.25	156.25
D										78.13	78.13	78.13
E										39.06	39.06	39.06
F										19.53	19.53	19.53
G										9.77	9.77	9.77
H										4.88	4.88	4.88

B

	1	2	3	4	5	6	7	8	9	10	11	12
	BDNF in pg/well (as measured) after removing the blank value									BDNF in pg/well (as measured) in triplicates		
A	6.04	4.31	2.67	2.26	6.66	4.68	4.23	1.42 << std range		625.31	663.54	646.79
B	7.19	6.43	4.48	3.96	4.50	2.78	Blank	Blank	Blank	312.22	336.59	299.70
C	8.20	5.68	5.09	3.89	5.01	2.18	4.88	2.23	2.79	168.48	153.35	143.63
D	10.32	9.63	7.29	6.40	4.85	2.79	1.39 << std range	<< std range		81.96	74.71	75.17
E	12.07	9.75	7.75	8.01	5.75	3.87	5.66	4.07	3.25	38.75	38.44	37.91
F	14.32	11.41	9.38	7.75	7.01	4.65	4.11	2.10 << std range		21.91	20.95	20.60
G	15.93	11.75	10.67	8.36	7.88	6.08	9.71	7.85	6.33	7.60	6.73	5.63
H	18.89	14.60	11.92	10.98	11.80	10.67	12.76	6.76	5.85	8.33	7.43	8.77

Figure 4.2 Different wells on ELISA plate gave different background values

A Only lysis buffer was loaded into the 96 -well plate (yellow highlighted wells) and amounts of recombinant BDNF used for the standard curve are represented in pg of protein per well (blue highlighted wells). **B** Background values differed up to 13-fold depending on their position on the 96-well plate (red values). Blue highlighted wells represent the standard curve as measured in the ELISA in pg of BDNF per well.

4.2.3 High background values are caused by the detergents contained in the lysis buffer

To identify the specific components of the lysis buffer causing high background signals in the BDNF ELISA, different buffers were tested (Figure 4.3). Triton X-100 as well as sodium deoxycholate (SDO) are typically included in the buffer used to solubilize the cells and both turn out to be responsible for the elevated background values (Figure 4.3). Of these two detergents, Triton X-100 seems to explain most of the background signal and even 0.1% was sufficient to interfere with BDNF measurements. Intriguingly, a cellular lysate from mouse ES cells known not to express the BDNF protein also added to the background levels. To exclude the possibility that an interaction between the detergents and the buffer itself caused these high background values, the incubation buffer already used in the ELISA was tested. This phosphate buffer has a neutral pH and does not contain any detergents (Materials and Methods, section 2.17). While it did not generate a high background by itself it did so upon the addition of Triton X-100 (Figure 4.3). Unfortunately, detergents turned out to be the only way to extract BDNF from the cells and at the same time keeping it in solution. As in the absence of carrier protein or detergents, BDNF is known to be adsorbed by the wall of plastic tubes and by pipette tips due to its physico-chemical properties. To prevent this phenomenon, bovine serum albumin (BSA) was also tested to prevent unspecific adsorption of BDNF, but this addition did not solve the problem of elevated background (Figure 4.3). The unsuitability of the standard BDNF ELISA for reliable measurements of the very low levels of BDNF generated by neurons derived from ES cells was finally confirmed by the observation that the expected proportionality of the signal was not obtained when testing the same samples at different volumes of lysate (Figure 4.4).

	RIPA	Incubation Buffer	Incubation Buffer	RIPA	RIPA	RIPA	RIPA	RIPA	RIPA	RIPA	RIPA	Incubation buffer
no detergents	x	x	x									
0.1 % Triton X-100				x	x	x	x					
0.2 % Triton X-100												x
1 % Triton X-100								x	x	x	x	
no Sodium deoxycholate				x	x			x	x			
0.2 % Sodium deoxycholate						x	x			x	x	
without any cell lysate	x	x	x	x		x		x		x	x	x
with ES cell lysate					x		x		x			
with BSA		x									x	
Background Value	0	0	0	81.34	121.57	59.79	74.34	73.93	117.28	70.04	90.49	80.16

Figure 4.3 Detergents in the lysis buffer identified as a cause of high background values

Different types of lysis buffers were tested to identify changes in background values in the ELISA. Triton X-100 containing buffers generated the highest background, which were further increased when cell lysate was present in the sample. Values show the mean of two measurements in pg of BDNF per ELISA-well.
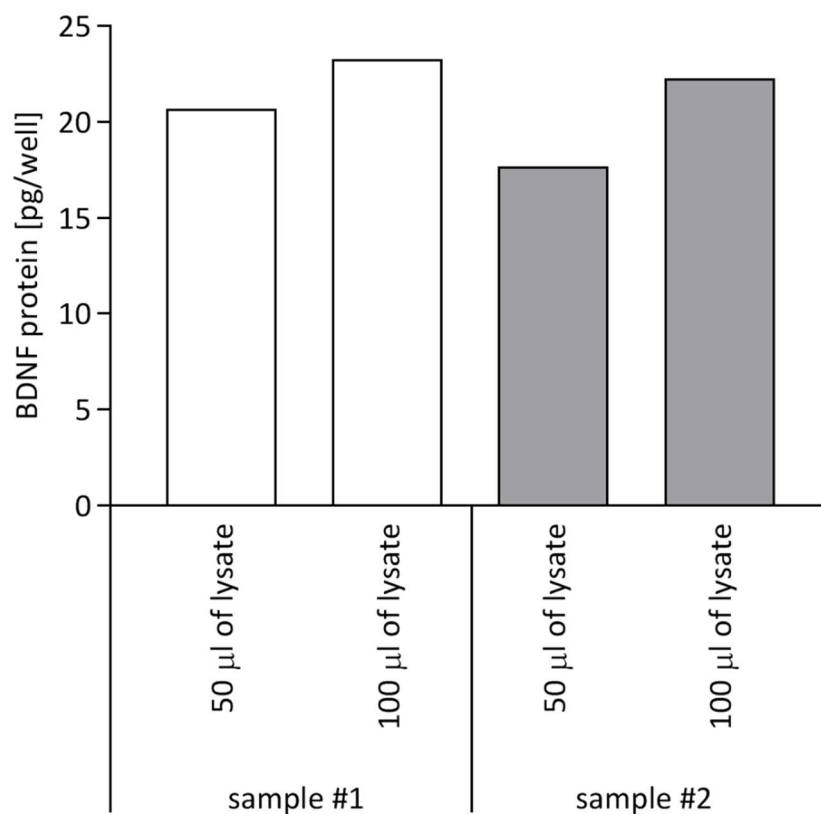
Figure 4.4 Lack of proportionality in the BDNF ELISA

The same neuronal lysates were analysed at two different concentrations with the ELISA. When adding double the amount of lysate, only 12 % (sample #1) or 25 % (sample #2), instead of 50 % more BDNF was quantified. Two independent lysates (#1 and #2) confirmed these results. Values are presented as pg of BDNF per μg total protein.

4.3   Detection of BDNF using Western blot

At the beginning of the project only BDNF polyclonal antibodies of variable quality were accessible. These antibodies typically detect multiple bands and made a reliable, let alone quantitative detection of BDNF difficult (Figure 4.5A). Fortunately, a new antibody became available very recently (Materials and Methods, section 2.18), the first monoclonal antibody allowing a specific and sensitive detection of BDNF on Western blot. Importantly, this new antibody also allows the detection of pro-BDNF as the sequence of mature BDNF (against which the antibody has been raised) is contained in pro-BDNF (Figure 4.5A and B; (Leibrock et al. 1989)).
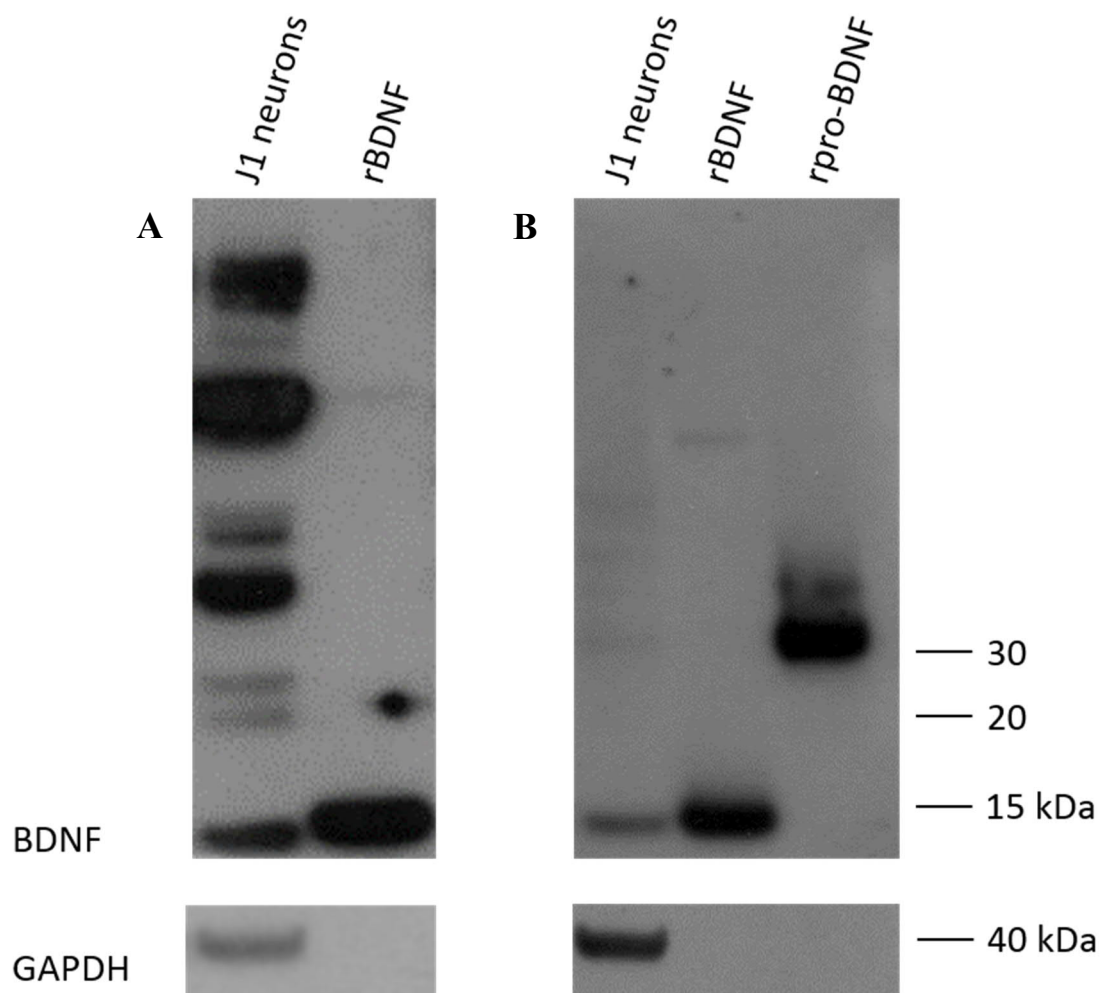
Figure 4.5 Monoclonal antibody improved BDNF detection and quantification

A BDNF detection using the long available polyclonal N-20 anti-BDNF antiserum from Santa Cruz. Note the multiple unspecific bands, including the area where pro-BDNF can be expected. **B** BDNF detection using the newly available BDNF monoclonal antibody 3C11 from Icosagen. Recombinant BDNF (rBDNF) and pro-BDNF (rpro-BDNF) confirmed specificity. GAPDH was used as internal control.

4.4   Discussion

BDNF levels in ES cell-derived neurons are low and sensitive methods are needed to ensure reliable detection. RT-qPCR is an effective tool for quantifying *Bdnf* mRNA due to the amplification of the target sequence, which enables the analysis of low abundance mRNAs. However, information relating to the protein levels of BDNF is crucial to determine the implications of a drug treatment, and therefore should not be overlooked in investigations concerning the FTY720-dependent increase of BDNF in neurons. Unfortunately, and for the reasons discussed in the above, the most straightforward method, namely quantification by BDNF ELISA turned out not to be feasible. The main reasons are the very low levels of BDNF coupled with elevated background values caused by the use of detergents needed to extract and carry BDNF to the ELISA plates. It is conceivable that detergents may disrupt the hydrophobic bonds formed between the first antibody (Ab #1) used to coat the plates and the plastic surface of the ELISA plate, thus possibly allowing direct binding of the HRP-conjugated secondary antibody (HRP-Ab #9). This possibility was tested and made likely by the observation that the ELISA procedure performed without the addition of Ab #1 did generate high background values (data not shown). Strong variability was also observed between the different wells which further complicated BDNF measurements by ELISA and while this variability may not be a problem when the levels of BDNF are relatively high as is the case for example in human serum or mouse brain, it did cause difficulties in the case of neurons generated from ES cells. Despite the inherent imperfect nature of protein quantification by Western blot techniques, the availability of a BDNF monoclonal antibody offered an alternative possibility.

Chapter 5

Effects of pFTY720 on J1 and B2 Neurons

5.1   Introduction

One of the most convincing ways of defining the role of a receptor in the mode of action of a drug is to look at the effects of the drug after genetically deleting the receptor. In the case of S1P1R, germ line deletion of the gene causes embryonic lethality (Introduction, section 1.2). Mouse embryos carrying a germ line deletion of *S1p1r* die at around E13 due to massive bleeding, caused by a lack of vascular smooth muscles cells enveloping the blood vessels (Liu et al. 2000). Deletion of floxed alleles of *S1p1r* using selective Cre drivers is one possibility to circumvent the problem of early lethality and while this strategy has been applied to *S1p1r*, it led thus far to some confusing results, including the conclusion that S1P1R may not be expressed by neurons and that the effects of FTY720 would be mediated by S1P1R on astrocytes (Choi et al. 2011). This notion is tentatively supported by immunohistochemical data using human brain tissue (Nishimura et al. 2010). However, subsequent studies indicating that FTY720 increases BDNF levels in mouse models (Deogracias et al. 2012; Di Pardo et al. 2014; Fukumoto et al. 2014) challenged these conclusions as neurons are the only cells in the intact brain expressing significant levels of BDNF (Rauskolb et al. 2010). After establishing and characterising the *S1p1r−/−* cell line B2 (Chapter 3) and validating the BDNF detection and quantification method (Chapter 4), the aim of the work described in this Chapter was to explore the role of the S1P1R in the pFTY720-dependent increase of BDNF levels in ES cell-derived neurons. As the S1P1R is a GPCR, further downstream targets including the ERK pathway, as well as CREB phosphorylation were investigated to gain further insights into

the mode of action and to delineate possible compensatory mechanisms by other S1P receptors in the *S1p1r*$^{-/-}$ cell line B2. Throughout the study the phosphorylated active form of FTY720 (pFTY720) was used to avoid variability due to unknown levels of its main phosphorylation enzyme, the kinase SphK2, in the culture system.

5.2 Investigating the Effects of pFTY720 on BDNF Levels in J1 and B2 Neurons

5.2.1 Analysis of BDNF levels after long-term exposure to pFTY720

The effects of pFTY720 on BDNF protein levels were investigated in J1 and B2 neurons treated with 10 nM and 100 nM pFTY720 from day two onwards (Materials and Methods, section 2.9). These experiments were limited to three weeks and to concentrations lower than 1 μM pFTY720 as pilot experiments indicated that prolonged exposure of J1 neurons to pFTY720 1 μM was toxic for the cells (data not shown). After three weeks in culture, neurons were lysed and BDNF levels were analysed using Western blot (Figure 5.1A and B). Densitometric analysis revealed a 45 %, significant increase of BDNF levels in J1 neurons (p (Ø *vs.* 100 nM) < 0.05), whilst this was not the case in B2 neurons (p (Ø *vs.* 100 nM) = 0.36; Figure 5.1C). However, it is important to note that the results obtained with J1 neurons also indicated a considerable variability with regard to the magnitude of the effect. This was a major difficulty observed with this culture system when assessing BDNF levels as well as those of other targets (see below and section 5.4 Discussion).

A

J1 neurons

BDNF — 15 kDa

βIII-tubulin — 50 kDa

pFTY720

B

B2 neurons

BDNF — 15 kDa

βIII-tubulin — 50 kDa

pFTY720

C
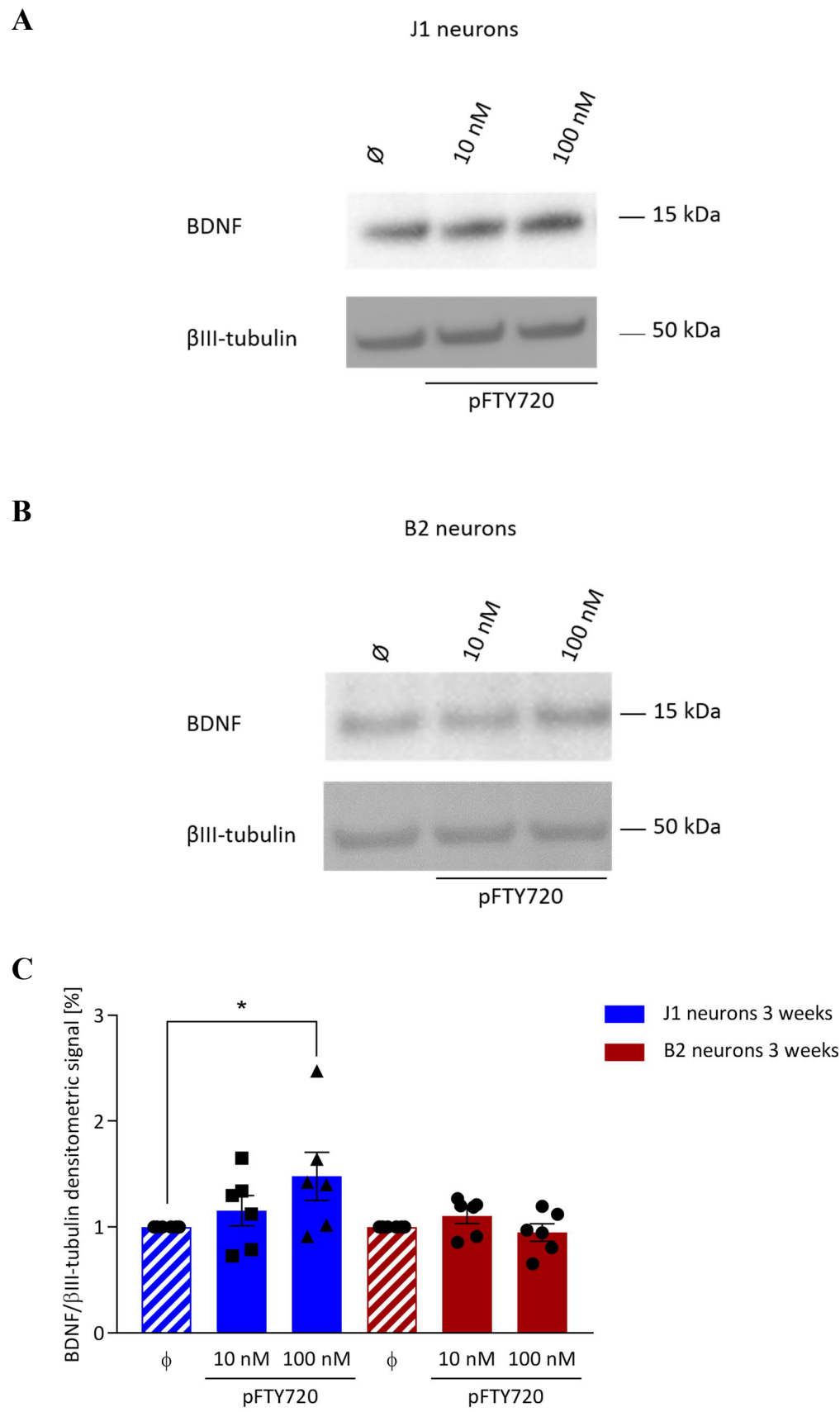
Figure 5.1 Long-term exposure of ES-cell derived neurons to pFTY720

Figure 5.1 Long-term exposure of ES cell-derived neurons to pFTY720

5-FdU-treated B2 and J1 neurons were exposed to pFTY720 10 nM or 100 nM from 2 DIV until lysis at three weeks. **A/B** Western blot of B2 and J1 neurons. 20 µl of lysate were loaded per lane. **C** pFTY720 100 nM significantly increased BDNF levels in J1 neurons compared to controls (Mann-Whitney test, *p < 0.05, n = 6). This was not the case in the B2 neurons treated with pFTY720 100 nM (Mann-Whitney test, p = 0.36, n = 6). Data are represented as mean ± SEM relative to βIII-tubulin and changes are in percentage *vs.* control. Ø: vehicle (DMSO) treated cells.

5.2.2 BDNF protein levels are unaffected by short-term treatment with pFTY720

Short-term treatment with pFTY720 10 nM has previously been shown to increase BDNF levels significantly in primary mouse cortical neurons (Deogracias et al. 2012). To investigate if this can also be observed in ES cell-derived neurons, short-term experiments were performed with J1 neurons at 14 DIV. Neurons were treated with pFTY720 10 nM for 8 h or 24 h, proteins extracted and BDNF levels analysed by Western blot (Figure 5.2A). pFTY720 was found not to increase BDNF levels significantly at either time point ($p > 0.05$; Figure 5.2B). Due to a lack of significant effect in J1 neurons, primary mouse cortical neurons at 12 DIV were also treated with pFTY720 10 nM at three different time points (4 h, 8 h and 24 h). However, also in primary cortical neurons BDNF levels were not affected by pFTY720 treatment ($p > 0.05$; Figure 5.2D). To investigate this further additional experiments were performed in primary mouse cortical neurons. None of these experiments led to a significant increase of BDNF levels (Appendix, Figure A.2 and A.3).
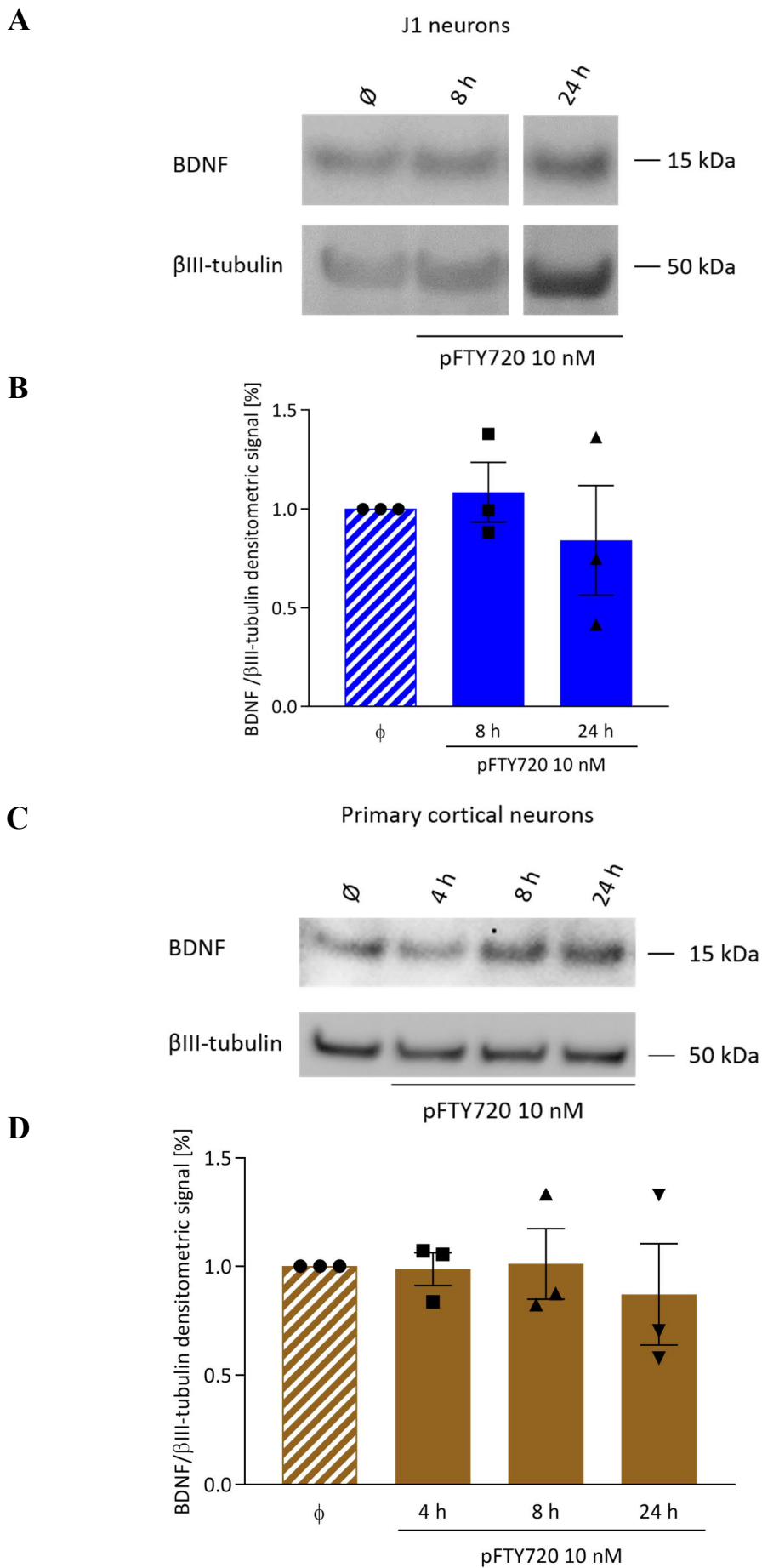
Figure 5.2 Short-term effects of pFTY720 on BDNF protein levels

Figure 5.2 Short-term effects of pFTY720 on BDNF protein levels

A 14 DIV old J1 neurons were treated with pFTY720 10 nM for 8 h and 24 h. Western blot represents BDNF expression of J1 neurons after short-term exposure to pFTY720 10 nM. 20 µl of neuronal lysate were loaded per lane. **B** pFTY720 at a concentration of 10 nM did not increase BDNF protein levels in J1 neurons significantly compared to controls (Kruskal-Wallis test, $p > 0.05$, $n = 3$). **C** 12 DIV old primary mouse cortical neurons were treated with pFTY720 10 nM for 4 h, 8 h and 24 h. Western blot represents BDNF expression of primary cortical neurons after short-term exposure to pFTY720 10 nM. 20 µl of neuronal lysate were loaded per lane. **D** pFTY720 at a concentration of 10 nM did not increase BDNF protein levels in primary cortical neurons 12 DIV significantly compared to controls (Kruskal-Wallis test, $p > 0.05$, $n = 3$ from 2 independent experiments). Data are represented as mean ± SEM relative to the internal control βIII-tubulin. Changes are in percentage *vs.* control. Ø: vehicle (DMSO) treated cells.

5.2.3 Are BDNF levels modulated by the sphingosine kinase inhibitor N,N-dimethylsphingosine in J1 neurons?

The moderate increase of BDNF levels in J1 neurons as well as the variability of the results may potentially be explained by the endogenous production of the natural ligand S1P of S1P1R. This hypothesis was tested by adding the sphingosine kinase inhibitor N,N-dimethylsphingosine (DMS) to the culture. DMS inhibits both sphingosine kinases (SphK1 and 2) and thus prevents the phosphorylation of sphingosine to S1P, leading to decreased levels of endogenous S1P in the culture system (Yatomi et al. 1996; Edsall et al. 1998).

Following a 16 h exposure of 14 DIV J1 neurons to DMS, the levels of BDNF were found to be unchanged (Figure 5.3B). Co-treatment of pFTY720 with DMS 100 nM and pFTY720 10 nM (Figure 5.4A) did also not lead to a change of BDNF levels ($p > 0.05$, Figure 5.4B). To this date it is therefore not possible to draw a conclusion on the role of endogenous S1P on BDNF levels in ES cell-derived neurons.

A
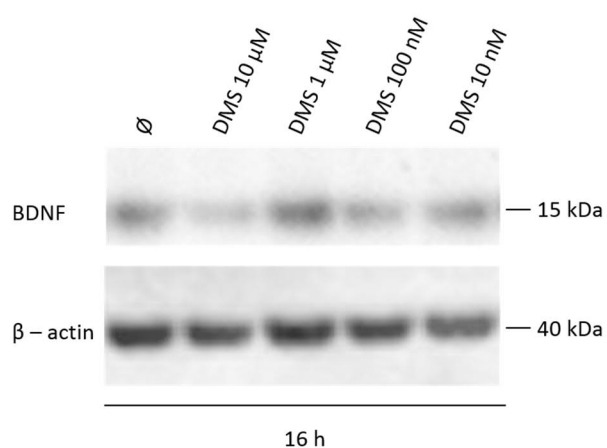
B
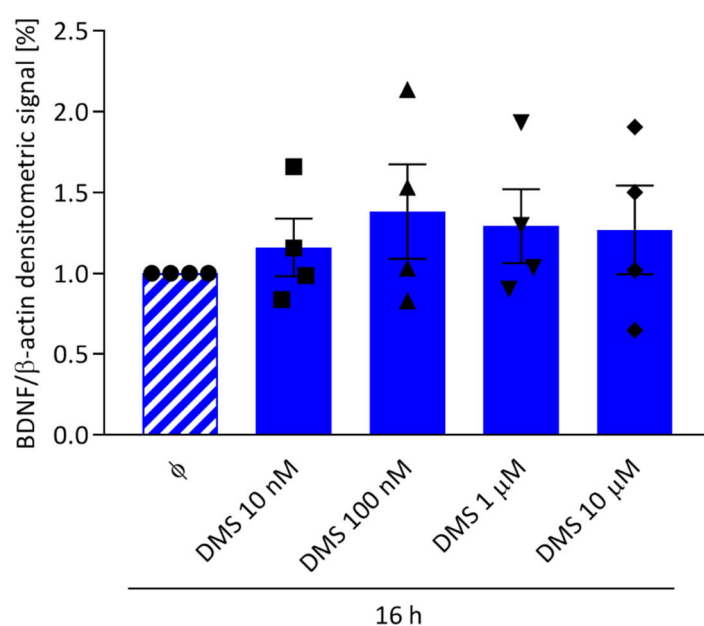
Figure 5.3 Effects of DMS on BDNF levels in WT neurons

14 DIV old J1 neurons were treated with different concentrations of DMS for 16 h.
A Western blot of BDNF levels in J1 neurons after DMS treatment. 40 μg of protein
were loaded per lane. **B** Graph represents densitometric analysis. DMS did not decrease
BDNF protein levels in J1 neurons significantly (One-way ANOVA, $p > 0.05$, n = 4).
Data are represented as mean ± SEM relative to internal control β-actin and changes
are in percentage *vs.* control. Ø: vehicle (EtOH) treated cells.

A

B
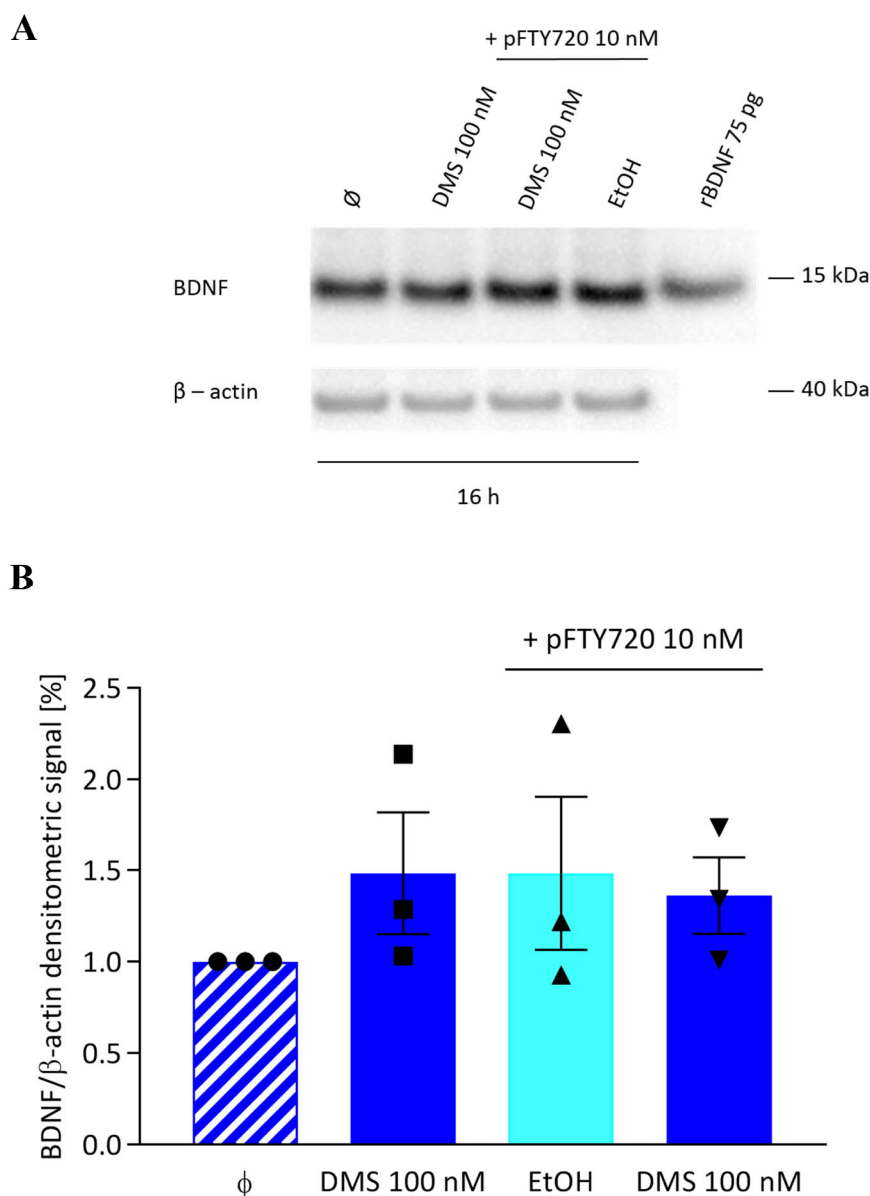
Figure 5.4 Effects of co-treatment of pFTY720 with DMS on BDNF levels

14 DIV old J1 neurons were treated with DMS 100 nM either alone or in combination with pFTY720 10 nM for 16 h. **A** Western Blot of BDNF levels in J1 neurons after co-treatment. 40 μg of protein were loaded per lane. **B** Graph represents densitometric analysis. Co-treatment of pFTY720 10 nM with DMS did not increase BDNF protein levels significantly (Mann-Whitney test, n.s. $p > 0.05$, n = 3). Data are represented as mean ± SEM relative to internal control β-actin and in percentage change *vs.* control. Ø: vehicle (EtOH) treated cells. The solid light blue bar represents cells treated with EtOH and pFTY720 10 nM.

5.3 Effects of pFTY720 on ERK1/2 and CREB Phosphorylation

Although the ES cell-derived neuronal culture used here delivered variable results in terms of BDNF induction by pFTY720, it is of interest to identify the possible mechanism downstream of S1P1R. Especially due to the availability of the B2 neurons and the results obtained with these cells (Figure 5.1). The enhancement of BDNF protein stability, an increased *Bdnf* mRNA translation or transcription could be possible explanations. Even though one report suggests that BDNF protein levels may be regulated by a rapid increase in translation following ketamine injections (Autry et al. 2011), there are currently no further indications that BDNF levels in neurons may be regulated by other mechanisms than increased transcription. Therefore, the focus of the current study was to investigate if pathways known to induce *Bdnf* mRNA transcription are affected by pFTY720 treatment in ES cell-derived neurons. GPCRs, including S1P1R are well known to act on the ERK pathway, as well as cAMP pathway (Choi and Chun 2013; Eishingdrelo and Kongsamut 2013). Importantly, there is considerable evidence that *Bdnf* transcription is regulated by CREB phosphorylation and the levels of intracellular calcium (West et al. 2001).

5.3.1 ERK1/2 phosphorylation following short-term pFTY20 addition to J1 and B2 neurons

To investigate the effects of pFTY720 on ERK1/2 phosphorylation, 14 DIV J1 and B2 neurons were exposed to different concentrations of pFTY720 (10 nM, 100 nM and 1 μM) for 10 min. Neuronal lysates were examined by Western blot and phosphorylation of ERK1/2 was analysed by densitometry (Figure 5.5). ERK1/2 phosphorylation was significantly increased in J1 neurons when treated with pFTY720 10 nM (**$p < 0.01$) and 100 nM for 10 min compared to controls (**$p < 0.01$, Figure 5.5C).

However, a One-way ANOVA analysis failed to reveal a statistically significant difference between the two cell lines regarding phosphorylation of ERK1/2 after 10 min ($p > 0.05$, Figure 5.5C). Importantly, whilst ERK1/2 phosphorylation was significantly increased in B2 neurons after treatment with pFTY720 1 μM compared to controls (**$p < 0.01$, Figure 5.5C), it should be noted that in a subsequent time course experiment, these findings could not be reproduced (Figure 5.6).

A

J1 neurons

B

B2 neurons

C
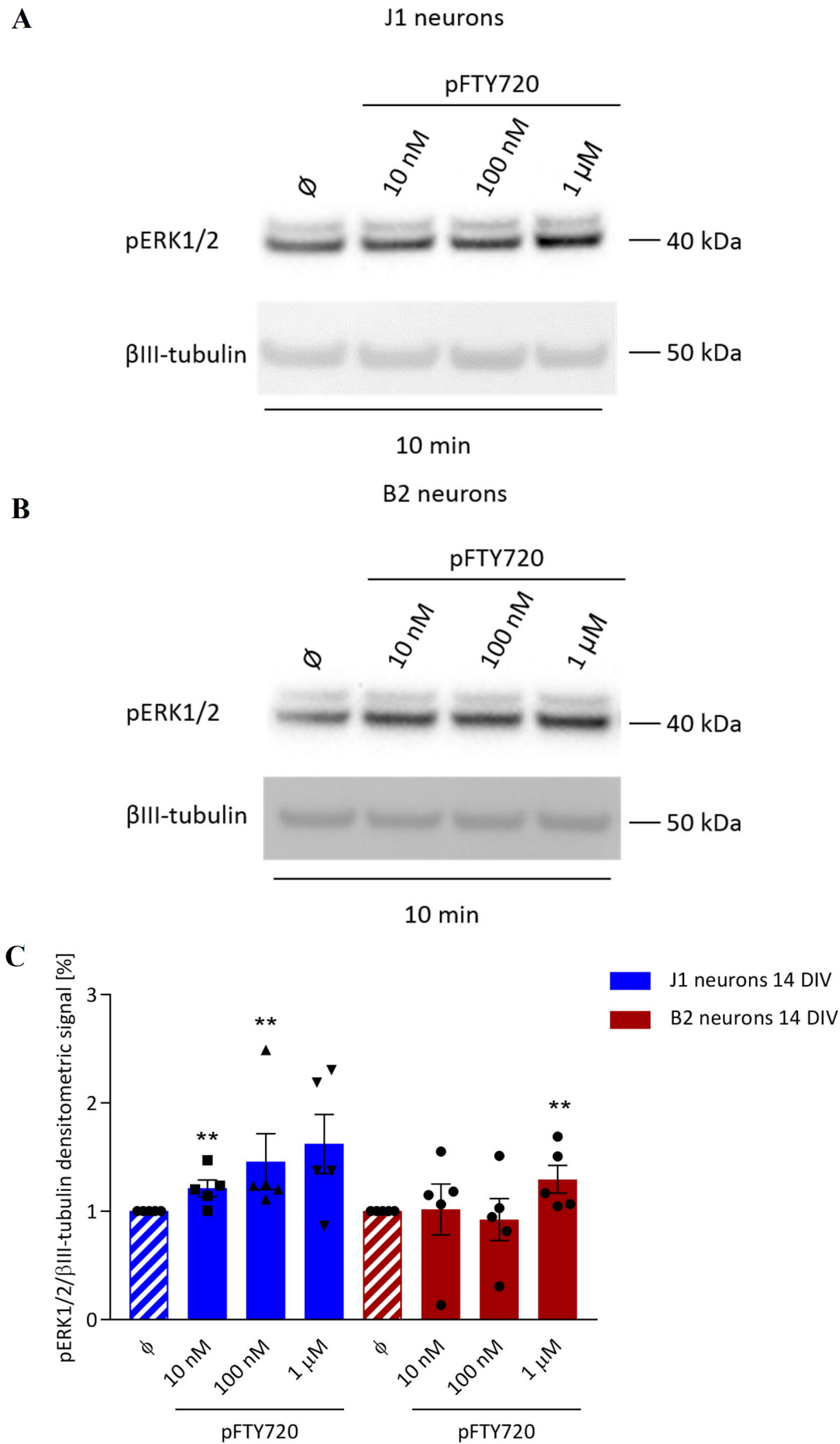
Figure 5.5 pFTY720 significantly increased pERK1/2 in J1 and B2 neurons

Figure 5.5 pFTY720 significantly increased pERK1/2 in J1 and B2 neurons

14 DIV J1 and B2 neurons were exposed to different concentrations of pFTY720 for 10 min. **A/B** Western blot for pERK1/2 expression in J1 and B2 neurons, respectively. 20 μl of neuronal lysate were loaded per lane. **C** Graph shows densitometric analysis. pFTY720 10 nM and 100 nM significantly increased the phosphorylation of ERK1/2 in J1 neurons compared to controls (Mann-Whitney test, **p (Ø vs pFTY720 10 nM and 100 nM) < 0.01, n = 5). In B2 neurons treatment with pFTY720 1 μM for 10 min led to a significant increase of ERK1/2 phosphorylation compared to controls (Mann-Whitney test, **p (Ø vs pFTY720 1 μM) < 0.01, n = 5). However, this result needs to be interpreted with caution as it could not be reproduced in a time course experiment performed with B2 neurons (Figure 5.6B and C). One-way ANOVA showed no differences between the phosphorylation of ERK1/2 in B2 and J1 neurons after pFTY720 exposure for 10 min (One-way ANOVA, p > 0.05). Data are represented as mean ± SEM relative to βIII-tubulin and changes are in percentage *vs.* control. Ø: vehicle (DMSO) treated cells.

5.3.2 Effects of pFTY720 on pERK1/2 in J1 and B2 neurons at different time points

Next, pFTY720 1 μM was tested at different time points using 14 DIV J1 and B2 neurons. Neuronal lysates were examined by Western blot (Figure 5.6A). As a result of the high variability observed, especially with the B2 neurons, the significant difference which was previously observed after 10 min exposure to pFTY720 1 μM (Figure 5.5) could not be reproduced ($p > 0.05$; Figure 5.6C).

A

J1 neurons

pERK1/2   — 40 kDa

βIII-tubulin   — 50 kDa

pFTY720 1 µM

B

B2 neurons

pERK1/2   — 40 kDa

βIII-tubulin   — 50 kDa

pFTY720 1 µM

C
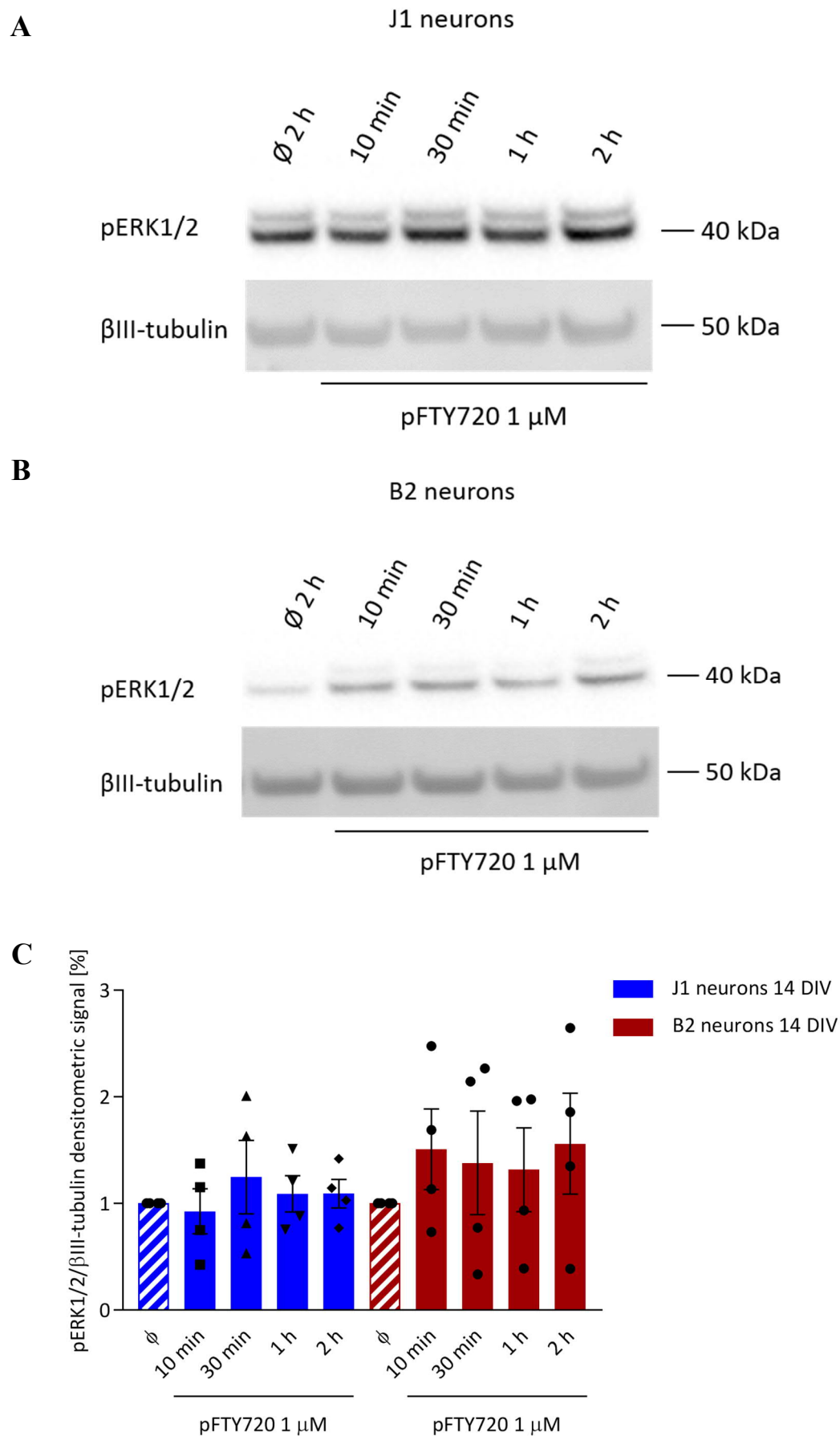
Figure 5.6 Effects of pFTY720 1 µM on pERK1/2 in J1 and B2 neurons

Figure 5.6 Effects of pFTY720 1 μM on pERK1/2 in J1 and B2 neurons

14 DIV J1 and B2 neurons were exposed to pFTY720 1 μM for the indicated time points. **A/B** Western blot for pERK1/2 expression in J1 and B2 neurons, respectively. 20 μl of neuronal lysate were loaded per lane. βIII-tubulin was used as internal control. **C** Graph shows densitometric analysis. No significant increase of ERK1/2 phosphorylation was observed in either cell line (One-way ANOVA, $p > 0.05$, n = 4). Data are represented as mean ± SEM relative to βIII-tubulin and changes are in percentage *vs.* control. Ø: vehicle (DMSO) treated cells.

5.3.3 Effects of pFTY720 on pCREB levels in J1 and B2 neurons

Next, 14 DIV ES cell-derived neurons J1 and B2 were exposed to different concentrations of pFTY720 for 10 min to explore a possible role of S1P1R in CREB phosphorylation. In both cell lines pFTY720 had similar effects after 10 min exposure ($p > 0.05$; Figure 5.7). After treatment with pFTY20 at a concentration of 1 μM CREB phosphorylation was significantly increased in J1 neurons compared to controls (* $p < 0.05$; Figure 5.7). However, when CREB phosphorylation was examined at different time points following pFTY720 1 μM addition, the previously observed increase of pCREB after 10 min exposure to the drug disappeared in J1 neurons ($p > 0.05$, Figure 5.8). Therefore, no conclusion can be drawn from this experiment and the significant effect seen in J1 neurons (Figure 5.7) needs to be interpreted with caution. In B2 neurons the time course experiment revealed a surprising and significant increase of CREB phosphorylation after pFTY720 1 μM treatment for 1 h and 2 h compared to controls (* $p < 0.05$; Figure 5.8C).
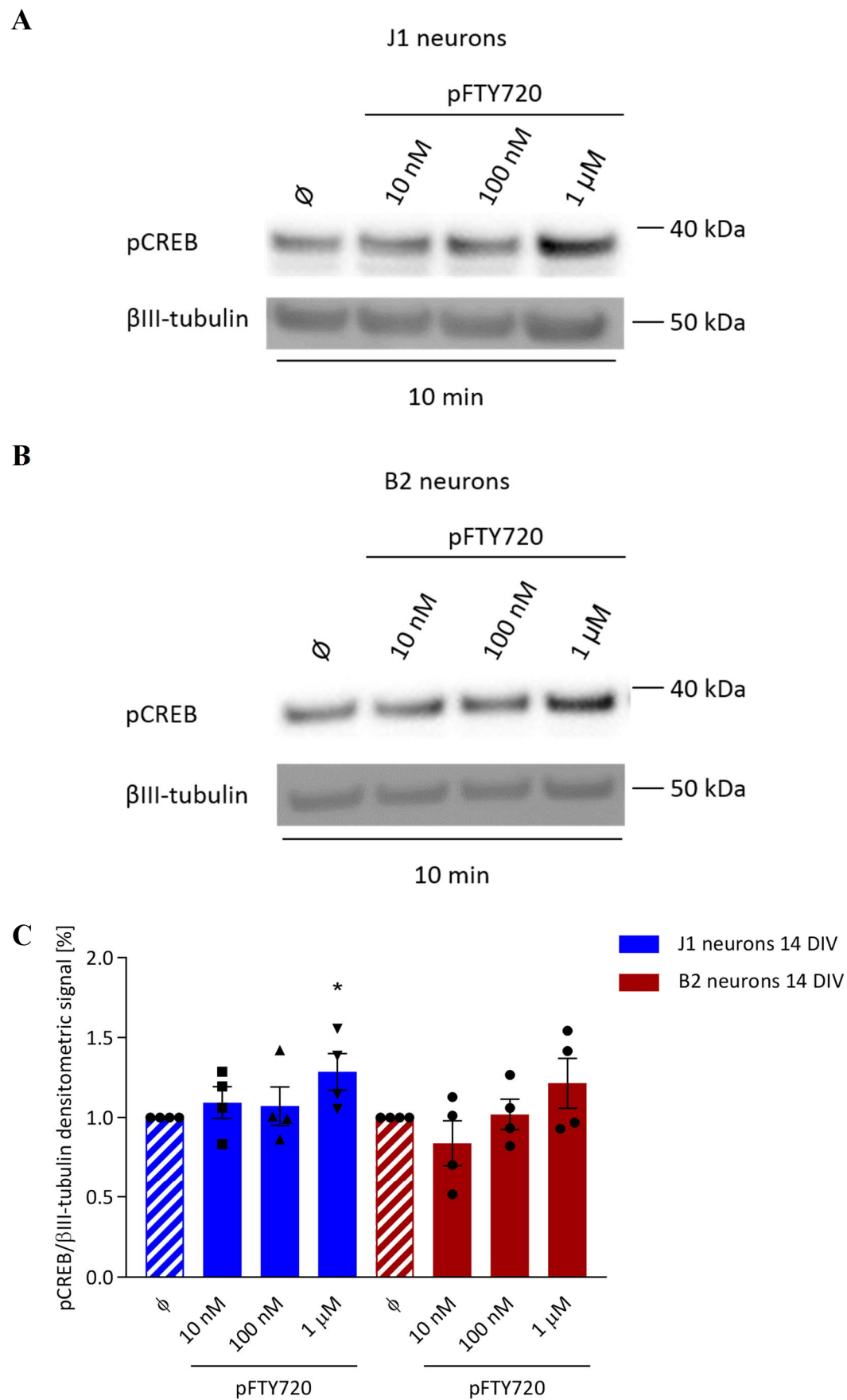
A

B

C

Figure 5.7 CREB phosphorylation following addition of pFTY720 to J1 and B2 neurons

Figure 5.7 CREB phosphorylation following addition of pFTY720 to J1 and B2 neurons

14 DIV old J1 and B2 neurons were exposed to different concentrations of pFTY720 for 10 min. **A/B** Western blot for pCREB expression in J1 and B2 neurons, respectively. 20 µl of neuronal lysate were loaded per lane. **B** Graph shows densitometric analysis. Although pFTY720 1 µM increased CREB phosphorylation significantly in J1 neurons compared to controls (Unpaired t test, $*p < 0.05$, n = 4), these results could not be reproduced in subsequent experiments and therefore need to be interpreted with caution (Figure 5.8A and C). No increase of pCREB levels was observed in B2 neurons with any concentration of pFTY720 after 10 min exposure (Unpaired t test, $p > 0.05$, n = 4). A One-way ANOVA did not reveal any significant differences between J1 and B2 neurons (One-way ANOVA, $p > 0.05$, n = 4). Data are represented as mean ± SEM relative to βIII-tubulin and changes are in percentage *vs.* control. Ø: vehicle (DMSO) treated cells.
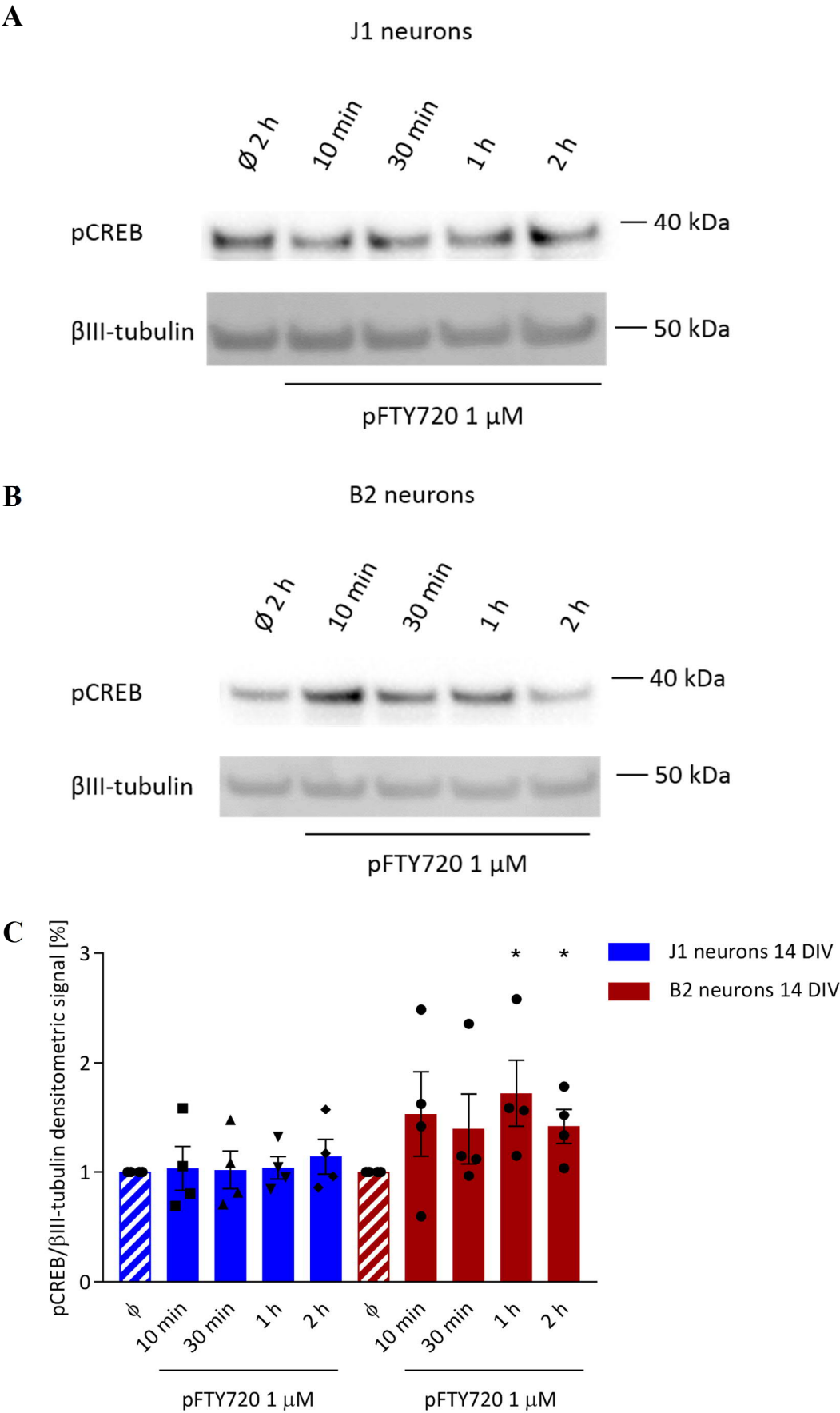
Figure 5.8 Levels of pCREB following addition of pFTY720 1 µM to J1 and B2 neurons

Figure 5.8 Levels of pCREB following addition of pFTY720 1 μM to J1 and B2 neurons

14 DIV J1 and B2 neurons were exposed to pFTY720 1 μM for the indicated time periods. **A/B** Western blot for pCREB expression in J1 and B2 neurons, respectively. 20 μl of neuronal lysate were loaded per lane. **B** Graph shows densitometric analysis. pFTY720 1 μM increased CREB phosphorylation significantly after 1 h and 2 h in B2, but not J1 neurons compared to controls (Mann-Whitney test, *p (Ø *vs.* pFTY720 1 μM 1 h and 2 h < 0.05, n = 4). The previously observed significant effect in J1 neurons after 10 min exposure to pFTY720 1 μM (Figure 5.7) could not be reproduced. No significant difference was found between J1 and B2 neurons (Kruskal-Wallis test, p > 0.05, n = 4). Data are represented as mean ± SEM relative to βIII-tubulin and changes are in percentage *vs.* control. Ø: vehicle (DMSO) treated cells.

5.3.4 pFTY720 increased Bdnf mRNA significantly in B2 neurons

Given the effects of pFTY720 addition on CREB phosphorylation (Figure 5.8) and the well-established role of the latter on BDNF transcription (Hong et al. 2008), J1 and B2 neurons were treated with pFTY720 at different concentrations for 8 h, RNA was extracted and the levels of *Bdnf* mRNA determined. A trend, but no significant differences were observed. Note however the variability between the individual values (Figure 5.9). Shorter time points were examined next and 1 h after the addition of pFTY720, the levels of *Bdnf* mRNA were significantly increased in B2 neurons compared to controls (*p (Ø *vs.* 1 h) < 0.05, Figure 5.10), but not in J1 neurons (p > 0.05, Figure 5.10).
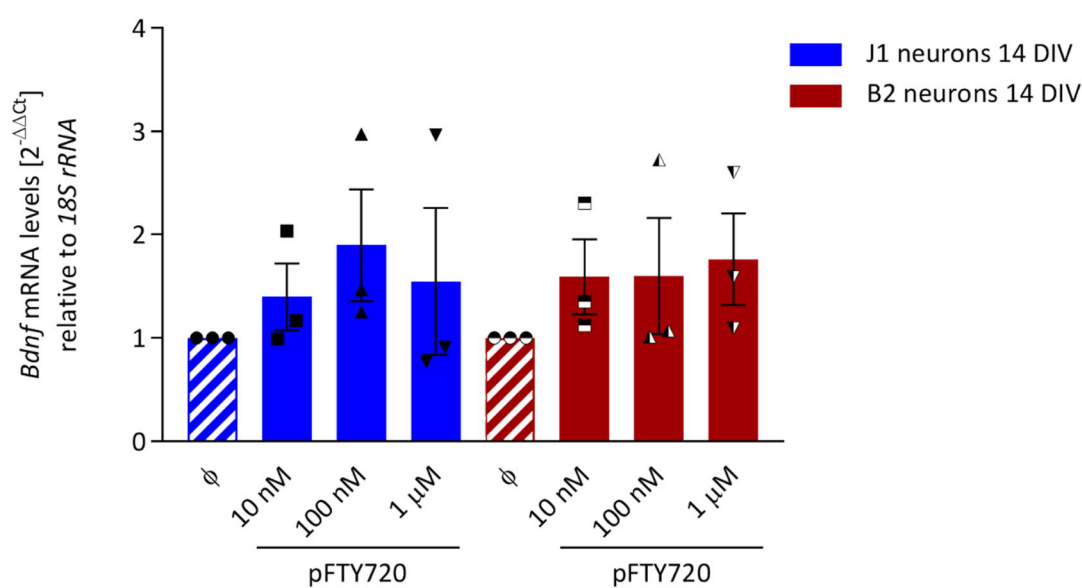
Figure 5.9 *Bdnf* mRNA levels in J1 and B2 neurons 8 h after pFTY720 addition

14 DIV old neurons were treated with different concentrations of pFTY720 for 8 h. pFTY720 did not increase *Bdnf* mRNA levels significantly in J1 nor in B2 neurons (Kruskal-Wallis test, $p > 0.05$, n = 3). Data are represented as mean of $2^{-\Delta\Delta Ct} \pm$ SEM relative to internal control *18S rRNA*. Ø: vehicle (DMSO) treated cells.
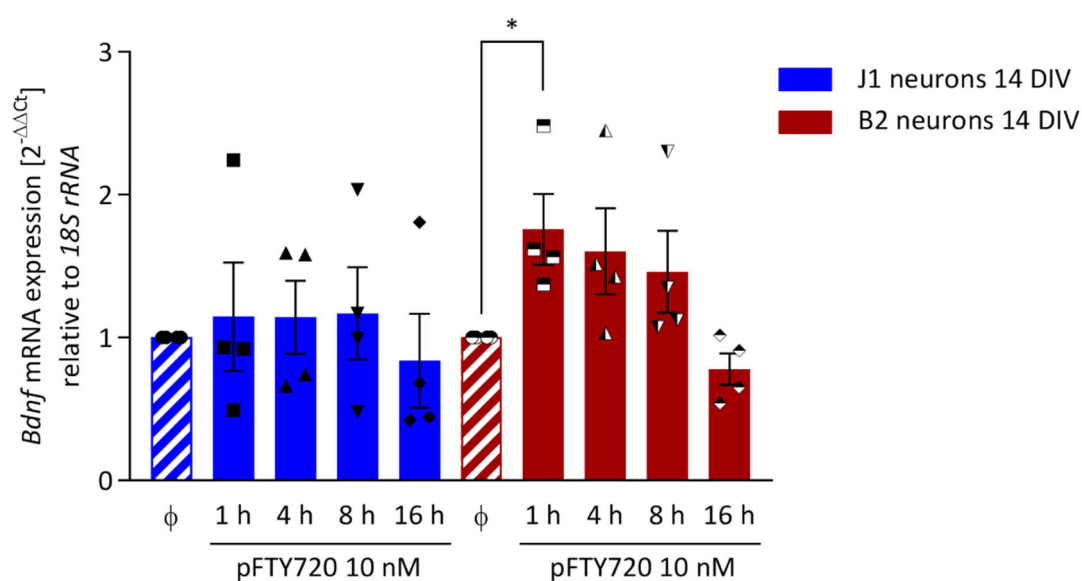
Figure 5.10 pFTY720 significantly increased *Bdnf* mRNA levels in B2 neurons

14 DIV old neurons were treated with pFTY720 10 nM for 1 h, 4 h, 8 h and 16 h. pFTY720 at a concentration of 10 nM increased *Bdnf* mRNA levels significantly in B2 neurons after 1 h compared to controls, but not in J1 neurons (Unpaired t-test, $p > 0.05$, $n = 4$). A one-way ANOVA did not reveal a significant difference between the two cell lines (One-way ANOVA, $p > 0.05$, $n = 4$). Data are represented as $2^{-\Delta\Delta Ct}$ mean $\pm$ SEM relative to internal control *18S rRNA*. Ø: vehicle (DMSO) treated cells.

5.4   Discussion

Long-term exposure of ES cell-derived neurons to pFTY720 suggested that the S1P1R may be involved in the upregulation of BDNF levels, as no significant effect was observed in the mutant cells lacking the receptor (Figure 5.1). Unfortunately, the high variability encountered in the culture system used here makes it difficult to draw firm conclusions as to an absolute requirement for S1P1R in mediating the effects of pFTY720 in neurons or the pathways recruited following the activation of S1P1R. Short-term experiments investigating the phosphorylation of ERK1/2 and CREB led to results that were even more variable than those related to BDNF levels upon long-term exposure (Figure 5.5-5.8). Significant effects which were found to occur after 10 min exposure to pFTY720 1 μM on pERK1/2 levels in B2 neurons and pCREB levels in J1 neurons could not be replicated in subsequent time course experiments (Figure 5.5-5.8). The reasons for the variability encountered in these experiments are unclear. Whilst this protocol was already extensively used by a number of groups to investigate the function of various genes, including p75[NTR] (Plachta et al. 2007), TrkA, TrkB and TrkC (Nikoletopoulou et al. 2010), Pax6 (Nikoletopoulou et al. 2007) and APP (Schrenk-Siemens et al. 2008), it appears that it may not be the optimal system to study the regulation of genes such as *Bdnf*. *Bdnf* is not only expressed at low levels but its expression also depends on the degree of neuronal maturation (Thoenen 1991). In young ES cell-derived neurons the levels of BDNF are barely detectable (Chapter 3, Figure 3.29), and it appears unlikely that neuronal activity develops similarly in all neurons even from one differentiation. Indeed, using the same differentiation protocol, a significant variability in terms of neuronal maturation between single neurons of the same differentiation as well as between cultures was reported using patch clamp recordings (Barth et al. 2014 and Discussion, section 8.4). As the protocol used consists of several sensitive steps and involves many different reagents (Material and Methods, section 2.9) multiple technical

factors could also be accounted for this variability. The most crucial aspect for the generation of a homogeneous population of neurons is the pluripotency of the ES cells used (Bibel et al. 2007). While the skills of the operator to maintain the pluripotency of the ES cells is one important aspect, culturing mouse ES cells in serum-containing medium and on feeder layers, as in this study, has been shown to increase the number of spontaneously differentiating cells compared to mouse ES cells cultured in serum-free conditions (Marks et al. 2012; Tamm et al. 2013). To investigate if the pluripotency of the ES cells may affect the variability observed in the neuronal cultures by generating heterogeneous populations (Bibel et al. 2007), future experiments should explore the expression pattern of different pluripotency markers, like the octamer-binding transcription factor 4 (Oct4) and the homeobox protein Nanog in ES cells of both cell lines (Loh et al. 2006). Additionally, the heterogeneity of ES cell-derived neuronal cultures should be investigated by immunohistochemical analysis of neuroglia and neuronal markers to facilitate the interpretation of the data obtained. Currently the results do not allow firm conclusions to be drawn and it is evident that more detailed characterisation studies of the J1 and B2 neurons are needed. What can be suggested due to the significant effect on pCREB levels in B2 neurons after 1 h and 2 h pFTY720 exposure (Figure 5.8) is that pFTY720 may also have other targets in ES cell-derived neurons apart from the S1P1R. This could be the S1P3R as the drug binds to it with similar affinity (Sykes et al. 2014) and the HDAC enzyme (Hait et al. 2014). However, other targets cannot be excluded at this preliminary stage as the significant increase of *Bdnf* mRNA levels after pFTY720 exposure in only B2 neurons (Figure 5.10), could possibly involve a modulation of intracellular Ca^{2+} levels by pFTY720 (Discussion, section 8.3.3). More importantly, to delineate if these effects are due to the difference in the background strain, the presence of the *Thy-1/Cre^ERT2* construct or indeed the lack of S1P1R a different control cell line to J1 should also have been used. It has been shown

that ES cells of different genetic background generated neurons of similar characteristics with the protocol used in this study (Bibel et al. 2004) and the rationale behind using the J1 cell line was to avoid any spontaneous recombination which could occur due to the presence of a *Cre^{ERT2}* construct (Zhang et al. 1996). However, spontaneous loxP recombination typically occurs at low level (Hayashi and McMahon 2002) and has been mainly reported *in vivo* (Kristianto et al. 2017). Therefore, experiments should be repeated with a cell line controlling for the different genetic background of the B2 neurons. A suitable cell line could be #48 (Chapter 3, Figure 3.16) which is of the same genetic background as B2 but does express the S1P1R.

In contrast to the long-term effects of pFTY720 on BDNF protein levels in J1 neurons, short-term exposure to 10 nM of pFTY720 did not induce any changes (Figure 5.2). This was unexpected as it was previously reported that pFTY720 10 nM increases BDNF protein levels after 24 h in primary mouse cortical cultures (Deogracias et al. 2012). To identify if the lack of increase could be due to differences between ES cell-derived and primary cortical neurons, the experiments performed by Deogracias and colleagues were replicated (Figure 5.2 and Appendix Figure A.2 and A.3). Although the number of wells investigated do not allow firm conclusions to be drawn, the current data suggests that also in primary cortical culture pFTY720 may not induce a significant increase in BDNF protein levels. To date it can only be speculated as to the reasons for the failure to reproduce the published data. Discussions with Ruben Deogracias revealed that differences in the experimental conditions, for example different media or the frequency of medium changes are unlikely to explain differences in experimental results with pFTY720. In the current study, fresh medium was added every third day until 9 DIV. In the study of Deogracias et al. 2012 however, the medium remained unchanged (R. Deogracias, personal communication). It is highly unlikely that the addition of medium abolished the increase of BDNF protein levels as rather the opposite would be expected.

Fresh medium appeared to induce increased spike counts and led to a significant increase of Arc protein in ES cell-derived neurons (Appendix, Figure A.6 and A.10), which can be predicted to occur in mouse primary cortical cultures in a similar fashion. Amongst one of few plausible explanations may be differences in the activity of pFTY720. The drug could have degraded into metabolites which would affect its potency. To investigate if this was indeed the case different batches of pFTY720 should have been tested as well as higher concentrations of up to 1 μM of pFTY720 for longer exposure times (e.g. 36 h, 48 h).

At present, it is not possible to draw a definite conclusion on the role of S1P1R in the effects of pFTY720 on ES cell-derived neurons. Although it seems to be implicated in the long-term effects of pFTY720 on BDNF protein levels (Figure 5.1) its role in mediating short-term effects is still unclear and further experiments are needed.

Chapter 6

In vivo Effects of FTY720 in Mice Conditionally Lacking S1P1R

6.1   Introduction

The *S1p1r*$^{\text{loxP/loxP/}}$*Cre*^{ERT2} mouse line described in the context of the isolation of ES cells (Chapter 3) was also used to investigate the role of the S1P1R on neurons *in vivo*. A randomly inserted *Thy-1/Cre*^{ERT2} construct allows the specific expression of the inducible recombinase in neurons only (Materials and Methods, section 2.2). The expression of *Cre*^{ERT2} mRNA in the adult hippocampus and cortex were assessed to learn about the potential of this mouse line designated SLICK-H (Young et al. 2008). The widespread expression of the S1P1R by essentially all cell types in the CNS suggests that a detectable decrease of *S1p1r* mRNA after tamoxifen injection may be unlikely (Choi and Chun 2013). This was tested in the cortex and compared to the hippocampus as it shows a comparatively high density of neuronal cell bodies, even though it is vascularised and endothelial cells are known to express the S1P1R at high levels.

6.2 Characterisation of the $S1p1r^{loxP/loxP}/Cre^{ERT2}$ Mouse Line

6.2.1 Cre^{ERT2} mRNA expression in two main adult brain areas

To identify the expression levels of Cre^{ERT2} mRNA the hippocampi and cortices of adult $S1p1r^{loxP/loxP}/Cre^{ERT2}$ mice were dissected and RNA isolated (Materials and Methods, section 2.14.2). RT-PCR experiments revealed that Cre^{ERT2} mRNA levels were higher in the adult hippocampus compared to adult cortex ($*p < 0.05$, Figure 6.1).

6.2.2 $S1p1r$ excision in the hippocampus and cortex

To test the efficacy of the tamoxifen treatment (75 mg/kg BW for five consecutive days), $S1p1r$ mRNA levels were determined in the hippocampus one week after the last injection. A small, but significant reduction could be observed ($**p < 0.01$, Figure 6.2A), suggesting that a proportion of neurons in the hippocampus are likely to express the S1P1R. Also in the cortex $S1p1r$ mRNA levels were analysed one week after the last injection. However, no reduction of $S1p1r$ mRNA levels was detectable in the cortex of tamoxifen compared to corn oil injected mice ($p > 0.05$, Figure 6.2B).
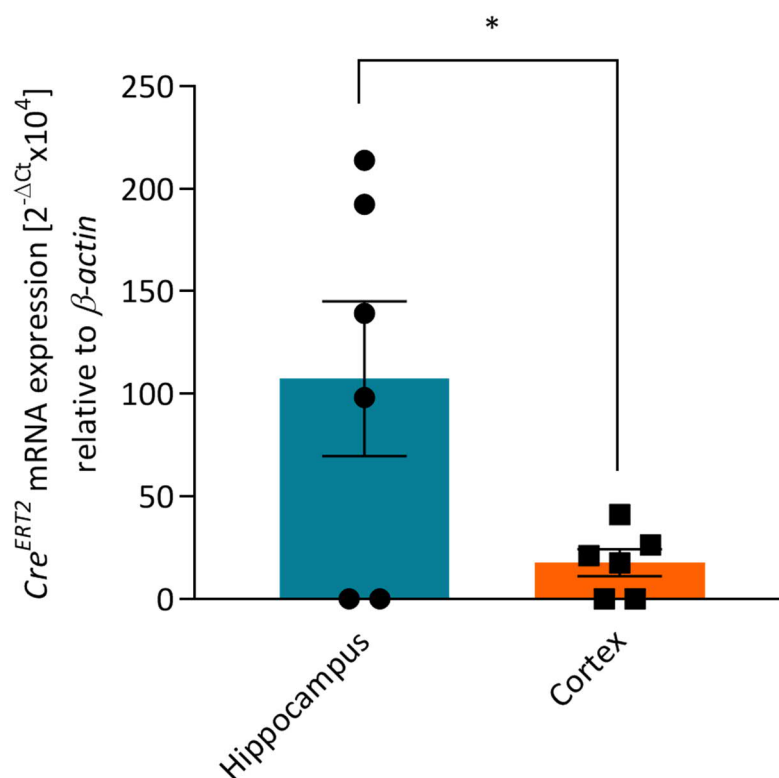
Figure 6.1 *Cre^ERT2* mRNA levels in the hippocampus and cortex

Cre^ERT2 levels were found to be expressed at significantly higher levels in the hippocampus compared to the cortex (Unpaired t test, *p (hippocampus *vs.* cortex) < 0.05, n = 6 mice). Data is represented as $2^{-\Delta Ct}x10^4$. *β-actin* was used as internal control. Graph represents mean ± SEM.

A
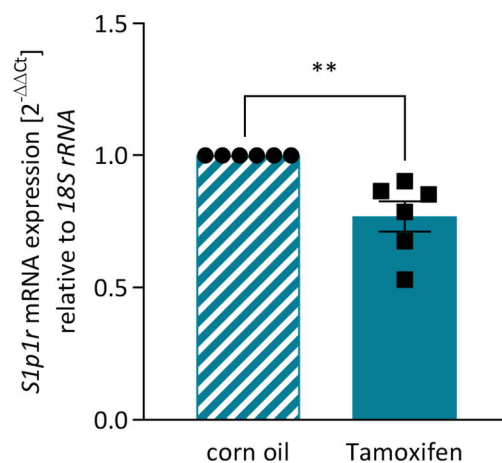
B
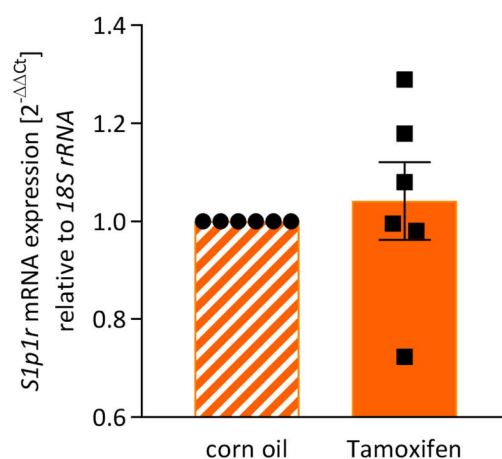
Figure 6.2 Tamoxifen injections decreased *S1p1r* mRNA levels in the hippocampus only

RNA extracted from the adult mouse hippocampus and cortex was used to analyse *S1p1r* mRNA levels after five consecutive tamoxifen injections. **A** Receptor expression was found to be significantly decreased in the hippocampus (Unpaired t-test, **$p < 0.01$, n = 6 mice). **B** In the cortex the levels of *S1p1r* mRNA remained unchanged (Unpaired t-test, $p > 0.05$, n = 6 mice). Data are represented as mean of $2^{-\Delta\Delta Ct} \pm$ SEM relative to internal control *18S rRNA*.

6.3　Molecular Changes in Various Brain Regions after FTY720 Injections *in vivo*

6.3.1　Effects of FTY720 on BDNF levels

Adult mice were injected every day for five consecutive days with tamoxifen. After a week FTY720 (0.1 mg/kg BW) injections started and were repeated every fourth day for four weeks (Materials and Methods, section 2.13). Cortices and hippocampi were dissected and BDNF levels analysed by Western blot (Figure 6.3). The effects of FTY720 on BDNF levels were relatively modest in the small cohort analysed. In the adult hippocampus of both corn oil and tamoxifen treated animals FTY720 injections induced only a trend towards an increase of BDNF levels compared to saline injected controls ($p = 0.054$, Figure 6.3). In the cortex FTY720 treatment did not affect BDNF levels whether in the corn oil nor in the tamoxifen treated mice ($p > 0.05$, Figure 6.4).

A
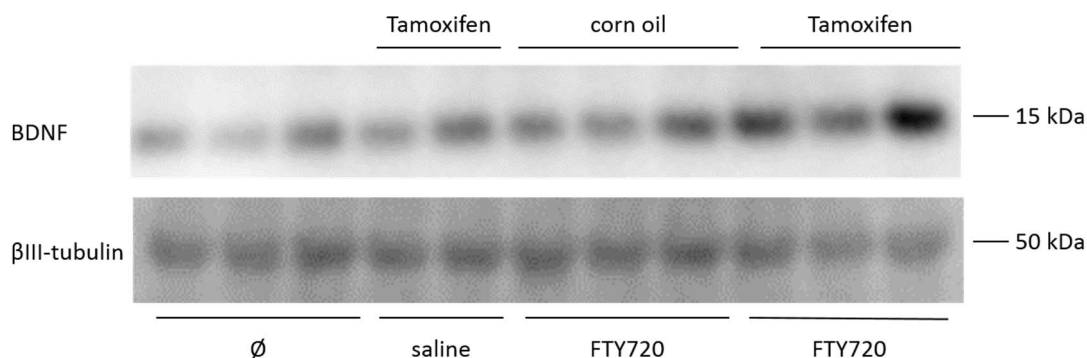
B
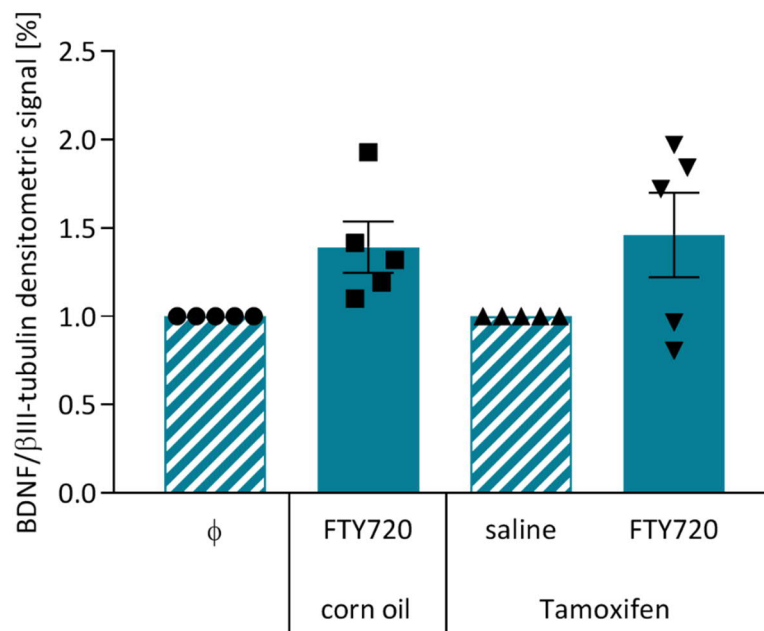
Figure 6.3 BDNF protein levels in the hippocampus following FTY720 injections

Mice were injected for five days with tamoxifen. After another week, mice were injected with FTY720 every fourth day for four weeks. BDNF levels showed overall a trend towards an increase after FTY720 exposure which is independent of the tamoxifen treatment (One-way ANOVA, p = 0.054, n = 5 mice). Ø: non-injected untreated mice. Graph represents change in percentage *vs.* control.

A
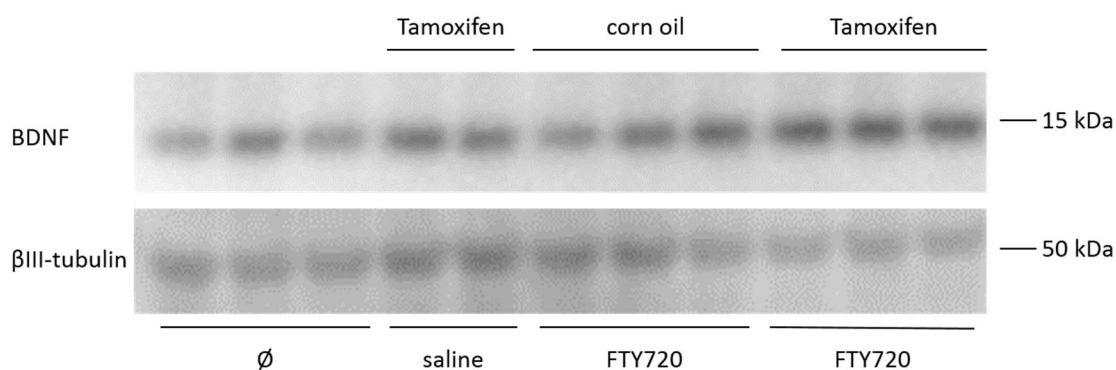
B
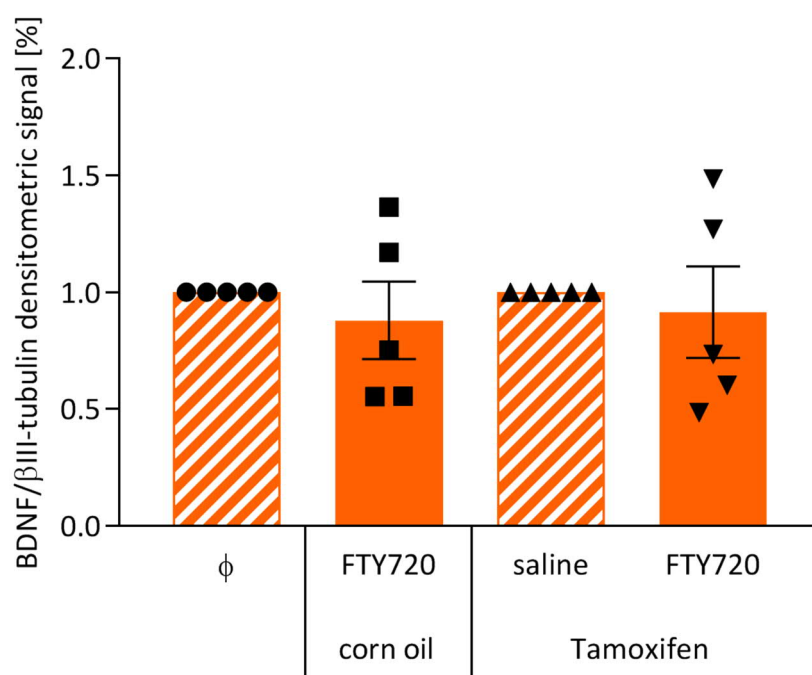
Figure 6.4 BDNF levels in the mouse cortex were unaffected by FTY720 injections

Mice were injected for five days with tamoxifen (75 mg/kg BW). Mice were allowed to rest for one week to let recombination take place. Subsequently, mice were injected with FTY720 (0.1 mg/kg BW) every fourth day for four weeks. BDNF levels remained unchanged in the mouse cortex after FTY720 treatment. Additionally, BDNF levels were not affected by tamoxifen treatment (One-way ANOVA, $p > 0.05$, n = 5 mice). Ø: non-injected untreated mice. Graph represents change in percentage *vs.* control.

6.3.2 Effects of FTY720 on ERK1/2 phosphorylation

The effects of FTY720 following a single FTY720 injection were also investigated with regard to ERK1/2 phosphorylation. Thirty minutes after FTY720 injections (0.1 mg/kg BW) hippocampi and cortices were dissected and proteins extracted. The mice were treated either with tamoxifen (75 mg/kg BW) or corn oil for five consecutive days, a week before the FTY720 or saline application. Despite tamoxifen treatment, injection of FTY720 led to a trend towards an increase of ERK1/2 phosphorylation compared to saline injected controls in the hippocampus (difference between medians = 1.07, Figure 6.5). In the cortex, no significant changes of ERK1/2 phosphorylation was induced by FTY720 treatment (Figure 6.6).

6.3.3 Effects of FTY720 on CREB phosphorylation

Using the same treatment regime as for the investigation of pERK1/2 levels, brain regions were assessed for changes in CREB phosphorylation after FTY720 treatment. In the hippocampus as well as the cortex of corn oil and tamoxifen treated adult mice no significant changes of CREB phosphorylation were observed 30 min after a single FTY720 injection of 0.1 mg/kg BW ($p > 0.05$, Figure 6.7 and 6.8).

A
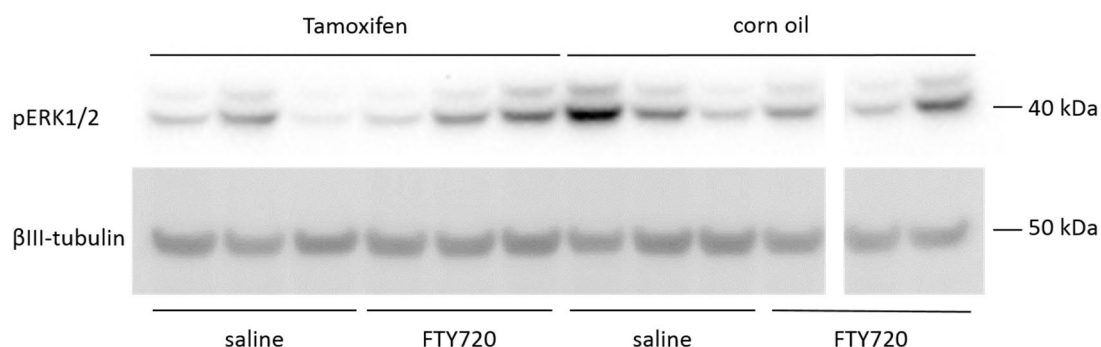
B
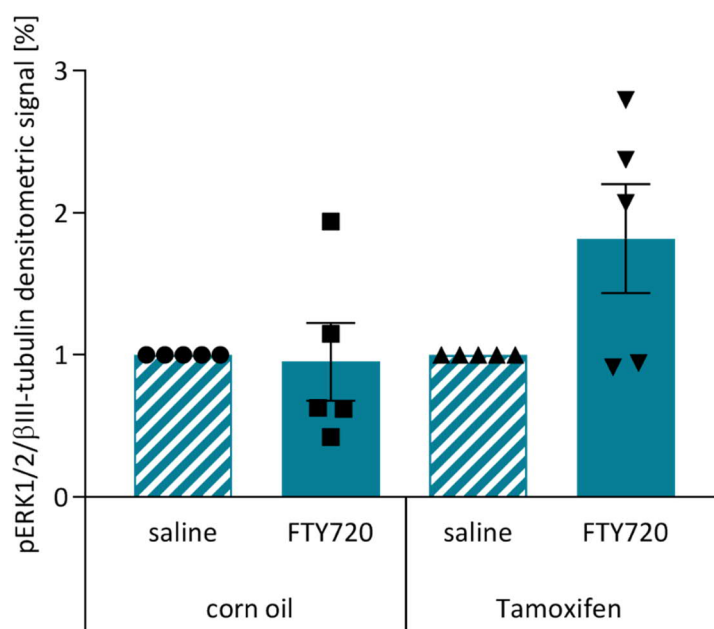
Figure 6.5 Short-term effects of FTY720 on ERK1/2 phosphorylation in the hippocampus

Corn oil or tamoxifen treated mice were injected with either FTY720 or the vehicle saline and culled 30 min after the injection. **A** Western blot of pERK1/2. 40 µg of protein were loaded per lane. **B** No changes of ERK1/2 phosphorylation was detected after FTY720 injections in corn oil treated mice (Mann-Whitney test, $p > 0.05$, n = 5 mice). In tamoxifen treated mice a trend towards an increase of ERK1/2 phosphorylation was observed after FTY720 injections (Mann-Whitney test, actual difference between medians (saline *vs.* FTY720) = 1.07, n = 5 mice). Data are represented as mean ± SEM relative to βIII-tubulin. Changes are in percentage *vs.* control.

A
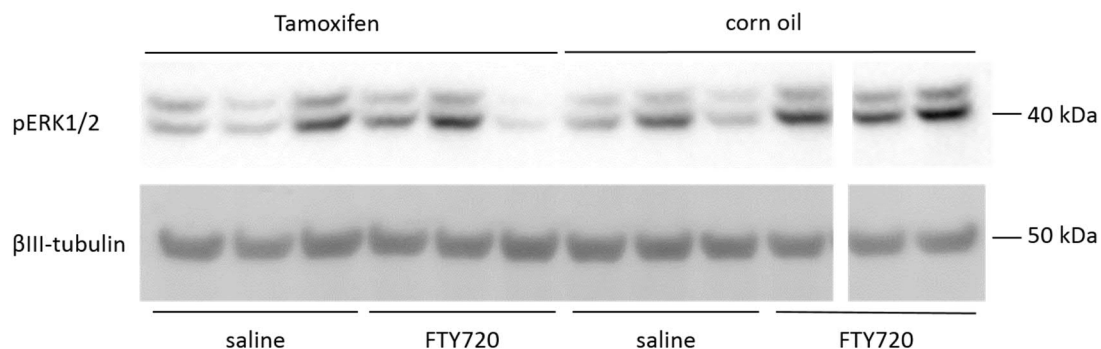
B
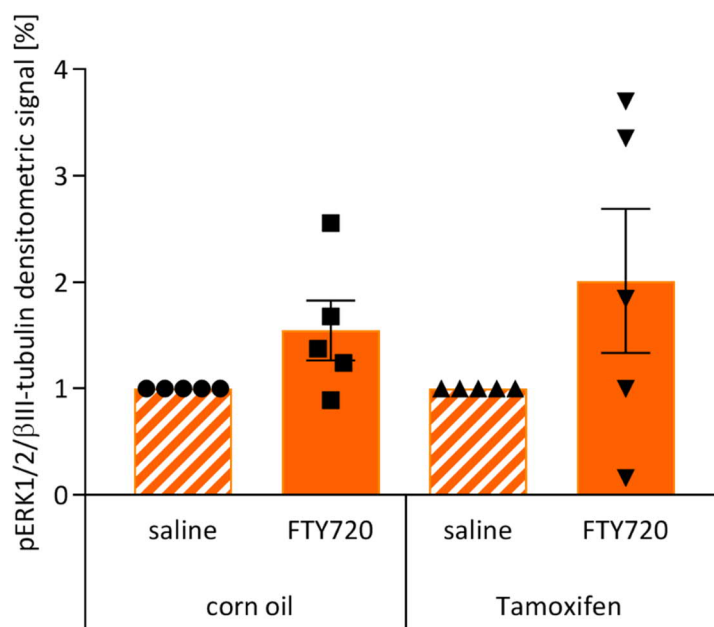
Figure 6.6 Short-term effects of FTY720 on ERK1/2 phosphorylation in the cortex

Corn oil or tamoxifen treated mice were injected with either FTY720 or the vehicle saline and culled 30 min after the injection. **A** Western blot of pERK1/2. 40 µg of protein were loaded per lane. **B** No changes in ERK1/2 phosphorylation were observed in the cortex of corn oil or tamoxifen treated mice (Unpaired t-test, p (saline *vs.* FTY720) > 0.05, n = 5 mice). Data are represented as mean ± SEM relative to βIII-tubulin. Changes are in percentage *vs.* control.

A
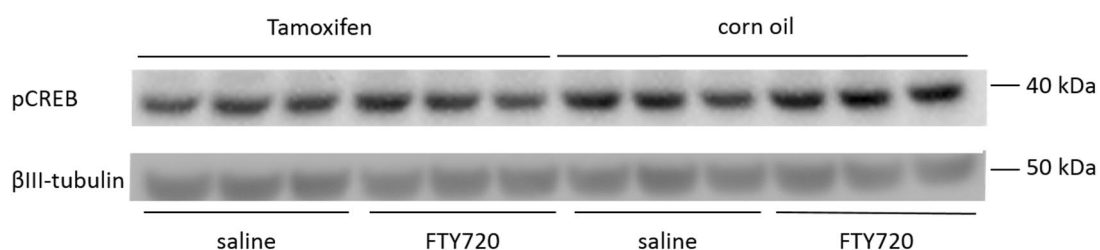
B
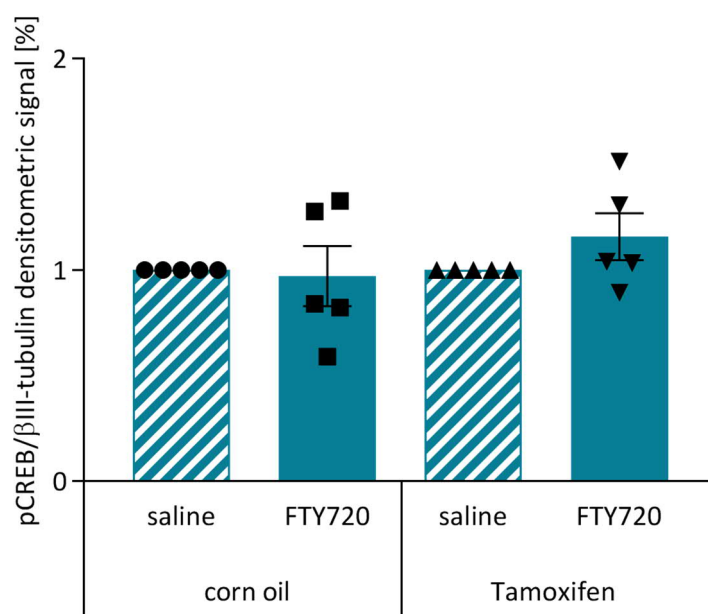
Figure 6.7 Levels of CREB phosphorylation after FTY720 treatment in the hippocampus

Corn oil or tamoxifen treated mice were injected with either FTY720 or the vehicle saline and culled 30 min after the injection. **A** Western blot of pCREB. 40 µg of protein were loaded per lane. **B** CREB phosphorylation was not affected by FTY720 injection in the hippocampus of corn oil or tamoxifen treated mice (Unpaired t-test, p (saline *vs.* FTY720) > 0.05, n = 5 mice). Data are represented as mean ± SEM relative to βIII-tubulin. Changes are in percentage *vs.* control.

A
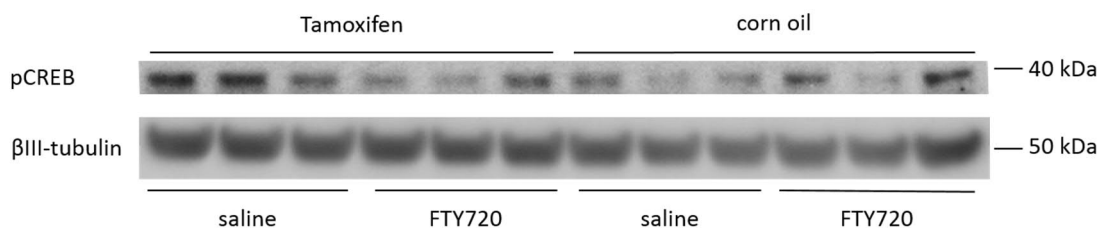
B
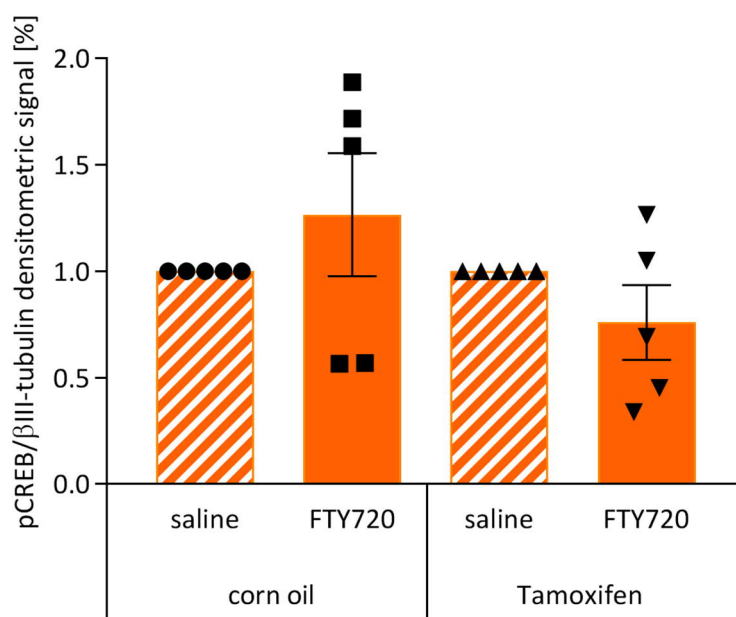
Figure 6.8 Levels of CREB phosphorylation after FTY720 treatment in the cortex

Corn oil or tamoxifen treated mice were injected with either FTY720 or the vehicle saline and culled 30 min after the injection. **A** Western blot of pCREB. 40 µg of protein were loaded per lane. **B** No significant effect on CREB phosphorylation was found in the cortex of tamoxifen or corn oil treated mice after a single FTY720 injection (Mann-Whitney test, p (saline *vs.* FTY720) > 0.05, n = 5 mice). Data are represented as mean ± SEM relative to βIII-tubulin. Changes are in percentage *vs.* control.

6.1   Discussion

To begin to evaluate whether the newly generated mouse line $S1p1r^{\text{loxP/loxP}}/Cre^{ERT2}$ could be used to excise S1P1R specifically in neurons and in brain regions of interest, the expression levels of Cre^{ERT2} driven by the *Thy-1* transgene were analysed prior to tamoxifen treatment. In contrast to other extensively used Thy-1 lines expressing YFP in small number of neurons, the *Thy-1/Cre^{ERT2}* SLICK-H line is characterised by a widespread neuron-specific expression of Cre^{ERT2} in the brain (Young et al. 2008). In theory, this line could help to delineate whether any effects of FTY720 in the brain may be caused directly by the activation of S1P1R on neurons, as opposed to indirectly through the activation of the receptor on other cell types, a major open question in the field. It was found that tamoxifen injections did decrease the levels of *S1p1r* mRNA in the hippocampus (Figure 6.2A). However, the level of reduction is only moderate and no reduction was seen in the cortex (Figure 6.2). This may seem surprising considering the fact that the *Thy-1/Cre^{ERT2}* SLICK-H line does show more than 90 % recombination efficiency in neurons of the hippocampus and the neocortex (Heimer-McGinn and Young 2011). This unexpected result may be due to the limited knowledge on the relative expression of S1P1R in neurons compared to non-neuronal cells (Blaho and Hla 2014). In addition, it is unclear if the $S1p1r^{\text{loxP/loxP}}/Cre^{ERT2}$ mouse line used in this study shows comparable levels of Cre^{ERT2} expression in the different brain areas to the mouse line previously examined by Heimer-McGinn and Young. Indeed, one of the problems encountered with lines based on random insertions of constructs such as *Thy-1/Cre^{ERT2}* is that they do not show the same stability over generations due to variations in the transgene copy number (Alexander et al. 2004). To more closely monitor Cre^{ERT2} expression in neurons as well as nuclear translocation after tamoxifen, it will be important in future experiments to monitor the efficiency of the process using sections of brain regions of interest and to stain them with Cre antibodies. This could be completed by *in situ*

hybridisation experiments to *S1p1r* mRNA in the hippocampus to identify the neuronal-specific excision and to visualise the expression levels of *S1p1r* mRNA in non-neuronal cells at the same time. In line with this, *S1p1r* mRNA levels would need to be normalised to a neuron-specific mRNA, given that the *Thy-1* promoter should drive a neuron-specifc expression of Cre^{ERT2}. The regime of tamoxifen administration also needs to be critically considered as it is known to be problematic in the context of studies dealing with the adult mouse brain. Here, mice were treated with tamoxifen (75 mg/kg BW) via intraperitoneal injections for five consecutive days. Intraperitoneal injections were preferred over oral administration by gavage to better control for the amounts of tamoxifen administered. Others have used more radical approaches in Thy-1/Cre^{ERT2} SLICK-H mice, including 250 mg tamoxifen per kg BW for five consecutive days administered by oral gavage followed by a rest of ten days and a final treatment of tamoxifen (same dosage) for another five days (Heimer-McGinn and Young 2011). It is conceivable that this much more extensive tamoxifen treatment may have led to significant reductions of levels in the hippocampus and the cerebral cortex.

Still, a small reduction of *S1p1r* mRNA levels could be achieved in the hipppocampus albeit not sufficient to prevent a trend towards an increase of BDNF levels following FTY720 injection (Figure 6.3). It will be interesting to see in future experiments if a more radical regime of tamoxifen treatment (see above) combined with the use of higher numbers of animals may lead to statistically significant results. The rationale behind investigating long-term effects of FTY720 on BDNF levels *in vivo* stems from the results obtained with ES cell-derived neurons indicating that long-term treatment of these cells led to a modest, albeit significant increase of BDNF protein levels *in vitro* provided S1P1R was expressed (see Chapter 5). However, it has been previously reported that BDNF levels already increased 48 h after a single FTY720 injection in the cerebral cortex, the hippocampus and the striatum (Deogracias et al. 2012). These experiments should be

replicated, especially as more recent results using the same long-term FTY720 injection paradigm (one injection every fourth day for four weeks) failed to detect an increase in BDNF protein levels in the hippocampus either (Miguez et al. 2015). Interestingly, in the same study *Bdnf* mRNA levels were found to be increased after FTY720 injections (Miguez et al. 2015), in line with another study where WT mice treated according to the same protocol showed an increase of *Bdnf* mRNA levels in the cerebral cortex (Di Pardo et al. 2014). In the current study no increase of BDNF protein levels in the cortex or hippocampus of corn oil or tamoxifen treated animals was observed after FTY720 treatment (Figure 6.4). Although it was a central objective to analyse the effects of FTY720 on BDNF protein expression levels (Introduction, section 1.4.4), it will be necessary in future experiments to first determine the conditions under which *Bdnf* mRNA levels may increase and the role of S1P1R in this effect. Additionally, considering the expression levels of S1P1R in non-neuronal cells, experiments analysing long-term effects of FTY720 on BDNF levels in animals lacking S1P1R expression in both neuronal and non-neuronal cells should also be included.

With regard to the short-term effects of FTY720 no significant changes could be observed whether in the cortex nor in the hippocampus (Figure 6.5-6.8). The high variability found in the biochemical measurements after FTY720 treatment in the cortex as well as the hippocampus, made it difficult to draw any conclusions and a higher number of animals needs to be investigated (see also Discussion, section 8.5).

Chapter 7

Sphingosine Receptors and Megakaryocytes

4.1 Introduction

S1P is involved in a wide variety of cell-cell interactions, its S1P receptors are widely distributed in tissues where they play a number of different roles ranging from the promotion of cell survival to migration and proliferation (Pyne et al. 2016). This is also the case in the vascular and hematopoietic system as illustrated by the results of germ line deletion of S1P1R and the role of FTY720 in preventing the egress of lymphocytes from lymph node (Introduction, section 1.2 and 1.3). The S1P gradient formed between the relatively high concentration in both lymph and blood is read by the S1P1R and not only directs lymphocytes out of the lymph nodes into the blood stream, but also helps guiding proplatelet protrusions from megakaryocytes to facilitate the release of platelets into the blood circulation (Hla et al. 2012; Zhang et al. 2012). As our laboratory recently reported that human and rat megakaryocytes express *BDNF/Bdnf* mRNA transcripts similar to neurons (Chacon-Fernandez et al. 2016), it was of interest to investigate which sub-type of sphingosine receptors is expressed by megakaryocytes and to test whether pFTY720 regulates *Bdnf* mRNA levels.

4.2   Rat Megakaryocytes Express *S1p receptor* mRNAs

RNA was extracted from primary cultures of rat megakaryocytes after 6-10 days and RT-qPCR was performed to analyse the expression of the five S1P receptors (Materials and Methods, section 2.16). All five receptors were found to be expressed whereby *S1p1r* and *S1p2r* mRNAs were found to be expressed at high levels with *S1p3r* being the least abundant member, followed by *S1p4r* and *S1p5r* using the levels of *Hprt* as a reference (Figure 7.1).
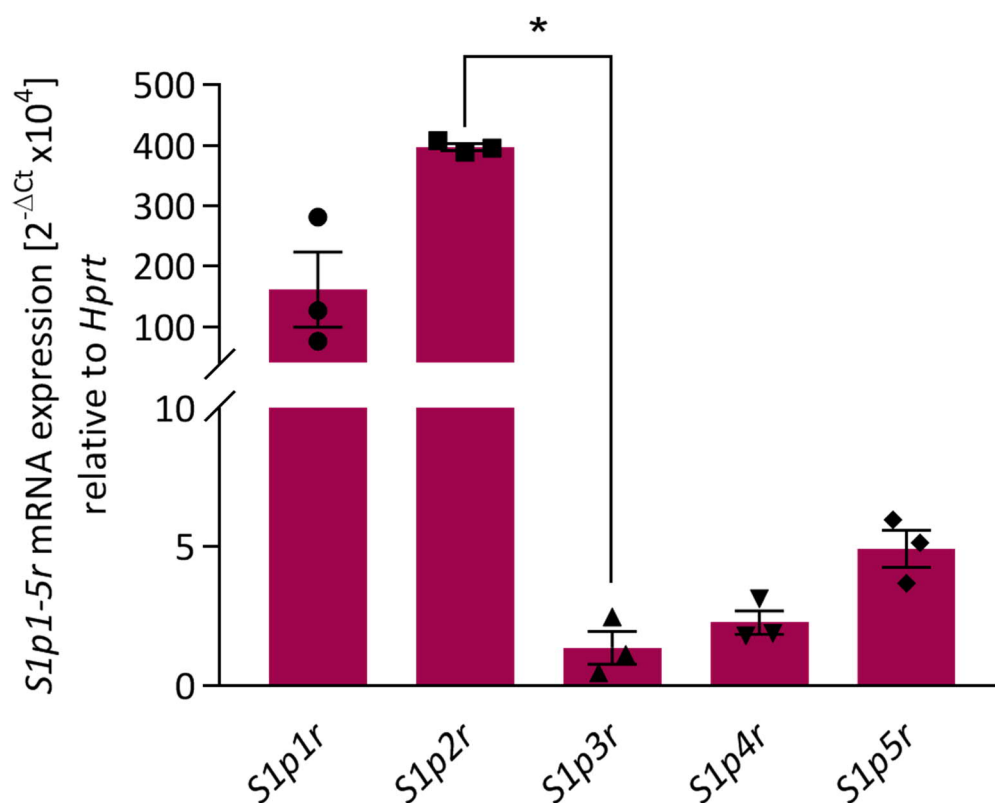
Figure 7.1 Expression pattern of *S1p receptors* in rat megakaryocytes

S1p1r and *S1p2r* mRNAs were expressed at comparatively high levels with lower, but clearly detectable expression of the three other members of the family. *S1p2r* mRNA is expressed at significantly higher levels than *S1p3r* mRNA (Kruskal-Wallis test followed by Dunn's multiple comparison test, $*p < 0.05$, n = 3). Data are represented as mean of $2^{-\Delta Ct} \times 10^4 \pm$ SEM relative to internal control *Hprt*.

4.3 *Bdnf* mRNA Levels in Megakaryocytes after Different Exposure Times to pFTY720

Primary megakaryocytes were treated for 6 and 16 h with pFTY720 10 nM, the cells lysed, RNA extracted and *Bdnf* mRNA levels analysed. These experiments revealed a significant decrease in *Bdnf* levels 6 h after treatment of megakaryocytes with pFTY720 10 nM (**$p < 0.01$). After 16 h exposure to pFTY720 a trend towards an increase of *Bdnf* mRNA levels was observed ($p = 0.06$, Figure 7.2).
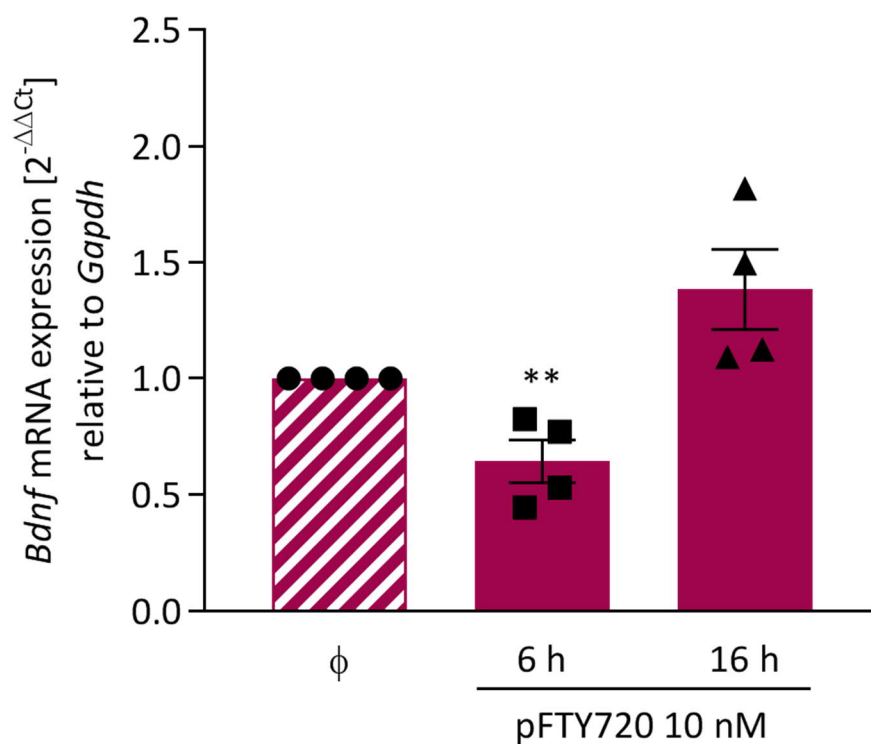
Figure 7.2 Effects of pFTY720 on *Bdnf* mRNA levels in rat megakaryocytes

Cultured megakaryocytes were treated with pFTY720 10 nM for 6 h or 16 h. *Bdnf* mRNA levels decreased significantly after 6 h exposure to pFTY720 10 nM (Unpaired t test, **p < 0.01, n = 4). After 16 h a trend towards an increase of *Bdnf* mRNA levels was observed (Unpaired t test, p (Ø *vs.* pFTY720 10 nM 16h) = 0.06, n = 4). Data are represented as mean ± SEM relative to internal control *Gapdh* and normalised to the control. Ø: vehicle (DMSO) treated cells.

4.4 Discussion

While all five sphingosine receptors were found to be expressed by rat megakaryocytes, it is of note that this seems not to be the case in mouse and human megakaryocytes where only *S1p1r*, *S1p2r* and *S1p4r* are expressed (Zhang et al. 2012). It more resembles the expression in immature megakaryocytes, where *S1p1r* and *S1p2r* are expressed at high levels, whilst *S1p3r* is only barely detectable (Zhang et al. 2012). While Zhang and colleagues used the same method to enrich the mature megakaryocytes, namely a BSA gradient (Materials and Methods, section 2.16), they additionally isolated the immature megakaryocytes by fluorescence activated cell sorting (FACS). It is therefore possible that in the present study, a mixture of mature and immature rat megakaryocytes has been investigated. This seems plausible given the observation that the rat megakaryocytes showed *S1p4r* as well as *S1p3r* expression. Although it has been shown that *Hprt* seems to be a stable reference gene for the detection of *S1pr* in three different tissues (Kays et al. 2012), the results of the current study would need to be extended using additional internal standards such as the attachment region binding protein *Arbp (attachment region binding protein)* or *Gapdh*.

The interpretation of the results regarding *Bdnf* mRNA levels after pFTY720 addition is complicated by the fact that towards the end of their *in vitro* maturation, cultured megakaryocytes can be observed to generate platelets (as they do *in vivo* in the bone marrow). This is relevant as our laboratory very recently demonstrated that not only megakaryocytes, but also platelets contain *Bdnf* mRNA transcripts, including those typically found in neurons (Chacon-Fernandez et al. 2016). As it remains unclear whether all platelets are collected in those experiments in addition to megakaryocytes, it is difficult at this point to interpret the results. The slight decrease seen at shorter time interval suggests that some of the platelet-contained transcripts may have been lost during the

extraction of the cells from the plate. The centrifugation step might not allow for all platelets to be spun down as they are considerably smaller than megakaryocytes (Materials and Methods, section 2.16). Also, the destruction of the megakaryocyte nucleus through apoptosis after platelet release (Gordge 2005), could explain a further loss of transcripts. Investigating the expression of a gene specifically found in megakaryocytes and platelets like the *von Willebrand factor* would allow to clarify this question and should be included in future experiments. Further, it will be interesting to explore the role of pFTY720 after purifying megakaryocytes and to investigate the supernatant separately as it is now clear that platelets are a complicating factor. Still, the preliminary results illustrated here are intriguing, including the trend towards an increase of *Bdnf* mRNA levels 16 h after pFTY720 addition show that investigating different time points, higher pFTY720 concentrations and BDNF protein levels will be of major interest. Finally, megakaryocytes may be additionally isolated by FACS using maturation-specific markers to ensure that they are analysed at similar degrees of maturation.

Chapter 8

Discussion

The main objective of this study was to explore the role of the S1P1R in mediating the effects of pFTY720 on neurons. As FTY720 has long been known to diffuse into the brain where it even accumulates there is a pressing need to understand how the drug may interact with what is generally thought to be one of its main targets, namely S1P1R. To this end, ES cells were isolated from the blastocysts of mutant animals carrying a conditional mutation of the receptor. S1P1R was excised from these ES cells, neurons generated and compared with those generated from WT ES cells. Using a modification of an existing differentiation protocol, neurons lacking S1P1R were successfully generated from these mutant ES cells and some of the biochemical changes following exposure to FTY720 compared with WT neurons. Although the excision of S1P1R affected the long-term effects of pFTY720 on BDNF levels in ES cell-derived neurons, the high variability encountered in the system used does not allow firm conclusions to be drawn about the role of S1P1R in these cells. Furthermore, some of the effects observed with neurons lacking S1P1R, including a transient increase of *Bdnf* mRNA, cannot solely be attributed to the lack of the receptor in the experimental setting used. This important point will require further investigation using a S1P1R-expressing cell line of the identical genetic background.

8.1   Generating Neurons Lacking S1P1R

As the role of sphingosine during early development only begins to be appreciated and mice lacking *S1p1r* die at the time when the CNS begins to develop (Introduction, section

1.2), it could not be assumed that neurons could be generated in the absence of S1P1R. This concern is of special relevance as WT ES cells express S1P1R (data not shown), and because the receptor has been suggested to play a role in neurogenesis (Liu et al. 2000; McGiffert et al. 2002; Mizugishi et al. 2005). Indeed, the standard differentiation protocol had to be modified due to the proliferation of non-neuronal cells observed with the progeny of *S1p1r^{-/-}* ES cells that affected long-term cultures of these neurons. While neither the identity of the proliferating cells nor the reasons for this altered proportion between neuron and non-neuronal cell progenitor could be investigated, these results suggest that S1P1R, and by extension sphingosine signalling, may play a role during the formation of cellular aggregate and the induction of neural commitment by retinoic acid. Not much is known about this process in the first place except for the interesting observation that the effects of the addition of retinoic acid can be replicated by interfering with Wnt signalling (Aubert et al. 2002). Following a brief, early pulse of 5- FdU, overgrowth of non-neuronal cells could be prevented and the phenotype of the resulting neurons seemed to be similar to those of WT neurons for certain characteristics. In particular, the extent as well as the developmental time course of synaptophysin and BDNF expression turned out to be similar as was the development of more specific markers such as two major glutamate transporters on mRNA level (Chapter 3). At the protein level, a significant increase of vGlut2 expression was found in B2 neurons compared to J1 neurons (Figure 3.31). The reasons for this increase are unclear at this point and further experiments involving immunocytochemical analysis to define the cellular composition of the cultures would be needed to understand the significance of this observation.

During the course of these studies, it was noted that the yield of progenitors dissociated from aggregates initiated with B2 ES cells ($10 \times 10^6 \pm 1.3 \times 10^6$ cells/dish) was significantly lower (Unpaired t test, **p < 0.01, n = 8) than the yield obtained with J1 ES cells (20×10^6

$\pm$ 1.1x10^6 cells/dish). While this observation is in line with a recent publication demonstrating that FTY720 promoted neural progenitor survival as well as proliferation in the adult mouse hippocampus (Efstathopoulos et al. 2015), it is more difficult to reconcile with recent results indicating that endogenous S1P may maintain neural stem cells quiescent in the sub-ventricular neurogenic niches (Codega et al. 2014). However, an analysis of *S1p1r* mRNA levels during the 8-day course of cellular aggregation revealed a progressive decrease of its expression in WT cells (data not shown). In the complete absence of the receptor, it is conceivable that S1P1R-dependent regulatory mechanisms may be missing thus hypothetically preventing an acceleration of progenitor amplification. New insights into mechanisms regulating expansion of neural progenitors may thus emerge from the use of mutant ES cells lacking S1P1R, a potentially valuable tool given the observation that proliferation of non-neuronal cells following the plating of these progenitors was considerably enhanced (see above). To better appreciate the relevance of these *in vitro* observations, further *in vivo* work is needed whereby an attractive possibility would be to cross the *S1p1r*$^{loxP/loxP}$ line with a lineage-specific line such as the *Glast/Cre*^{ERT2} line allowing the excision of the receptor in radial glial cells as well as in mature astrocytes following tamoxifen injections (Mori et al. 2006).

8.2   Using *S1p1r*$^{-/-}$ Neurons to Test Antibody Specificity

The availability of cells lacking *S1p1r* as evidenced by genomic DNA as well as RT-qPCR analyses made it possible to test the specificity of commercially available antibodies targeting this receptor. A widely used reagent is a polyclonal antibody from Cayman Chemicals (Kohno et al. 2002; Crousillac et al. 2009; Nishimura et al. 2010; Healy et al. 2013; Lukas et al. 2014). It detected S1P1R at a molecular weight slightly in excess of 50 kDa while S1P1R has an estimated molecular weight of

43 kDa (UniProtConsortium 2014), a discrepancy that may be explained by the N-glycosylation consensus sequences in the extracellular domain of the receptor (Kohno et al. 2002). Consistent with the mRNA data (Figure 3.33), the intensity of the Western blot signal increased significantly with time in culture and was quite prominent after three weeks (Figure 3.20-3.21). However, this is also the case with neuronal lysates prepared from B2 ES cell-derived neurons, a result incompatible with the genomic DNA and mRNA analyses. Further, a monoclonal antibody raised against S1P1R (Nakajima et al. 2014), detected a band at about 43 kDa that became more prominent during neuronal differentiation and was also present in neurons derived from ES cells lacking the gene encoding S1P1R. Hence, the specificity of both antibodies could not be confirmed, which may explain in part the state of confusion in the field, especially regarding the important question as to whether S1P1R is expressed at all by neurons (Chae et al. 2004; Nishimura et al. 2010; Choi et al. 2011). In this regard, the results presented in Chapter 3 are interesting as they indicate that the *S1p1r* gene is expressed in the cultures of ES cell-derived neurons and that this expression increases during the differentiation (Figure 3.33). Additionally, preliminary results in Chapter 5 suggest that S1P1R might be involved in the long-term effects of pFTY720 on BDNF levels in ES cell-derived neurons. What this study does not address, is the exact cellular composition of the cultures used. Preliminary results on GFAP expression analysis by Western blot suggest that under suboptimal culturing conditions and without mitotic inhibitor treatment, different cell types may be present in these cultures (Figure 3.27). It is unclear if these cells would also express S1P1R and thereby contribute to the effects seen in J1 cultures. As currently no specific antibodies are available these additional investigations could involve *in situ* hybridisation assays or fluorescence-activated cell sorting (FACS) with subsequent RT-PCR analysis for *S1p1r* in the isolated cell types. There are published specificity tests of the S1P1R polyclonal antibody showing an immunohistochemistry analysis of S1P1R expression on

vascular endothelial cells in E12.5 mouse tissue, using *S1p1r*^{-/-} tissue as control (Akiyama et al. 2008). This prompted further investigations and an immunocytochemistry analysis of J1 and B2 ES cell-derived neurons, thereby testing the possibility that the polyclonal antibody might recognise the receptor on tissue sections, as opposed to Western blot. However, these additional experiments revealed a weak granular-type of staining on neuronal processes (Figure 3.22 and 3.23). While this staining pattern would as such be compatible with the expression of a membrane protein it was of comparable intensity using neurons derived from B2 ES cells not expressing S1P1R. Therefore, this staining cannot be attributed to S1P1R, but possibly to another receptor such as S1P3R. This would explain the discrepancy with the previous study by Akiyama et al. as the developing mouse vasculature only expresses very low levels of S1P3R as revealed by *in situ* hybridisation analysis (Ishii et al. 2001). Also, the germ line deletion of *S1p3r* does not lead to embryonic lethality, unlike germ line deletion of *S1p1r* (Liu et al. 2000), suggesting very low to no expression of S1P3R on E12.5 mouse endothelial cells. Additional studies are needed to analyse a possible cross-reactivity of the polyclonal antibody with S1P3R and to clearly define its specificity.

8.3 Effects of pFTY720 on J1 and B2 Neurons *in vitro*

8.3.1 Pathways activated upon prolonged pFTY720 exposure

After prolonged exposure of WT and mutant ES cell-derived neurons to pFTY720, a significant increase of BDNF levels was observed in WT, but not in neurons lacking S1P1R (Figure 5.1). This suggests that the increase may be a S1P1R-dependent effect. The mode of action of FTY720 was originally described as that of a functional antagonist due to its effect observed in lymphocytes. Indeed, long-term exposure of lymphocytes to FTY720 and its phosphorylated form induce the internalisation of S1P1R, thereby

hindering its activation by S1P (Graler and Goetzl 2004; Matloubian et al. 2004). Subsequent studies reported on S1P1R internalisation in transfected Chinese hamster ovary (CHO) (Mullershausen et al. 2009; Sykes et al. 2014), human umbilical vein endothelial cells (HUVEC) (Mullershausen et al. 2009), and astrocytes (Choi et al. 2011; Healy et al. 2013). These studies have shown that the drug's action is complex and that pFTY720 triggers a sustained cAMP signalling over S1P1R even after its internalisation in HUVEC and astrocytes (Figure 8.1 and (Mullershausen et al. 2009; Healy et al. 2013)). This persistent activation of the $G_{i/o}$ protein leads to the continuous inhibition of adenylyl cyclase and induction of ERK1/2 phosphorylation (Healy et al. 2013). If the internalisation of S1P1R also occurs in neurons is unclear at this point. Should this indeed be the case the induction of ERK1/2 phosphorylation could possibly be an explanation for the reported increase of *Bdnf* transcription *in vitro* and *in vivo* (Deogracias et al. 2012). By contrast, the increase in intracellular Ca^{2+}, known to occur soon after S1P1R activation is not sustained following prolonged exposure to pFTY720 in astrocytes (Healy et al. 2013), for reasons that are not well understood. It is possibly caused by a conformational change of S1P1R elicited by its ligands and/or an uncoupling of the S1P1R from the PLC pathway, known to induce intracellular Ca^{2+} release after its activation through the $G_{\beta\gamma}$ subunit (Figure 8.1 and (Werry et al. 2003; Healy et al. 2013)). This is important as it is well known that *Bdnf* transcription in neurons is induced by rapid Ca^{2+} influx (Introduction, section 1.4.2 and (West et al. 2014)). At this point, the continuous activation of the ERK pathway seems to be the most likely explanation for the increase of BDNF levels in WT neurons (Figure 5.1). In mutant neurons lacking S1P1R, the drug will likely first bind to S1P3R, as the affinity of pFTY720 to S1P1R and S1P3R is similar (Sykes et al. 2014) and the expression of the two receptors in cultured J1 and B2 neurons at the mRNA level is comparable (Figure 3.33). S1P3R is also coupled to $G_{i/o}$ protein and the ERK pathway (Ishii et al. 2002). However, the results suggest that this does not occur

at significant levels in the B2 neurons as no BDNF increase could be observed after long-term exposure to pFTY720 in these neurons lacking S1P1R (Figure 5.1). Also, the results on the phosphorylation of ERK1/2 is difficult to interpret due to the high variability encountered in the culture system used (Figure 5.5 and 5.6, Discussion Chapter 5). Intriguingly, pFTY720 acts as a weak partial agonist on S1P3R by blocking the signalling of S1P *via* the G_q protein and at the same time activating the $G_{i/o}$ protein-dependent pathways. This distinct activation of S1P3R by S1P and pFTY720 is thought to occur because of different conformational changes of the receptor caused by pFTY720 compared to S1P (Sensken et al. 2008). Presumably, long-term exposure of mutant neurons to pFTY720 may inhibit adenylyl cyclase and abrogate Ca^{2+} signalling while still activating the ERK pathway. However, the activation of S1P1R by pFTY720 is more efficient than activation of S1P3R as the intrinsic activity of pFTY720 on S1P1R (pEC_{50} = 9.32) is significantly higher compared to S1P3R (pEC_{50} = 8.44), as examined by a $[^{35}S]$-GTPγS incorporation assay (Sykes et al. 2014), possibly explaining the lack of an increase in BDNF expression in B2 neurons compared to J1 neurons.

In addition to receptor-mediated mechanisms, it has recently been reported that FTY720 enters the cell to be phosphorylated in the nucleus where it acts as an HDAC inhibitor (Hait et al. 2014). HDAC inhibitors have been known to induce *Bdnf* transcription (Chen et al. 2006) and this was confirmed by the study of Hait et al., showing increased *Bdnf* mRNA levels after FTY720 treatment (Hait et al. 2014). However, if the HDAC inhibition by pFTY720 played a significant role following long-term exposure of neurons to the drug, a BDNF increase would be expected in mutant neurons lacking S1P1R. Although pFTY720 is unlikely to cross the cell membrane, due to its polar head groups, it could still be entering through two different mechanisms. Either by binding S1P3R, which also results in internalisation, followed by the release of pFTY720 in the intracellular compartment and subsequent recycling of the receptor (Sykes et al. 2014) or

after its dephosphorylation by the lipid phosphate phosphatase 3 (LPP3) (Mechtcheriakova et al. 2007), which then enables its crossing of the cell membrane as FTY720. However, this seems not to occur at a significant level as shown by the lack of increase of BDNF in the mutant neurons (Figure 5.1). This was further confirmed by exploring the vascular endothelial growth factor D (*Vegfd*) mRNA levels after a short-term exposure to pFTY720. In the study of Hait et al. a significant increase of *Vegfd* levels was observed in the hippocampus of FTY720-treated mice due to HDAC inhibition. However, in ES cell-derived neurons *Vegfd* mRNA levels remained unchanged in J1 and B2 neurons following pFTY720 treatment (Appendix, Figure A.11).

At this point it is very difficult to draw a final conclusion about the functional significance of S1P1R expressed on neurons and its role in regulating BDNF levels, not least because of the rather weak effects of long-term exposure of pFTY720 on BDNF levels (Figure 5.1). As such this is surprising considering previous effects *in vivo* of FTY720 in mice lacking *Mecp2*$^{-/-}$. It was shown that FTY720 treatment over the course of four weeks significantly increased BDNF protein levels in various brain regions of *Mecp2*$^{-/-}$ mice (Deogracias et al. 2012). It is conceivable that this increase may somehow be linked with decreased levels of BDNF in the brain of *Mecp2*$^{-/-}$ mice. However, in the same study exposure of WT mice to FTY720 for 48 h, also increased BDNF levels significantly in the mouse brain (Deogracias et al. 2012), suggesting that other factors must play a role in neuronal cultures. Whether BDNF accumulation in long-term neuronal cultures may mask any increase of BDNF levels caused by pFTY720 treatment was investigated using a monoclonal antibody (mAb #9) able to capture secreted BDNF. However, the addition of this antibody to J1 neurons several days before experiments were conducted did not affect BDNF levels following treatment of the cultures with pFTY720 (Appendix, Figure A.14). Also, changing the density of the neuronal culture or treating the neurons earlier than 14 DIV failed to induce a larger increase of BDNF levels following drug addition,

although the steady state levels of BDNF were lower (Appendix, Figure A.15-A.17). Possibly, neurons younger than 14 DIV may still be too immature to respond to pFTY720, as suggested by the relatively low expression levels of the synaptic protein synaptophysin (Figure 3.28). Indeed, previous work with primary cultures of neurons has indicated that BDNF increase was dependent on active synaptic transmission (Deogracias et al. 2012). Hence, effects of pFTY720 on ES cell-derived neurons were therefore not further investigated in cultures before 14 DIV. More experiments are needed to understand the lack of a significant increase of BDNF protein level. It is evident however, that the high variability in the culture system, which will be discussed below (section 8.4) may remain problematic. A promising strategy for future studies could be to try and accelerate the maturation of ES cell-derived neurons, such that a robust synaptic activity may develop sooner (see below section 8.3.2). Additionally, the synaptic activity should be monitored by for example patch-clamp recordings to ensure comparable levels of basal activity in all the conditions analysed.
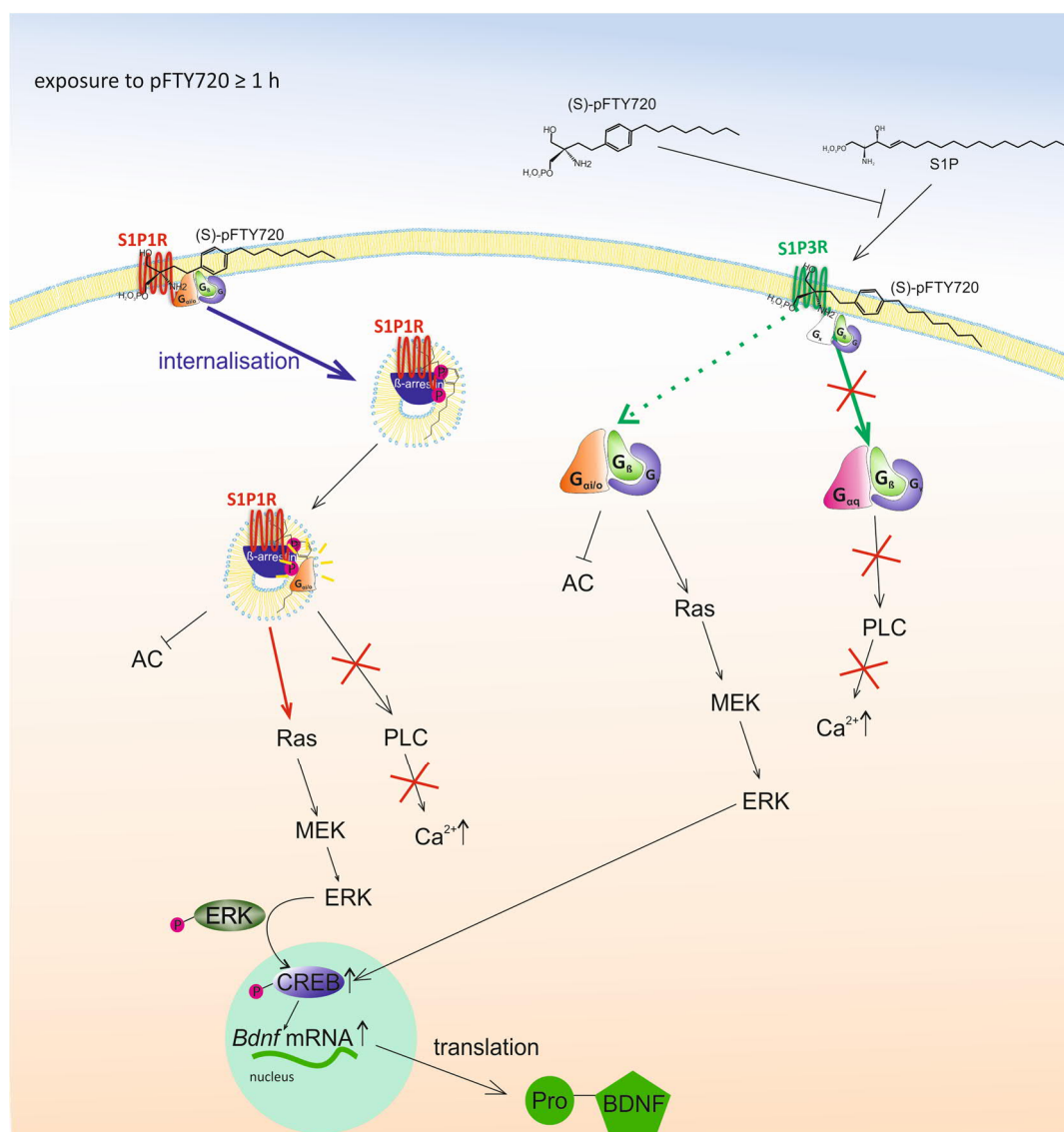
Figure 8.1 Proposed mechanism of action following long-term exposure to pFTY720

$G_{i/o}$ coupled pathways can be activated through the internalised S1P1R, activating the ERK pathway, which induces CREB phosphorylation with subsequent *Bdnf* mRNA transcription. pFTY720 also binds S1P3R which is proposed to be the primary target in the mutant neurons and thereby inhibits the binding of S1P. It activates the $G_{i/o}$ coupled ERK pathway with a lower intrinsic activity than over S1P1R (dotted green arrow) and inhibits activation of G_q coupled pathways, thereby acting as a partial agonist. Original figure including information from Ishii et al. 2004; Mullershausen et al. 2009; Healy et al. 2013; Park and Poo 2013; Sykes et al. 2014; West et al. 2014.

8.3.2 Short-term effects of pFTY720 on BDNF levels

ES cell-derived WT neurons treated at 14 DIV for 8 h or 24 h failed to increase BDNF protein levels (Figure 5.2). The difficulties encountered in obtaining a significant and reproducible increase of BDNF levels in ES cell-derived neurons were not only unexpected in view of previous *in vivo* results (see above) but also in the face of what has been reported with primary cultures derived from the embryonic mouse cortex. In primary cortical cultures short-term exposure of neurons to 10 nM and 100 nM pFTY720 for 24 h increased BDNF protein as well as *Bdnf* mRNA levels significantly (Deogracias et al. 2012). This discrepancy in BDNF levels observed in response to pFTY720 treatment further underlines the difference between primary cortical and ES cell-derived neurons. This includes the observation that ES cell-derived neurons do not seem to mature at the same rate as neurons freshly isolated from the developing brain (Chuang et al. 2013; Sadegh and Macklis 2014). As it was previously shown that primary cortical neurons reach maturity between 10-20 DIV (Lesuisse and Martin 2002), it is possible that ES cell-derived neurons need to be cultured for longer than 14 DIV to attain a similar level of maturity. It has been noted that it is possible to enhance neuronal maturation in ES cell-derived neurons by manipulating various conditions (for review see (Chuang et al. 2015)). These involve among others the activation of the Wnt signalling pathway (Jing et al. 2011), or addition of a nitric oxide donor to the culturing system (Arnhold et al. 2002). In spite of the limitations of ES cell-derived neurons, the inherent flexibility of this system confers many advantages justifying its use. They bear the potential to generate an unlimited number of post-mitotic cells and facilitate the generation of genetically modified neurons (Bibel et al. 2004; Gordon et al. 2013). However, the failure to replicate the data of Deogracias and colleagues in primary cortical culture demands for the consideration of other factors. It seems plausible that the quality or stability of the drug pFTY720 may have been affected. This could be further investigated by testing pFTY720

using simpler biochemical assays based on cells transfected with S1P1R and the analysis of downstream biochemical measurements (Sanna et al. 2004; Jo et al. 2005; Mullershausen et al. 2009). An additional difficulty when studying the role of S1P1R in transducing biological signals is likely to result from the endogenous production of the receptor ligand, namely S1P (see Introduction, section 1.2). In an attempt to decrease the concentration of endogenous S1P, neurons were exposed to the sphingosine kinase inhibitor DMS. Surprisingly, a trend towards an increase in BDNF expression was observed (Figure 5.4). This result may suggest that the chronic exposure of ES cell-derived neurons to endogenous ligand, especially in the context of high density culture may chronically desensitise the receptor. In view of this result, future experiments should include measurements of endogenous S1P, especially in the context of dense cultures to better understand not only the pharmacology but also the physiology of this signalling system, the complexity of which only begins to be appreciated.

8.3.3 Effects of pFTY720 on ERK1/2 and CREB phosphorylation

In an attempt to simplify the analysis by decreasing the complexity resulting from receptor internalisation caused by prolonged drug exposure, parameters thought to be close to receptor activation were explored at short time intervals after exposure to pFTY720. To this end, ERK1/2 and CREB phosphorylation were investigated as wells as their possible impact on *Bdnf* mRNA levels. Due to the high variability encountered in B2 neurons no conclusion can be drawn regarding the effects of pFTY720 on ERK1/2 phosphorylation and the significant increase seen in WT neurons following exposure to 10 nM and 100 nM pFTY720 must be interpreted with caution (Figure 5.5). Both S1P1R and S1P3R activate the ERK pathway after binding pFTY720 (Sensken et al. 2008; Healy et al. 2013), with the drug being more potent in its action through S1P1R compared with

S1P3R (Sykes et al. 2014). This may explain a stronger response observed in J1 neurons (see also above). pFTY720 has been shown to phosphorylate Akt a downstream target of both receptors (Figure 1.2 and (Brinkmann 2007)), which is known to subsequently increase pCREB (Du and Montminy 1998). In B2 neurons, pFTY720 seemed to induce a significant increase of pCREB levels and significantly increased *Bdnf* mRNA levels whereas this could not be consistently observed in J1 neurons (Figure 5.7-5.8 and 5.10). The high variability encountered in the system used here might explain why previous results in primary cortical cultures of WT mice report on an increase of pERK1/2, pCREB and *Bdnf* mRNA levels after pFTY720 addition (Deogracias et al. 2012). Also, the fact that $G_{i/o}$ protein activation signals to the PI3K/Akt and ERK pathway implies that CREB phosphorylation should also occur in WT neurons following S1P1R stimulation (Radeff-Huang et al. 2004; McCubrey et al. 2007; Tao et al. 2009; Safarian et al. 2015). It has been shown that in cells lacking both S1P2R and S1P3R, stimulation of S1P1R does not induce an activation of the Akt pathway (Zhang et al. 2007; Means et al. 2008). In WT cells however, the Akt pathway is activated in a $G_{i/o}$ protein-dependent manner, indicative of a possible interplay between the different receptors (Zhang et al. 2007; Means et al. 2008). How this complexity of S1P signalling affected the results obtained in this study is unknown. But as this finding supports the notion that the phosphorylation of CREB should still occur in the WT neurons through the activation of the $G_{i/o}$ protein and its downstream pathways (Figure 8.2), it is conceivable that pFTY720 may act on other targets in B2 neurons. This may lead to a stronger Ca^{2+} increase, a notion supported by the increase of CREB phosphorylation (Figure 5.8) and the significant increase of *Bdnf* mRNA in the mutant neurons only (Figure 5.10). Activation of S1P1R does increase intracellular Ca^{2+} levels in a $G_{i/o}$ protein-dependent manner provided exposure to pFTY720 is shorter than 1 h. Following this brief exposure time, significant number of receptors may be internalised (Figure 8.1 and 8.2 and (Healy et al. 2013)). However, the

increase of intracellular Ca^{2+} was not strong enough to induce CREB phosphorylation consistently in J1 neurons as the pCREB increase seen after 10 min exposure to pFTY720 1 μM (Figure 5.7) could not be reproduced in subsequent experiments (Figure 5.8). This could be further explored by measuring intracellular Ca^{2+} levels after pFTY720 addition to B2 neurons with and without blocking S1P3R to investigate if another target may be involved as predicted by previous studies. Indeed, pFTY720 has been shown not to induce a Ca^{2+} response through S1P3R due to its inhibition of the G_q-dependent pathway (Ishii et al. 2002; Sensken et al. 2008).
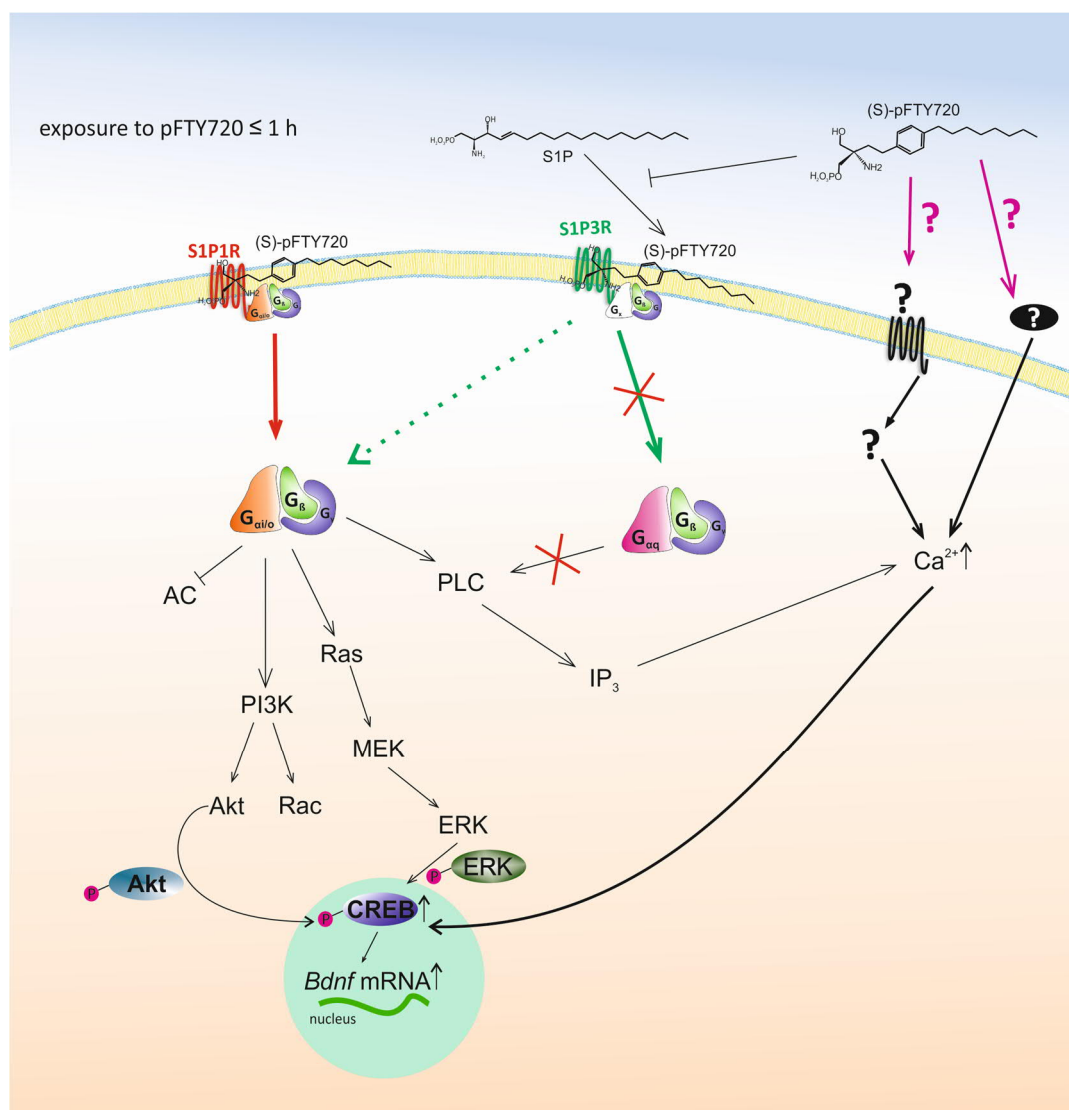
Figure 8.2 Proposed mechanism of action following short-term exposure to pFTY720

pFTY720 stimulates S1P1R thereby activating the ERK pathway, as well as the PI3K/Akt pathway, and inducing Ca^{2+} increase which all lead to CREB phosphorylation with subsequent *Bdnf* mRNA transcription. pFTY720 binds S1P3R and thereby inhibits the binding of S1P. It acts as a partial agonist as it has inhibitory actions on the G_q coupled pathway, while it stimulates the $G_{i/o}$ coupled ERK pathway but with a lower intrinsic activity compared to S1P1R (dotted green arrow). It is suggested that pFTY720 binds another target (indicated by the question mark), which is either a receptor or a direct mediator of intracellular Ca^{2+} increase. Original figure including information from Ishii et al. 2002; Brinkmann 2007; Zhang et al. 2007, Means et al. 2008; Sensken et al. 2008 and Sykes et al. 2014.

8.4 Variability in Culture System

While the generation of neurons from ES cells is an invaluable tool to neuroscientists as exemplified by the clarification of various gene functions (see for example (Schrenk-Siemens et al. 2008; Nikoletopoulou et al. 2010; Yazdani et al. 2012)), its use in the context of quantitative biochemical measurements turned out to be significantly more problematic than initially anticipated. Indeed, an unexpectedly large variability was observed in all measurements performed, irrespective of the molecule under investigation. One plausible reason at the core of the variability may be differences in the temporal development of synaptic activity. This is not only supported by the data obtained from extracellular recordings (Figure A.9 and A.10), but also by the results of other investigators using the same basic differentiation protocol (Bibel et al. 2007; Barth et al. 2014). Intracellular recordings performed by Barth and colleagues revealed considerable variations between cells in relation to the development of synaptic activity. The variability was not due to the differences of one differentiation to the other, as already within one differentiation changes were observed (Barth et al. 2014). Previous results on the activity of pFTY720 on primary cultures of neurons have suggested that the effects of the drug on BDNF levels where dependent on both pre-as well as postsynaptic mechanisms (Deogracias et al. 2012). Therefore, it is likely that at least part of the variability observed in the parameters investigated in this study may be a consequence of asynchronous development of the connectivity between neurons and of synaptic activity. In line with this, spike count measurements performed here using Micro Electrode Arrays (Materials and Methods, section 2.12) revealed considerable differences between single wells (Figure A.9). Despite the high variability encountered with ES cell-derived neurons, primary cultures do not represent a straight-forward alternative. As primary cultures from *S1p1r$^{-/-}$* mice cannot be established due to lethality of the deletion at the embryonic stage (Liu et al. 2000), a conditional gene deletion would be needed. Cre-mediated excision of

target genes in primary cultures of neurons is typically not efficient enough to allow subsequent biochemical analyses of cell lysates and therefore, other approaches need to be considered. For example, $S1p1r^{loxP/loxP}Emx1/Cre^{ERT2}$ mice could be used as it allows significant expression of Cre^{ERT2} earlier during brain development than *Thy-1*. The homeobox protein *Emx1* is already detected at E10 in the mouse forebrain (Boncinelli et al. 1993; Cecchi and Boncinelli 2000). It has been used previously to successfully excise genes specifically in neurons of the forebrain (Baquet et al. 2004; Kessaris et al. 2006). Also, primary cultures prepared from the mouse line $GLAST/Cre^{ERT2}$ would allow to investigate the role of S1P1R both in neurons and astrocytes and to compare the results with those obtained from cells isolated from the $Emx1/Cre^{ERT2}$ line (Mori et al. 2006).

8.5   Effects of FTY720 *in vivo*

Not unexpectedly, the tamoxifen-induced excision of *S1p1r* failed to significantly alter the effects of FTY720 in the two brain regions investigated, even if a small, but significant reduction in the levels of *S1p1r* mRNA was noted in the hippocampus (Figure 6.2A). While this small decrease shows that as expected the majority of S1P1R-expressing cells are non-neuronal cells it does suggest that the *S1p1r* gene might also be expressed by neurons, given that Cre expression is driven by a *Thy-1* construct exclusively expressed in neurons as documented by the expression of YFP (Young et al. 2008). As noted in the above, more detailed investigations of the important point of the relative levels of expression of S1P1R by neurons *versus* other cell types will need the development of more specific reagents than the S1P1R antibodies available so far (Discussion, section 8.2). A previous study used human *GFAP*, *nestin* as well as *synapsin* promoters to drive the expression of Cre for the excision of a floxed *S1p1r* allele to explore the role of the receptor in mice challenged by EAE (Choi et al. 2011). Interestingly, this study revealed

that the excision of S1P1R in cells targeted by the *GFAP* and the *nestin*, but not the *synapsin* promoter decreased the EAE score following injection of the myelin oligodendrocyte glycoprotein (MOG) peptide. In both cases, FTY720 also lost its protective effects and failed to ameliorate the clinical scores of treated animals. The overall conclusion of the study was that an important part of the mode of action of FTY720 towards ameliorating the symptoms of EAE can be accounted for by its ability to downregulate S1P1R expression on astrocytes which were suggested to be the main S1P1R-expressing cells. The same study also concluded that S1P1R is not expressed by neurons. However, the interpretation of these S1P1R localisation results was largely based on the use of Cre deleter lines (Choi et al. 2011). Indeed, the *synapsin* promoter used to drive Cre is not expressed in all neurons (Zhu et al. 2001), while at the same time the human *GFAP* promoter is known to be expressed by the progenitors of both neurons and astrocytes (Malatesta et al. 2003), thus undermining the conclusion reached by Choi and colleagues that S1P1R may not be expressed by neurons. The mouse line generated in this study might help to clarify this question of S1P1R expression on neurons further. Though this would require *in situ* hybridisation studies given the lack of specific S1P1R antibodies (see above, section 8.2).

This study also investigated the effects of FTY720 on BDNF protein levels *in vivo* (Figure 6.3 and 6.4). In line with another report investigating the long-term effects of FTY720 on BDNF levels in the hippocampus (Miguez et al. 2015), no increase could be observed in the brain regions investigated. However, shorter treatments of just one injection 48 h prior BDNF level assessment should be considered in future studies as this led to a significant increase in multiple major brain regions (Discussion Chapter 6 and Deogracias et al. 2012). Furthermore, a significant increase on ERK1/2 (Di Pardo et al. 2014), and CREB phosphorylation was reported 30 min after FTY720 injections *in vivo* (Deogracias et al. 2012). Currently it remains unclear why it was not possible to replicate this data in the

hippocampus and cortex of corn oil treated *Thy-1/Cre^{ERT2} S1p1r^{loxP/loxP}* mice (Figure 6.5-6.8). However, a high variability was encountered between single mice and it appears likely that significantly more animals should be examined before definite conclusions could be drawn on the effects of FTY720 on ERK1/2 and CREB phosphorylation in these mice. Additionally, the mouse strain was different in the studies reporting on a significant increase compared to the one used in this study and the choice of mouse strain could also impact the results (Sandberg 2000; Wahlsten et al. 2006; Mouri et al. 2012).

8.6 Sphingosine Receptors on Megakaryocytes

S1P receptors are present on a wide variety of cell types and S1P gradients are used for various chemotactic processes including the generation of platelets from proplatelets (Introduction, section 1.2). As cultured rat megakaryocytes express all five *S1P receptors* at the mRNA levels (Figure 7.1), and especially *S1p1r* and *S1p2r* at high levels, it was of interest to test whether or not pFTY720 would regulate *Bdnf* mRNA levels, given work recently published by our laboratory indicating that the expression pattern of the *Bdnf* transcripts in megakaryocytes is identical to the pattern found in neurons (Chacon-Fernandez et al. 2016). The suggestion that *Bdnf* transcription might be regulated similarly in neurons and megakaryocytes was further supported by the finding that increased levels of intracellular calcium enhanced *Bdnf* transcription in megakaryocytes, which is known to be also the case in neurons (Chacon-Fernandez et al. 2016). While the results suggest that pFTY720 may modulate *Bdnf* mRNA levels (Figure 7.2) the interpretation of these experiments is complicated by the fact that the addition of pFTY720 most likely affects the maturation of proplatelets as well as the release of platelets. This is important given the realisation that *Bdnf* mRNA is present in platelets, at least in humans (Rowley et al. 2011). Rats were used here as the *Bdnf* gene is not

expressed at significant levels in mice (Chacon-Fernandez et al. 2016). Interestingly, platelet counts analysed 12 h after FTY720 administration are significantly increased in the blood circulation, indicating an increased release by megakaryocytes (Zhang et al. 2012). In contrast platelet counts are decreased in humans after several weeks of drug administration, possibly due to the functional antagonistic action of FTY720 after long-term treatments (EMA 2014).

8.7 Conclusion and Perspectives

One of the most unexpected finding of these investigations is that short-term exposure of pFTY720 to neurons lacking S1P1R elicited a transient increase of *Bdnf* mRNA levels not observed with WT neurons. However, this intriguing result needs to be interpreted with caution as an additional control cell line still expressing S1P1R of the same genetic background as B2 should be analysed additionally. This would be needed to exclude other explanations such as differences in the genetic background of the different ES cell lines used in this study. Another important result is that following long-term exposure, it appears that S1P1R may be involved in the pFTY720-dependent increase of BDNF protein levels in ES cell-derived neurons *in vitro* (Figure 5.1). When comparing the results of this study with the findings previously obtained in primary cortical cultures (Deogracias et al. 2012), it cannot be excluded that cells others than neurons are required for pFTY720 to deploy its full activity.

In sum, it appears that the mode of action of FTY720 even in the simplified *in vitro* system used here is complex and requires further detailed investigations. It will be of particular interest to delineate the possibility that pFTY720 may also act through other receptors, including S1P3R expressed by these neurons. This could be explored by reconstituting a system based on for example CHO cells expressing just one of the five S1P receptors at a time as well as constructs reporting on activation of CREB phosphorylation. This strategy would allow the investigation of the signalling pathways elicited by one of the receptor's subtype only, and introduction of additional receptors can be controlled and interactions therefore better understood. In addition, the role of the endogenous production of sphingosine, most likely an intrinsic complicating factor would need to be investigated in detail. In the context of developing new drugs targeting S1P receptors, an elegant approach has been recently developed allowing the efficient screening of

exceptionally large libraries of agonist antibody candidates (Xie et al. 2013). This system could also be used to screen receptor-activating antibodies by infecting a S1P receptor-expressing CHO reporter cell line with viruses expressing this large antibody libraries. Such receptor-selective reagents may help delineating what appears to be a complex interplay between different S1P receptors and to better define their potential to treat neurodegenerative diseases.

Bibliography

Abeliovich, A. and Gitler, A. D. 2016. Defects in trafficking bridge Parkinson's disease pathology and genetics. *Nature* 539(7628), pp. 207-216. doi: 10.1038/nature20414

Adachi, K. et al. 1995. Design, synthesis, and structure-activity relationships of 2-substituted-2-amino-1,3-propanediols: Discovery of a novel immunosuppressant, FTY720. Bioorganic and Medical Chemistry Letters

Ahn, M. et al. 2007. Regulation of Na(v)1.2 channels by brain-derived neurotrophic factor, TrkB, and associated Fyn kinase. *J Neurosci* 27(43), pp. 11533-11542. doi: 10.1523/jneurosci.5005-06.2007

Aid, T. et al. 2007. Mouse and rat BDNF gene structure and expression revisited. *J Neurosci Res* 85(3), pp. 525-535. doi: 10.1002/jnr.21139

Akiyama, T. et al. 2008. Immunohistochemical detection of sphingosine-1-phosphate receptor 1 in vascular and lymphatic endothelial cells. *J Mol Histol* 39(5), pp. 527-533. doi: 10.1007/s10735-008-9193-y

Albert, R. et al. 2005. Novel immunomodulator FTY720 is phosphorylated in rats and humans to form a single stereoisomer. Identification, chemical proof, and biological characterization of the biologically active species and its enantiomer. *J Med Chem* 48(16), pp. 5373-5377. doi: 10.1021/jm050242f

Alexander, G. M. et al. 2004. Effect of transgene copy number on survival in the G93A SOD1 transgenic mouse model of ALS. *Brain Res Mol Brain Res* 130(1-2), pp. 7-15. doi: 10.1016/j.molbrainres.2004.07.002

Allen, S. J. et al. 2013. GDNF, NGF and BDNF as therapeutic options for neurodegeneration. *Pharmacol Ther* 138(2), pp. 155-175. doi: 10.1016/j.pharmthera.2013.01.004

Allende, M. L. et al. 2004. Expression of the sphingosine 1-phosphate receptor, S1P1, on T-cells controls thymic emigration. *J Biol Chem* 279(15), pp. 15396-15401. doi: 10.1074/jbc.M314291200

Amir, R. E. et al. 1999. Rett syndrome is caused by mutations in X-linked MECP2, encoding methyl-CpG-binding protein 2. *Nat Genet* 23(2), pp. 185-188. doi: 10.1038/13810

An, S. et al. 1999. Transduction of intracellular calcium signals through G protein-mediated activation of phospholipase C by recombinant sphingosine 1-phosphate receptors. *Mol Pharmacol* 55(5), pp. 787-794.

Ancellin, N. and Hla, T. 1999. Differential pharmacological properties and signal transduction of the sphingosine 1-phosphate receptors EDG-1, EDG-3, and EDG-5. *J Biol Chem* 274(27), pp. 18997-19002.

Aoki, M. et al. 2016. Sphingosine-1-Phosphate Signaling in Immune Cells and Inflammation: Roles and Therapeutic Potential. *Mediators Inflamm* 2016, p. 8606878. doi: 10.1155/2016/8606878

Arnhold, S. et al. 2002. NOS-II is involved in early differentiation of murine cortical, retinal and ES cell-derived neurons—an immunocytochemical and functional approach. *International Journal of Developmental Neuroscience* 20(2), pp. 83-92. doi: http://dx.doi.org/10.1016/S0736-5748(02)00020-5

Arnon, T. I. et al. 2011. GRK2-dependent S1PR1 desensitization is required for lymphocytes to overcome their attraction to blood. *Science* 333(6051), pp. 1898-1903. doi: 10.1126/science.1208248

Asle-Rousta, M. et al. 2013. FTY720 (fingolimod) attenuates beta-amyloid peptide (Abeta42)-induced impairment of spatial learning and memory in rats. *J Mol Neurosci* 50, doi: 10.1007/s12031-013-9979-6

Aubert, J. et al. 2002. Functional gene screening in embryonic stem cells implicates Wnt antagonism in neural differentiation. *Nat Biotechnol* 20(12), pp. 1240-1245. doi: 10.1038/nbt763

Autry, A. E. et al. 2011. NMDA receptor blockade at rest triggers rapid behavioural antidepressant responses. *Nature* 475(7354), pp. 91-95. doi: 10.1038/nature10130

Bagyinszky, E. et al. 2014. The genetics of Alzheimer's disease.*Clin Interv Aging*. Vol. 9. pp. 535-551.

Baquet, Z. C. et al. 2004. Early striatal dendrite deficits followed by neuron loss with advanced age in the absence of anterograde cortical brain-derived neurotrophic factor. *J Neurosci* 24(17), pp. 4250-4258. doi: 10.1523/jneurosci.3920-03.2004

Barakat, T. S. and Gribnau, J. 2010. X chromosome inactivation and embryonic stem cells. *Adv Exp Med Biol* 695, pp. 132-154. doi: 10.1007/978-1-4419-7037-4_10

Barbacid, M. 1994. The Trk family of neurotrophin receptors. *J Neurobiol* 25(11), pp. 1386-1403. doi: 10.1002/neu.480251107

Barbacid, M. 1995. Neurotrophic factors and their receptors. *Curr Opin Cell Biol* 7(2), pp. 148-155.

Barde, Y. A. et al. 1982. Purification of a new neurotrophic factor from mammalian brain. *Embo j* 1(5), pp. 549-553.

Barth, L. et al. 2014. Functional differentiation of stem cell-derived neurons from different murine backgrounds. *Front Cell Neurosci* 8, doi: 10.3389/fncel.2014.00049

Bathina, S. and Das, U. N. 2015. Brain-derived neurotrophic factor and its clinical implications.*Arch Med Sci*. Vol. 11. pp. 1164-1178.

Batlle-Morera, L. et al. 2008. Parameters influencing derivation of embryonic stem cells from murine embryos. *Genesis* 46(12), pp. 758-767. doi: 10.1002/dvg.20442

Bennett, M. L. et al. 2016. New tools for studying microglia in the mouse and human CNS. *Proc Natl Acad Sci U S A* 113(12), pp. E1738-1746. doi: 10.1073/pnas.1525528113

Berdyshev, E. V. et al. 2009. FTY720 inhibits ceramide synthases and up-regulates dihydrosphingosine 1-phosphate formation in human lung endothelial cells. *J Biol Chem* 284(9), pp. 5467-5477. doi: 10.1074/jbc.M805186200

Bibel, M. and Barde, Y.-A. 2000. Neurotrophins: key regulators of cell fate and cell shape in the vertebrate nervous system. *Genes & Development* 14(23), pp. 2919-2937. doi: 10.1101/gad.841400

Bibel, M. et al. 2007. Generation of a defined and uniform population of CNS progenitors and neurons from mouse embryonic stem cells. *Nat Protoc* 2(5), pp. 1034-1043. doi: 10.1038/nprot.2007.147

Bibel, M. et al. 2004. Differentiation of mouse embryonic stem cells into a defined neuronal lineage. *Nat Neurosci* 7(9), pp. 1003-1009. doi: 10.1038/nn1301

Blaho, V. A. and Hla, T. 2014. An update on the biology of sphingosine 1-phosphate receptors. *J Lipid Res* 55(8), pp. 1596-1608. doi: 10.1194/jlr.R046300

Blow, D. M. et al. 1974. Mode of action of soybean trypsin inhibitor (Kunitz) as a model for specific protein-protein interactions. *Nature* 249(5452), pp. 54-57.

Boncinelli, E. et al. 1993. Emx and Otx homeobox genes in the developing mouse brain. *J Neurobiol* 24(10), pp. 1356-1366. doi: 10.1002/neu.480241008

Braak, H. and Braak, E. 2000. Pathoanatomy of Parkinson's disease. *J Neurol* 247 Suppl 2, pp. Ii3-10. doi: 10.1007/pl00007758

Bramham, C. R. et al. 2008. The immediate early gene arc/arg3.1: regulation, mechanisms, and function. *J Neurosci* 28(46), pp. 11760-11767. doi: 10.1523/jneurosci.3864-08.2008

Bredy, T. W. et al. 2007. Histone modifications around individual BDNF gene promoters in prefrontal cortex are associated with extinction of conditioned fear. *Learn Mem* 14(4), pp. 268-276. doi: 10.1101/lm.500907

Brinkmann, V. 2007. Sphingosine 1-phosphate receptors in health and disease: mechanistic insights from gene deletion studies and reverse pharmacology. *Pharmacol Ther* 115(1), pp. 84-105. doi: 10.1016/j.pharmthera.2007.04.006

Brinkmann, V. et al. 2004. FTY720: sphingosine 1-phosphate receptor-1 in the control of lymphocyte egress and endothelial barrier function. *Am J Transplant* 4(7), pp. 1019-1025. doi: 10.1111/j.1600-6143.2004.00476.x

Brizuela, L. et al. 2014. Osteoblast-derived sphingosine 1-phosphate to induce proliferation and confer resistance to therapeutics to bone metastasis-derived prostate cancer cells. *Molecular Oncology* 8(7), pp. 1181-1195. doi: http://dx.doi.org/10.1016/j.molonc.2014.04.001

Bronstein, J. M. et al. 1997. Oligodendrocyte-specific protein (OSP) is a major component of CNS myelin. *J Neurosci Res* 50(5), pp. 713-720. doi: 10.1002/(sici)1097-4547(19971201)50:5<713::aid-jnr8>3.0.co;2-k

Brunkhorst, R. et al. 2014. Fingolimod for the treatment of neurological diseases—state of play and future perspectives. *Frontiers in Cellular Neuroscience* 8, doi: 10.3389/fncel.2014.00283

Buchman, A. S. et al. 2016. Higher brain BDNF gene expression is associated with slower cognitive decline in older adults. *Neurology* 86(8), pp. 735-741. doi: 10.1212/wnl.0000000000002387

Buckley, P. F. et al. 2011. Brain-derived neurotrophic factor: findings in schizophrenia. *Curr Opin Psychiatry* 24(2), pp. 122-127. doi: 10.1097/YCO.0b013e3283436eb7

Bus, B. A. et al. 2015. Chronic depression is associated with a pronounced decrease in serum brain-derived neurotrophic factor over time. *Mol Psychiatry* 20(5), pp. 602-608. doi: 10.1038/mp.2014.83

Bünemann, M. et al. 1995. Activation of muscarinic K+ current in guinea-pig atrial myocytes by sphingosine-1-phosphate. *J Physiol* 489(Pt 3), pp. 701-707.

Camm, J. et al. 2014. Cardiac and vascular effects of fingolimod: mechanistic basis and clinical implications. *Am Heart J* 168(5), pp. 632-644. doi: 10.1016/j.ahj.2014.06.028

Canter, R. G. et al. 2016. The road to restoring neural circuits for the treatment of Alzheimer's disease. *Nature* 539(7628), pp. 187-196. doi: 10.1038/nature20412

Castren, E. et al. 1993. Differential effects of MK-801 on brain-derived neurotrophic factor mRNA levels in different regions of the rat brain. *Exp Neurol* 122(2), pp. 244-252.

Cazorla, M. et al. 2011. Pharmacological characterization of six trkB antibodies reveals a novel class of functional agents for the study of the BDNF receptor. *Br J Pharmacol* 162(4), pp. 947-960. doi: 10.1111/j.1476-5381.2010.01094.x

Cecchi, C. and Boncinelli, E. 2000. Emx homeogenes and mouse brain development. *Trends Neurosci* 23(8), pp. 347-352.

Chacon-Fernandez, P. et al. 2016. Brain-derived Neurotrophic Factor in Megakaryocytes. *J Biol Chem* 291(19), pp. 9872-9881. doi: 10.1074/jbc.M116.720029

Chae, S. S. et al. 2004. Constitutive expression of the S1P1 receptor in adult tissues. *Prostaglandins Other Lipid Mediat* 73(1-2), pp. 141-150.

Chang, Q. et al. 2006. The disease progression of Mecp2 mutant mice is affected by the level of BDNF expression. *Neuron* 49(3), pp. 341-348. doi: 10.1016/j.neuron.2005.12.027

Chao, M. V. 2003. Neurotrophins and their receptors: a convergence point for many signalling pathways. *Nat Rev Neurosci* 4(4), pp. 299-309. doi: 10.1038/nrn1078

Chen, P. S. et al. 2006. Valproate protects dopaminergic neurons in midbrain neuron/glia cultures by stimulating the release of neurotrophic factors from astrocytes. *Mol Psychiatry* 11(12), pp. 1116-1125. doi: 10.1038/sj.mp.4001893

Chen, W. G. et al. 2003. Upstream stimulatory factors are mediators of Ca2+-responsive transcription in neurons. *J Neurosci* 23(7), pp. 2572-2581.

Chen, Y. et al. 2008. NS21: Re-defined and Modified Supplement B27 for Neuronal Cultures. *J Neurosci Methods* 171(2), pp. 239-247. doi: 10.1016/j.jneumeth.2008.03.013

Choi, J. W. and Chun, J. 2013. Lysophospholipids and their receptors in the central nervous system. *Biochim Biophys Acta* 1831(1), pp. 20-32. doi: 10.1016/j.bbalip.2012.07.015

Choi, J. W. et al. 2011. FTY720 (fingolimod) efficacy in an animal model of multiple sclerosis requires astrocyte sphingosine 1-phosphate receptor 1 (S1P1) modulation. *Proc Natl Acad Sci U S A* 108(2), pp. 751-756. doi: 10.1073/pnas.1014154108

Chuang, J.-H. et al. 2013. Differentiation of glutamatergic neurons from mouse embryonic stem cells requires raptor S6K signaling. *Stem Cell Research* 11(3), pp. 1117-1128. doi: http://dx.doi.org/10.1016/j.scr.2013.08.003

Chuang, J. H. et al. 2015. Neural differentiation from embryonic stem cells in vitro: An overview of the signaling pathways. *World J Stem Cells* 7(2), pp. 437-447. doi: 10.4252/wjsc.v7.i2.437

Chun, J. and Brinkmann, V. 2011. A mechanistically novel, first oral therapy for multiple sclerosis: the development of fingolimod (FTY720, Gilenya). *Discov Med* 12(64), pp. 213-228.

Chun, J. et al. 2002. International Union of Pharmacology. XXXIV. Lysophospholipid receptor nomenclature. *Pharmacol Rev* 54(2), pp. 265-269.

Ciechanover, A. 2005. Proteolysis: from the lysosome to ubiquitin and the proteasome.*Nat Rev Mol Cell Biol*. Vol. 6. England, pp. 79-87.

Clapcote, S. J. and Roder, J. C. 2005. Simplex PCR assay for sex determination in mice. *Biotechniques* 38(5), pp. 702, 704, 706.

Clarkson, A. N. et al. 2015. Combined ampakine and BDNF treatments enhance poststroke functional recovery in aged mice via AKT-CREB signaling. *J Cereb Blood Flow Metab* 35(8), pp. 1272-1279. doi: 10.1038/jcbfm.2015.33

Clayton, D. F. and George, J. M. 1998. The synucleins: a family of proteins involved in synaptic function, plasticity, neurodegeneration and disease. *Trends Neurosci* 21(6), pp. 249-254.

Codega, P. et al. 2014. Prospective identification and purification of quiescent adult neural stem cells from their in vivo niche. *Neuron* 82(3), pp. 545-559. doi: 10.1016/j.neuron.2014.02.039

Couttas, T. A. et al. 2014. Loss of the neuroprotective factor Sphingosine 1-phosphate early in Alzheimer's disease pathogenesis. *Acta Neuropathologica Communications* 2(1), p. 9. doi: 10.1186/2051-5960-2-9

Crousillac, S. et al. 2009. Sphingosine-1-Phosphate Elicits Receptor-Dependent Calcium Signaling in Retinal Amacrine Cells. *Journal of Neurophysiology* 102(6), pp. 3295-3309. doi: 10.1152/jn.00119.2009

Cuvillier, O. et al. 1996. Suppression of ceramide-mediated programmed cell death by sphingosine-1-phosphate. *Nature* 381, doi: 10.1038/381800a0

Cyster, J. G. and Schwab, S. R. 2012. Sphingosine-1-phosphate and lymphocyte egress from lymphoid organs. *Annu Rev Immunol* 30, pp. 69-94. doi: 10.1146/annurev-immunol-020711-075011

Czubowicz, K. and Strosznajder, R. 2014. Ceramide in the molecular mechanisms of neuronal cell death. The role of sphingosine-1-phosphate. *Mol Neurobiol* 50(1), pp. 26-37. doi: 10.1007/s12035-013-8606-4

D'Amico, E. et al. 2016. Treatment-Related Progressive Multifocal Leukoencephalopathy in Multiple Sclerosis: A Comprehensive Review of Current Evidence and Future Needs. *Drug Saf* 39(12), pp. 1163-1174. doi: 10.1007/s40264-016-0461-6

DeFreitas, M. F. et al. 2001. A novel p75NTR signaling pathway promotes survival, not death, of immunopurified neocortical subplate neurons. *J Neurosci* 21(14), pp. 5121-5129.

Deogracias, R. et al. 2012. Fingolimod, a sphingosine-1 phosphate receptor modulator, increases BDNF levels and improves symptoms of a mouse model of Rett syndrome. *Proc Natl Acad Sci U S A* 109(35), pp. 14230-14235. doi: 10.1073/pnas.1206093109

Di Menna, L. et al. 2013. Fingolimod protects cultured cortical neurons against excitotoxic death. *Pharmacol Res* 67(1), pp. 1-9. doi: 10.1016/j.phrs.2012.10.004

Di Pardo, A. et al. 2014. FTY720 (fingolimod) is a neuroprotective and disease-modifying agent in cellular and mouse models of Huntington disease. *Hum Mol Genet* 23(9), pp. 2251-2265. doi: 10.1093/hmg/ddt615

Di Pardo, A. et al. 2012. Ganglioside GM1 induces phosphorylation of mutant huntingtin and restores normal motor behavior in Huntington disease mice. *Proc Natl Acad Sci U S A* 109(9), pp. 3528-3533. doi: 10.1073/pnas.1114502109

Dieni, S. et al. 2012. BDNF and its pro-peptide are stored in presynaptic dense core vesicles in brain neurons. *J Cell Biol* 196(6), pp. 775-788. doi: 10.1083/jcb.201201038

Doi, Y. et al. 2013. Fingolimod phosphate attenuates oligomeric amyloid beta-induced neurotoxicity via increased brain-derived neurotrophic factor expression in neurons. *PLoS One* 8, doi: 10.1371/journal.pone.0061988

Donoviel, M. S. et al. 2015. Spinster 2, a sphingosine-1-phosphate transporter, plays a critical role in inflammatory and autoimmune diseases. *Faseb j* 29(12), pp. 5018-5028. doi: 10.1096/fj.15-274936

Du, K. and Montminy, M. 1998. CREB is a regulatory target for the protein kinase Akt/PKB. *J Biol Chem* 273(49), pp. 32377-32379.

Dusaban, S. S. et al. 2017. Sphingosine 1-phosphate receptor 3 and RhoA signaling mediate inflammatory gene expression in astrocytes. *J Neuroinflammation* 14(1), p. 111. doi: 10.1186/s12974-017-0882-x

Edsall, L. C. et al. 1998. N,N-Dimethylsphingosine is a potent competitive inhibitor of sphingosine kinase but not of protein kinase C: modulation of cellular levels of sphingosine 1-phosphate and ceramide. *Biochemistry* 37(37), pp. 12892-12898. doi: 10.1021/bi980744d

Efstathopoulos, P. et al. 2015. Fingolimod induces neurogenesis in adult mouse hippocampus and improves contextual fear memory. *Transl Psychiatry* 5, p. e685. doi: 10.1038/tp.2015.179

Egan, M. F. et al. 2003. The BDNF val66met polymorphism affects activity-dependent secretion of BDNF and human memory and hippocampal function. *Cell* 112(2), pp. 257-269. doi: 10.1016/S0092-8674(03)00035-7

Eishingdrelo, H. and Kongsamut, S. 2013. Minireview: Targeting GPCR Activated ERK Pathways for Drug Discovery. *Curr Chem Genom Transl Med* 7, pp. 9-15. doi: 10.2174/2213988501307010009

Elliott, R. C. et al. 1994. An improved method detects differential NGF and BDNF gene expression in response to depolarization in cultured hippocampal neurons. *Molecular Brain Research* 26(1–2), pp. 81-88. doi: http://dx.doi.org/10.1016/0169-328X(94)90077-9

EMA. 2014. *Gilenya-Scientific conclusions and grounds recommending the variation to the terms of the marketing authorisation*. Available at: http://www.ema.europa.eu/ema/

Emamzadeh, F. N. 2016. Alpha-synuclein structure, functions, and interactions.*J Res Med Sci*. Vol. 21. India.

English, A. W. et al. 2013. Small-molecule trkB agonists promote axon regeneration in cut peripheral nerves. *Proc Natl Acad Sci U S A* 110(40), pp. 16217-16222. doi: 10.1073/pnas.1303646110

Erickson, K. I. et al. 2012. The Aging Hippocampus. *The Neuroscientist* 18(1), pp. 82-97. doi: doi:10.1177/1073858410397054

Ernfors, P. et al. 1995. Studies on the physiological role of brain-derived neurotrophic factor and neurotrophin-3 in knockout mice. *Int J Dev Biol* 39(5), pp. 799-807.

Ernfors, P. et al. 1994. Mice lacking brain-derived neurotrophic factor develop with sensory deficits. *Nature* 368(6467), pp. 147-150. doi: 10.1038/368147a0

Ernst, C. et al. 2006. Antidepressant effects of exercise: evidence for an adult-neurogenesis hypothesis? *J Psychiatry Neurosci* 31(2), pp. 84-92.

Faber, H. et al. 2013. Prolonged and symptomatic bradycardia following a single dose of fingolimod. *Mult Scler* 19(1), pp. 126-128. doi: 10.1177/1352458512447596

FDA. 2015. FDA Drug Safety Communication: FDA warns about cases of rare brain infection with MS drug Gilenya (fingolimod) in two patients with no prior exposure to immunosuppressant drugs. *Drug Safety Communications*, p. 4.

Federman, N. et al. 2013. Nuclear factor kappaB-dependent histone acetylation is specifically involved in persistent forms of memory. *J Neurosci* 33(17), pp. 7603-7614. doi: 10.1523/jneurosci.4181-12.2013

Filippov, V. et al. 2012. Increased ceramide in brains with Alzheimer's and other neurodegenerative diseases. *J Alzheimers Dis* 29(3), pp. 537-547. doi: 10.3233/jad-2011-111202

Fischer, I. et al. 2011. Sphingosine kinase 1 and sphingosine 1-phosphate receptor 3 are functionally upregulated on astrocytes under pro-inflammatory conditions. *PLoS One* 6, doi: 10.1371/journal.pone.0023905

Forrest, M. et al. 2004. Immune cell regulation and cardiovascular effects of sphingosine 1-phosphate receptor agonists in rodents are mediated via distinct receptor subtypes. *J Pharmacol Exp Ther* 309(2), pp. 758-768. doi: 10.1124/jpet.103.062828

Foster, C. A. et al. 2007. Brain penetration of the oral immunomodulatory drug FTY720 and its phosphorylation in the central nervous system during experimental autoimmune encephalomyelitis: consequences for mode of action in multiple sclerosis. *J Pharmacol Exp Ther* 323(2), pp. 469-475. doi: 10.1124/jpet.107.127183

Foster, C. A. et al. 2009. FTY720 rescue therapy in the dark agouti rat model of experimental autoimmune encephalomyelitis: expression of central nervous system genes and reversal of blood-brain-barrier damage. *Brain Pathol* 19(2), pp. 254-266. doi: 10.1111/j.1750-3639.2008.00182.x

Fremeau Jr, R. T. et al. 2001. The Expression of Vesicular Glutamate Transporters Defines Two Classes of Excitatory Synapse. *Neuron* 31(2), pp. 247-260. doi: http://dx.doi.org/10.1016/S0896-6273(01)00344-0

Fukumoto, K. et al. 2014. Fingolimod increases brain-derived neurotrophic factor levels and ameliorates amyloid beta-induced memory impairment. *Behav Brain Res* 268, pp. 88-93. doi: 10.1016/j.bbr.2014.03.046

Garris, C. S. et al. 2014. Sphingosine-1-phosphate receptor 1 signalling in T cells: trafficking and beyond. *Immunology* 142(3), pp. 347-353. doi: 10.1111/imm.12272

Gartner, A. et al. 2006. Hippocampal long-term potentiation is supported by presynaptic and postsynaptic tyrosine receptor kinase B-mediated phospholipase Cgamma signaling. *J Neurosci* 26(13), pp. 3496-3504. doi: 10.1523/jneurosci.3792-05.2006

Gauthier, L. R. et al. 2004. Huntingtin controls neurotrophic support and survival of neurons by enhancing BDNF vesicular transport along microtubules. *Cell* 118(1), pp. 127-138. doi: 10.1016/j.cell.2004.06.018

Gergely, P. et al. 2012. The selective sphingosine 1-phosphate receptor modulator BAF312 redirects lymphocyte distribution and has species-specific effects on heart rate. *Br J Pharmacol* 167(5), pp. 1035-1047. doi: 10.1111/j.1476-5381.2012.02061.x

Ghosh, A. et al. 1994. Requirement for BDNF in activity-dependent survival of cortical neurons. *Science* 263(5153), pp. 1618-1623.

Gonda, K. et al. 1999. The novel sphingosine 1-phosphate receptor AGR16 is coupled via pertussis toxin-sensitive and -insensitive G-proteins to multiple signalling pathways. *Biochem J* 337 (Pt 1), pp. 67-75.

Gonzalez-Fernandez, B. et al. 2016. Inhibition of the SphK1/S1P signaling pathway by melatonin in mice with liver fibrosis and human hepatic stellate cells. *Biofactors*, doi: 10.1002/biof.1342

Gordge, M. P. 2005. Megakaryocyte apoptosis: sorting out the signals. *Br J Pharmacol* 145(3), pp. 271-273. doi: 10.1038/sj.bjp.0706202

Gordon, J. et al. 2013. General overview of neuronal cell culture. *Methods Mol Biol* 1078, pp. 1-8. doi: 10.1007/978-1-62703-640-5_1

Gordon, J. W. et al. 1987. Regulation of Thy-1 gene expression in transgenic mice. *Cell* 50(3), pp. 445-452.

Gorshkova, I. et al. 2008. Protein kinase C-epsilon regulates sphingosine 1-phosphate-mediated migration of human lung endothelial cells through activation of phospholipase D2, protein kinase C-zeta, and Rac1. *J Biol Chem* 283(17), pp. 11794-11806. doi: 10.1074/jbc.M800250200

Graler, M. H. and Goetzl, E. J. 2004. The immunosuppressant FTY720 down-regulates sphingosine 1-phosphate G-protein-coupled receptors. *Faseb j* 18(3), pp. 551-553. doi: 10.1096/fj.03-0910fje

Graler, M. H. et al. 2003. The sphingosine 1-phosphate receptor S1P4 regulates cell shape and motility via coupling to Gi and G12/13. *J Cell Biochem* 89(3), pp. 507-519. doi: 10.1002/jcb.10537

Gray, J. et al. 2006. Hyperphagia, severe obesity, impaired cognitive function, and hyperactivity associated with functional loss of one copy of the brain-derived neurotrophic factor (BDNF) gene. *Diabetes* 55(12), pp. 3366-3371. doi: 10.2337/db06-0550

Griffin, E. W. et al. 2011. Aerobic exercise improves hippocampal function and increases BDNF in the serum of young adult males. *Physiol Behav* 104(5), pp. 934-941. doi: 10.1016/j.physbeh.2011.06.005

Gunawardena, S. et al. 2003. Disruption of axonal transport by loss of huntingtin or expression of pathogenic polyQ proteins in Drosophila. *Neuron* 40(1), pp. 25-40.

Haapasalo, A. et al. 2002. Regulation of TRKB surface expression by brain-derived neurotrophic factor and truncated TRKB isoforms. *J Biol Chem* 277(45), pp. 43160-43167. doi: 10.1074/jbc.M205202200

Hait, N. C. et al. 2014. Active, phosphorylated fingolimod inhibits histone deacetylases and facilitates fear extinction memory. *Nat Neurosci* 17(7), pp. 971-980. doi: 10.1038/nn.3728

Hall, J. et al. 2000. Rapid and selective induction of BDNF expression in the hippocampus during contextual learning. *Nat Neurosci* 3(6), pp. 533-535. doi: 10.1038/75698

Han, J. C. et al. 2008. Brain-derived neurotrophic factor and obesity in the WAGR syndrome. *N Engl J Med* 359(9), pp. 918-927. doi: 10.1056/NEJMoa0801119

Han, J. C. et al. 2013. Association of brain-derived neurotrophic factor (BDNF) haploinsufficiency with lower adaptive behaviour and reduced cognitive functioning in WAGR/11p13 deletion syndrome. *Cortex* 49(10), pp. 2700-2710. doi: 10.1016/j.cortex.2013.02.009

Hanson, M. A. et al. 2012. Crystal structure of a lipid G protein-coupled receptor. *Science* 335(6070), pp. 851-855. doi: 10.1126/science.1215904

Hardy, J. A. and Higgins, G. A. 1992. Alzheimer's disease: the amyloid cascade hypothesis. *Science* 256(5054), pp. 184-185.

Harward, S. C. et al. 2016. Autocrine BDNF–TrkB signalling within a single dendritic spine. *Nature* 538(7623), pp. 99-103. doi: 10.1038/nature19766

Hasegawa, Y. et al. 2010. Activation of sphingosine 1-phosphate receptor-1 by FTY720 is neuroprotective after ischemic stroke in rats. *Stroke* 41(2), pp. 368-374. doi: 10.1161/strokeaha.109.568899

Hayashi, S. and McMahon, A. P. 2002. Efficient recombination in diverse tissues by a tamoxifen-inducible form of Cre: a tool for temporally regulated gene activation/inactivation in the mouse. *Dev Biol* 244(2), pp. 305-318. doi: 10.1006/dbio.2002.0597

Healy, L. M. et al. 2013. Pathway specific modulation of S1P1 receptor signalling in rat and human astrocytes. *Br J Pharmacol* 169(5), pp. 1114-1129. doi: 10.1111/bph.12207

Heimer-McGinn, V. and Young, P. 2011. Efficient inducible Pan-neuronal cre-mediated recombination in SLICK-H transgenic mice. *Genesis* 49(12), pp. 942-949. doi: 10.1002/dvg.20777

Heldt, S. A. et al. 2007. Hippocampus-specific deletion of BDNF in adult mice impairs spatial memory and extinction of aversive memories. *Mol Psychiatry* 12(7), pp. 656-670. doi: 10.1038/sj.mp.4001957

Hevner, R. F. et al. 2001. Tbr1 regulates differentiation of the preplate and layer 6. *Neuron* 29(2), pp. 353-366.

Heyden, A. et al. 2011. Hippocampal enlargement in Bassoon-mutant mice is associated with enhanced neurogenesis, reduced apoptosis, and abnormal BDNF levels. *Cell Tissue Res* 346(1), pp. 11-26. doi: 10.1007/s00441-011-1233-3

Hla, T. et al. 2012. S1P and the birth of platelets.*J Exp Med*. Vol. 209. pp. 2137-2140.

Hla, T. et al. 1999. Sphingosine-1-phosphate: extracellular mediator or intracellular second messenger? *Biochem Pharmacol* 58(2), pp. 201-207.

Hla, T. and Maciag, T. 1990. An abundant transcript induced in differentiating human endothelial cells encodes a polypeptide with structural similarities to G-protein-coupled receptors. *J Biol Chem* 265(16), pp. 9308-9313.

Hol, E. M. et al. 2003. Neuronal expression of GFAP in patients with Alzheimer pathology and identification of novel GFAP splice forms. *Mol Psychiatry* 8(9), pp. 786-796. doi: 10.1038/sj.mp.4001379

Hong, E. J. et al. 2008. A biological function for the neuronal activity-dependent component of Bdnf transcription in the development of cortical inhibition. *Neuron* 60(4), pp. 610-624. doi: 10.1016/j.neuron.2008.09.024

Hyman, B. T. et al. 2012. National Institute on Aging-Alzheimer's Association guidelines for the neuropathologic assessment of Alzheimer's disease. *Alzheimers Dement* 8, doi: 10.1016/j.jalz.2011.10.007

Igarashi, J. et al. 2001. Sphingosine 1-phosphate and activation of endothelial nitric-oxide synthase. differential regulation of Akt and MAP kinase pathways by EDG and bradykinin receptors in vascular endothelial cells. *J Biol Chem* 276(15), pp. 12420-12426. doi: 10.1074/jbc.M008375200

Im, D. S. et al. 1997. Characterization of sphingosine 1-phosphate-induced actions and its signaling pathways in rat hepatocytes. *Am J Physiol* 272(5 Pt 1), pp. G1091-1099.

Im, D. S. et al. 2000. Characterization of a novel sphingosine 1-phosphate receptor, Edg-8. *J Biol Chem* 275(19), pp. 14281-14286.

Ippolito, D. M. and Eroglu, C. 2010. Quantifying synapses: an immunocytochemistry-based assay to quantify synapse number. *J Vis Exp* (45), doi: 10.3791/2270

Ishii, I. et al. 2001. Selective loss of sphingosine 1-phosphate signaling with no obvious phenotypic abnormality in mice lacking its G protein-coupled receptor, LP(B3)/EDG-3. *J Biol Chem* 276(36), pp. 33697-33704. doi: 10.1074/jbc.M104441200

Ishii, I. et al. 2004. Lysophospholipid receptors: signaling and biology. *Annu Rev Biochem* 73, pp. 321-354. doi: 10.1146/annurev.biochem.73.011303.073731

Ishii, I. et al. 2002. Marked perinatal lethality and cellular signaling deficits in mice null for the two sphingosine 1-phosphate (S1P) receptors, S1P(2)/LP(B2)/EDG-5 and S1P(3)/LP(B3)/EDG-3. *J Biol Chem* 277(28), pp. 25152-25159. doi: 10.1074/jbc.M200137200

Ito, K. and Enomoto, H. 2016. Retrograde transport of neurotrophic factor signaling: implications in neuronal development and pathogenesis. *The Journal of Biochemistry* 160(2), pp. 77-85. doi: 10.1093/jb/mvw037

Jaillard, C. et al. 2005. Edg8/S1P5: an oligodendroglial receptor with dual function on process retraction and cell survival. *J Neurosci* 25(6), pp. 1459-1469. doi: 10.1523/jneurosci.4645-04.2005

Jang, S. et al. 2011. Modulation of sphingosine 1-phosphate and tyrosine hydroxylase in the stress-induced anxiety. *Neurochem Res* 36(2), pp. 258-267. doi: 10.1007/s11064-010-0313-1

Jing, Y. et al. 2011. In Vitro Differentiation of Mouse Embryonic Stem Cells into Neurons of the Dorsal Forebrain.*Cell Mol Neurobiol*. Vol. 31. Boston, pp. 715-727.

Jo, E. et al. 2005. S1P1-selective in vivo-active agonists from high-throughput screening: off-the-shelf chemical probes of receptor interactions, signaling, and fate. *Chem Biol* 12(6), pp. 703-715. doi: 10.1016/j.chembiol.2005.04.019

Jones, K. R. et al. 1994. Targeted Disruption of the BDNF Gene Perturbs Brain and Sensory Neuron Development but Not Motor Neuron Development. *Cell* 76(6), pp. 989-999.

Kajimoto, T. et al. 2007. Involvement of sphingosine-1-phosphate in glutamate secretion in hippocampal neurons. *Mol Cell Biol* 27, doi: 10.1128/mcb.01465-06

Kaplan, D. R. et al. 1991. Tyrosine phosphorylation and tyrosine kinase activity of the trk proto-oncogene product induced by NGF. *Nature* 350(6314), pp. 158-160. doi: 10.1038/350158a0

Kappos, L. et al. 2010. A placebo-controlled trial of oral fingolimod in relapsing multiple sclerosis. *N Engl J Med* 362(5), pp. 387-401. doi: 10.1056/NEJMoa0909494

Kawahara, A. et al. 2009. The sphingolipid transporter spns2 functions in migration of zebrafish myocardial precursors. *Science* 323(5913), pp. 524-527. doi: 10.1126/science.1167449

Kays, J. S. et al. 2012. Expression of sphingosine 1-phosphate receptors in the rat dorsal root ganglia and defined single isolated sensory neurons. *Physiol Genomics* 44(18), pp. 889-901. doi: 10.1152/physiolgenomics.00053.2012

Kernie, S. G. et al. 2000. BDNF regulates eating behavior and locomotor activity in mice. *Embo j* 19(6), pp. 1290-1300. doi: 10.1093/emboj/19.6.1290

Kessaris, N. et al. 2006. Competing waves of oligodendrocytes in the forebrain and postnatal elimination of an embryonic lineage. *Nat Neurosci* 9(2), pp. 173-179. doi: http://www.nature.com/neuro/journal/v9/n2/suppinfo/nn1620_S1.html

Kim, J. H. et al. 2000. Sphingosine 1-phosphate activates Erk-1/-2 by transactivating epidermal growth factor receptor in rat-2 cells. *IUBMB Life* 50(2), pp. 119-124. doi: 10.1080/713803698

Kimura, A. et al. 2008. Antagonism of sphingosine 1-phosphate receptor-2 enhances migration of neural progenitor cells toward an area of brain. *Stroke* 39(12), pp. 3411-3417. doi: 10.1161/strokeaha.108.514612

Kitatani, K. et al. 2008. The sphingolipid salvage pathway in ceramide metabolism and signaling. *Cell Signal* 20(6), pp. 1010-1018. doi: 10.1016/j.cellsig.2007.12.006

Klein, R. et al. 1990. The trkB tyrosine protein kinase gene codes for a second neurogenic receptor that lacks the catalytic kinase domain. *Cell* 61(4), pp. 647-656.

Kohno, T. et al. 2002. N-glycans of sphingosine 1-phosphate receptor Edg-1 regulate ligand-induced receptor internalization. *FASEB J* 16(9), pp. 983-992. doi: 10.1096/fj.01-0809com

Kokaia, Z. et al. 1993. Rapid increase of BDNF mRNA levels in cortical neurons following spreading depression: regulation by glutamatergic mechanisms independent of seizure activity. *Molecular Brain Research* 19(4), pp. 277-286. doi: http://dx.doi.org/10.1016/0169-328X(93)90126-A

Kolbeck, R. et al. 1999. Brain-derived neurotrophic factor levels in the nervous system of wild-type and neurotrophin gene mutant mice. *J Neurochem* 72(5), pp. 1930-1938.

Kollias, G. et al. 1987. Differential regulation of a Thy-1 gene in transgenic mice. *Proc Natl Acad Sci U S A* 84(6), pp. 1492-1496.

Kon, J. et al. 1999. Comparison of intrinsic activities of the putative sphingosine 1-phosphate receptor subtypes to regulate several signaling pathways in their cDNA-transfected Chinese hamster ovary cells. *J Biol Chem* 274(34), pp. 23940-23947.

Kono, M. et al. 2004. The sphingosine-1-phosphate receptors S1P1, S1P2, and S1P3 function coordinately during embryonic angiogenesis. *J Biol Chem* 279(28), pp. 29367-29373. doi: 10.1074/jbc.M403937200

Koppel, I. et al. 2015. Efficient use of a translation start codon in BDNF exon I. *J Neurochem* 134(6), pp. 1015-1025. doi: 10.1111/jnc.13124

Korte, M. et al. 1995. Hippocampal long-term potentiation is impaired in mice lacking brain-derived neurotrophic factor. *Proc Natl Acad Sci U S A* 92(19), pp. 8856-8860.

Koyrakh, L. et al. 2005. The heart rate decrease caused by acute FTY720 administration is mediated by the G protein-gated potassium channel I. *Am J Transplant* 5(3), pp. 529-536. doi: 10.1111/j.1600-6143.2005.00754.x

Kristianto, J. et al. 2017. Spontaneous recombinase activity of Cre–ERT2 in vivo. *Transgenic Res* 26(3), pp. 411-417. doi: 10.1007/s11248-017-0018-1

Laske, C. et al. 2011. Higher BDNF serum levels predict slower cognitive decline in Alzheimer's disease patients. *Int J Neuropsychopharmacol* 14(3), pp. 399-404. doi: 10.1017/s1461145710001008

Lauterborn, J. C. et al. 2009. Ampakines cause sustained increases in brain-derived neurotrophic factor signaling at excitatory synapses without changes in AMPA receptor subunit expression. *Neuroscience* 159(1), pp. 283-295. doi: 10.1016/j.neuroscience.2008.12.018

Lee, B. H. and Kim, Y. K. 2010. The Roles of BDNF in the Pathophysiology of Major Depression and in Antidepressant Treatment. *Psychiatry Investig* 7(4), pp. 231-235. doi: 10.4306/pi.2010.7.4.231

Lee, F. S. and Chao, M. V. 2001. Activation of Trk neurotrophin receptors in the absence of neurotrophins. Vol. 98. pp. 3555-3560.

Lee, F. S. et al. 2002. Activation of Trk neurotrophin receptor signaling by pituitary adenylate cyclase-activating polypeptides. *J Biol Chem* 277(11), pp. 9096-9102. doi: 10.1074/jbc.M107421200

Lee, M. J. et al. 1998. Sphingosine-1-phosphate as a ligand for the G protein-coupled receptor EDG-1. *Science* 279(5356), pp. 1552-1555.

Leibrock, J. et al. 1989. Molecular cloning and expression of brain-derived neurotrophic factor. *Nature* 341(6238), pp. 149-152. doi: 10.1038/341149a0

Leid, M. et al. 2004. CTIP1 and CTIP2 are differentially expressed during mouse embryogenesis. *Gene Expression Patterns* 4(6), pp. 733-739. doi: https://doi.org/10.1016/j.modgep.2004.03.009

Lesuisse, C. and Martin, L. J. 2002. Long-term culture of mouse cortical neurons as a model for neuronal development, aging, and death. *J Neurobiol* 51(1), pp. 9-23.

Li, E. et al. 1992. Targeted mutation of the DNA methyltransferase gene results in embryonic lethality. *Cell* 69(6), pp. 915-926.

Lindholm, J. S. O. and Castrén, E. 2014. Mice with altered BDNF signaling as models for mood disorders and antidepressant effects. *Front Behav Neurosci* 8, doi: 10.3389/fnbeh.2014.00143

Liot, G. et al. 2013. Mutant Huntingtin alters retrograde transport of TrkB receptors in striatal dendrites. *J Neurosci* 33(15), pp. 6298-6309. doi: 10.1523/jneurosci.2033-12.2013

Liu, J. et al. 2012. Brain-derived neurotrophic factor (BDNF) genetic polymorphism greatly increases risk of leucine-rich repeat kinase 2 (LRRK2) for Parkinson's disease. *Parkinsonism Relat Disord* 18(2), pp. 140-143. doi: 10.1016/j.parkreldis.2011.09.002

Liu, Y. et al. 2000. Edg-1, the G protein-coupled receptor for sphingosine-1-phosphate, is essential for vascular maturation. *J Clin Invest* 106(8), pp. 951-961. doi: 10.1172/jci10905

Lo, C. G. et al. 2005. Cyclical modulation of sphingosine-1-phosphate receptor 1 surface expression during lymphocyte recirculation and relationship to lymphoid organ transit. *J Exp Med* 201(2), pp. 291-301. doi: 10.1084/jem.20041509

Loh, Y. H. et al. 2006. The Oct4 and Nanog transcription network regulates pluripotency in mouse embryonic stem cells. *Nat Genet* 38(4), pp. 431-440. doi: 10.1038/ng1760

Lukas, S. et al. 2014. No differences observed among multiple clinical S1P1 receptor agonists (functional antagonists) in S1P1 receptor down-regulation and degradation. *J Biomol Screen* 19(3), pp. 407-416. doi: 10.1177/1087057113502234

Lyons, M. R. et al. 2016. The transcription factor calcium-response factor limits NMDA receptor-dependent transcription in the developing brain. *J Neurochem* 137(2), pp. 164-176. doi: 10.1111/jnc.13556

MacLennan, A. J. et al. 1994. Cloning and Characterization of a Putative G-Protein Coupled Receptor Potentially Involved in Development. *Molecular and Cellular Neuroscience* 5(3), pp. 201-209. doi: http://dx.doi.org/10.1006/mcne.1994.1024

MacLennan, A. J. et al. 2001. An essential role for the H218/AGR16/Edg-5/LP(B2) sphingosine 1-phosphate receptor in neuronal excitability. *Eur J Neurosci* 14(2), pp. 203-209.

Maisonpierre, P. C. et al. 1990. NT-3, BDNF, and NGF in the developing rat nervous system: parallel as well as reciprocal patterns of expression. *Neuron* 5(4), pp. 501-509.

Malatesta, P. et al. 2003. Neuronal or glial progeny: regional differences in radial glia fate. *Neuron* 37(5), pp. 751-764.

Mansoor, M. and Melendez, A. J. 2008. Recent trials for FTY720 (fingolimod): a new generation of immunomodulators structurally similar to sphingosine. *Rev Recent Clin Trials* 3(1), pp. 62-69.

Marks, H. et al. 2012. The transcriptional and epigenomic foundations of ground state pluripotency. *Cell* 149(3), pp. 590-604. doi: 10.1016/j.cell.2012.03.026

Martinez-Garay, I. et al. 2016. Normal radial migration and lamination are maintained in dyslexia-susceptibility candidate gene homolog Kiaa0319 knockout mice. *Brain Structure and Function*, pp. 1-18. doi: 10.1007/s00429-016-1282-1

Marty, S. et al. 1996. GABAergic stimulation regulates the phenotype of hippocampal interneurons through the regulation of brain-derived neurotrophic factor. *Neuron* 16(3), pp. 565-570.

Matloubian, M. et al. 2004. Lymphocyte egress from thymus and peripheral lymphoid organs is dependent on S1P receptor 1. *Nature* 427(6972), pp. 355-360. doi: 10.1038/nature02284

Matsuda, N. et al. 2009. Differential activity-dependent secretion of brain-derived neurotrophic factor from axon and dendrite. *J Neurosci* 29(45), pp. 14185-14198. doi: 10.1523/jneurosci.1863-09.2009

Matsumoto, T. et al. 2008. Biosynthesis and processing of endogenous BDNF: CNS neurons store and secrete BDNF, not pro-BDNF. *Nat Neurosci* 11(2), pp. 131-133. doi: 10.1038/nn2038

Mazurais, D. et al. 2002. Cell type-specific localization of human cardiac S1P receptors. *J Histochem Cytochem* 50(5), pp. 661-670. doi: 10.1177/002215540205000507

McCubrey, J. A. et al. 2007. ROLES OF THE RAF/MEK/ERK PATHWAY IN CELL GROWTH, MALIGNANT TRANSFORMATION AND DRUG RESISTANCE. *Biochim Biophys Acta* 1773(8), pp. 1263-1284. doi: 10.1016/j.bbamcr.2006.10.001

McCudden, C. R. et al. 2005. G-protein signaling: back to the future.*Cell Mol Life Sci*. Vol. 62. Basel, pp. 551-577.

McDonald, N. Q. and Hendrickson, W. A. 1993. A structural superfamily of growth factors containing a cystine knot motif. *Cell* 73(3), pp. 421-424.

McGiffert, C. et al. 2002. Embryonic brain expression analysis of lysophospholipid receptor genes suggests roles for s1p(1) in neurogenesis and s1p(1-3) in angiogenesis. *FEBS Lett* 531(1), pp. 103-108.

Means, C. K. et al. 2008. S1P(1) Receptor Localization Confers Selectivity for Gi-mediated cAMP and Contractile Responses. *The Journal of Biological Chemistry* 283(18), pp. 11954-11963. doi: 10.1074/jbc.M707422200

Mechtcheriakova, D. et al. 2007. FTY720-phosphate is dephosphorylated by lipid phosphate phosphatase 3. *FEBS Lett* 581, doi: 10.1016/j.febslet.2007.05.069

Middeldorp, J. and Hol, E. M. 2011. GFAP in health and disease. *Progress in Neurobiology* 93(3), pp. 421-443. doi: http://dx.doi.org/10.1016/j.pneurobio.2011.01.005

Miguez, A. et al. 2015. Fingolimod (FTY720) enhances hippocampal synaptic plasticity and memory in Huntington's disease by preventing p75NTR up-regulation and astrocyte-mediated inflammation. *Human molecular genetics* 24(17), pp. 4958-4970. doi: 10.1093/hmg/ddv218

Mizugishi, K. et al. 2005. Essential role for sphingosine kinases in neural and vascular development. *Mol Cell Biol* 25(24), pp. 11113-11121. doi: 10.1128/mcb.25.24.11113-11121.2005

Moberly, J. B. et al. 2012. Pharmacological effects of CS-0777, a selective sphingosine 1-phosphate receptor-1 modulator: results from a 12-week, open-label pilot study in multiple sclerosis patients. *J Neuroimmunol* 246(1-2), pp. 100-107. doi: 10.1016/j.jneuroim.2012.03.007

Molendijk, M. L. et al. 2014. Serum BDNF concentrations as peripheral manifestations of depression: evidence from a systematic review and meta-analyses on 179 associations (N=9484). *Mol Psychiatry* 19(7), pp. 791-800. doi: 10.1038/mp.2013.105

Morales-Ruiz, M. et al. 2001. Sphingosine 1-phosphate activates Akt, nitric oxide production, and chemotaxis through a Gi protein/phosphoinositide 3-kinase pathway in endothelial cells. *J Biol Chem* 276(22), pp. 19672-19677. doi: 10.1074/jbc.M009993200

Mori, T. et al. 2006. Inducible gene deletion in astroglia and radial glia--a valuable tool for functional and lineage analysis. *Glia* 54(1), pp. 21-34. doi: 10.1002/glia.20350

Mouri, A. et al. 2012. Mouse strain differences in phencyclidine-induced behavioural changes. *International Journal of Neuropsychopharmacology* 15(6), pp. 767-779. doi: 10.1017/S146114571100085X

Muhle, C. et al. 2013. Sphingolipids in psychiatric disorders and pain syndromes. *Handb Exp Pharmacol* (216), pp. 431-456. doi: 10.1007/978-3-7091-1511-4_22

Mullershausen, F. et al. 2009. Persistent signaling induced by FTY720-phosphate is mediated by internalized S1P1 receptors. *Nat Chem Biol* 5(6), pp. 428-434. doi: 10.1038/nchembio.173

Naegelin, Y. et al. 2015. OP24 – 2321: FINGORETT – An ongoing phase I clinical study to assess safety and efficacy of oral fingolimod (FTY720) in children with Rett syndrome. *European Journal of Paediatric Neurology* 19, p. S8. doi: http://dx.doi.org/10.1016/S1090-3798(15)30025-8

Nagahara, A. H. et al. 2009. Neuroprotective effects of brain-derived neurotrophic factor in rodent and primate models of Alzheimer's disease. *Nat Med* 15(3), pp. 331-337. doi: 10.1038/nm.1912

Nagappan, G. et al. 2009. Control of extracellular cleavage of ProBDNF by high frequency neuronal activity. *Proc Natl Acad Sci U S A* 106(4), pp. 1267-1272. doi: 10.1073/pnas.0807322106

Nakajima, C. et al. 2014. The lipoprotein receptor LRP1 modulates sphingosine-1-phosphate signaling and is essential for vascular development. *Development* 141(23), pp. 4513-4525. doi: 10.1242/dev.109124

Nikoletopoulou, V. et al. 2010. Neurotrophin receptors TrkA and TrkC cause neuronal death whereas TrkB does not. *Nature* 467(7311), pp. 59-63. doi: 10.1038/nature09336

Nikoletopoulou, V. et al. 2007. Neurotrophin receptor-mediated death of misspecified neurons generated from embryonic stem cells lacking Pax6. *Cell Stem Cell* 1(5), pp. 529-540. doi: 10.1016/j.stem.2007.08.011

Nishimura, H. et al. 2010. Cellular localization of sphingosine-1-phosphate receptor 1 expression in the human central nervous system. *J Histochem Cytochem* 58(9), pp. 847-856. doi: 10.1369/jhc.2010.956409

Notaras, M. et al. 2015. The BDNF gene Val66Met polymorphism as a modifier of psychiatric disorder susceptibility: progress and controversy. *Mol Psychiatry* 20(8), pp. 916-930. doi: 10.1038/mp.2015.27

Novgorodov, A. S. et al. 2007. Activation of sphingosine-1-phosphate receptor S1P5 inhibits oligodendrocyte progenitor migration. *Faseb j* 21(7), pp. 1503-1514. doi: 10.1096/fj.06-7420com

Nygaard, R. et al. 2009. Ligand binding and micro-switches in 7TM receptor structures. *Trends Pharmacol Sci* 30(5), pp. 249-259. doi: 10.1016/j.tips.2009.02.006

O'Sullivan, S. and Dev, K. K. 2016. Sphingosine-1-phosphate receptor therapies: Advances in clinical trials for CNS-related diseases. *Neuropharmacology*, doi: 10.1016/j.neuropharm.2016.11.006

Okada, T. et al. 2009. Sphingosine kinase/sphingosine 1-phosphate signalling in central nervous system. *Cellular Signalling* 21(1), pp. 7-13. doi: http://dx.doi.org/10.1016/j.cellsig.2008.07.011

Okamoto, H. et al. 1998. EDG1 is a functional sphingosine-1-phosphate receptor that is linked via a Gi/o to multiple signaling pathways, including phospholipase C activation, Ca2+ mobilization, Ras-mitogen-activated protein kinase activation, and adenylate cyclase inhibition. *J Biol Chem* 273(42), pp. 27104-27110.

Okamoto, H. et al. 2000. Inhibitory regulation of Rac activation, membrane ruffling, and cell migration by the G protein-coupled sphingosine-1-phosphate receptor EDG5 but not EDG1 or EDG3. *Mol Cell Biol* 20(24), pp. 9247-9261.

Oldham, W. M. and Hamm, H. E. 2008. Heterotrimeric G protein activation by G-protein-coupled receptors. *Nat Rev Mol Cell Biol* 9(1), pp. 60-71. doi: 10.1038/nrm2299

Oliveri, S. 2014. *Biosynthesis and release of Brain-derived neurotrophic factor: a study using neurons derived from embryonic stem cells.* University Basel.

Pappu, R. et al. 2007. Promotion of lymphocyte egress into blood and lymph by distinct sources of sphingosine-1-phosphate. *Science* 316(5822), pp. 295-298. doi: 10.1126/science.1139221

Pardridge, W. M. et al. 1994. Transport of human recombinant brain-derived neurotrophic factor (BDNF) through the rat blood-brain barrier in vivo using vector-mediated peptide drug delivery. *Pharm Res* 11(5), pp. 738-746.

Park, H. and Poo, M. M. 2013. Neurotrophin regulation of neural circuit development and function. *Nat Rev Neurosci* 14(1), pp. 7-23. doi: 10.1038/nrn3379

Paterson, R. R. 2008. Cordyceps: a traditional Chinese medicine and another fungal therapeutic biofactory? *Phytochemistry* 69(7), pp. 1469-1495. doi: 10.1016/j.phytochem.2008.01.027

Pebay, A. et al. 2001. Sphingosine-1-phosphate induces proliferation of astrocytes: regulation by intracellular signalling cascades. *Eur J Neurosci* 13(12), pp. 2067-2076.

Pelleymounter, M. A. et al. 1995. Characteristics of BDNF-induced weight loss. *Exp Neurol* 131(2), pp. 229-238.

Pham, T. H. et al. 2010. Lymphatic endothelial cell sphingosine kinase activity is required for lymphocyte egress and lymphatic patterning. *J Exp Med* 207(1), pp. 17-27. doi: 10.1084/jem.20091619

Pitman, M. R. et al. 2015. A selective ATP-competitive sphingosine kinase inhibitor demonstrates anti-cancer properties. *Oncotarget* 6(9), pp. 7065-7083. doi: 10.18632/oncotarget.3178

Plachta, N. et al. 2007. Identification of a lectin causing the degeneration of neuronal processes using engineered embryonic stem cells. *Nat Neurosci* 10(6), pp. 712-719. doi: 10.1038/nn1897

Polacchini, A. et al. 2015. A method for reproducible measurements of serum BDNF: comparison of the performance of six commercial assays. *Sci Rep* 5, p. 17989. doi: 10.1038/srep17989

Potenza, R. L. et al. 2016. Fingolimod: A Disease-Modifier Drug in a Mouse Model of Amyotrophic Lateral Sclerosis. *Neurotherapeutics* 13(4), pp. 918-927. doi: 10.1007/s13311-016-0462-2

Prasher, V. P. et al. 1998. Molecular mapping of Alzheimer-type dementia in Down's syndrome. *Ann Neurol* 43(3), pp. 380-383. doi: 10.1002/ana.410430316

Przedborski, S. et al. 2003. Neurodegeneration: what is it and where are we? *J Clin Invest* 111(1), pp. 3-10. doi: 10.1172/jci17522

Putney, J. W. and Tomita, T. 2012. Phospholipase C Signaling and Calcium Influx. *Adv Biol Regul* 52(1), pp. 152-164. doi: 10.1016/j.advenzreg.2011.09.005

Pyne, N. J. et al. 2007. Receptor tyrosine kinase-G-protein coupled receptor complex signaling in mammalian cells. *Adv Enzyme Regul* 47, pp. 271-280. doi: 10.1016/j.advenzreg.2006.12.011

Pyne, S. et al. 2016. Sphingosine 1-phosphate and sphingosine kinases in health and disease: Recent advances. *Prog Lipid Res* 62, pp. 93-106. doi: 10.1016/j.plipres.2016.03.001

Qin, X. Y. et al. 2016. Decreased peripheral brain-derived neurotrophic factor levels in Alzheimer's disease: a meta-analysis study (N=7277). *Mol Psychiatry*, doi: 10.1038/mp.2016.62

Radeff-Huang, J. et al. 2004. G protein mediated signaling pathways in lysophospholipid induced cell proliferation and survival. *J Cell Biochem* 92(5), pp. 949-966. doi: 10.1002/jcb.20094

Radziejewski, C. et al. 1992. Dimeric structure and conformational stability of brain-derived neurotrophic factor and neurotrophin-3. *Biochemistry* 31(18), pp. 4431-4436.

Rakhit, S. et al. 1999. Sphingosine 1-phosphate stimulation of the p42/p44 mitogen-activated protein kinase pathway in airway smooth muscle. Role of endothelial differentiation gene 1, c-Src tyrosine kinase and phosphoinositide 3-kinase. *Biochem J* 338(Pt 3), pp. 643-649.

Rao, V. R. et al. 2006. AMPA receptors regulate transcription of the plasticity-related immediate-early gene Arc. *Nature neuroscience* 9(7), pp. 887-895. doi: 10.1038/nn1708

Rauskolb, S. et al. 2010. Global deprivation of brain-derived neurotrophic factor in the CNS reveals an area-specific requirement for dendritic growth. *J Neurosci* 30(5), pp. 1739-1749. doi: 10.1523/jneurosci.5100-09.2010

Reichardt, L. F. 2006. Neurotrophin-regulated signalling pathways. *Philos Trans R Soc Lond B Biol Sci* 361(1473), pp. 1545-1564. doi: 10.1098/rstb.2006.1894

Rodriguez-Tebar, A. et al. 1990. Binding of brain-derived neurotrophic factor to the nerve growth factor receptor. *Neuron* 4(4), pp. 487-492.

Roux, P. P. et al. 1999. p75 neurotrophin receptor expression is induced in apoptotic neurons after seizure. *J Neurosci* 19(16), pp. 6887-6896.

Rowley, J. W. et al. 2011. Genome-wide RNA-seq analysis of human and mouse platelet transcriptomes. *Blood* 118(14), pp. e101-111. doi: 10.1182/blood-2011-03-339705

Saarelainen, T. et al. 2003. Activation of the TrkB neurotrophin receptor is induced by antidepressant drugs and is required for antidepressant-induced behavioral effects. *J Neurosci* 23(1), pp. 349-357.

Sadegh, C. and Macklis, J. D. 2014. Established Monolayer Differentiation of Mouse Embryonic Stem Cells Generates Heterogeneous Neocortical-Like Neurons Stalled at a Stage Equivalent to Midcorticogenesis. *J Comp Neurol* 522(12), pp. 2691-2706. doi: 10.1002/cne.23576

Safarian, F. et al. 2015. Activation of S1P(1) receptor regulates PI3K/Akt/FoxO3a pathway in response to oxidative stress in PC12 cells. *J Mol Neurosci* 56(1), pp. 177-187. doi: 10.1007/s12031-014-0478-1

Sakane, T. and Pardridge, W. M. 1997. Carboxyl-directed pegylation of brain-derived neurotrophic factor markedly reduces systemic clearance with minimal loss of biologic activity. *Pharm Res* 14(8), pp. 1085-1091.

Sanchez, T. and Hla, T. 2004. Structural and functional characteristics of S1P receptors. *J Cell Biochem* 92(5), pp. 913-922. doi: 10.1002/jcb.20127

Sanchez, T. et al. 2005. PTEN as an effector in the signaling of antimigratory G protein-coupled receptor. *Proc Natl Acad Sci U S A* 102(12), pp. 4312-4317. doi: 10.1073/pnas.0409784102

Sandberg, R. 2000. Regional and strain-specific gene expression mapping in the adult. Vol. 97. pp. 11038-11043.

Sanna, M. G. et al. 2004. Sphingosine 1-phosphate (S1P) receptor subtypes S1P1 and S1P3, respectively, regulate lymphocyte recirculation and heart rate. *J Biol Chem* 279(14), pp. 13839-13848. doi: 10.1074/jbc.M311743200

Santarelli, L. et al. 2003. Requirement of hippocampal neurogenesis for the behavioral effects of antidepressants. *Science* 301(5634), pp. 805-809. doi: 10.1126/science.1083328

Scharfman, H. et al. 2005. Increased neurogenesis and the ectopic granule cells after intrahippocampal BDNF infusion in adult rats. *Experimental Neurology* 192(2), pp. 348-356. doi: http://dx.doi.org/10.1016/j.expneurol.2004.11.016

Schiffmann, S. et al. 2012. Inhibitors of specific ceramide synthases. *Biochimie* 94(2), pp. 558-565. doi: 10.1016/j.biochi.2011.09.007

Schmittgen, T. D. and Livak, K. J. 2008. Analyzing real-time PCR data by the comparative C(T) method. *Nat Protoc* 3, doi: 10.1038/nprot.2008.73

Schrader, C. et al. 2012. PCR inhibitors – occurrence, properties and removal. *Journal of Applied Microbiology* 113(5), pp. 1014-1026. doi: 10.1111/j.1365-2672.2012.05384.x

Schrenk-Siemens, K. et al. 2008. Embryonic stem cell-derived neurons as a cellular system to study gene function: lack of amyloid precursor proteins APP and APLP2 leads to defective synaptic transmission. *Stem Cells* 26(8), pp. 2153-2163. doi: 10.1634/stemcells.2008-0010

Schwab, S. R. et al. 2005. Lymphocyte sequestration through S1P lyase inhibition and disruption of S1P gradients. *Science* 309(5741), pp. 1735-1739. doi: 10.1126/science.1113640

Sensken, S. C. et al. 2008. Selective activation of G alpha i mediated signalling of S1P3 by FTY720-phosphate. *Cell Signal* 20(6), pp. 1125-1133. doi: 10.1016/j.cellsig.2008.01.019

Serra-Millas, M. 2016. Are the changes in the peripheral brain-derived neurotrophic factor levels due to platelet activation? *World J Psychiatry* 6(1), pp. 84-101. doi: 10.5498/wjp.v6.i1.84

Shepherd, R. K. et al. 2005. Chronic depolarization enhances the trophic effects of BDNF in rescuing auditory neurons following a sensorineural hearing loss. *J Comp Neurol* 486(2), pp. 145-158. doi: 10.1002/cne.20564

Shiow, L. R. et al. 2006. CD69 acts downstream of interferon-alpha/beta to inhibit S1P1 and lymphocyte egress from lymphoid organs. *Nature* 440(7083), pp. 540-544. doi: 10.1038/nature04606

Siehler, S. et al. 2001. Sphingosine 1-phosphate activates nuclear factor-kappa B through Edg receptors. Activation through Edg-3 and Edg-5, but not Edg-1, in human embryonic kidney 293 cells. *J Biol Chem* 276(52), pp. 48733-48739. doi: 10.1074/jbc.M011072200

Silva, V. R. R. et al. 2017. Hypothalamic S1P/S1PR1 axis controls energy homeostasis in Middle-Aged Rodents: the reversal effects of physical exercise.*Aging (Albany NY)*. Vol. 9. pp. 142-154.

Simpson, E. M. et al. 1997. Genetic variation among 129 substrains and its importance for targeted mutagenesis in mice. *Nat Genet* 16(1), pp. 19-27. doi: 10.1038/ng0597-19

Solter, D. and Knowles, B. B. 1975. Immunosurgery of mouse blastocyst. *Proc Natl Acad Sci U S A* 72(12), pp. 5099-5102.

Sorensen, S. D. et al. 2003. Common signaling pathways link activation of murine PAR-1, LPA, and S1P receptors to proliferation of astrocytes. *Mol Pharmacol* 64, doi: 10.1124/mol.64.5.1199

Spiegel, S. 2000. Sphingosine 1-phosphate: a ligand for the EDG-1 family of G-protein-coupled receptors. *Ann N Y Acad Sci* 905, pp. 54-60.

Stevens, L. C. 1973. A new inbred subline of mice (129-terSv) with a high incidence of spontaneous congenital testicular teratomas. *J Natl Cancer Inst* 50(1), pp. 235-242.

Strand, A. D. et al. 2007. Expression profiling of Huntington's disease models suggests that brain-derived neurotrophic factor depletion plays a major role in striatal degeneration. *J Neurosci* 27(43), pp. 11758-11768. doi: 10.1523/jneurosci.2461-07.2007

Suen, P. C. et al. 1997. Brain-derived neurotrophic factor rapidly enhances phosphorylation of the postsynaptic N-methyl-D-aspartate receptor subunit 1. *Proc Natl Acad Sci U S A* 94(15), pp. 8191-8195.

Sugimoto, N. et al. 2003. Inhibitory and stimulatory regulation of Rac and cell motility by the G12/13-Rho and Gi pathways integrated downstream of a single G protein-coupled sphingosine-1-phosphate receptor isoform. *Mol Cell Biol* 23(5), pp. 1534-1545.

Sulzer, D. et al. 2017. T cells from patients with Parkinson's disease recognize alpha-synuclein peptides. *Nature* 546(7660), pp. 656-661. doi: 10.1038/nature22815

Sun, Y. et al. 2016. The sphingosine-1-phosphate analogue, FTY-720, promotes the proliferation of embryonic neural stem cells, enhances hippocampal neurogenesis and learning and memory abilities in adult mice. *Br J Pharmacol* 173(18), pp. 2793-2807. doi: 10.1111/bph.13557

Sung, G. H. et al. 2007. Phylogenetic classification of Cordyceps and the clavicipitaceous fungi. *Studies in Mycology* 57, pp. 5-59. doi: 10.3114/sim.2007.57.01

Swift, J. L. et al. 2011. Quantification of receptor tyrosine kinase transactivation through direct dimerization and surface density measurements in single cells. *Proc Natl Acad Sci U S A* 108(17), pp. 7016-7021. doi: 10.1073/pnas.1018280108

Sykes, D. A. et al. 2014. Investigating the molecular mechanisms through which FTY720-P causes persistent S1P receptor internalisation. *Br J Pharmacol*, doi: 10.1111/bph.12620

Szuhany, K. L. et al. 2015. A meta-analytic review of the effects of exercise on brain-derived neurotrophic factor. *J Psychiatr Res* 60, pp. 56-64. doi: 10.1016/j.jpsychires.2014.10.003

Takasugi, N. et al. 2013. FTY720/fingolimod, a sphingosine analogue, reduces amyloid-beta production in neurons. *PLoS One* 8, doi: 10.1371/journal.pone.0064050

Takuwa, Y. et al. 2002. The Edg family G protein-coupled receptors for lysophospholipids: their signaling properties and biological activities. *J Biochem* 131(6), pp. 767-771.

Tamm, C. et al. 2013. A Comparative Study of Protocols for Mouse Embryonic Stem Cell Culturing. *PLOS ONE* 8(12), p. e81156. doi: 10.1371/journal.pone.0081156

Tani, M. et al. 2005. Mechanisms of sphingosine and sphingosine 1-phosphate generation in human platelets. *J Lipid Res* 46(11), pp. 2458-2467. doi: 10.1194/jlr.M500268-JLR200

Tao, R. et al. 2009. Cardiomyocyte S1P(1) Receptor–mediated Extracellular Signal–related Kinase Signaling and Desensitization. *J Cardiovasc Pharmacol* 53(6), pp. 486-494. doi: 10.1097/FJC.0b013e3181a7b58a

Taylor, A. et al. 2012. Motoneuron Programmed Cell Death in Response to proBDNF. *Dev Neurobiol* 72(5), pp. 699-712. doi: 10.1002/dneu.20964

Thoenen, H. 1991. The changing scene of neurotrophic factors. *Trends in Neurosciences* 14(5), pp. 165-170. doi: 10.1016/0166-2236(91)90097-E

Todd, A. J. et al. 2003. The expression of vesicular glutamate transporters VGLUT1 and VGLUT2 in neurochemically defined axonal populations in the rat spinal cord with emphasis on the dorsal horn. *Eur J Neurosci* 17(1), pp. 13-27.

Tucker, K. and Fadool, D. 2002. Neurotrophin modulation of voltage-gated potassium channels in rat through TrkB receptors is time and sensory experience dependent. *J Physiol* 542(Pt 2), pp. 413-429. doi: 10.1113/jphysiol.2002.017376

Tuon, T. et al. 2014. Physical training prevents depressive symptoms and a decrease in brain-derived neurotrophic factor in Parkinson's disease. *Brain Res Bull* 108, pp. 106-112. doi: 10.1016/j.brainresbull.2014.09.006

UniProtConsortium. 2014. UniProt: a hub for protein information. *Nucleic Acids Research* 43(D1), pp. D204-D212. doi: 10.1093/nar/gku989

Van Brocklyn, J. R. et al. 2000. Sphingosine-1-phosphate is a ligand for the G protein-coupled receptor EDG-6. *Blood* 95(8), pp. 2624-2629.

van Doorn, R. et al. 2012. Sphingosine 1-phosphate receptor 5 mediates the immune quiescence of the human brain endothelial barrier. *J Neuroinflammation* 9, p. 133. doi: 10.1186/1742-2094-9-133

Van Doorn, R. et al. 2010. Sphingosine 1-phosphate receptor 1 and 3 are upregulated in multiple sclerosis lesions. *Glia* 58(12), pp. 1465-1476. doi: 10.1002/glia.21021

van Echten-Deckert, G. and Walter, J. 2012. Sphingolipids: critical players in Alzheimer's disease. *Prog Lipid Res* 51(4), pp. 378-393. doi: 10.1016/j.plipres.2012.07.001

van Praag, H. et al. 1999. Running enhances neurogenesis, learning, and long-term potentiation in mice.*Proc Natl Acad Sci U S A*. Vol. 96. pp. 13427-13431.

Vargas, W. S. and Perumal, J. S. 2013. Fingolimod and cardiac risk: latest findings and clinical implications.*Ther Adv Drug Saf*. Vol. 4. Sage UK: London, England, pp. 119-124.

Ventimiglia, R. et al. 1995. The neurotrophins BDNF, NT-3 and NT-4/5 promote survival and morphological and biochemical differentiation of striatal neurons in vitro. *Eur J Neurosci* 7(2), pp. 213-222.

Vidal-Martinez, G. et al. 2016. FTY720/Fingolimod Reduces Synucleinopathy and Improves Gut Motility in A53T Mice: CONTRIBUTIONS OF PRO-BRAIN-DERIVED NEUROTROPHIC FACTOR (PRO-BDNF) AND MATURE BDNF. *J Biol Chem* 291(39), pp. 20811-20821. doi: 10.1074/jbc.M116.744029

Wahlsten, D. et al. 2006. Stability of inbred mouse strain differences in behavior and brain size between laboratories and across decades. *Proceedings of the National Academy of Sciences* 103(44), pp. 16364-16369. doi: 10.1073/pnas.0605342103

Wang, L. and Dudek, S. M. 2009. Regulation of vascular permeability by sphingosine 1-phosphate. *Microvasc Res* 77(1), pp. 39-45. doi: 10.1016/j.mvr.2008.09.005

Wang, W. et al. 2005. Type 4 sphingosine 1-phosphate G protein-coupled receptor (S1P4) transduces S1P effects on T cell proliferation and cytokine secretion without signaling migration. *Faseb j* 19(12), pp. 1731-1733. doi: 10.1096/fj.05-3730fje

Weissmiller, A. M. and Wu, C. 2012. Current advances in using neurotrophic factors to treat neurodegenerative disorders. *Transl Neurodegener* 1(1), p. 14. doi: 10.1186/2047-9158-1-14

Werry, T. D. et al. 2003. Mechanisms of cross-talk between G-protein-coupled receptors resulting in enhanced release of intracellular Ca2+. *Biochem J* 374(Pt 2), pp. 281-296. doi: 10.1042/bj20030312

West, A. E. et al. 2001. Calcium regulation of neuronal gene expression. *Proc Natl Acad Sci U S A* 98(20), pp. 11024-11031. doi: 10.1073/pnas.191352298

West, A. E. et al. 2002. Regulation of transcription factors by neuronal activity. *Nat Rev Neurosci* 3(12), pp. 921-931. doi: 10.1038/nrn987

West, A. E. et al. 2014. Neurotrophins: transcription and translation. *Handb Exp Pharmacol* 220, pp. 67-100. doi: 10.1007/978-3-642-45106-5_4

Wetsel, W. C. et al. 2013. Disruption of the expression of the proprotein convertase PC7 reduces BDNF production and affects learning and memory in mice. *Proc Natl Acad Sci U S A* 110(43), pp. 17362-17367. doi: 10.1073/pnas.1314698110

Wyss-Coray, T. 2016. Ageing, neurodegeneration and brain rejuvenation. *Nature* 539(7628), pp. 180-186. doi: 10.1038/nature20411

Xie, J. et al. 2013. Autocrine signaling based selection of combinatorial antibodies that transdifferentiate human stem cells. *Proc Natl Acad Sci U S A* 110(20), pp. 8099-8104. doi: 10.1073/pnas.1306263110

Xu, B. et al. 2000. The role of brain-derived neurotrophic factor receptors in the mature hippocampus: modulation of long-term potentiation through a presynaptic mechanism involving TrkB. *J Neurosci* 20(18), pp. 6888-6897.

Yamaguchi, F. et al. 1996. Molecular Cloning of the Novel Human G Protein-Coupled Receptor (GPCR) Gene Mapped on Chromosome 9. *Biochemical and Biophysical Research Communications* 227(2), pp. 608-614. doi: http://dx.doi.org/10.1006/bbrc.1996.1553

Yamamoto, H. and Gurney, M. E. 1990. Human platelets contain brain-derived neurotrophic factor. *J Neurosci* 10(11), pp. 3469-3478.

Yanagida, K. and Hla, T. 2016. Vascular and Immunobiology of the Circulatory Sphingosine 1-Phosphate Gradient. *Annu Rev Physiol*, doi: 10.1146/annurev-physiol-021014-071635

Yang, J. et al. 2009. Neuronal release of proBDNF. *Nat Neurosci* 12(2), pp. 113-115. doi: 10.1038/nn.2244

Yatomi, Y. et al. 1996. N,N-dimethylsphingosine inhibition of sphingosine kinase and sphingosine 1-phosphate activity in human platelets. *Biochemistry* 35(2), pp. 626-633. doi: 10.1021/bi9515533

Yazdani, M. et al. 2012. Disease modeling using embryonic stem cells: MeCP2 regulates nuclear size and RNA synthesis in neurons. *Stem Cells* 30(10), pp. 2128-2139. doi: 10.1002/stem.1180

Ye, Y. et al. 2016. Activation of Sphingosine 1-Phosphate Receptor 1 Enhances Hippocampus Neurogenesis in a Rat Model of Traumatic Brain Injury: An Involvement of MEK/Erk Signaling Pathway. *Neural Plasticity* 2016, p. 13. doi: 10.1155/2016/8072156

Ying, Q. L. et al. 2008. The ground state of embryonic stem cell self-renewal. *Nature* 453(7194), pp. 519-523. doi: 10.1038/nature06968

Young, P. et al. 2008. Single-neuron labeling with inducible Cre-mediated knockout in transgenic mice. *Nat Neurosci* 11(6), pp. 721-728. doi: 10.1038/nn.2118

Yuan, J. and Yankner, B. A. 2000. Apoptosis in the nervous system. *Nature* 407(6805), pp. 802-809. doi: 10.1038/35037739

Zafra, F. et al. 1990. Activity dependent regulation of BDNF and NGF mRNAs in the rat hippocampus is mediated by non-NMDA glutamate receptors. *Embo j* 9(11), pp. 3545-3550.

Zemann, B. et al. 2006. Sphingosine kinase type 2 is essential for lymphopenia induced by the immunomodulatory drug FTY720. *Blood* 107(4), pp. 1454-1458. doi: 10.1182/blood-2005-07-2628

Zhang, G. et al. 1999. Comparative analysis of three murine G-protein coupled receptors activated by sphingosine-1-phosphate. *Gene* 227(1), pp. 89-99.

Zhang, J. et al. 2007. Signals from Type 1 Sphingosine 1-Phosphate Receptors Enhance Adult Mouse Cardiac Myocyte Survival During Hypoxia. *American Journal of Physiology - Heart and Circulatory Physiology*, doi: 10.1152/ajpheart.00587.2006

Zhang, L. et al. 2012. A novel role of sphingosine 1-phosphate receptor S1pr1 in mouse thrombopoiesis. *J Exp Med* 209(12), pp. 2165-2181. doi: 10.1084/jem.20121090

Zhang, L. et al. 2015. FTY720 induces autophagy-related apoptosis and necroptosis in human glioblastoma cells. *Toxicol Lett* 236(1), pp. 43-59. doi: 10.1016/j.toxlet.2015.04.015

Zhang, Y. et al. 1996. Inducible site-directed recombination in mouse embryonic stem cells. *Nucleic Acids Res* 24(4), pp. 543-548.

Zhang, Y. H. et al. 2006. Intracellular sphingosine 1-phosphate mediates the increased excitability produced by nerve growth factor in rat sensory neurons. *J Physiol* 575(Pt 1), pp. 101-113. doi: 10.1113/jphysiol.2006.111575

Zheng, F. et al. 2011. Regulation of brain-derived neurotrophic factor exon IV transcription through calcium responsive elements in cortical neurons. *PLoS One* 6(12), p. e28441. doi: 10.1371/journal.pone.0028441

Zheng, F. et al. 2012. Regulation of brain-derived neurotrophic factor expression in neurons. *Int J Physiol Pathophysiol Pharmacol* 4(4), pp. 188-200.

Zhu, Y. et al. 2001. Ablation of NF1 function in neurons induces abnormal development of cerebral cortex and reactive gliosis in the brain. *Genes Dev* 15(7), pp. 859-876. doi: 10.1101/gad.862101

Zondag, G. C. et al. 1998. Sphingosine 1-phosphate signalling through the G-protein-coupled receptor Edg-1. *Biochem J* 330 (Pt 2), pp. 605-609.

Zuccato, C. and Cattaneo, E. 2007. Role of brain-derived neurotrophic factor in Huntington's disease. *Prog Neurobiol* 81(5-6), pp. 294-330. doi: 10.1016/j.pneurobio.2007.01.003

Zuccato, C. et al. 2001. Loss of huntingtin-mediated BDNF gene transcription in Huntington's disease. *Science* 293(5529), pp. 493-498. doi: 10.1126/science.1059581

Appendix

Analysing the potency of 4-OHT

The potency of 4-OHT was tested on *Rosa26/Cre^ERT2* x *HA-TrkA-127* ES cells (Figure A.1A). The time course experiment revealed that 0.8 μM 4-OHT is most potent between 8 h and 20 h and therefore subsequent experiments were performed overnight. These results demonstrated that 0.05 μM 4-OHT treatment activated Cre^ERT2 in the *Rosa26/Cre^ERT2* x *HA-TrkA-127* ES cells, which led to the successful excision of the stop cassette and the subsequent expression of HA-TrkA as demonstrated by Western blot (Figure A.1B).
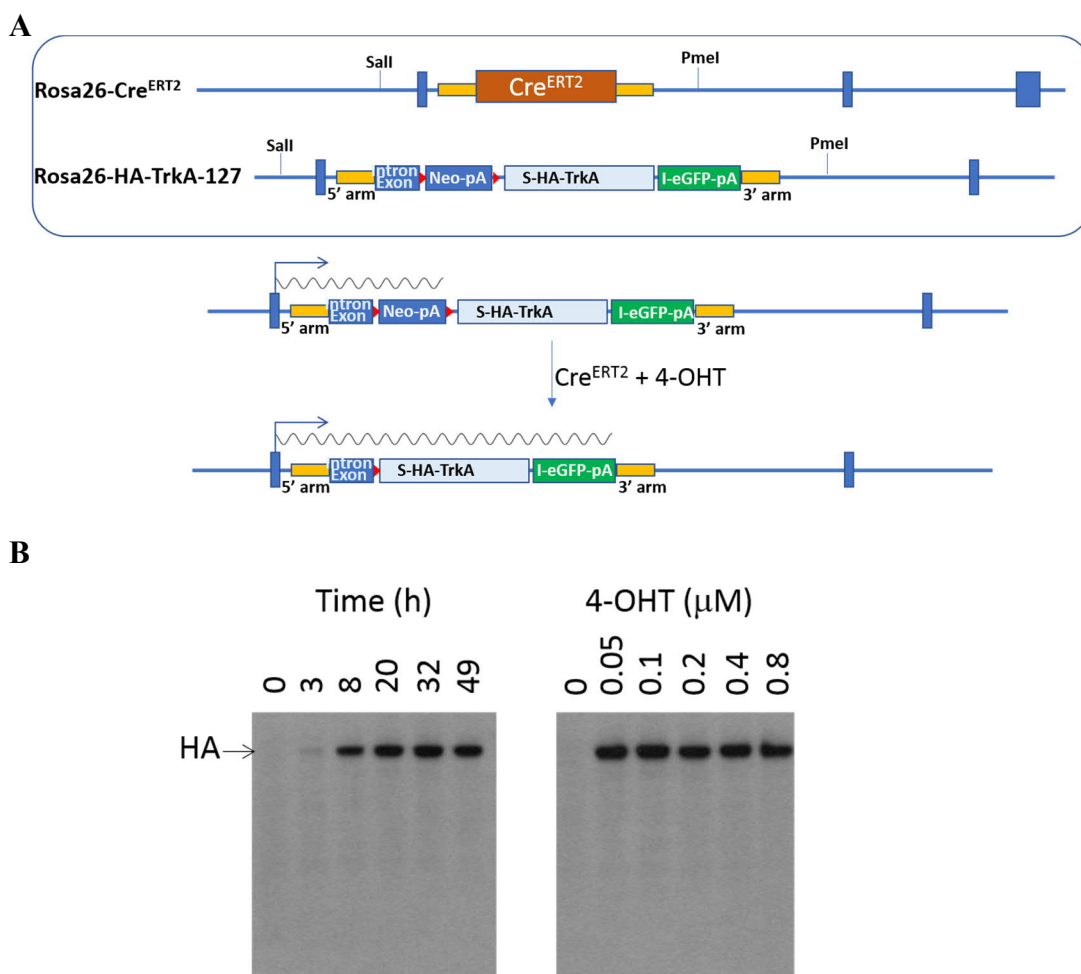
Figure A.1 4-OHT induced Cre^{ERT2} mediated recombination in mouse ES cells

A ES cells carrying a Cre^{ERT2} transgene in one allele of the Rosa26 locus and an HA-TrA-127 transgene with a stop-cassette (Neo-pA) flanked by two lox P site (red arrows) at its 5' end on the other Rosa26 allele were used to test the potency of 4-OHT. Map kindly provided by Dr. Xinsheng Nan. **B** Western blot represents HA-TrkA recognised by an antibody against the HA tag. 40 µg cell lysate was loaded per lane. ES cells were treated with 0.8 µM of 4-OHT for 3 to 49 h. Dose response experiment was performed overnight with 0.05 – 0.8 µM 4-OHT. The successful excision of the stop cassette was demonstrated by the expression of HA-TrkA on Western blot. These results were performed and analysed by Dr. Xinsheng Nan.

Effects of pFTY720 on BDNF levels in primary mouse cortical neurons

pFTY720 has recently been shown to induce increased BDNF protein expression in primary mouse cortical neurons (Deogracias et al. 2012). In the current study, these experiments were repeated to serve as a positive control for short-term experiments with pFTY720 on ES cell-derived neurons. First, primary mouse cortical neurons 8 DIV were exposed to different concentrations of pFTY720 for 24 h, followed by a time course experiment with pFTY720 10 nM. Both experiments revealed no significant effect by pFTY720 on BDNF protein levels (Figure A.2B and D). However, the lack of increase could be due to immaturity of the neurons, as a previous report has shown that primary mouse cortical neurons reach their maturity between 10 and 20 DIV (Lesuisse and Martin 2002). Also, characterisation experiments by Deogracias et al. 2012 were done in 2 weeks old neurons. This led to the repetition of dose response and time course experiments in primary cortical neurons 12 DIV. Nevertheless, in both experiments no significant increase of BDNF protein levels was observed after pFTY720 exposure (Figure A.3B and D).
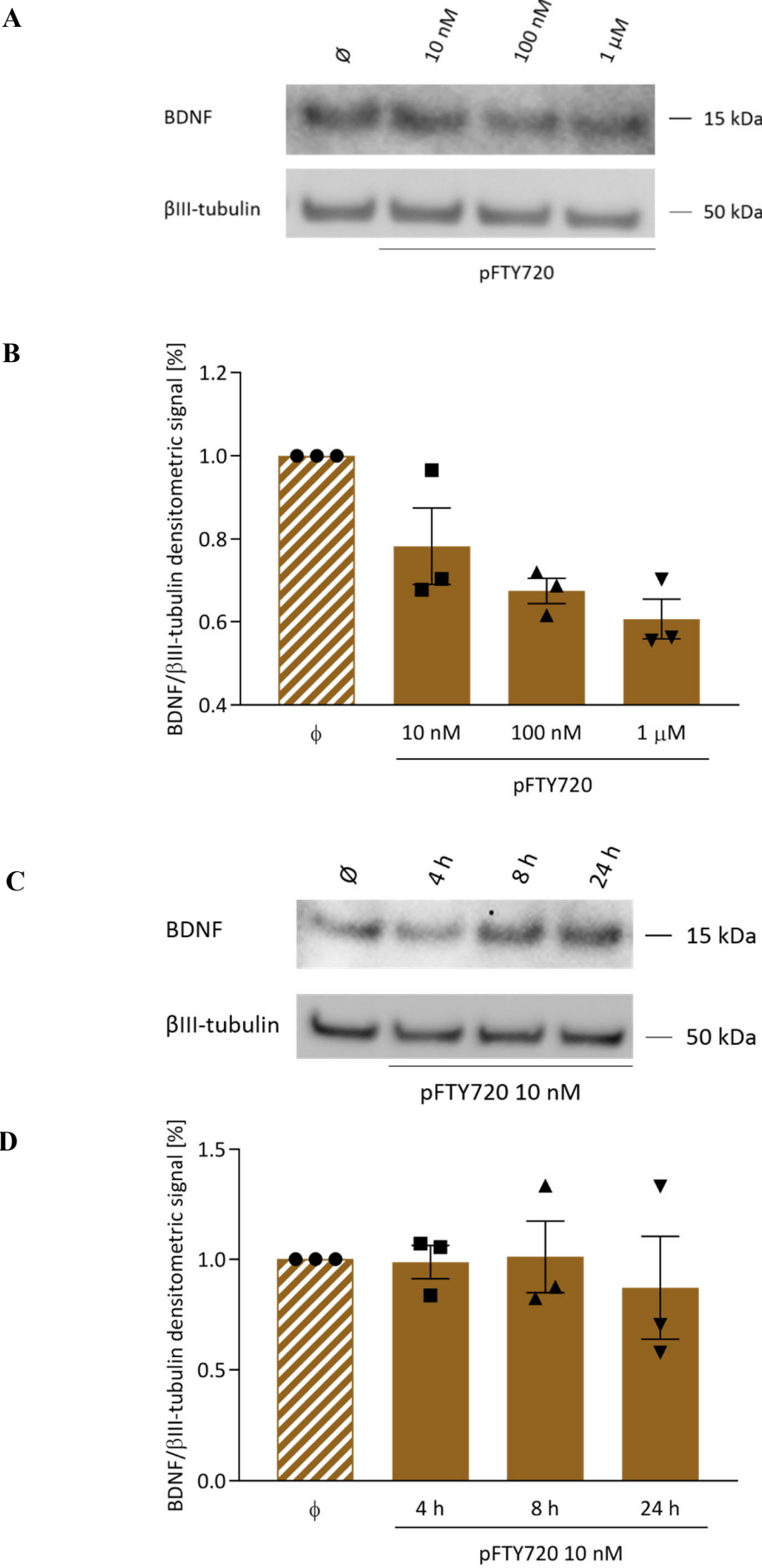
A

B

C

D
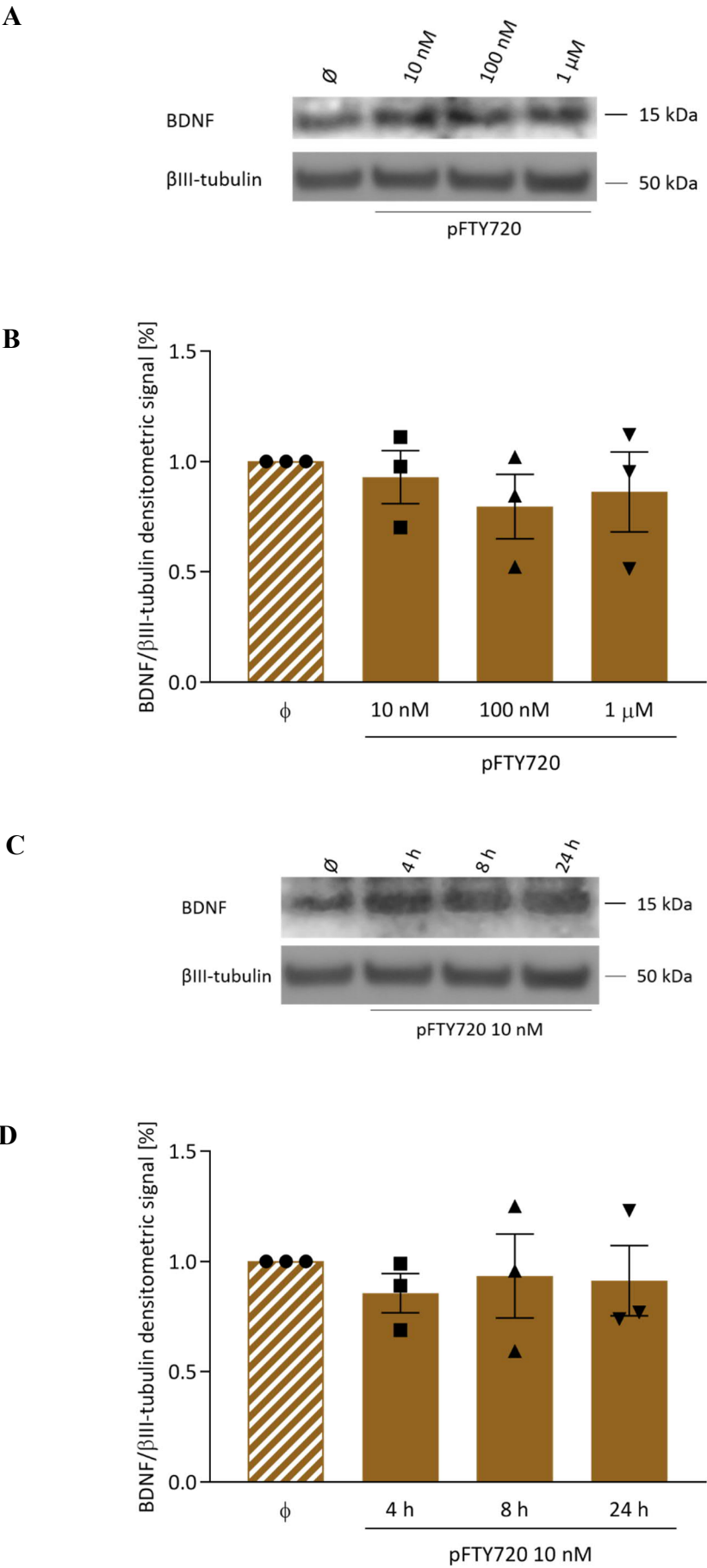
Figure A.2 Short-term effects of pFTY720 on primary cortical neurons 8 DIV

**Figure A.2 Short-term effects of pFTY720 on primary cortical neurons 8 DIV**

A 8 DIV old primary mouse cortical neurons were treated with different concentrations of pFTY720 for 24 h. Western blot represents BDNF expression of primary cortical neurons after short-term exposure to pFTY720 10 nM, 100 nM and 1 µM. 20 µl of neuronal lysate was loaded per lane. **B** pFTY720 did not increase BDNF protein levels at any concentration in primary cortical neurons significantly compared to controls (Kruskal-Wallis test, $p > 0.05$, n = 3). **C** A time course experiment with primary cortical neurons 8 DIV was performed. Neurons were treated with pFTY720 10 nM for 4 h, 8 h or 24 h and BDNF levels were analysed using Western blot. **D** BDNF levels were not increased by pFTY720 10 nM at any time point compared to controls. Data are represented as mean ± SEM relative to internal control βIII-tubulin. Changes are in percentage vs. control. Ø: vehicle (DMSO) treated cells.

A

B

C

D

Figure A.3 Short-term effects of pFTY720 on primary cortical neurons 12 DIV

Figure A.3 Short-term effects of pFTY720 on primary cortical neurons 12 DIV

A 12 DIV old primary mouse cortical neurons were treated with different concentrations of pFTY720 for 24 h. Western blot represents BDNF expression of primary cortical neurons after short-term exposure to pFTY720 10 nM, 100 nM and 1 μM. 20 μl of neuronal lysate was loaded per lane. **B** pFTY720 did not change BDNF protein levels significantly at any concentration in primary cortical neurons (Kruskal-Wallis test, $p > 0.05$, n = 3). **C** Neurons were treated with pFTY720 10 nM for 4 h, 8 h or 24 h and BDNF levels were analysed using Western blot. **D** BDNF levels were not increased by pFTY720 10 nM at any time point compared to vehicle-treated controls. Data are represented as mean ± SEM relative to internal control βIII-tubulin. Changes are in percentage vs. control. Ø: vehicle (DMSO) treated cells.

Exploring possible causes of biochemical endpoint variability in ES cell-derived neurons

As the biochemical parameters investigated all show significant variability attempts were made to test whether some could be the results of the tissue culture conditions used, including in particular medium exchange as the system requires a complete medium exchange on day 2, 4, 8 and 12 of neuronal culture (see Materials and Methods). To this end, 14 DIV cultured J1 neurons were subjected to a complete medium exchange and BDNF protein levels analysed at different time points. As shown in Figure A.4, BDNF protein levels did not change significantly 8 h after a complete medium exchange. At 16 h however, a trend towards an increase can be observed (Figure A.4). In view of these results, *Bdnf* mRNA levels were also analysed under the assumption that while medium exchange may not be sufficient to stimulate the translational machinery, it may be sufficient to activate the MAPK pathway activation and the transcription of the *Bdnf* gene. However, this turned out not to be the case (Figure A.5).

As a potentially sensitive indicator of the metabolic state of cultured neurons, the levels of Arc were also investigated. Unlike BDNF, which is stored in large dense core vesicles until its release from neurons, Arc is known to rapidly turn over, not only at the level of its mRNA, but also as a protein that is rapidly degraded after its biosynthesis. For this reason, Arc is attracting considerable attention in studies related to the biochemistry of synaptic plasticity (Rao et al. 2006; Bramham et al. 2008) . When 14 DIV J1 neurons were lysed 2 h after the medium exchange reference, Arc protein levels were significantly increased (Figure A.6).

A

B
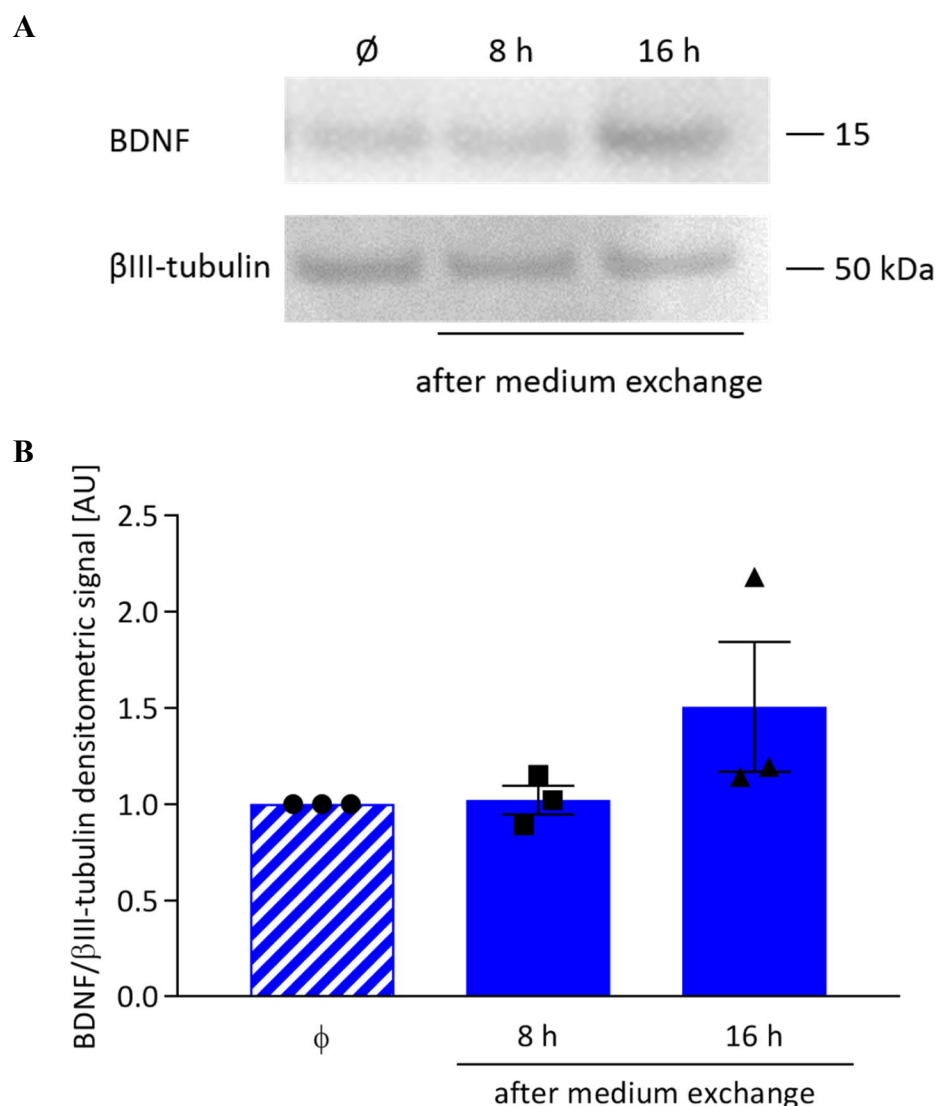
Figure A.4 Effects of medium exchange on BDNF protein levels in J1 neurons 14 DIV

A complete medium exchange was performed and neurons were lysed after either 8 or 16 h. A 20 µl of neuronal lysate were loaded per lane. B Densitometric analysis did not reveal a significant BDNF increase (Kruskal-Wallis test, $p > 0.05$, $n = 3$). Data are represented as mean $\pm$ SEM relative to internal control βIII-tubulin. Ø stands for cells where no medium exchange was performed.
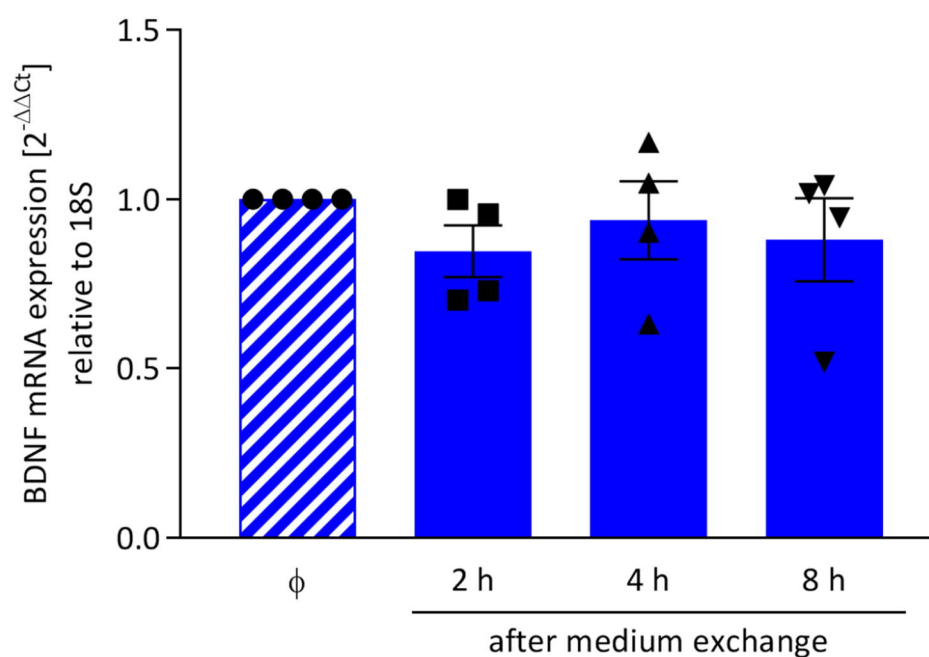
Figure A.5 Effects of medium exchange on *Bdnf* mRNA levels in J1 neurons 14 DIV

A complete medium exchange was performed and neurons were lysed after either 2, 4 or 8 h.

BDNF mRNA levels did not change significantly after medium exchange (Kruskal-Wallis

test, $p > 0.05$, n = 4 individual experiments). Data are represented as mean ± SEM relative to

A

B
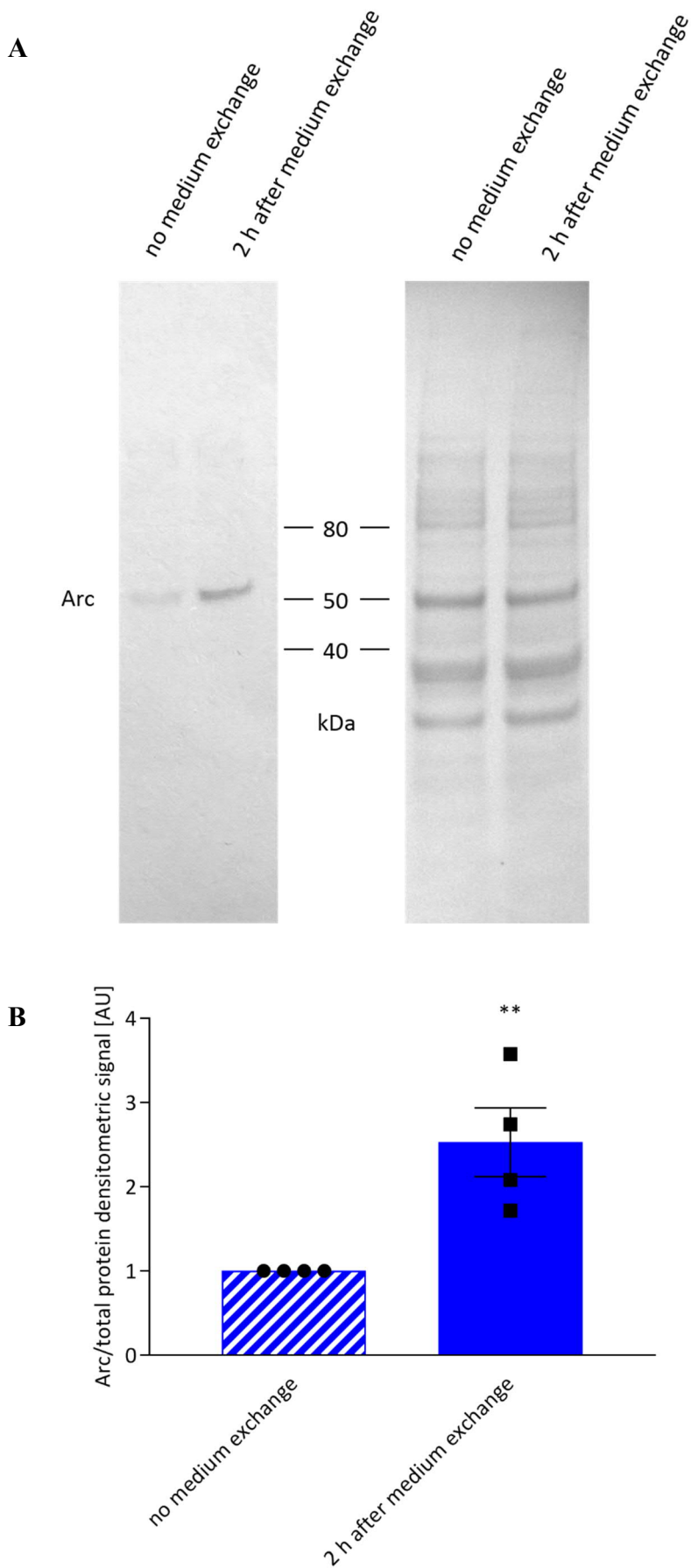
Figure A.6 Effects of medium exchange on Arc protein expression in J1 neurons

Figure A.6 Effects of medium exchange on Arc protein expression in J1 neurons

Arc protein levels were analysed in J1 neurons 14 DIV 2 h after a complete medium exchange. **A** Representative western blot of Arc in J1 neurons before and after medium exchange. Pierce staining for densitometric analysis of total protein is shown on the right. **B** Graph represents densitometric analysis. Arc levels increased significantly (Unpaired t-test, **p (no medium exchange vs. medium exchange) < 0.01, n = 4). Data are represented as medium ± SEM.

Effects of pFTY720 on Arc protein levels in ES cell-derived neurons

Arc levels were also investigated following exposure to pFTY720. Fourteen day-old J1 ES cell-derived neurons were treated with different concentrations of pFTY720 for 7 h and Arc protein levels analysed by Western blot (Figure A.7). These experiments failed to reveal any consistent increase of Arc levels following pFTY720 treatment. A time-course experiment performed with 10 nM did indicate a transient, but not significant increase of Arc levels 2 h after treatment (Figure A.8).

A

B
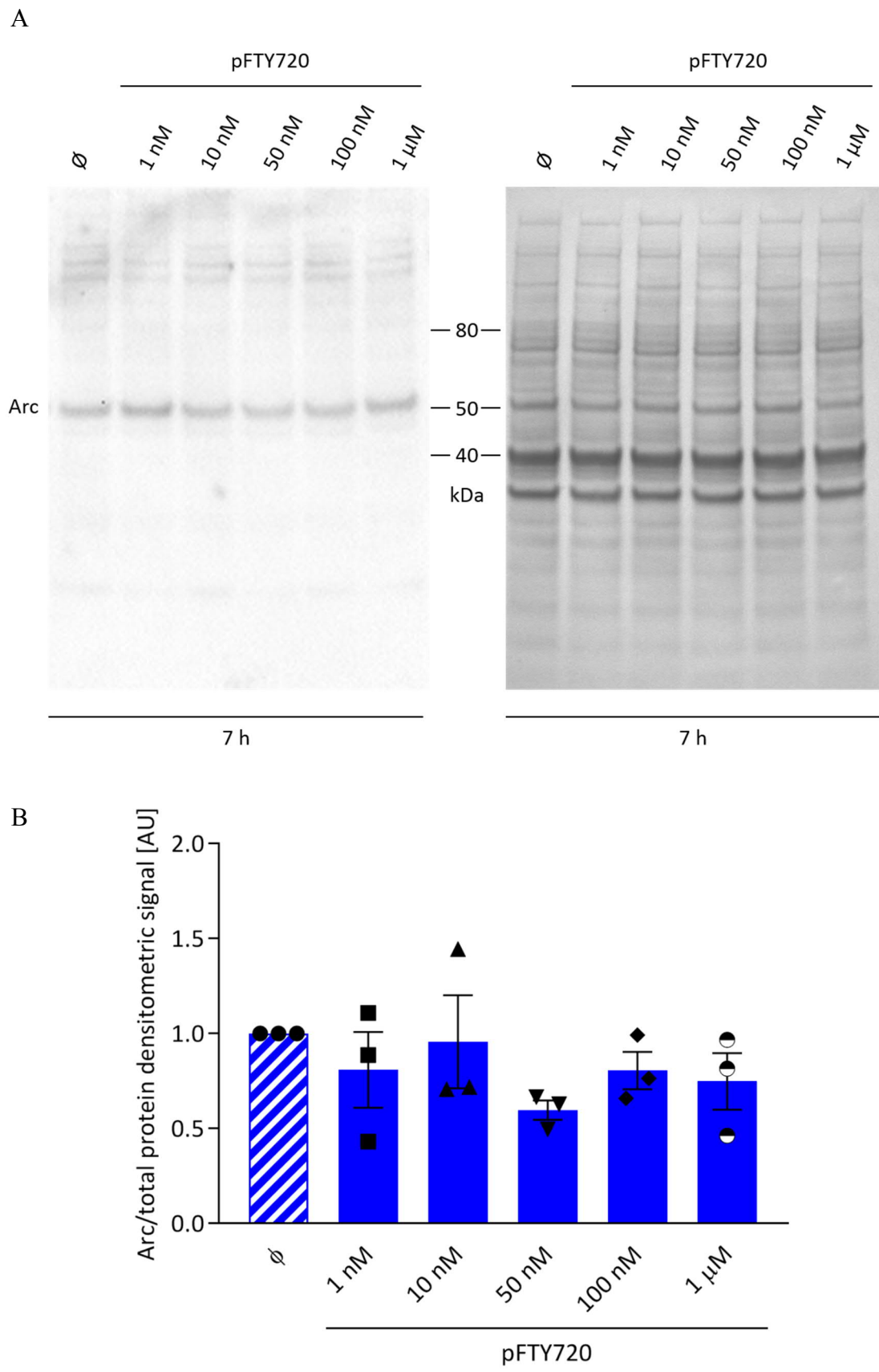
Figure A.7 Dose response experiment – Effects of pFTY720 on Arc expression

Figure A.7 Dose response experiment - Effects of pFTY720 on Arc expression

14 DIV J1 neurons were exposed to different concentrations of pFTY720 10 nM for 7 h. **A** Western blot for Arc expression in J1 neurons. 30 μg of protein were loaded per lane. Pierce staining for densitometric analysis of total protein is shown on the right panel. **B** Graph shows densitometric analysis. Arc protein expression did not change after 7 h exposure to different concentrations of pFTY720 (Kruskal-Wallis test, n.s. $p > 0.05$, n = 3). Data are represented as mean ± SEM relative to total protein and normalised to the control. Ø stands for vehicle (DMSO) treated cells.

A

B
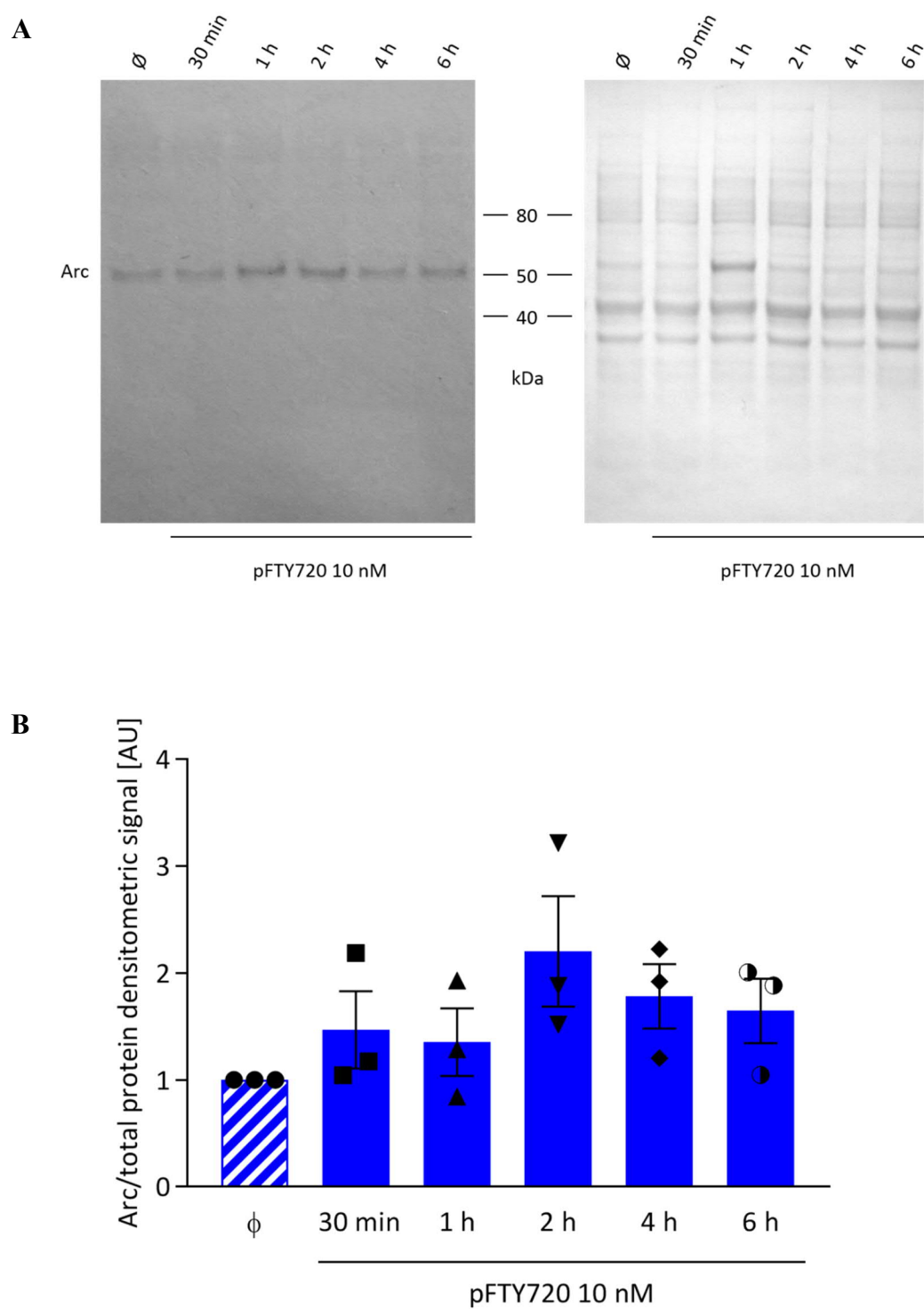
Figure A.8 Time course experiment - Effects of pFTY720 10 nM on Arc expression

Figure A.8 Time course experiment - Effects of pFTY720 10 nM on Arc expression

14 DIV J1 neurons were exposed to pFTY720 10 nM for the indicated time periods. **A** Western blot for Arc expression in J1 neurons. 30 μg of protein were loaded per lane. Pierce staining for densitometric analysis of total protein is shown on the right. **B** Graph shows densitometric analysis. Arc protein expression was not significantly increased at any time point (Mann-Whitney test, $p > 0.05$, $n = 3$). At 2 h a trend was observed (differences between medians = 0.882). Data are represented as mean ± SEM relative to total protein and normalised to the control. Ø stands for the vehicle DMSO.

Recording activity of neurons derived from ES cells

One possibility to explain the variability of the biochemical results, is the neuronal activity in the cultures. Indeed, neither the maturation of the neurons themselves nor the time-course of the development of synaptic contacts can be controlled. Yet, FTY720 has been shown to require ongoing neuronal activity to exert biochemical effects, including the regulation of BDNF levels (Deogracias et al. 2012). In addition, previous studies by others using the same *in vitro* differentiation system reported significant variability even between individual neurons in the same cultures by monitoring activity using intracellular recording (Barth et al., 2014). In an attempt to approach this question, ES cell-derived neurons were plated on MEA plates suitable for extracellular recordings allowing data on spike counts to be collected (see Materials and Methods). The difference between single wells was striking (Figure A.9). Neurons generated from J1 and B2 ES cells were examined at different time points and in five different wells. The results indicate that in every well, different spike counts were recorded even though the neurons originated from the very same progenitors (Figure A.9). These neurons were also treated with either DMSO or pFTY720 10 nM and spike counts determined after 60 min, with and without medium change (Figure A.10). While the medium exchange did increase spike counts in J1 neurons, this was not the case with B2 neurons. However, spike counts were very low in mutant neurons for reasons that remained unclear. Neither did the addition of DMSO or of pFTY720 10 nM alter the spike counts whereby the differences in spike counts between single wells remain remarkable (Figure A.10).

A

J1 neurons

B
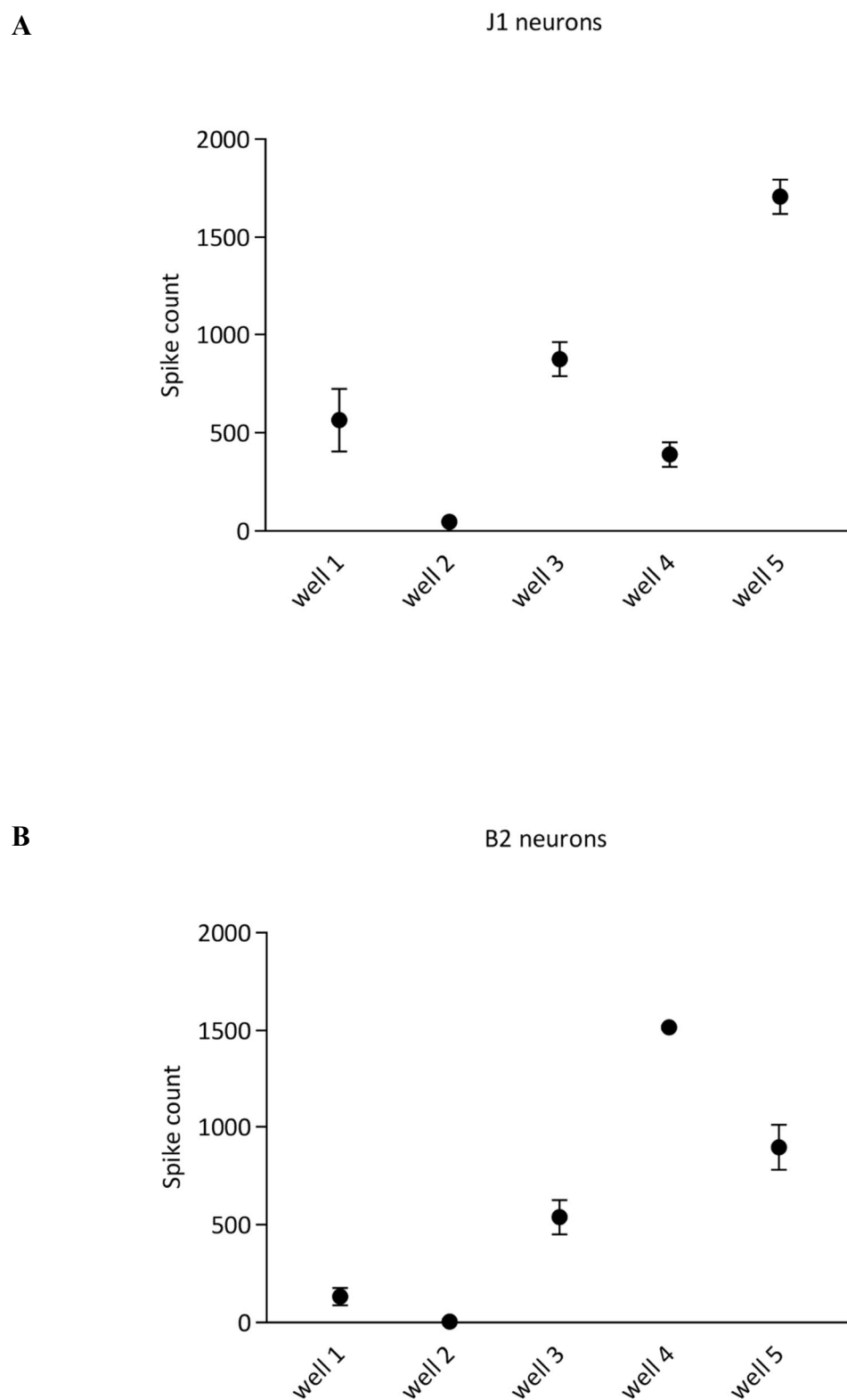
B2 neurons

Figure A.9 Spike count measurements in J1 and B2 neurons

Spike counts in J1 and B2 neurons 14 DIV were measured in five different wells

(n = 3 measurements of the same well). Spike counts vary between wells.

A

J1 neurons

B
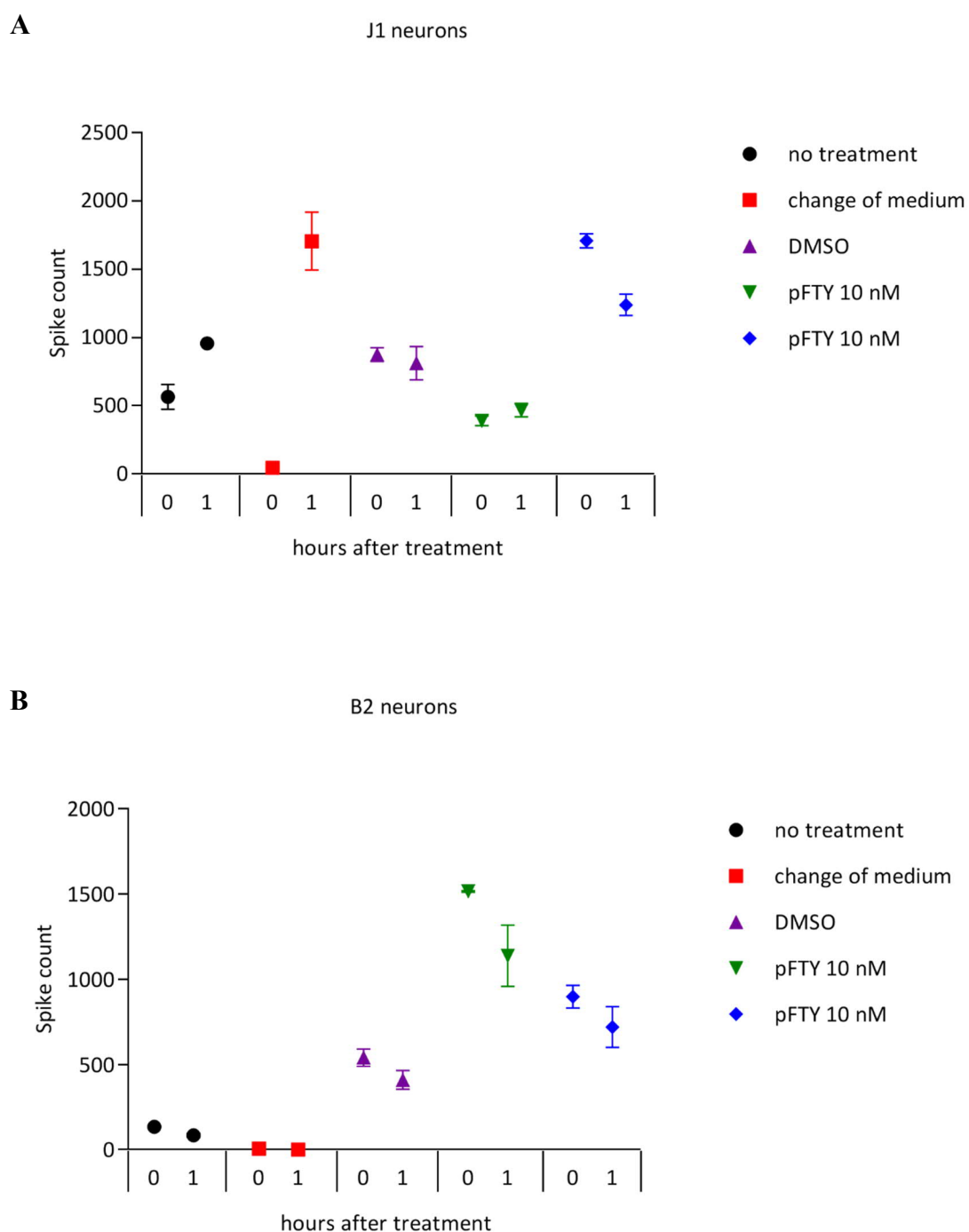
B2 neurons

Figure A.10 Spike Counts in J1 and B2 neurons after treatment

Neurons were exposed to the indicated treatment for 1 h before another measurement

of the spike counts was performed. In J1 neurons medium exchange increased the spike

count by 330 %. In J1 and B2 neurons treatment with pFTY720 10 nM did not result

in an increased spike count.

Vegfd mRNA levels were unaffected by pFTY720 treatment in ES cell-derived neurons

A recent *in vivo* study on FTY720 showed that mRNA of the vascular endothelial growth factor (*Vegfd*) is significantly increased in mice treated with the drug (Hait et al. 2014). The researchers showed that the increase is mediated through the inhibition of the class I histone deacetylases by pFTY720. This mode of action was shown to be independent of the S1P1R (Hait et al. 2014). As the generated mutant cell line B2 is the ideal tool to confirm this result both J1 and B2 neurons were treated with pFTY720 10 nM for different time periods and *Vegfd* mRNA levels were analysed using RT-PCR (Figure A.11).

In J1 and B2 neurons no significant increase of *Vegfd* mRNA levels was induced after treatment with 10 nM pFTY720 (Figure A.11).
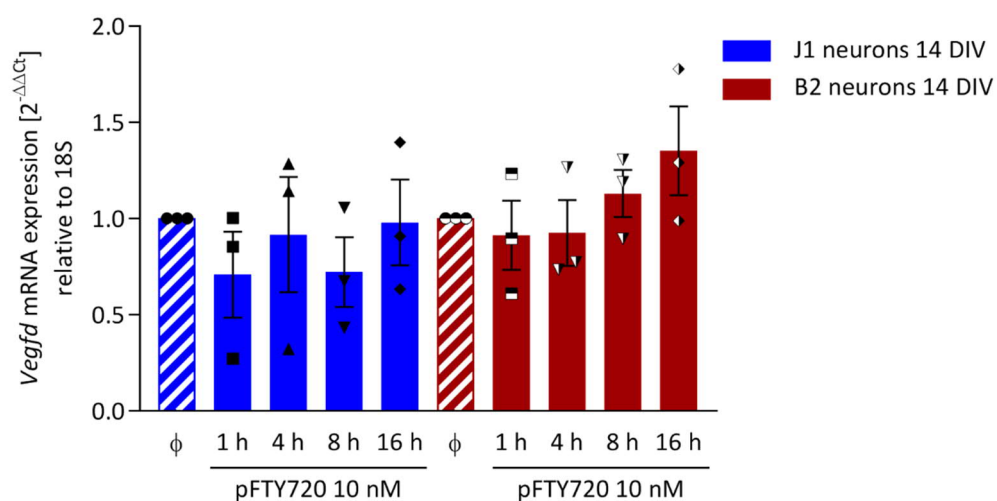
Figure A.11 *Vegfd* mRNA levels in J1 nor B2 neurons after pFTY720 treatment

14 DIV old neurons were treated with pFTY720 10 nM for 1 h, 4 h, 8 h and 16 h. No change

of *Vegfd* mRNA levels was observed after exposure to 10 nM pFTY720 (Kruskal-Wallis test,

$p > 0.05$, n = 3). Data are represented as mean ± SEM relative to internal control *18S rRNA*.

Ø: vehicle (DMSO) treated cells.

Exposure of J1 and B2 neurons to KCl

It is well established in the BDNF field that membrane depolarisation in neurons induces increased transcription of the *Bdnf* gene (Kokaia et al. 1993; Elliott et al. 1994) and thereby enhances neuronal survival (Ghosh et al. 1994; Shepherd et al. 2005). To understand if the ES cell-derived neurons used here behave similar, J1 neurons 21 DIV were exposed to 60 mM KCl for 24 h and BDNF protein levels were analysed by Western blot. However, no significant increase could be found (Figure A.12). In 14 days old B2 neurons the same experiment was conducted and a clear trend towards an increase was observed compared to NaCl-treated neurons (Mann-Whitney test, actual difference between medians = 10.27, Figure A.13). However, no firm conclusion can be drawn from this experiments as a higher number of repeats is needed. The lack of a significant increase suggests that BDNF protein levels could have been secreted during KCl treatment. Indeed, it has been shown before that a significant amount of BDNF is secreted after overnight treatment with 50 mM KCl in J1 ES cell-derived neurons (Oliveri 2014). This could be investigated by BDNF immunoprecipitation in the supernatant of the neuronal cultures. In line with this *Bdnf* mRNA levels should be measured in both cell lines upon depolarisation of the neurons with KCl (Zafra et al. 1990).
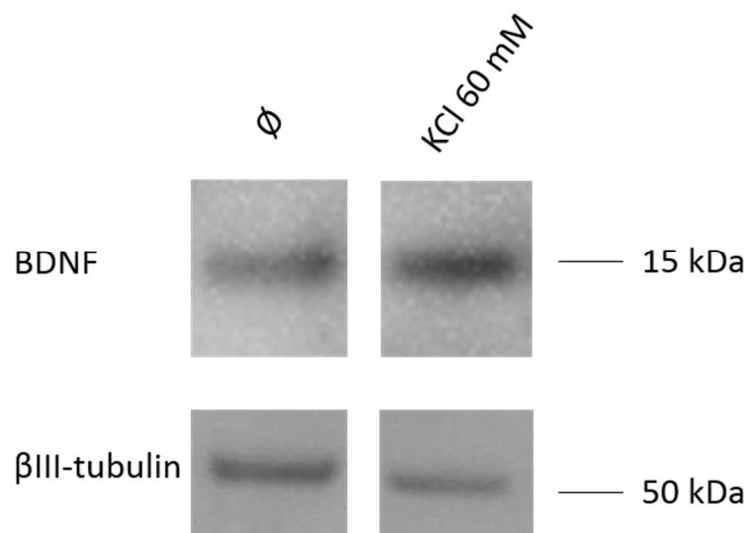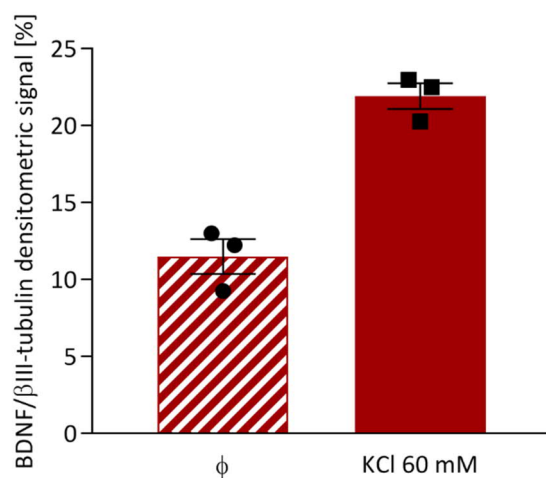
A
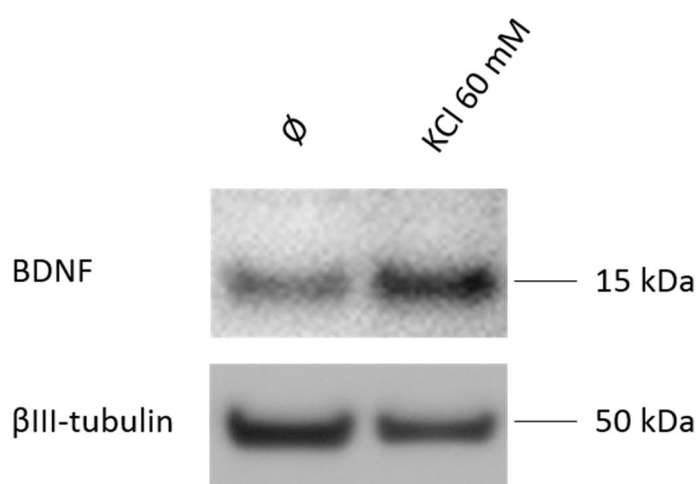
B
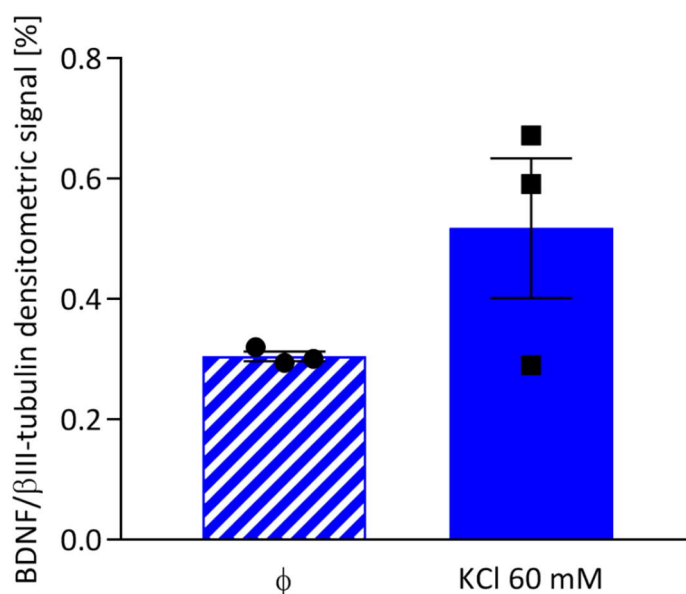
**Figure A.12 BDNF expression levels in J1 neurons after exposure to 60 mM KCl**

J1 neurons 21 DIV were exposed to 60 mM KCl for 24 h and BDNF levels were analysed.

A Western blot of BDNF. 20 μl of neuronal lysate was loaded per lane. **B** BDNF levels were

not significantly increased after 24 h exposure to 60 mM KCl (Mann-Whitney test, $p > 0.05$,

$n = 3$ independent wells). Data are presented as mean ± SEM relative to βIII-tubulin. Ø: vehicle

(NaCl) treated cells.

A

B

Figure A.13 BDNF expression levels in B2 neurons after exposure to 60 mM KCl

B2 neurons 14 DIV were exposed to 60 mM KCl for 24 h and BDNF levels were analysed.

A Western blot of BDNF. 20 μl of neuronal lysate was loaded per lane. **B** BDNF levels were

not significantly increased after 24 h exposure to 60 mM KCl but a trend towards an increase

was observed (Mann-Whitney test, actual difference between medians = 10.26, $p > 0.05$,

n = 3 independent wells). Data are presented as mean ± SEM relative to βIII-tubulin. Ø: vehicle

(NaCl) treated cells.

# Analysis of different culture conditions to investigate BDNF modulation by pFTY720

Results in J1 neurons 14 DIV revealed no significant modulation of BDNF levels by short-term treatment with pFTY720 (Figure 5.2). It was unclear if this lack of effect might be due to the accumulation of BDNF in these cultures. It is conceivable that these relatively high levels could induce a negative feedback loop thereby inhibiting further *Bdnf* transcription (see Introduction and Haapasalo et al. 2002). This hypothesis was tested with a monoclonal antibody (mAb #9) capturing secreted BDNF (Materials and Methods, section 2.11). However, BDNF levels were not affected by 50 nM pFTY720. Also, there was no difference observed in BDNF levels between antibody-treated and untreated controls (Figure A.14).

Another approach to decrease basal BDNF levels was tested by lowering the plating density of J1 neurons. Plating densities of as low as 0.85×10^5 cells/cm^2 and 1.4×10^5 cells/cm^2 were tested. At the lowest plating density BDNF was barely detectable by Western blot in J1 neurons 14 DIV, so that a quantification by densitometry was not possible (Figure A.15). In neurons of a slightly higher plating density detection of BDNF protein levels was improved allowing quantification of BDNF expression levels. Also in these cultures, no increase in BDNF expression was induced by 10 nM pFTY720 treatment after 24 h (Figure A.16).
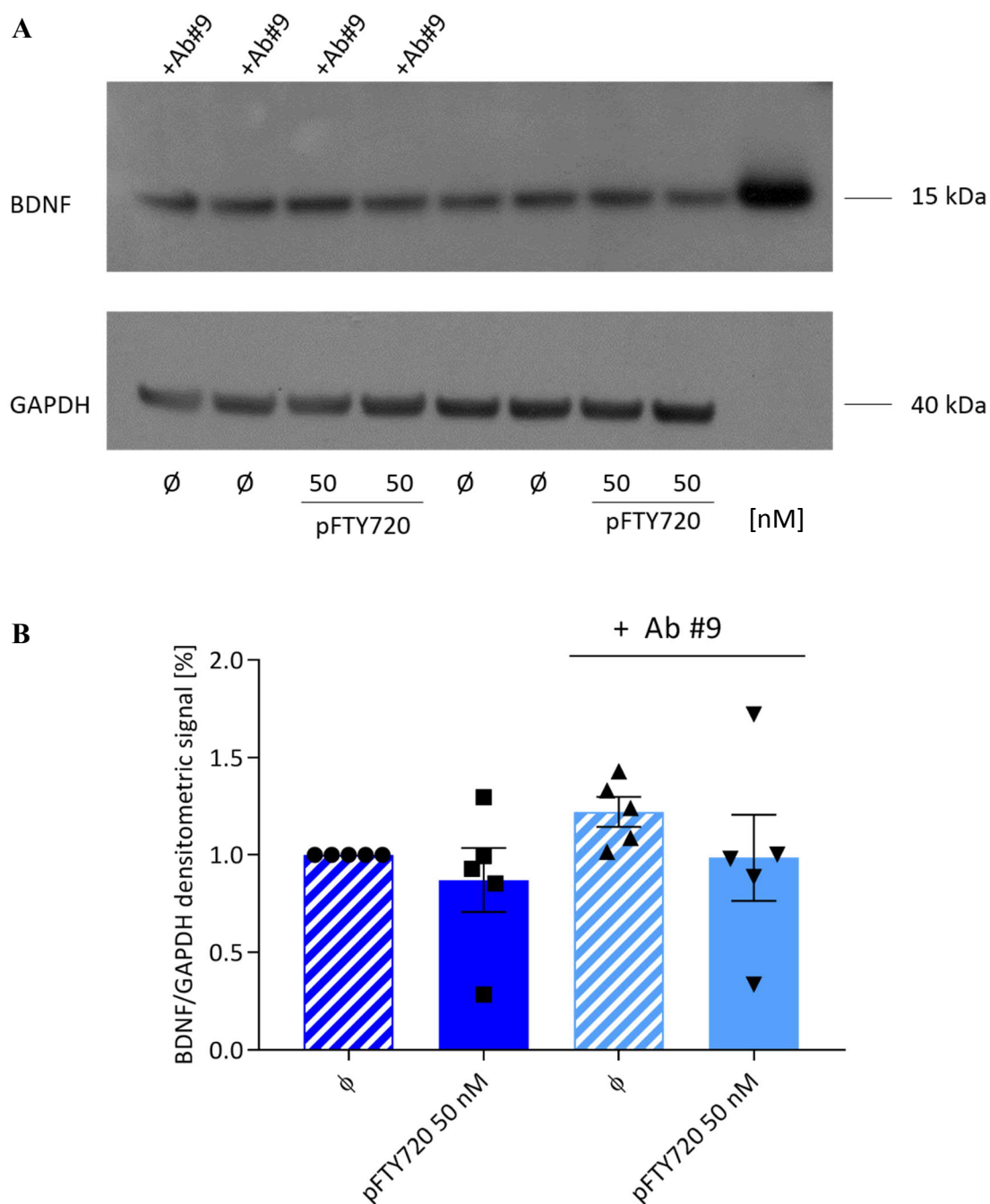
Figure A.14 Pre-treatment of J1 neurons with mAb #9

J1 neurons 14 DIV were exposed to 10 μg/ml mAb #9 for seven days before they were treated at 21 DIV with 50 nM pFTY720 for 8 h. **A** Western blot of BDNF. 20 μl of neuronal lysate was loaded per lane. **B** BDNF levels were not significantly affected by 50 nM pFTY720 treatment (Kruskal Wallis test, $p > 0.05$, n = 5 from 3 independent experiments). Data are presented as mean ± SEM relative to GAPDH. Changes are in percentage *vs.* control. Ø: vehicle (DMSO) treated cells.
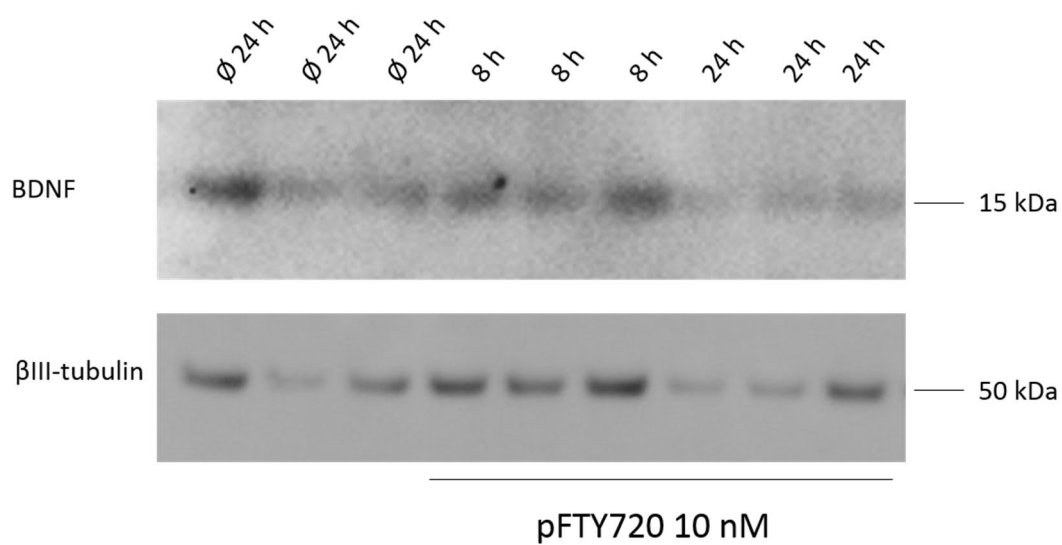
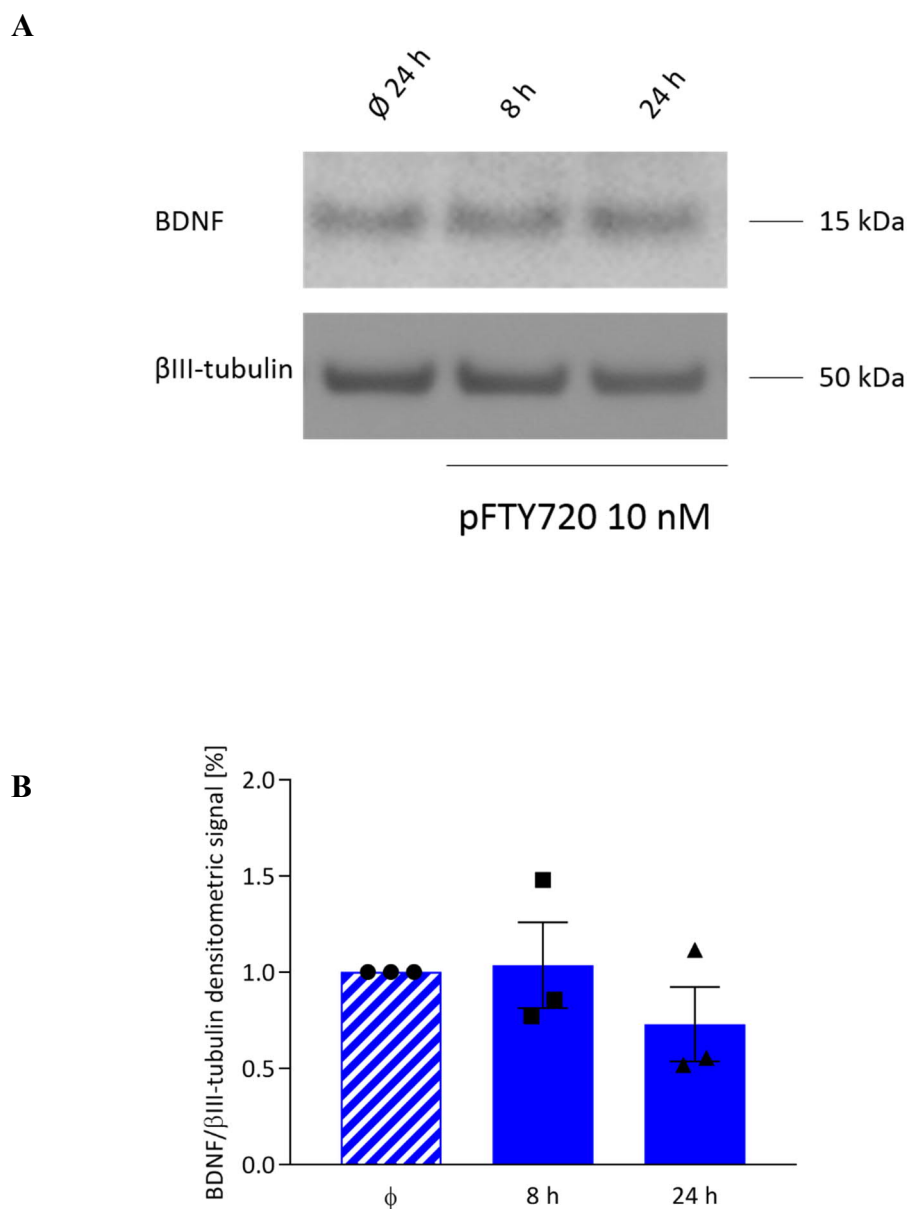**Figure A.15 BDNF levels in J1 neurons cultured at low density**

J1 neurons were cultured at a density of 0.85×10^5 cells/cm^2 and treated at 14 DIV with 10 nM pFTY720 for 8 h and 24 h. **A** Western blot shows that BDNF was barely detectable in J1 neurons cultured at this low plating density and a quantification of BDNF levels by densitometry was not possible. 20 µl of neuronal lysate was loaded per lane. Observation from 2 independent experiments. Ø: vehicle (DMSO) treated cells.

A
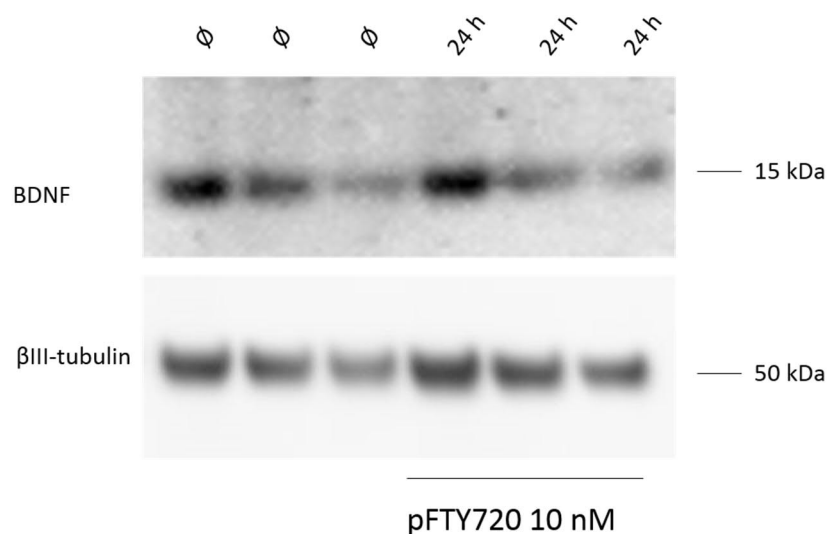
B
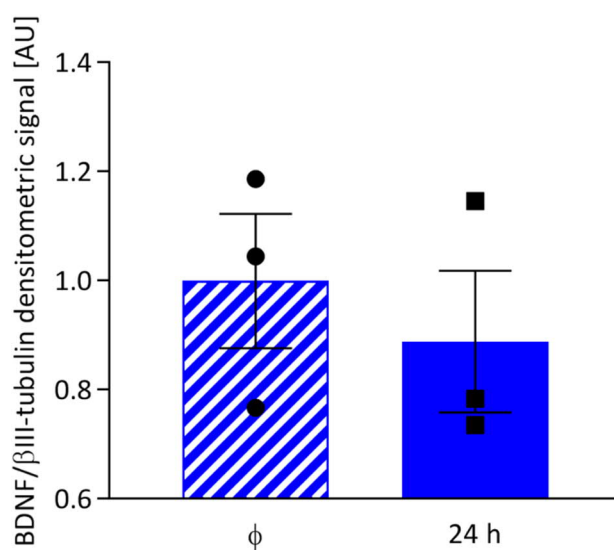
Figure A.16 BDNF levels were unaffected in neurons cultured at 1.4 x 10^5 cells/cm^2

J1 neurons were cultured at a density of 1.4 x 10^5 cells/cm^2 and treated at 14 DIV with 10 nM

pFTY720 for 24 h. **A** BDNF detection was improved in J1 cultures of 1.4 x 10^5 cells/cm^2

density. 20 μl of lysate was loaded per lane. **B** No increase of BDNF expression was induced

by a 24 h exposure to 10 nM pFTY720 (Mann-Whitney test, $p > 0.05$, n = 3 independent

wells). Data are presented as mean ± SEM relative to βIII-tubulin. Ø: vehicle (DMSO) treated

cells.

Investigations of the longitudinal expression of BDNF in ES cell-derived neurons showed that levels start to be detectable around 10 DIV onwards (Figure 3.29B). This was also seen for the expression levels of synaptophysin and suggested that low levels of synaptic transmission might be detectable. By treating ES cell-derived neurons with pFTY720 as early as 10 DIV it was investigated if this level of neuronal activity would be high enough to induce a pFTY720-dependent increase in BDNF expression. However, BDNF expression levels were not affected by 10 nM pFTY720 treatment for 8 h or 24 h (Figure A.17), suggesting that these neurons might indeed be too immature.

A

B

Figure A.17 BDNF levels in J1 neurons 10 DIV after pFTY720 treatment

J1 neurons 10 DIV were exposed to 10 nM pFTY720 for 8 h and 24 h. **A** Western blot for BDNF. 20 µl of neuronal lysate was loaded per lane. **B** No change in BDNF expression was observed after 24 h exposure to 10 nM pFTY720 (Kruskal Wallis test, $p > 0.05$, n = 3 from 2 independent experiments). Data are presented as mean ± SEM relative to βIII-tubulin. Changes are in percentage *vs.* control. Ø: vehicle (DMSO) treated cells.